UNIVERSIDADE FEDERAL DE PERNAMBUCO
CENTRO DE TECNOLOGIA E GEOCIÊNCIAS
PROGRAMA DE PÓS-GRADUAÇÃO EM GEOCIÊNCIAS

JUAN DAVID VALLEJO RAMÍREZ

CARACTERIZAÇÃO PALEOAMBIENTAL DA FASE PÓS-RIFTE DAS BACIAS DO ARARIPE E JATOBÁ, NORDESTE DO BRASIL: INFERÊNCIAS PALINOLÓGICAS E PALINOFACIOLÓGICAS

Tese de Doutorado

Recife – PE
2024

JUAN DAVID VALLEJO RAMIREZ

CARACTERIZAÇÃO PALEOAMBIENTAL DA FASE PÓS-RIFTE DAS BACIAS DO ARARIPE E JATOBÁ, NORDESTE DO BRASIL: INFERÊNCIAS PALINOLÓGICAS E PALINOFACIOLÓGICAS

Tese apresentada ao Programa de Pós-Graduação em Geociências do Cento de Tecnologia e Geociências da Universidade Federal de Pernambuco como preenchimento parcial dos requisitos para obtenção do grau de Doutor em Geociências.

Área de Concentração: Geologia Sedimentar e Ambiental

Orientadora: Dra. Enelise Katia Piovesan

Coorientador: Dr. Marcelo de Araujo Carvalho

Recife

2024

.Catalogação de Publicação na Fonte. UFPE - Biblioteca Central

Vallejo Ramírez, Juan David.
Caracterização paleoambiental da fase pós-rifte das bacias do Araripe e Jatobá, Nordeste do Brasil: inferências palinológicas e palinofaciológicas / Juan David Vallejo Ramírez. - Recife, 2024.
115f.: il.

Tese (Doutorado) - Universidade Federal de Pernambuco, Centro de Tecnologia e Geociências, Programa de Pós-Graduação em Geociências, 2024.
Orientação: Enelise Katia Piovesan.
Coorientação: Marcelo de Araujo Carvalho.

1. MOA; 2. Andar locar Alagoas; 3. Palinofácies; 4. Paleoambiente. I. Piovesan, Enelise Katia. II. Carvalho, Marcelo de Araujo. III. Título.

UFPE-Biblioteca Central

JUAN DAVID VALLEJO RAMIREZ

CARACTERIZAÇÃO PALEOAMBIENTAL DA FASE PÓS-RIFTE DAS BACIAS DO ARARIPE E JATOBÁ, NORDESTE DO BRASIL: INFERÊNCIAS PALINOLÓGICAS E PALINOFACIOLÓGICAS

APROVADA EM:

Banca Examinadora

____

Dra. Enelise Katia Piovesan

Universidade Federal de Pernambuco (UFPE)

____

Dra. Alessandra da Silva dos Santos (Examinador Externo)

Universidade do Vale do Rio dos Sinos (UNISINOS)

____

Dra. Luzia Antonioli (Examinador Externo)

Universidade do Estado do Rio de Janeiro (UERJ)

____

Dr. Mitsuru Arai (Examinador Externo)

Universidade Estadual Paulista Júlio de Mesquita Filho (UERJ)

____

Dr. Rodolfo Dino (Examinador Externo)

Universidade do Estado do Rio de Janeiro (UERJ)

____

Dr. Claus Fallgatter

Universidade Federal de Pernambuco (UFPE)

31 de Julho de 2024

Agradecimentos

A todas as pessoas que, de forma positiva ou negativa, contribuíram para meu crescimento profissional.

Ao Programa de Pós-Graduação em Geociências do Centro de Tecnologia e Geociências da Universidade Federal de Pernambuco, pela assistência e acompanhamento durante o meu tempo de permanência;

Ao projeto 'Bioestratigrafia de alta resolução e paleoambientes das bacias do Araripe, Tucano Norte e Jatobá (Rifte e Pós-rifte), pela concessão da bolsa;

Ao Laboratório de Micropaleontologia Aplicada (LMA), por ser meu lar e me acolher em tempos de incertezas;

Aos meus pais, meu irmão e irmãs, pelo apoio incondicional, por serem meu estímulo durante estes anos. Sua disciplina, responsabilidade, amor e vontade de fazer as coisas certas foram essenciais para enfrentar este desassossego;

Ao meu capitão, meu 01, por acreditar em mim, por topar desde o começo, sua ajuda foi fundamental para conferir, descrever e aprender mais sobre geologia. Você foi parte de minha motivação. Para sempre, vou te amar. Obrigado, Regina Buarque de Gusmão.

“A ciência é muito mais que um corpo de conhecimentos.

É uma maneira de pensar.”

Carl Sagan

RESUMO

Localizadas no Nordeste brasileiro, as bacias do Jatobá e do Araripe ainda geram discussões sobre o contexto de sua evolução, no que diz respeito à influência marinha e ao seu intervalo temporal. Essas bacias são compostas por rochas siliciclásticas intercaladas com níveis de calcário e evaporitos, das quais foram analisadas 250 amostras palinológicas. Com esses dados, foi possível refinar o intervalo temporal e as condições deposicionais das sequências neoptianas das bacias do Araripe e Jatobá. Evidências palinológicas identificaram, para as duas bacias, 156 táxons. A determinação de fóssil-guia é marcada pela biozona P-270, definida pela espécie *Sergipea variverrucata*. A presença de palinomorfos marinhos em alguns níveis (e.g., *Subtilisphaera* sp. e palinoforaminíferos) indica incursões marinhas em ambas as bacias. Com base em associações palinofaciológicas e fácies sedimentares, determinou-se que o sistema deposicional do Grupo Santana em ambas as bacias compreende um sistema fluvio-deltaico depositado durante o Eoaptiano, bem como ambientes lagunares semifechados e ambientes marinhos rasos depositados durante o Neoaptiano. Adicionalmente, são registradas ocorrências de palinoforaminíferos em amostras da Formação Crato, evidenciando as primeiras incursões marinhas nas bacias.

Palavras-chave: MOA, Andar local Alagoas, Palinofácies, Paleoambiente.

ABSTRACT

Located in northeastern Brazil, the Jatobá and Araripe basins continue to spark discussions regarding their evolutionary context, particularly concerning marine influence and their temporal interval. They are composed of siliciclastic rocks intercalated with levels of limestone and evaporites, from which 250 palynological samples have been described. With this data, it was possible to refine the temporal interval and depositional conditions of the Neo-Aptian sequences of the Araripe and Jatobá basins. Palynological evidence identifies, for both basins, biozone (P-270), in addition to the identification of 156 taxa. The determination of guide species is marked by palynozone P-270, defined by the occurrence of *Sergipea variverrucata*. The presence of marine palynomorphs (e.g., *Subtilisphaera* sp. and foraminiferal linings) indicates marine incursions into the basins. Based on palynological associations and sedimentary facies, it was determined that the depositional system of the Santana Group in both basins comprises a fluvio-deltaic system deposited during the Lower Aptian, as well as semi-enclosed lagoon and shallow marine environments deposited during the Upper Aptian. Additionally, occurrences of foraminiferal linings in samples from the Crato Formation are recorded, providing evidence of the first marine incursions into the basins.

Key words: AOM, Alagoas local Stage, Palynofacies, Paleoenvironment

LISTA DE FIGURAS

SUMÁRIO

1. INTRODUÇÃO

Estudos palinológicos aplicados a depósitos do Mesozoico têm desempenhado um papel importante na compreensão e ampliação do conhecimento sobre os padrões bioestratigráficos nas bacias sedimentares brasileiras (e.g. Regali *et al*., 1974a,b; Regali, 1989; Dino, 1994; Regali & Santos, 1999; Arai, *et al*., 2001; Coimbra *et al*., 2002; Heimhofer & Hochuli, 2010; Portela *et al*., 2014; Nascimento *et al*., 2017; Souza-Lima & Silva, 2018; Michels *et al*., 2018; Ferreira *et al*., 2016; 2020; Carvalho *et al*., 2019; Arai & Assine, 2020; Nascimento *et al*., 2023).

Um foco significativo dessas pesquisas tem sido o reconhecimento dos bioeventos que ocorreram durante a deposição da fase pós-rifte, composta de estratos depositados em ambiente continental a marinho durante o Aptiano (idade local Alagoas) (Chang *et al*., 1988).

O Andar Local Alagoas (Schaller, 1969) foi reconhecido praticamente em todas as bacias cretácicas brasileiras por meio de correlações palinológicas (Dino, 1992). Ele é marcado pela superzona *Exesipollenites tumulus* (P-200), a qual é caracterizada por seis zonas palinológicas: P-230, P-240, P-250, P-260, P-270 e P-280 (Regali *et al*., 1974a). As palinozonas P-230 e P-280, representam as idades inferior e superior do Andar Alagoas, tendo uma ampla distribuição temporal e as zonas P-270 e P-280 marcam o intervalo correspondente ao Alagoas superior (Regali, 1987, 1989; Beurlen & Regali, 1987; Regali & Viana, 1989; Regali & Santos, 1999).

O Andar Alagoas foi identificado nas bacias do Araripe e Jatobá (Lima, 1978; Coimbra *et al*., 2002; Nascimento *et al*., 2017) que corresponde a um intervalo de tempo com grandes mudanças ambientais, relacionada à formação de importantes reservas de hidrocarbonetos (Gomes *et al*., 2021).

Na Bacia do Araripe, o Grupo Santana é a unidade litoestratigráfica que abrange sucessões do Andar Local Alagoas, correspondendo a uma sequência transicional "pós-rifte" (Coimbra *et al*., 2002; Assine *et al*., 2014), sendo constituído, da base para topo, pelas formações Barbalha, Crato, Ipubi e Romualdo (Neumann & Cabrera, 1999; Assine *et al*., 2014). Na Bacia de Jatobá, a Formação Marizal é correlata à Formação Barbalha e, com exceção da Formação Ipubi, as demais unidades do Grupo Santana são registradas (Neumann & Rocha, 2014; Varejão *et al*., 2016).

Existem várias contribuições importantes da palinologia para as bacias do Araripe e Jatobá (Lima, 1978; Lima, 1984; Arai & Coelho, 2001; Coimbra *et al*., 2002; Neumann *et al*., 2003; Heimhofer & Hochuli, 2010; Nascimento *et al*., 2017; Teixeira *et al*., 2017; Goldberg *et al*., 2019; Arai & Assine, 2020; Coimbra & Freire, 2021; Lacerda *et al*., 2023; Vallejo *et al*., 2023; Nascimento et al., 2023). No entanto, mesmo após um longo histórico de pesquisas, algumas questões ainda permanecem sem uma resposta satisfatória, como a possível presença ou ausência de depósitos albianos, dentro do Andar Alagoas.

A opção de usar os palinomorfos para o refinamento cronoestratigráfico nessas bacias deve-se à sua alta resolução bioestratigráfica. Palinomorfo é o termo geral adotado para todos os espécimes não dissolvidos por ácidos (e.g., ácido clorídrico e ácido fluorídrico) nas preparações em rochas sedimentares (Tyson, 1995; Traverse, 2007).

O estudo da matéria orgânica sedimentar (MOS) em rochas sedimentares visa a interpretação da conexão entre a biosfera e a geosfera, na qual interagem diversas disciplinas e técnicas para sua caracterização. A utilização integrada dessas técnicas requer um entendimento dos fatores ambientais que controlam a produção de matéria orgânica na biosfera, dos processos ecológicos e sedimentológicos que controlam sua distribuição, e decomposição dos fatores geomicrobiológicos e biogeoquímicos que influenciam sua preservação, além dos processos geoquímicos e físicos que determinam a modificação da MOS durante sua incorporação na geosfera. Isso torna o estudo da MOS um dos segmentos mais multidisciplinares das Ciências da Terra (Tyson, 1995; Mendonça Filho *et al*., 2014).

A palinofácies é uma técnica que estuda a composição da matéria orgânica sedimentar, potencial para interpretação paleoambiental, que fornece uma visão sobre os sistemas transgressivo-regressivos nos paleoambientes deposicionais (e.g. Carvalho *et al*., 2006a, 2006b; Teixeira *et al*., 2017; Gonzalez *et al*., 2020; Vallejo *et al*., 2023), principalmente considerando seu tipo de associação. Esporos, grãos de pólen, dinocistos, algas, acritarcos e todos os outros palinomorfos são naturalmente incluídos em uma análise de palinofácies.

O presente trabalho visa descrever, classificar, quantificar a matéria orgânica sedimentar e correlacionar a associação palinoflorística das amostras de testemunhos (poços 2-AR-SR-1A-CE e 2-AR-SR-1B-CE da Bacia do Araripe, 2-JB-SN-2A-PE e 2-JB-SN-2B-PE da Bacia de Jatobá) e amostras de rochas coletados em afloramentos do Grupo Santana, da Bacia do Araripe, abordando a aplicação bioestratigráfica e contribuindo com novos dados concernentes à evolução dos paleoambientes nas bacias interiores cretáceas no Nordeste do Brasil.

2. OBJETIVOS

2.1. Objetivo geral

Caracterizar qualitativa e quantitativamente as partículas da matéria orgânica sedimentar nos depósitos da fase pós-rifte do Andar Alagoas e refinar o posicionamento cronoestratigráfico das bacias do Araripe e Jatobá, Nordeste do Brasil.

2.2. Objetivos específicos

1. Interpretar os paleoambientes de deposição;
2. Realizar a correlação cronoestratigráfica das unidades pós-rifte das bacias do Araripe e Jatobá com eventos regionais;
3. Reconhecimento do arcabouço bioestratigrafico com base em palinomorfos nas bacias estudadas.

3. CONTEXTOS GEOLÓGICO E BIOESTRATIGRÁFICO

As bacias do Araripe e Jatobá representam bacias interiores localizadas na região Nordeste do Brasil, que foram implantadas sobre terrenos cristalinos pré-cambrianos que constituem a Província Borborema (PB). A PB abrange a parte oeste de um cinturão móvel Brasiliano, que se estende desde o Nordeste do Brasil até o Noroeste da África, englobando o Escudo Tuareg, o Escudo Benino-Nigeriano e as províncias em Camarões (Almeida *et al*., 1981; Brito neves *et al*., 2000) (Figura 1).

A Província Borborema é dividida em três Subprovíncias crustais: Norte, Transversal e Sul (Brito Neves *et al*., 2000; Van Schmus *et al*., 2011). A Subprovíncia Norte está localizada ao norte da Zona de Cisalhamento Patos e é composta pelos domínios Médio Coreaú, Ceará Central e Rio Grande do Norte (Brito Neves *et al*., 2000). Por sua vez, a Subprovíncia Transversal abrange os domínios Piancó-Alto Brígida, Alto Pajeú, Alto Moxotó e Rio Capibaribe (Santos, 1995). Já a Subprovíncia Sul está situada ao sul da Zona de Cisalhamento Pernambuco e é composta pelos domínios Pernambuco-Alagoas, Sergipano e Riacho do Pontal (Neves, 2021). Essas subprovíncias são separadas pelas Zonas de Cisalhamento Patos e Pernambuco, que possuem direção leste-oeste.

A PB limita-se ao norte pelo Cráton São Luís, ao sul pelo Cráton São Francisco, a oeste pela Bacia do Parnaíba e a Leste por bacias costeiras da margem passiva brasileira (Oliveira, 2008).

O registro estratigráfico do Mesozoico nas bacias da margem continental brasileira foi consolidado por Ponte *et al*. (1978), que identificaram cinco megassequências: continental, transicional evaporítica, plataforma carbonática rasa, marinha transgressiva e marinha regressiva. De acordo com Chang *et al*. (1988; 1992), a megassequência continental é composta por três sequências de estágios sin-rifte, que são definidas com base em suas associações de fácies e arcabouço estrutural. Essas sequências são as seguintes: (1) sin-rifte I, correspondente ao estágio inicial de subsidência relacionado ao estiramento litosférico inicial (Garcia, 1991), que resultou na formação da "Depressão Afro-brasileira" (Cesero *et al*., 1997) no final do Jurássico (idade Dom João); (2) sin-rifte II, depositada durante o Eocretáceo (idades Rio da Serra–Aratu), quando o rifteamento atingiu seu clímax e a rápida extensão da crosta levou ao aprofundamento acelerado dos grabens, onde lagos de água doce permanentemente estratificados foram estabelecidos; (3) sin-rifte III, com uma taxa de subsidência maior, em que a sedimentação dos lagos foi sucedida pela deposição de sedimentos alúvio-fluviais no Barremiano (idades Buracica–Jiquiá).

Figura 1 - Mapa da Província Borborema, Nordeste do Brasil, apresentando as bacias fanerozoicas da região: Destacam-se as bacias do Araripe e de Jatobá.

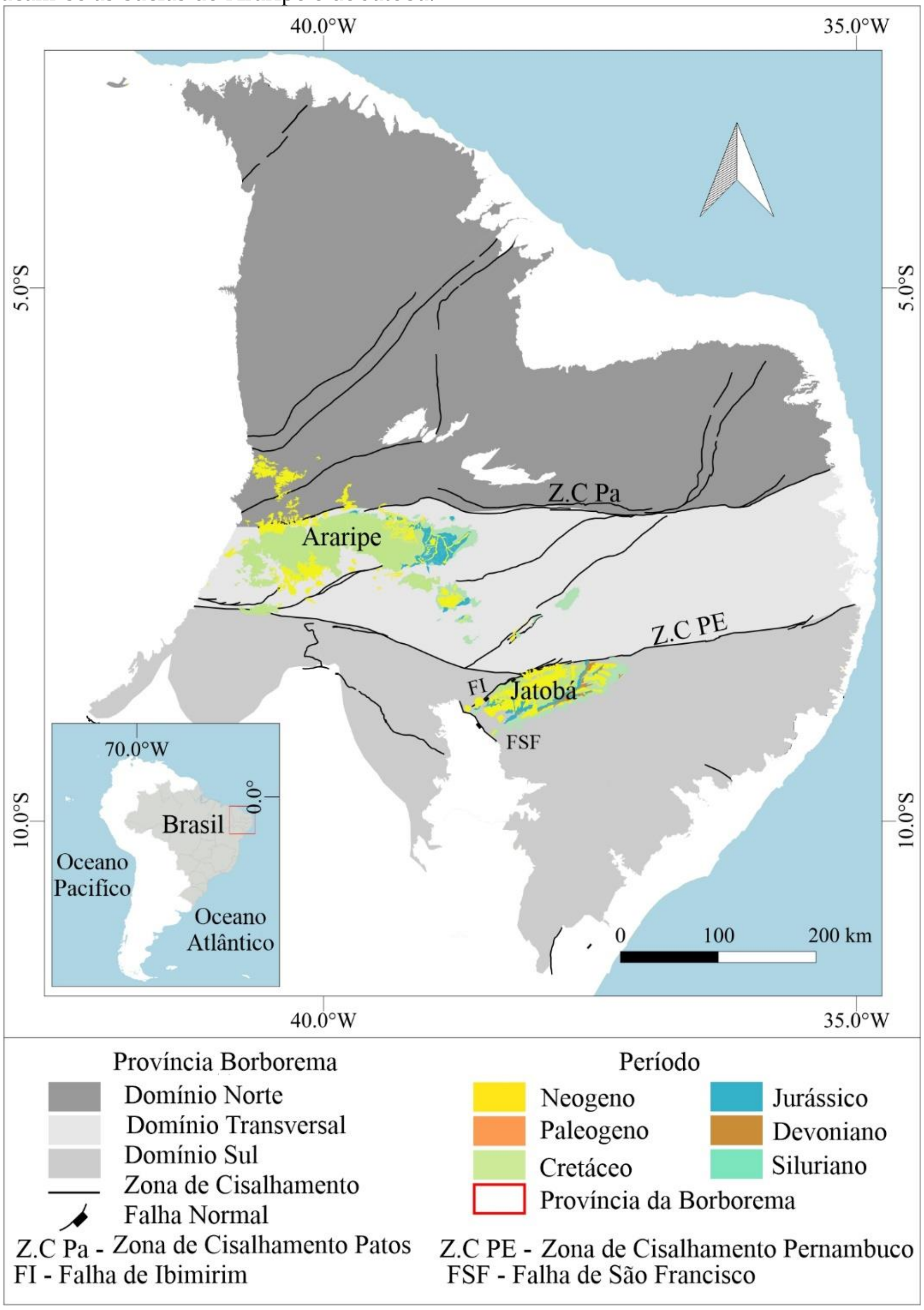

Fonte: Autor.

A estratigrafia das bacias interiores do Araripe e Jatobá é subdividida em sinéclise paleozoica, início de rifte, desenvolvimento do hemi-graben, clímax de rifte e pós-rifte, seguindo o modelo proposto por Prosser (1993) e modificado por Kuchle & Scherer

(2010); Kuchle *et al*., (2011); Scherer *et al*., (2014); Guzmán *et al*., (2015); Nascimento *et al*., (2017) (Figura 2).

Nas bacias do Araripe e Jatobá, a sequência pós-rifte é subdividida em duas unidades: pós-rifte I e pós-rifte II (Assine, 2007; Neumann & Rocha, 2014).

Figura 2 - Atualização da carta estratigráfica das Bacia do Araripe e Jatobá ilustrando o Andar Alagoas, ambiente deposicional e sequências tectonoestratigráficas.

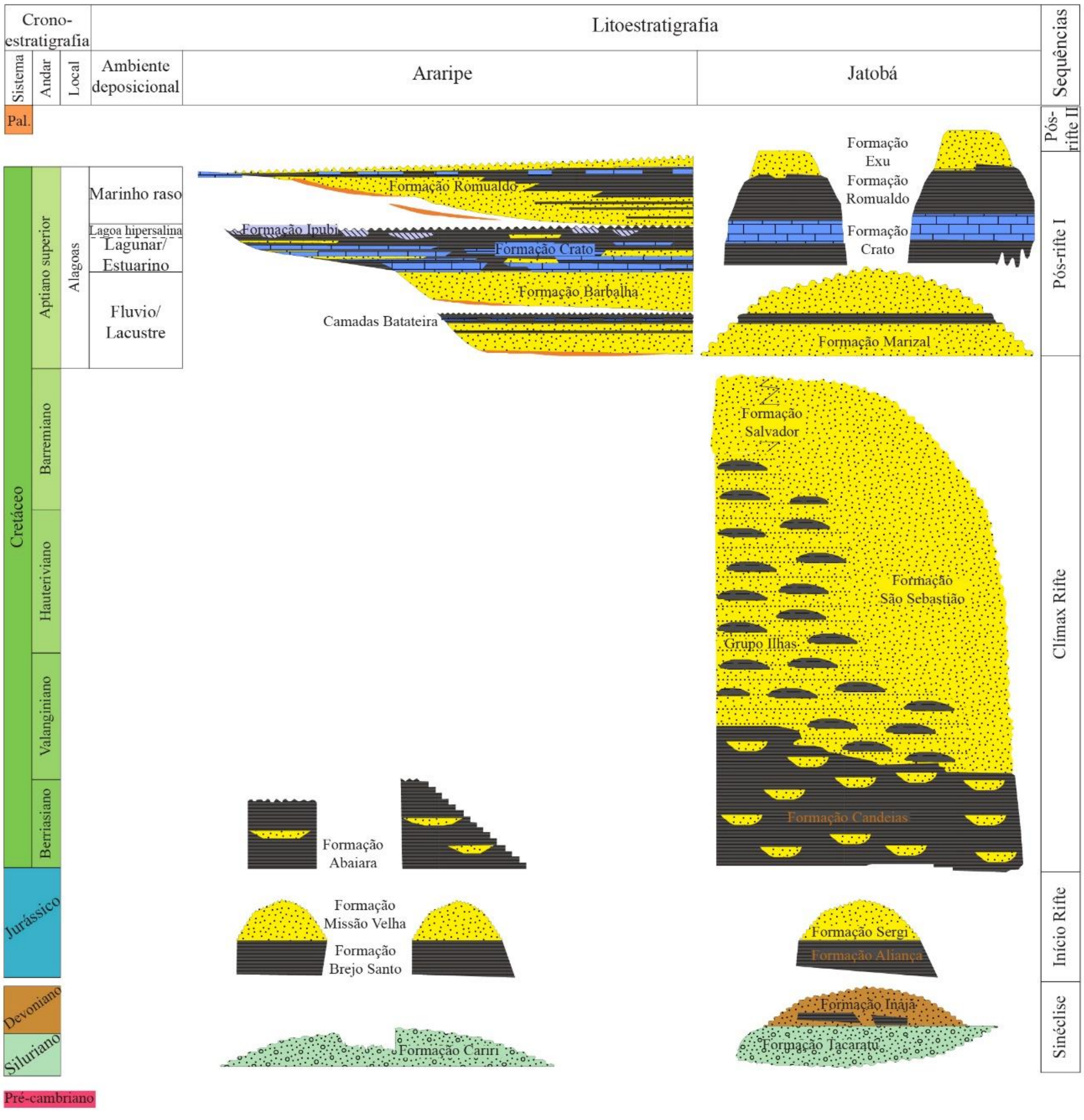

Fonte: Baseada em Assine (2007), Nascimento *et al*. (2017), Mendes *et al*. (2020), Varejão *et al*. (2021b), Guzmán *et al.* (2023).

A sequência pós-rifte I corresponde a uma sequência transicional evaporítica caracterizada por rochas de idade aptiana (Andar Local Alagoas). Essas rochas apresentam pequena espessura, porém grande extensão lateral, e são originadas de sedimentos siliciclásticos provenientes de ambientes flúvio-lacustres e aluviais. Gradualmente, esses sedimentos são substituídos por carbonatos e folhelhos, associados localmente a evaporitos depositados em ambientes costeiros de supramaré. O topo dessa unidade é marcado pela transgressão marinha no interior do nordeste do Brasil (Chang *et al*., 1992; Assine, 2007; Assine *et al*., 2014). A sequência pós-rifte II registra a deposição alúvio-fluvial e marca o retorno das condições continentais nas bacias interiores (Assine, 2007; Neumann & Rocha, 2014).

3.1. Bacia do Araripe

Localizada no Nordeste do Brasil, foi formada por processos extensionais relacionados a abertura tectônica do Atlântico Sul decorrente da separação dos continentes América do Sul e África (Assine *et al*., 2014; Scherer *et al*., 2015). A Bacia do Araripe abarca as formações Barbalha, Crato, Ipubi e Romualdo, que compõem o Grupo Santana (Neumann & Assine, 2015). Essas formações apresentam uma evolução tectono-sedimentar complexa, formada pelo empilhamento de várias sequências estratigráficas limitadas por discordâncias regionais associadas às formações Cariri, Brejo Santo, Missão Velha e Abaiara (Assine, 2007; Assine *et al*., 2014; Neumann & Assine, 2015).

O Grupo Santana, de acordo com as proposições de nomenclatura litoestratigráfica de Assine *et al*. (2014) e Neumann & Assine (2015), envolve calcários laminados, evaporitos de gipsita, arenitos, concreções carbonáticas, folhelhos, siltitos, pelitos e folhelhos escuros (Assine *et al*., 2014; Fambrini *et al*., 2020). Na base deste grupo, ocorre a Formação Barbalha, que apresenta intercalações de arenitos e folhelhos, incluindo também folhelhos das Camadas Batateira, que são um importante marco estratigráfico na bacia e representam a implantação de um lago pautado por flutuações do nível de água, registrando eventos de anoxia (Assine, 2007; Assine *et al*., 2014; Scherer *et al*., 2015). Acima da Formação Barbalha, está depositada a Formação Crato, uma unidade com espessura aproximada de 70 m (Assine, 2007). Essa formação é composta predominantemente por calcários com estratificação plano paralela (Neumann, 1999), intercaladas com folhelhos entre os intervalos de calcário (Neumann & Cabrera, 1999). As camadas evaporíticas descontínuas da Formação Ipubi são depositadas logo acima da Formação Crato e consistem em sucessões ricas de gipsita, associadas a *sabkhas* costeiras (Assine, 2007) ou a um sistema de *playa lake* (Nascimento *et al*., 2016). Por fim, a

Formação Romualdo é a unidade litoestratigráfica do topo do Grupo Santana, sendo principalmente composta por folhelhos, reconhecida mundialmente por sua preservação excepcional de fósseis (*Konservat-Lagerstätte*) dentro de concreções carbonáticas presentes em alguns níveis (Martill, 1988). Esta compreende uma ampla variedade de litologias, incluindo conglomerados estratificados, arenitos de granulação fina a média, calcários, margas e folhelhos, que caracterizam uma transição de ambiente costeiro para marinho (Assine *et al*., 2014).

O Grupo Santana é limitado por uma discordância erosiva em sua parte superior com as formações aluviais Araripina e Exu (Assine *et al*., 2014). Estas formações fazem parte da sequência pós-rifte II, constituída por duas unidades com características litológicas distintas (Assine, 2007).

3.2. Bacia do Jatobá

A Bacia de Jatobá está localizada no Norte do sistema Recôncavo-Tucano-Jatobá, que é uma ramificação do rifte abortado do Atlântico Sul, formada durante o Eocretáceo. Ela abrange uma área de aproximadamente 5000 km^2 nos estados de Pernambuco e Bahia, no nordeste do Brasil. Os limites da bacia são definidos pela falha de Ibimirim ao norte, pela falha de São Francisco, que a separa da sub-bacia do Tucano Norte, a oeste, e por margens flexurais nas outras direções (Costa *et al*., 2003). A estratigrafia da Bacia de Jatobá apresenta diferenças no seu registro sedimentar e tectono-estrutural em comparação com a Bacia de Tucano Norte. Estas diferenças encontram-se na fase rifte, que é menos evidente na Bacia de Jatobá do que na Bacia de Tucano Norte (Guzmán *et al*., 2015).

Rochas sedimentares pertencentes ao Grupo Jatobá (formações Tacaratu e Inajá) caracterizam a sequência sinéclise siluro-devoniana. As Formações Aliança e Sergi constituem a base do Grupo Brotas e representam a primeira etapa tectônica do início de rifte da Bacia de Jatobá (Kuchle *et al*., 2011), este grupo é composto por intercalações de lamitos vermelhos e cinza-esverdeadas, juntamente com arenitos muito finos, de cor bege a marrom e coquinas de ostracodes (Mendes *et al.*, 2020). Esta representa a porção distal dos sistemas aluviais do Jurássico Superior (Andar Dom João). A Formação Candeias representa o início da fase de clímax de rifte (Kuchle, 2010). As sequências clímax e fase final do rifte (Berriasiano–Eoaptiano) compreendem depósitos relacionáveis à Formação Candeias, ao Grupo Ilhas e à Formação São Sebastião.

No interior da Bacia de Jatobá, no intervalo atribuído ao Aptiano–Albiano inferior, há depósitos correspondentes à fase pós-rifte que se correlacionam com um contexto de subsidência térmica, em uma bacia tipo sag (Costa *et al*., 2007). A sequência aptiana é composta pelas formações Crato e Romualdo, essas formações, juntamente com as formações Marizal e Exu, fazem parte da tectonossequência pós-rifte (Rocha & Leite, 1999; Rocha, 2011).

Segundo Rocha (2011), a Bacia de Jatobá é constituída por um pacote predominantemente carbonático, com intercalações siliciclásticas, aflorando na Serra Negra e na Serra do Periquito, que corresponde à última fase lacustre. O registro sedimentar composto por depósitos aluviais siliciclásticos, como conglomerados e arenitos, caracteriza a Formação Marizal, cobrindo uma grande parte da bacia. Segundo Lima (2018), a Formação Marizal está depositada sobre um sistema fluvial associado a deltas, caracterizado por arenitos intercalados com sedimentos pelíticos (siltitos e argilitos), que apresentam estruturas de sobrecarga. Esses depósitos sobrepõem-se à Formação São Sebastião através de uma discordância angular, correspondendo ao evento de ruptura (Magnavita *et al*., 2003).

Depósitos lacustres de ambiente raso à profundo estão sobrepostos à Formação Marizal. Esses depósitos estão correlacionados com estratos contemporâneos na região de Araripe e são caracterizados pelas Formações Crato (calcário laminado intercalado com arenitos e folhelhos), Romualdo, de ambiente lacustre raso (folhelhos, margas e calcário intercalados), e Formação Exu (arenitos grossos a conglomerados), que afloram nas localidades de Serra do Periquito e Serra Negra (Carvalho *et al*., 2010; Rocha, 2011; Santos *et al*., 2011; Lima, 2018).

3.3. Palinoestratigrafia

Os depósitos sedimentares de idade mesozoica nas bacias do Araripe e Jatobá representam as fases rifte (início do rifte e clímax do rifte) e pós-rifte, que se desenvolveram do final do Jurássico ao final do Eocretáceo, durante o processo de quebra do Supercontinente Gondwana, resultando na separação dos continentes Africano e Sul Americano.

Os intervalos estudados correspondem ao Andar local Alagoas (Coimbra *et al*., 2002; Nascimento *et al*., 2017). A Bacia do Araripe foi estudada por Lima (1978), que encontrou dificuldades para correlacionar seu biozoneamento com o proposto por Regali *et al*. (1974a). No entanto, Lima (1978) sugeriu que a maior parte da Formação Santana poderia ser correlacionada à Superzona *Inaperturopollenites microclavatus* (P-300). Mais tarde, Regali (1990) reavaliou os dados de Lima (1978) e correlacionou-os com a parte inferior da Zona P-280. Estudos posteriores subdividiram o Grupo Santana em quatro intervalos bioestratigráficos correlacionáveis com as biozonas P-270 e P-280 (Portela, 2008; Rios-Netto *et al*., 2012). No entanto, Arai & Assine (2020) estabeleceram que todo o Grupo Santana corresponde à P-270.

O desenvolvimento de correlações bioestratigráficas nas Bacias do Araripe e Jatobá, com base em diferentes estudos (Coimbra *et al*., 2002; Tomé *et al*., 2014; Nascimento *et al*., 2017; Guzmán *et al*., 2023), revela que é provável que a sequência pós-rifte para as bacias possa ter sido depositada durante o Neoaptiano e início do Albiano.

De acordo com Rios-Netto et al. (2012), os sedimentos da Formação Santana foram depositados durante o Neoaptiano, conforme indicado pela caracterização da palinozona *Sergipea variverrucata* (P-270) e Subzona Tricolpados ornamentados (P-270.2), e palinozona *Complicatisaccus cearensis* (P-280) e Subzona *Equisetosporites maculosus* (P-280.1). No zoneamento bioestratigrafico proposto por Regali (1989a), Regali & Santos (1999) e Ferreira *et al*. (2016, 2020) o Grupo Santana enquadram-se na palinozona *Complicatisaccus cearensis* (P-280) correspondente a uma idade neoaptiana.

Lima (1984) identificou distintas biozonas para a Bacia de Jatobá, estudadas em amostras de sondagem de rochas portadoras das camadas linhíticas. Segundo o autor, as espécies *Exesipollenites tumulus*, *Reyrea polymorphus*, *Inaperturopollenites turbatus* e *Sergipea variverrucata* correspondem às Biozonas P-260/270 (Regali *et al*., 1974a), correspondente do Aptiano superior.

Nascimento *et al.* (2017) apresentam para a Bacia de Jatobá uma análise bioestratigráfica correspondente ao Aptiano–Albiano inferior, na qual identificaram o limite superior da palinozona de *Inaperturopollenites turbatus* (P-260) e da palinozona *Sergipea variverrucata* (P-270), bem como o limite inferior da palinozona *Complicatisaccus cearensis* (P-280).

4. MATERIAL E MÉTODOS

O presente estudo está inserido no projeto "BIOESTRATIGRAFIA DE ALTA RESOLUÇÃO E PALEOAMBIENTES DAS BACIAS DO ARARIPE, TUCANO NORTE E JATOBÁ (SEÇÕES RIFTE E PÓS-RIFTE).

O material é constituído por seções estratigráficas provenientes de afloramentos da Bacia do Araripe, além de dois furos de sondagens provenientes desta mesma bacia e duas sondagens provenientes da Bacia de Jatobá (Tabela 1; Figuras 3, 4 e 5).

Tabela 1 – Coordenadas das seções estratigráficas estudadas e amostras coletadas.

Coordenadas	Tipo	Seção	Local	Bacia	Nº de Amostras
N9163029/E481969	Afloramento	4BAr01	Sítio Sobradinho	Araripe	9
N9204540/E420538	Afloramento	1BAr11	Pedreira Conceição Preta	Araripe	6
N9213217/E422963	Afloramento	1BAr17	Pedreira Três Irmãos	Araripe	8
N9186456/E490069	Afloramento	2BAr04	Serra do Mãozinha	Araripe	8
N9198774/E449987	Afloramento	3BAr06	Rio Batateira	Araripe	5
N9198829/E450069	Afloramento	3BAr05	Rio Batateira	Araripe	1
N9200254/E450933	Afloramento	3BAr03	Rio Batateira	Araripe	1
N9200279/E450993	Afloramento	3BAr02	Rio Batateira	Araripe	1
N9200385/E451227	Afloramento	3BAr01	Rio Batateira	Araripe	2
N9193984/E456617	Poço	2-AR-SR-1A-CE	Sítio Romualdo	Araripe	59
N9197712/E455205	Poço	2-AR-SR-1B-CE	Sítio Romualdo	Araripe	43
N9042782/E607985	Poço	2-JB-SN-2A-PE	Serra Negra	Jatobá	47
N9044544/E610733	Poço	2-JB-SN-2B-PE	Serra Negra	Jatobá	60

Fonte: Autor.

Figura 3 - Localização dos afloramentos e testemunhos de sondagem da fase pós-rifte amostrados: Bacia do Araripe e Bacia de Jatobá.

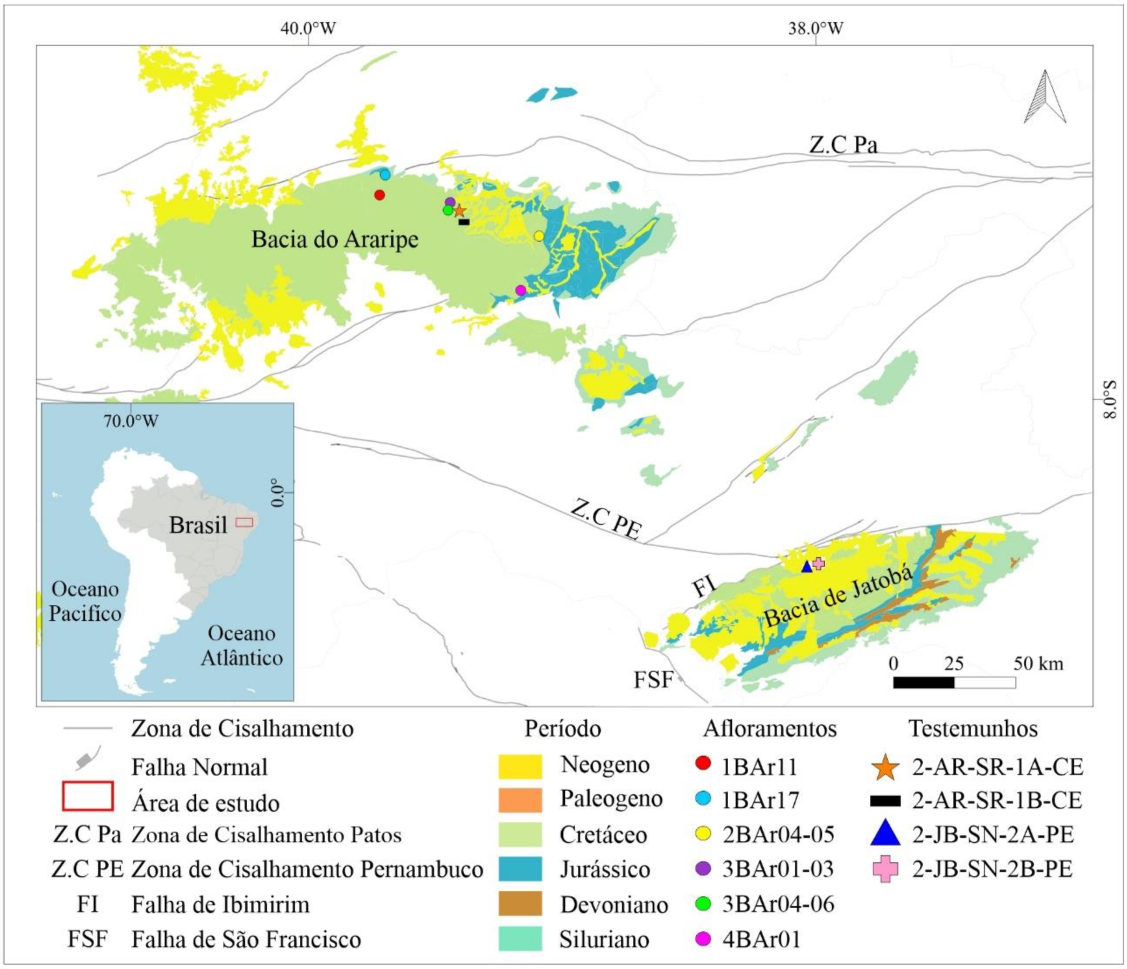

Fonte: Autor.

4.1. Preparação das amostras

O material foi preparado utilizando os procedimentos de palinofácies descritos por Tyson (1995) e Mendonça Filho *et al.* (2014), com algumas modificações. Este procedimento envolveu a destruição de todo o material mineral por acidificação, utilizando tratamento ácido convencional que envolve a dissolução de constituintes minerais a partir do uso de ácido clorídrico (HCl) e ácido fluorídrico (HF) para remover carbonatos e silicatos. Foi adicionado HCl (37%) suficiente para cobrir completamente a amostra, deixando reagir por 24 horas. As amostras foram lavadas com água destilada e posteriormente foi adicionado HF (40%), cobrindo a amostra e deixando reagir por 24 horas. As amostras foram novamente lavadas com água destilada e peneiradas em malha de abertura de 10 μm. Foi adicionado HCl (10%) ao resíduo, cobrindo a amostra por 24 horas, e finalmente lavado com água destilada em abundância. A matéria orgânica residual foi separada em duas partes: a não oxidada para análise de MOS e oxidada usando ácido nítrico para limpar e elucidar os palinomorfos. O resíduo foi montado em lâminas utilizando álcool polivinílico (PVA) e adesivo óptico *Norland* curado sob luz ultravioleta e luz solar. Em cada lâmina, foram contadas e analisadas 300 partículas de matéria orgânica e 300 palinomorfos sob microscópio de luz transmitida. A MOS foi classificada de acordo com Tyson (1995) e Mendonça Filho *et al*. (2014). Para cada amostra, foi determinada a abundância relativa em porcentagem da MOS, e os constituintes representativos foram fotografados usando uma câmera digital Axiocam 503 acoplada a um microscópio Zeiss (Axio Imager A.2) com objetiva de 20X e imersão em óleo de 63X e 100X. Todas as lâminas e resíduos estão armazenados e catalogados no Laboratório de Micropaleontologia Aplicada (LMA) da Universidade Federal de Pernambuco (UFPE).

4.2. Análise de palinofácies

As associações de palinofácies foram reveladas pelo dendrograma da análise de cluster no modo R, designadas por sua composição e partículas dominantes de MOS. Posteriormente, os percentuais das associações foram plotados usando o site RiojaPlot para determinar os intervalos paleoambientais. Além disso, inferências paleoambientais foram baseadas nas tendências deposicionais das partículas orgânicas que compõem cada associação (Tyson, 1995; Carvalho, 2001).

4.3. Análise Palinológica

Os percentuais dos palinomorfos são apresentados (Apêndice A), juntamente com os palinomorfos mais representativos. A taxonomia e identificação das morfoespécies de pólen e esporos foram baseadas em Jansonius & Hills (1976 e suplementos), assim como em vários artigos clássicos (Regali *et al*., 1974a; b; 1985; Lima, 1978; Regali & Viana, 1989; Regali, 1989a; Dino, 1992; 1994; Coimbra *et al*., 2002) e no Banco de dados do *Instituto Smithsonian de Pesquisas Tropicais* (Jaramillo & Rueda, 2023).

4.4. Análise de fácies sedimentares

O princípio da análise de fácies consiste em diferenciar o conteúdo sedimentar baseado na litologia (e.g. composição), textura (e.g. granulometria), estruturas e sedimentares. Estruturas biogênicas, conteúdo fossilífero e cor podem auxiliar na definição e distinção de litofácies (Miall, 1996; Tucker, 2014). O conjunto das características que constituem uma fácies permite a interpretações dos processos e condições deposicionais (Ashley, 1990; Nichols, 2009). Diferentes fácies podem ser agrupadas em associações de fácies, implicando em sucessivos processos deposicionais geneticamente relacionados a um mesmo contexto sedimentar (Collinson, 1996). Esse procedimento permite a interpretação e reconstrução do paleoambiente deposicional, que pode ser comparado com modelos de referência da literatura (e.g. Walker & James, 1992; Reading, 1996; Posamentier & Walker, 2006).

Nesse trabalho, a metodologia de análise de fácies, suas associações e superfícies limitantes seguiu os preceitos de Miall (1996; 2000); Walker & James (1992) e Tucker (2014), e consistiu basicamente em: 1) Registro fotográfico dos testemunhos; 2) Demarcação das principais litologias; 3) Identificação e descrição das fácies presentes; 4) Elaboração dos perfis sedimentológicos.

5. RESULTADOS E DISCUSSÕES

Os resultados e as interpretações da presente pesquisa serão apresentados em quatro partes. Na primeira, é apresentada a descrição da litologia das seções estratigráficas de amostragem, seguida dos três artigos: o primeiro, já publicado; o segundo atualmente em submissão, e o terceiro que se encontra em fase de revisão.

5.1. Caracterização e amostragem dos afloramentos e testemunhos de sondagem

5.1.1. Afloramentos

Na Bacia Araripe, a sequência pós-rifte I foi estudada em detalhe nos afloramentos localizados nas encostas da Chapada do Araripe (Figura 4). O Grupo Santana, da base para o topo, é composto pelas formações Barbalha, Crato, Ipubi e Romualdo, amostrado superficialmente nas bordas nordeste, leste e sudeste da bacia. A Formação Barbalha, correlacionada crono e litologicamente com a Formação Marizal da Bacia de Jatobá, aflora ao longo do Rio da Batateira, correspondendo ao Geossítio Batateiras na área do Parque Estadual Sítio Fundão, Crato, Ceará.

O afloramento 3BAr01 corresponde às 'Camadas Batateira' (correlacionadas com as Camadas Amargosa da Formação Marizal) e possui 1,70 m de altura de folhelhos pretos bioclásticos, onde uma amostra foi coletada no nível que apresentava menor alteração (Figura 4C). Percorrendo o Rio da Batateira em sentido sudoeste, mais cinco amostras dos afloramentos 3BAr02, 3BAr03, 3BAr04 e 3BAr05 (Figura 4A-C, Figura 5C), compostas por argilitos e folhelhos cinzas intercalados aos arenitos da Formação Barbalha, foram coletadas. A Formação Barbalha é sobreposta pela Formação Crato, onde foram coletadas amostras do afloramento 3BAr06 constituído por folhelhos pretos e calcários laminados (Figura 4D, Figura 5C).

Na Serra da Mãozinha, localizada no município de Abaiara, Ceará, os afloramentos 2Bar04 e 2Bar05 (Figura 5D), são compostos por folhelhos cinza, intercalados com calcários laminados, e um nível de arenito fino enriquecido em micas, pertencentes a Formação Crato.

Nos municípios de Nova Olinda e Santana do Cariri, Ceará, são encontradas abundantes minas de exploração de calcário da Formação Crato, para cimento ou lajes, e de gipsita da Formação Ipubi. Na Pedreira Três Irmãos, afloramento 1BAr17, foi coletado calcário laminado intercalado por siltitos, folhelhos e finos níveis de gipsita da Formação Crato (Figura 4F, Figura 5A). Na Pedreira Conceição Preta, o afloramento 1BAr11 (Figura 4G, Figura 5B), apresenta uma sucessão de gipsita/anidrita, folhelho, siltito e calcário com aproximadamente 16 m de altura.

O Sítio Sobradinho, afloramento 4BAr01 (Figura 4H, Figura 5E), localizado a sudeste da Chapada do Araripe, corresponde a um afloramento com aproximadamente 100 m de altura que registra a seção estratigráfica mais espessa e completa da Formação Romualdo, do Grupo Santana. Nesta seção, ocorrem depósitos costeiros transicionais, quartzo arenitos de granulometria areia fina, argilitos, siltitos e folhelhos, além de calcários presentes como níveis interestratificados e concreções, sobrepostas sobre as fácies carbonática-siliciclásticas da Formação Crato.

Figura 4 - Afloramentos do Grupo Santana, Bacia do Araripe: A (3BAr01); B (3BAr03); C (3BAr05) Rio Batateira, Formação Barbalha; D (3BAr06) Rio Batateira, Formação Crato; E (2BAr05a) Serra da Mãozinha, Formação Crato; F (1BAr17) Pedreira Três Irmãos, Formação Crato; G (1BAr11) Pedreira Conceição Preta, Formação Ipubi; H (4BAr01) Sítio Sobradinho, Formação Romualdo

Fonte: Autor.

Figura 5 - Afloramentos do Grupo Santana, Bacia do Araripe: Perfis litológicos dos afloramentos (em metros), mostrando os intervalos coletados e analisados. Seção: A. Pedreira Três Irmãos (1BAr17); B. Pedreira Conceição Preta (1BAr11); C. Rio Batateira (3BAr06) é um perfil composto contendo as formações Barbalha e Crato; D. Serra da Mãozinha (2BAr04-05) e E. Sítio Sobradinho (4BAr01). Perfis adaptados de Assine *et al.* (2014), Custódio *et al.* (2017), Varejão *et al.* (2021a; b) e Vallejo *et al.* (2023). A seta preta indica a direção vertical de amostragem em cada afloramento. Escala 1:20.

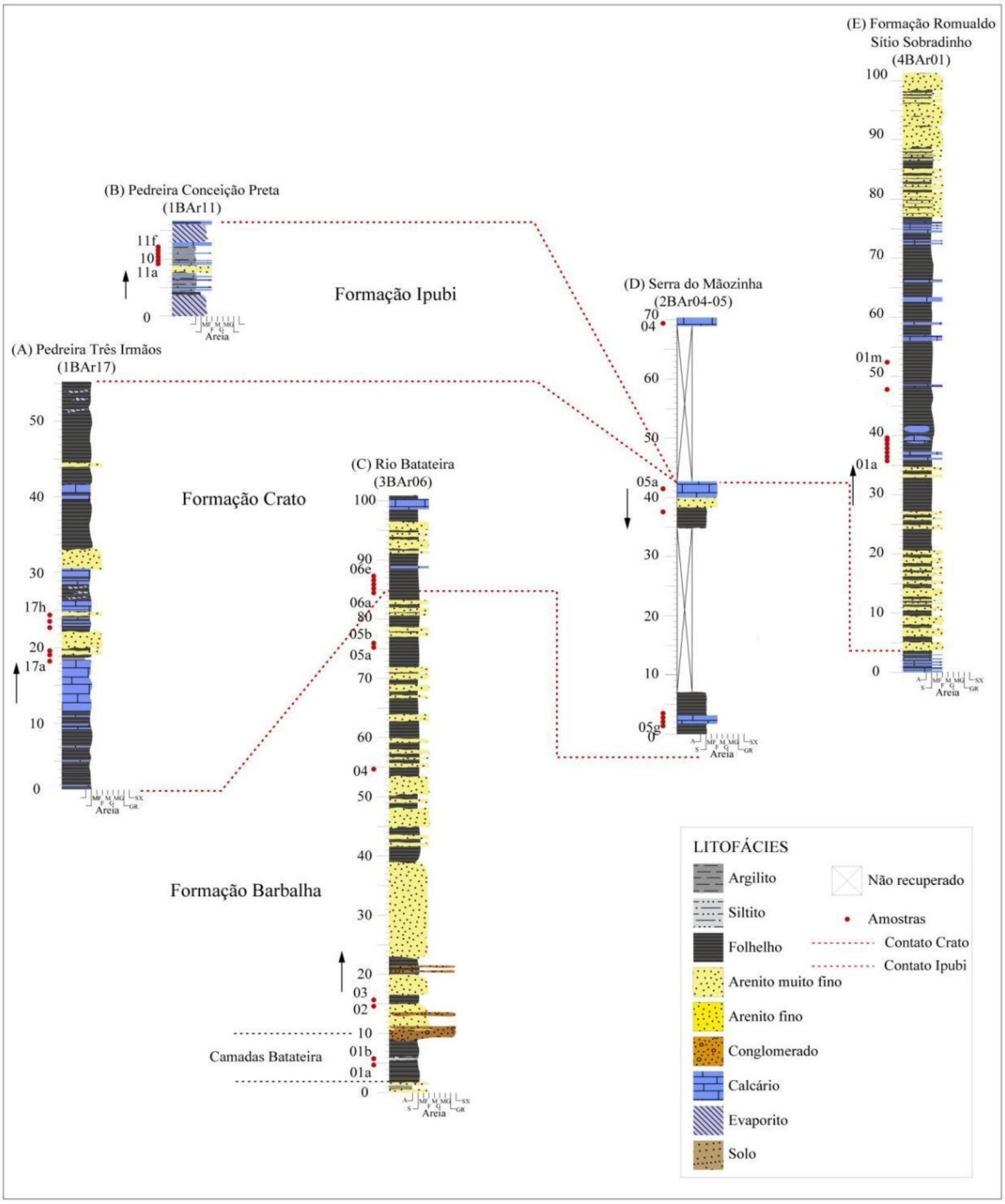

Fonte: Modificada de Vallejo *et al.* (2023).

5.1.2. Testemunhos

Foram confeccionados quatro perfis estratigráficos em escala 1:100. O poço 2-AR-SR-1A-CE (Figura 6A), foi recuperado na localidade do Sítio Romualdo, município do Crato, Ceará. Com uma profundidade de 140 m, apresenta uma ampla variedade litológica no testemunho. A porção superior é predominantemente siliciclástica, registrando intercalações de arenitos com granulometria de areia fina e estratificações de *climbing ripples*, além de argilitos. No intervalo de 37 a 65 m, há a presença de evaporitos e argilitos escuros, seguidos por calcários laminados e siltitos, além de uma lente de microbialito. No intervalo seguinte, encontram-se calcários laminados, com intercalações de rochas pelíticas, até 125 m. Na base, observa-se um aumento no tamanho de grão, variando de granulometria silte a areia média. Os estratos registrados nesse furo estão associados às formações Romualdo, Ipubi e Crato, bem como ao topo da Formação Barbalha do Grupo Santana (Apêndice A).

O poço 2-AR-SR-1B-CE (Figura 6B), foi perfurado no Sítio Romualdo, localizado no município de Crato, Ceará. com uma profundidade de 105 m, onde a porção superior do testemunho é composta por solo até aproximadamente 20 m. No intervalo de 21 até 37 m, é composto por arenitos de granulometria areia muito fina a fina, com estratificações de *climbing ripples* intercaladas com siltitos e argilitos. No intervalo de 39 até 62, é composto por solo. Posteriormente, entre 66 e 73 metros, encontra-se um arenito com granulometria de areia grossa, apresentando *climbing ripples*. Entre 75 e 86 metros, há um pacote de argilito com *climbing ripples* e estratificações cruzadas de baixo ângulo. Na profundidade de 79.5 metros, foi registrada a presença de uma lente de microbialito. Na base, observa-se um pacote de arenito de granulometria areia média e solo inconsolidado. Este furo registra parte da Formação Crato (Apêndice B).

O poço 2-JB-SN-2A-PE (Figura 6C), foi amostrado na localidade de Serra Negra, no município de Ibimirim, Pernambuco. Com uma profundidade de 105 m, a porção superior é composta por solo até aproximadamente 26 m. No intervalo de 27 até 84 m, apresenta uma sucessão siliciclástica com intercalações de arenito de granulometria muito fina, com *climbing ripples*, folhelho preto e siltitos. Na profundidade de 84 até 88 m, há um pacote de calcário laminado, seguido por um folhelho com uma camada de microbialito. Na base do perfil, ocorrem intercalações de argilito e siltito. Essa seção registra a ocorrência das formações Romualdo e Crato (Apêndice C).

Poço 2-JB-SN-2B-PE (Figura 6D), foi perfurado na localidade de Serra Negra, no município de Ibimirim, Pernambuco. Com uma profundidade de 72,5 m, apresenta no topo a presença de solo até 10 m. Entre as profundidades de 10 e 13 m, ocorre a presença de calcário laminado. Entre as profundidades de 21 e 43 m, observam-se intercalações de arenito muito fino a fino, com presença de estratificações cruzadas e *climbing ripples*, além de siltitos e argilitos com *climbing ripples*. Na profundidade de 44 m, há a presença de um microbialito. Na base, ocorrem intercalações de arenito médio a grosso, com estratificação cruzada e *climbing ripples*, siltito e argilito, além de uma lente de calcário. Esses sedimentos encontram-se associados às formações Crato e Marizal (Apêndice D).

Figura 6 - Perfis sedimentológicos dos testemunhos da Bacia do Araripe (2-AR-SR-1A CE) - (2-AR-SR-1B-CE) e Bacia de Jatobá (2-JB-SN-2A-PE) - (2-JB-SN-2B-PE). Profundidade em metros. Escala 1:100.

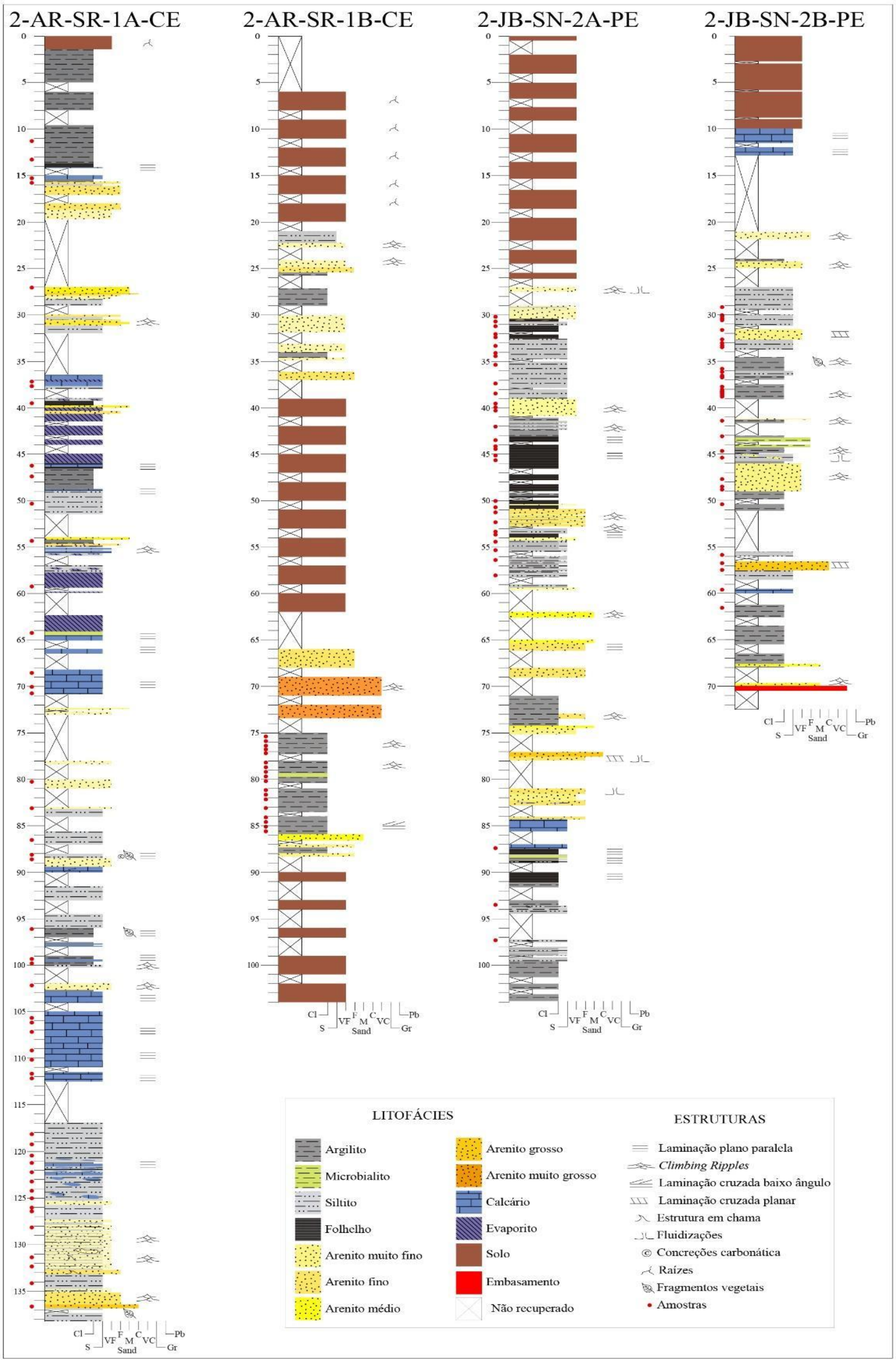

Fonte: Autor

5.2. Artigos

5.2.1. Primeiro artigo

No primeiro artigo que compõem a tese é apresentado a análise paleoambiental da matéria orgânica sedimentar (MOS) encontrada em depósitos transicionais aluviais-lacustres na Bacia do Araripe. As amostras foram coletadas em quatro formações que englobam o Grupo Santana. Essas foram analisadas com a técnica de palinofácies para contabilizar e agrupar as categorias de querogênio. A MOS foi subdividida em seis grupos com base em sua composição. A distribuição estratigráfica das palinofácies reflete uma mudança de um ambiente fluvial para um ambiente lacustre e eventualmente para um sistema estuarino. Os dados registrados indicam que o Grupo Santana apresenta a idade Aptiano superior. Encontra-se publicado em: *Jornal of South American Earth Sciences*, volume 121 (2023) 104154, https://doi.org/10.1016/j.jsames.2022.104154. O artigo publicado corresponde ao Apêndice E desta tese.

5.2.2. Segundo artigo

Neste artigo, é apresentada a distribuição estratigráfica da matéria orgânica sedimentar ao longo do poço 2-AR-SR-1A CE, o qual contém as quatro formações que compõem o Grupo Santana, na Bacia do Araripe. Além disso, são identificadas as associações de palinofácies e determinados os palinomorfos que caracterizam um paleoambiente deposicional durante o Aptiano superior. O artigo intitulado "*Sedimentary organic matter and paleoenvironmental reconstruction of the Santana Group (Early Cretaceous), Araripe Basin, Northeast Brazil*". Encontra-se publicado em: *Cretaceous Research*, volume (2024) 106016, https://doi.org/10.1016/j.cretres.2024.106016. O artigo publicado corresponde ao Apêndice F desta tese.

5.2.3. Terceiro artigo

Neste artigo, é apresentada a distribuição estratigráfica dos palinomorfos das bacias do Araripe e Jatobá, identificando as palinozona *Sergipea variverrucata* (P-270). Além disso, registra-se a ocorrência de palinomorfos marinhos na bacia do Jatobá.

Palynoflora of the Early Cretaceous (late Aptian) in the Araripe and Jatobá basins, Northeast Brazil

Juan David Vallejo[1,2]*, Regina Buarque de Gusmão[1,2], Alessandra Santos[3], Claus Fallgatter[1,2], Virgínio Henrique de Miranda Lopes Neumann[1,2], Marcelo de Araujo Carvalho[4], Enelise Katia Piovesan[1,2]

[1] Applied Micropaleontology Laboratory (LAGESE/LITPEG), Department of Geology, Federal University of Pernambuco, Recife-PE, Av. Da Arquitetura, s/n, CEP 50740-550, Brazil

[2] Graduate Program in Geosciences, Technology and Geosciences Centre, Federal University of Pernambuco, Recife-PE, Av. da Arquitetura, s/n, CEP 50740-550, Brazil

[3] Technological Institute of Paleoceanography and Climate Changes (itt Oceaneon), UNISINOS University, Avenida Unisinos, 950 - Cristo Rei, São Leopoldo, RS 93022-750, Brazil

[4] Plant Paleoecology Laboratory (LAPAV), Department of Geology and Paleontology, National Museum, Federal University of Rio de Janeiro, Rio de Janeiro-RJ, Brazil

* Corresponding author.

Abstract

The Santana Group, Upper Aptian (Alagoas local stage) records the post-rift stage of the Araripe and Jatobá basins after Gondwana break-up. Palynological zones and geological evolution is still controversial and requires review as new information becomes available. This study integrates palynological and sedimentological analyses from the Araripe and Jatobá Basins, which comprise siliciclastic rocks intercalated with levels of limestone and evaporites. With our analyses, it was possible to refine the temporal interval and depositional conditions of the late Aptian sequences of the Araripe and Jatobá basins. Palynological evidence determines, *Sergipea variverrucata* biozone (P-270), leading to the identification of 156 taxa. The determination of guide species is defined by their last occurrence of *S. variverrucata*. The presence of marine palynomorphs (e.g., *Subtilisphaera* sp. and foraminiferal test linings) indicates marine incursions into the basins. Based on palynological associations and sedimentary facies, the depositional system of the Santana Group in both basins comprises a fluvio-deltaic setting deposited during the Early Aptian, from semi-enclosed lagoon and shallow marine environments. Additionally, occurrences of foraminiferal linings in samples from the Crato Formation have been recorded, further reinforcing evidence of marine incursions into the basins.

Keywords: Alagoas local Stage, biostratigraphy, palynomorphs, paleoenvironment, post-rift sequence

1.Introduction

Applied palynological analysis of samples from the Cretaceous deposits has contributed to the elucidation and expansion of the biostratigraphic frameworks of sedimentary basins in Northeast of Brazil (Dino, 1994; Regali and Santos, 1999; Arai, et al., 2001; Coimbra et al., 2002; Heimhofer and Hochuli, 2010; Portela et al., 2014; Souza Lima and Silva, 2018; Ferreira et al., 2016, 2020; Nascimento et al., 2017, 2023; Michels et al., 2018; Carvalho et al., 2019; Arai and Assine, 2020), performing a crucial role in determining the age and environmental conditions of sedimentary deposits.

Given the similar features between the Araripe and Jatobá basins (Neumann and Rocha, 2014; Lima, 2018; Varejão et al., 2021a), these basins began to experience sedimentation that was almost synchronous, likely due to a significant eustatic rise (Arai, 2009). However, the age of the Aptian deposits, where the post-rift I sequence of the basins is recorded, as well as the extent of marine influence during this geological and temporal interval, remain poorly understood.

Data from previous studies, primarily on deposits of the Romualdo Formation, suggest deposition from the Aptian to the late Aptian and early Albian (Araripe et al., 2021; 2022; Barreto et al., 2022; Guerrini et al., 2023; Lemos et al., 2023; Nascimento et al., 2023). However, Arai and Assine (2020) argued that the palynological data indicate that the entire Santana Group is of Aptian age due to the conspicuous presence of *Sergipea variverrucata*, which they attribute to an upper Aptian biozone (P-270). This finding corroborates what Melo et al. (2020) proposed regarding the upper Aptian age of the Romualdo Formation. In a more comprehensive study of the Santana Group, Guzmán et al. (2023) identified the lower Aptian in the Barbalha Formation, which is stratigraphically positioned in the *Leupoldina cabri* Zone, as supported by Fauth et al. (2023). In addition, Guzmán et al. (2023) dated the Crato, Ipubi, and Romualdo formations as upper Aptian.

Through the description of the palynofloristic association, Nascimento et al. (2017) identified an Aptian–lower Albian age for the Crato Formation in the Jatobá Basin. This finding aligns with the previous suggestions of Tomé et al. (2014), which indicate an Aptian–early Albian age for the fauna found in both basins located in the Alagoas Local Stage. The Alagoas Local Stage consists of a transitional sequence characterized by rocks of Aptian and Albian ages, representing a time interval marked by significant environmental changes (Hay and Floegel, 2012; Carvalho et al., 2017; Gomes et al., 2021).

This study aimed to identify the palynoflora and sedimentary characteristics and to infer the paleoenvironmental conditions during deposition. The data presented refine the understanding of the age, contributing to a better comprehension of the depositional history by focusing on the distribution of palynomorphs across four well cores in Northeastern Brazil, which span the post-rift I sequence.

2. Geological and Stratigraphical framework

The Araripe and Jatobá basins are settled above the Precambrian crystalline terrains of the Borborema Province, in the Northeastern part of Brazil (Fig. 1). Both the Jatobá and Araripe Basin share similar features on their post-rift I sequence (Aptian age) (Neumann and Cabrera, 1999; Neumann et al., 2010). According to Rocha and Leite (1999) these basins are divided into four megasequences based on its the regional unconformities: (a) Paleozoic sequence (Upper Ordovician–Lower Silurian); (b) The early rift sequence (Upper Jurassic); (c) The rift climax sequence (Lower Cretaceous); (d) post-rift sequences. The post-rift sequence is divided into a lower post-rift I sequence that corresponds to the Alagoas Stage, and the upper post-rift II sequence (summarized by Fambrini et al., 2020).

These different megasequences, include the continental syn-rift phase, transitional evaporitic, shallow marine carbonate platform of the early drift stage, and open marine-transgressive and regressive cycles of the passive margin stage (Ponte and Asmus, 1978; Ponte and Ponte Filho, 1996; Assine, 2007; Assine et al., 2014; Neumann and Assine, 2015). These are followed by deposits associated with extensional processes during Gondwana break-up and the opening of the South Atlantic Ocean during the Early Cretaceous (Guzmán et al., 2023; Azevedo et al., 2024).

The Araripe Basin has a complex stratigraphic framework, during the Aptian and is recorded by the Santana Group. This unit comprises a variety of depositional settings, from fluvial to bayhead delta, and coastal to marine, including, from base to top, the Barbalha, Crato, Ipubi, and Romualdo formations (Assine et al., 2014; Neumann and Assine, 2015; Custódio et al., 2017; Varejão et al., 2019, 2021a, b; Guzmán et al., 2023). According to Assine et al. (2014), two disconformities led to the division of the Santana Group into three depositional sequences. The first sequence encompasses the lower part of the Barbalha Formation, and the top of the Batateira Beds interpreted as a coastal transgressive system, from a fluvial-deltaic environment, influenced by seawater (Varejão et al., 2021a; Fauth et al., 2023). The second sequence comprises the upper part of the Barbalha Formation, and the Crato and Ipubi formations, and the third sequence corresponds to the Romualdo Formation.

The Jatobá Basin is part of the Recôncavo-Tucano-Jatobá system, located in the states of Pernambuco and Bahia, covering an area of approximately 5,000 km². Its boundaries are defined by the Ibimirim fault to the north which also conditions the preferential orientation of the basin and its depocenter (Magnavita et al., 2012); the São Francisco fault to the west (separating it from the North-Tucano sub-basin), and flexural edges in other directions (Costa et al., 2003). In the Jatobá Basin, the Aptian–Lower Albian deposits represent the post-rift phase and are associated with a thermal subsidence related to a sag-type basin (Costa et al., 2007). The sedimentary record is dominated by alluvial deposits, including conglomerates and sandstones of the Marizal Formation, which cover a significant portion of the basin. Above the Marizal Formation, typical lacustrine deposits are correlated with the Barbalha Formation in the Araripe Basin (Neumann and Cabrera, 1999).

these deposits are correlate with strata in the Araripe Basin and represent the Crato Formation (laminated limestone and shales), the Romualdo Formation (interbedded shales, marls, and limestone), and the Exu Formation (coarse-grained sandstones to conglomerates with thin beds). These formations are exposed in the localities of Serra do Periquito and Serra Negra (Carvalho et al., 2010; Santos et al., 2011; Rocha, 2011) in the Jatobá Basin.

3. Material and Methods

The database for this study includes four cored wells from Northeastern Brazil. The cores exhibit a wide range of lithologies, primarily dominated by siliciclastic sediments intercalated with laminated limestone packages and occasional evaporites. Sedimentary logs, at a scale of 1:100, with sampling positions, are shown in Figure 2. Facies associations were compared to the depositional models for continental environments proposed by Miall (1996). The dataset includes 209 samples, summarized in Table 1.

Basin	Well ID	Coordinates	Number of Samples Analyzed
Araripe	2-AR-SR-1A-CE	N9193984/E456617	59
Araripe	2-AR-SR-1B-CE	N9197712/E455205	43
Jatobá	2-JB-SN-2A-PE	N9042782/E607985	47
Jatobá	2-JB-SN-2B-PE	N9044544/E610733	60

For palynological analyses, the samples were treated with hydrochloric acid (HCl) to remove carbonates and hydrofluoric acid (HF) to remove silicates (Uesugui, 1979; Wood et al., 1996). The residual organic matter was divided into two parts: one non-oxidized and one oxidized (using nitric acid to clean and concentrate the palynomorphs). The residual matter was mounted on slides using polyvinyl Alcohol (PVA) and Norland Optical Adhesive, cured under ultraviolet light. Up to 300 palynomorphs were counted per slide and analyzed under transmitted light microscopy, observed using a Zeiss microscope (Axio Imager A.2) with objectives immersion oil 63X and 100X. The representative constituents were photographed using a digital Axiocam 503 camera. All slides and residues are stored and cataloged at the Applied LMA/UFPE, under P00280 code.

All the palynomorphs present on the slides were identified and counted. Taxonomic identification was based on the works of Regali et al. (1974a,b); Lima (1978); and Dino (1992); (1994). Additionally, based on Carvalho et al. (2019) and Santos et al. (2022) the proportions of the pollen grains and spores were compared among the main paleoclimate indicators, humid (e.g., fern spores), semi-arid-arid (e.g., *Classopollis*), warmer, drier (e.g., *Equisetosporites*) and warmer, wet highlands (*Araucariacites*+*Inaperturopollenites*).

4. Results

A total of 26.017 palynomorphs were counted in four well-studied cores. The abundance of palynomorphs in the cores ranged from very high to low, showing considerable variation (Supplementary material 1, 1–14). The preservation of terrestrial palynomorphs was good, while marine palynomorph preservation ranged from poor to good. Terrestrial palynomorphs included pollen, spores, fungi, and freshwater algae (e.g., *Pediastrum*, *Botryococcus*), and marine palynomorphs including, dinoflagellate cysts (e.g, *Subtilisphaera* sp.), foraminiferal test linings, and scolecodonts. Paleozoic palynomorphs, including acritarchs (e.g., *Maranhites*), also occur and interpreted as reworking.

Gymnosperm pollen grains dominated, averaging 68.31%, followed by pteridophyte spores at 12.25%, marine elements 9.72% and angiosperms at 4.5% of the total palynomorphs. The identified palynoflora comprised 158 taxa. The more abundant taxa included *Classopollis*, *Equisetosporites*, *Araucariacites*, *Inaperturopollenites*, *Gnetaceaepollenites*, *Steevesipollenites*, *Uesuguipollenites*, and spores with *Cicatricosisporites*, and *Deltoidospora*. Angiosperm taxa were less abundant, represented by *Trisectoris reticulatus, Penetetrapites mollis, Pennipollis reticulatus, Afropollis* sp. And *Stellatopollis* sp. Additionally, palynomorphs of biostratigraphic significance, such as *Exesipollenites tumulus*, *Sergipea variverrucata*, *Equisetosporites maculosus* and *Complicatisaccus cearensis*, were identified. In addition to the rare occurrence of *Elaterosporites klaszii* together with *Retistephanocolpites* sp. was also registered (Fig. 3).

The samples yielded a rich and abundant palynoflora, with an assemblage comparable to those reported from the Upper Aptian in the Brazilian continental margin basins. The assemblage shows a strong affinity with the *Sergipea variverrucata* biozone (P-270), based on the standard biozonation scheme (Regali and Santos, 1999).

4.1 Palynostratigraphy of the studied cores from the basins

4.1.1. late Aptian Araripe Basin

In the wells of the Araripe Basin, a total of 9,496 palynomorphs were counted, including 7,532 pollen grains, 1,384 spores, 580 others (including fungi, scolecodonts, and spheromorphs), as well as seven dinoflagellate cysts and two foraminiferal test linings (Supplementary Material x?). A total of 127 taxa were identified, with abundance recorded in the Barbalha and Crato formations.

The lower interval (127-138 m), Barbalha Formation contains a mixture of palynomorphs restricted to Upper Aptian, this is characterized by the occurrence of *S. variverrucata* is recorded at 134 m, associated with *C. classoides*, *A. australis*, *L verrucatus*, *A. jardinus*, *S. dubius*, *I. foveolatus*, *C. avnimelechi*, *S. punctata*, *P. mamelonatus*, in addition to *G. retangularis*, *G. jansonii*, *P. reticulatus*, *T. reticulatus*, *S. araripensis*, *C. brevilaesuratus*, and *C. cearensis*, which is recorded at 131.74 m. The interval (64-127 m), Crato Formation registered the presence of foraminiferal test linings at a depth of 126 m; furthermore, it has presented high abundance palynological. The occurrence of *S. variverrucata* is recorded at 106.73 m, and *C. cearensis* is recorded at 99.78 m, in addition to *G. retangularis*, *G. jansonii*, *G. barghoornii*, *S. densiornatus*, *S. araripensis*, *Regalipollenites amphoriformis*, *B. regaliae*, *Sergipea naviformis*, *P. mollis*, *C. nuni*, *C. avnimelechi*, *C. brevilaesuratus*, *I. foveolatus* and *M. silvai*. The occurrence of *E. maculosus* is recorded from 105.73 m (Fig. 4), while the rare occurrence of *E. klaszii* is noted at 80 m (Fig. 5). The Ipubi Formation exhibits a low palynoflora, with taxa such as *C. classoides*, *A. jardinus*, *S. araripensis*, *C. avnimelechi*, and *Eucommiidites troedssonii*. The Romualdo Formation, characterized by the presence of marine palynomorphs, has a lower palynoflora. The presence of the *Subtilisphaera* genus is associated with *C. classoides*, *A. australis*, *A. jardinus*, and *C. brevilaesuratus*.

4.1.2. late Aptian Jatobá Basin

In the wells of the Jatobá Basin, a total of 16,516 palynomorphs were counted, including 11,417 pollen grains, 1,803 spores, 771 others (including fungi, scolecodonts, and spheromorphs), 2,451 dinoflagellate cysts, and 74 foraminiferal test linings (Supplementary Material x?). A total of 128 taxa were identified, with abundance recorded in the Romualdo and Crato formations.

In the lower interval (55-70 m) of the Marizal Formation (Fig. 7), palynomorph abundance is low. From the base of the core, an assemblage consisting of *C. classoides*, *A. australis*, *B. regaliae, G. jansonii*, *S. densiornatus, E. maculosus*, *G. retangularis*, *S. tenuiverrucata*, *T. reticulatus*, *C. dampieri*, *D. australis*, *Crybelosporites pannuceus*, *C. avnimelechi*, *C. brevilaesuratus*, *C. microstriatus, M. silvai* and *I. foveolatus* is recorded. The Crato Formation presents an abundance of palynomorphs, with this assemblage comprising *S. variverrucata*, *C. cearensis*, *Ischyosporites pseudoreticulatus*, *C. purbeckensis*, *G. barghoornii*, *G. oreadis*, *R. amphoriformis*, *U. callosus*, *Cycadopites glottus*, *S. tenuiverrucata*. The occurrence of foraminiferal linings is recorded at a depth of 87.2 m (Fig. 6). In the interval (30-59 m), the Romualdo Formation exhibits an abundance of palynomorphs, with notable occurrences of *S. variverrucata* and dinocysts of the genus *Subtilisphaera* sp.

4.2 Facies distribution

Individual facies encountered in the core datasets (Fig. 2) are summarized in Table 2. These facies combine into common facies associations, representing different depositional environments.

Facies analysis was carried out on four cores and allowed for the interpretation of 21 facies, which were grouped into 4 facies associations: FA1 – Estuarine facies association, FA2 – Shallow marine facies association, FA3 – Lacustrine facies association, FA4 – Fluvial facies association.

Facies	Grain Size	Description	Interpretation	Facies Association
F1	Clay	claystone; low angle planar cross lamination	sediments deposited under low-energy flow conditions	FA1
F2		shale; foliated; eventually with very fine-grained sandstone lenses	settling of fine-grained sediments from suspension, low energy flow fallout	FA2
F3	Clay	shale; foliated; sometimes interbedded with siltstone	settling of fine-grained sediments from suspension plumes	FA1
F4	Silt	Calcilutite with planar cross-lamination	low energy conditions decantation of micritic mud in shallow waters and possibly high salinity. Such characteristics are compatible with occurrences in lakes from areas with an arid climate (sabkhas)	FA2
F5	Silt	massive calcilutite	formed in low-energy settings where finer particles settled out from suspension, indicating that it was deposited relatively uniformly and without significant interruption or changes in sedimentation conditions	FA2
F6	Silt	siltstone with evaporite lenses	fluctuations in lake base level during brief periods of saltwater input (Collinson and Thompson, 1982)	FA3

F7	Silt and clay	siltstone with claystone intercalation	settling of fine-grained sediments from suspension fallout	FA3
F8	Silt and fine-grained sand	siltstone; lenses of fine-grained sandstone, with fluidization	settling of sediments from suspension fallout, showing soft sediment deformation structures	FA3
F9	Silt and very fine-grained sand	siltstone with intercalations of very fine-grained sandstone, eventually with flame structure, fine-grained sandstone lenses and climbing ripples cross-laminations	migration of subaqueous ripples under lower flow regime (Miall, 1996)	FA4
F10	Clay and silt	massive siltstone and claystone	settling of fine-grained sediments from suspension fallout	FA1
F11	Clay and silt	claystone and siltstone; with climbing ripple cross-laminations	migration of subaqueous ripples under lower flow regime (Miall, 1996)	FA4
F12	Clay and silt	laminated claystone and siltstone; showing carbonate concretions and plant fragments	sediments deposited under low-energy flow conditions	FA3
F13		massive evaporite	precipitation of gypsum in shallow waters under conditions of extreme aridity. (Collinson and Thompson, 1982)	FA2
F14		microbialite	lithified microbial mats that generated in shallow restricted settings, probably intertidal to supratidal settings	FA2
F15	fine-grained sand	sandstone with lenses of claystone		FA3
F16	fine-grained sand and clay	sandstone; intercalation of claystone with climbing ripples cross-lamination	migration of 3D subaqueous ripples under lower flow regime (Miall, 1977)	FA4
F17	very fine to fine-grained sand	sandstone showing climbing ripples cross-lamination and with flame structures	traction and suspension fallout showing, soft sediment deformation structures	FA4
F18	coarse to very fine-grained sand	sandstone with planar cross lamination in the thinnest parts, eventually fluidized	Migration of subaqueous ripples (lower flow regime) (Miall, 1977; 1990)	FA4
F19	very coarse to very fine-grained sands	massive sandstone	concentrated flow deposits as a result of rapid deposition (Miall, 1996)	FA1
F20	very fine-grained sand	sandstone showing climbing ripples cross-laminations	migration of subaqueous ripples (Miall, 1977)	FA1
F21	very coarse to fine-grained sands	sandstone showing ripple cross-laminations	lower flow regime (Miall, 1996)	FA4

4.2.1. FA1 - Estuarine facies association

This facies association consists of very fine-grained sandstone with climbing ripples cross-lamination, as well as massive sandstone with particle sizes ranging from very coarse to very fine sand. Additionally, black shale is present, sometimes interbedded with siltstone, while massive claystone and siltstone are also observed. Facies F10, F19, and F20 are present in four cores, while Facies F1 occurs in core 2-AR-SR-1B-CE, and Facies F3 in core 2-JB-SN-2A-PE. Guzmán (2023) documented the occurrence of mixohaline ostracods and benthic foraminifera in the stratigraphic intervals associated with this grouping.

This facies association is interpreted as an environment influenced by tidal currents (Nichols, 2009), with fine-grained sediments settling from suspension fallout and concentrated flow deposits resulting from rapid deposition. The tidal influence is further supported by the presence of benthic foraminifera and mixohaline ostracods reported by Guzmán (2023).

4.2.2. FA2 - Shallow marine facies association

The association includes evaporites, shale with occasional very fine-grained sandstone lenses, massive and laminated calcilutite, as well as microbialite lenses. Facies F2 is present in wells 2-AR-SR-1A-CE and 2-JB-SN-2A-PE; Facies F4 in wells 2-AR-SR-1A-CE and 2-JB-SN-2B-PE; Facies F5 in wells 2-AR-SR-1A-CE, 2-JB-SN-2A-PE and 2-JB-SN-2B-PE; Facies F13 in well 2-AR-SR-1A-CE; and Facies 14 in all four cores. Guzmán (2023) reported the presence of mixohaline ostracods and benthic foraminifera in the stratigraphic intervals grouped within this association.

The interpretation of shallow marine facies, not influenced by terrigenous material, suggest that carbonate sedimentation particularly occurs in warm climates. Sediment accumulation is slow, and the calm waters favor marine life (Nichols, 2009), such as the faunal associations described by Guzmán (2023). In arid conditions, evaporite minerals such as gypsum, anhydrite, and halite precipitate (Collinson and Thompson, 1982). The key factor for evaporite formation is climate, with these environments typically found in subtropical regions characterized by high temperatures and low rainfall (Nichols, 2009). Microbial mats are generated in shallow, restricted settings, likely in intertidal to supratidal zones (Noffke, 2010).

4.2.3. FA3 - Lacustrine facies association

A predominantly siliciclastic rock association was described, consisting of siltstone with evaporite lenses and occasional claystone intercalations. Fine-grained sandstone lenses with fluidization features are present within the siltstone. Laminated claystone and siltstone, along with carbonate concretions and plant fragments, are also observed. Additionally, sandstone with claystone lenses was noted. Facies F6 and F12 are present in well 2-AR-SR-1A-CE; Facies F7 and F8 in well 2-JB-SN-2B-PE; and Facies F15 in well 2-JB-SN-2A-PE. The presence of non-marine and mixohaline ostracods in the cores was reported by Guzmán (2023).

This is interpreted as the depositional setting of clay, silt, and fine-grained sandstone from suspended sediments in shallow water bodies under low-energy flow conditions. The presence of evaporite mineral lenses supports cycles of climate change (Nichols, 2009). Ostracods described by Guzmán (2023) suggest a lacustrine environment for this stratigraphic interval.

4.2.4. FA4 - Fluvial facies association

The fluvial facies association features siliciclastic rocks, including siltstone and claystone, with intercalations of very fine to very coarse-grained sandstone, sometimes exhibiting flame structures, fine-grained sandstone lenses, and climbing ripples cross-laminations. Additionally, claystone and siltstone with climbing ripples cross-laminations are present, along with sandstone showing climbing ripples cross-lamination, flame structures and planar cross-lamination in the fine-grained sand portion. Facies F11 and F21 are present in all four cores; Facies 18 is found in well 2-AR-SR-1A-CE and in two cores from the Jatobá Basin; Facies F9 is present in core 2-AR-SR-1A-CE; Facies F16 is found in well 2-JB-SN-2B-PE; and Facies F17 is present in well 2-JB-SN-2A-PE. The records of non-marine and mixohaline ostracods were reported in the four cores (Guzmán, 2023) within the intervals assigned to the aforementioned facies.

The migration of subaqueous ripples within this lower flow regime highlights the dynamic interaction between sediment transport processes and flow conditions (Miall, 1977; 1990). These structures form through a combination of traction and suspension sorting, often accompanied by soft sediment deformation (Miall, 1977; 1996). Compared to marine environments, this setting has a lower potential for fossil preservation. The most abundant fossils are sporomorphs, which are highly resistant to degradation and can survive long periods of transport before being deposited and preserved (Nichols, 2009).

5. Discussion

5.1 Biostratigraphy

The relative ages assigned to the post-rift I sequence for the Araripe and Jatobá basin was based mainly on the stratigraphic ranges of palynomorphs compiled from the palynostratigraphy scheme of the Sergipe and Alagoas Basin proposed by Regali and Santos (1999).

The palynoflora of the boreholes is primarily characterized by a high abundance of *Classopollis*. This genus first appeared in the Late Triassic and reached its peak abundance during the Jurassic and Early Cretaceous periods (Song and Shang, 2000). A significant proportion of *Classopollis* is also widely distributed in Early to middle Aptian strata (Carvalho et al., 2017, 2019; Santos et al., 2022). Considering the dominance of gymnosperms and the high proportion of *Classopollis,* along with a small amount of the angiosperm pollen and the presence of *Sergipea variverrucata*, this study defines the age of the current boreholes section as corresponding to the Aptian stage.

The palynoflora is comparable to those reported from the Upper Aptian of Brazilian continental margin basins (e.g., Dino, 1992, 1994; Arai et al., 2001; Regali and Santos, 1999;

Heimhofer and Hochuli, 2010; Rios-Netto et al., 2012; Michels et al., 2018; Ferreira et al., 2020; Arai and Assine, 2020; Nascimento et al., 2023).

In these studies, the micropaleontological results show a good correlation between age assignments, demonstrating that the *S. variverrucata* biozone (P-270) is generally applicable to the post-rift I sequence, although some adjustments are necessary. Comparisons of deposits from the late Aptian to early Albian, along with the absence of species of biostratigraphic value, reveal challenges due to the limited core record from these ages.

The limited recovery of guide palynomorphs in the Araripe Basin hinders comparisons with the Jatobá Basin and other zonations, restricting the recognition of biozone (P-270). In contrast, a recognized late Aptian palynomorph assemblage represented by *S. variverrucata*, *B. regaliae*, *C. classoides*, *G. jansonii*, *A. australis*, *U. callosus*, *C. segmentatus*, *T. reticulatus*, *A. jardinus*, *G. retangularis*, *E. maculosus*, *C. cearensis*, *C. avnimelechi*, *M. silvai*, *C. pannuceus*, *C. microstriatus* is consistent with the Early Cretaceous assemblage reported in northeastern Brazil (Carvalho et al., 2017; 2019; Arai and Assine, 2020; Nascimento et al., 2023).

Ostracods and foraminifera indicate a lower to late Aptian age in the Araripe Basin (Melo et al., 2020; Gúzman et al., 2023). In the same basin, a late Aptian palynomorph assemblage was identified, composed of *S. variverrucata*, *C. classoides*, *A. jardinus*, *G. jansonii*, *U. callosus*, *C. segmentatus*, *B. regaliae*, *A. australis* and *Subtilisphaera* sp. This assemblage is consistent with those reported by Teixeira et al. (2017), Arai and Assine (2020) and Vallejo et al. (2023), Nascimento et al. (2023). Reference records indicate the occurrence of *S. variverrucata*, and its presence may suggest a late Aptian age.

According to Guzmán et al. (2023), the presence of *Favusella hoterivica* at the top of the Barbalha Formation in the Araripe Basin suggests a chronostratigraphic position within the lower Aptian, partially correlating with the *Leupoldina cabri* Zone. This was confirmed by Fauth et al. (2023), who, for the first time, dated the Barbalha Formation deposits based on the recovery of the planktonic foraminiferal genera *Leupoldina* and *Globigerinelloides*. These genera mark the *L. cabri* to *G. algerianus* zones, which corresponds to the early Aptian/early late Aptian interval.

Nascimento et al. (2017) reported that the Aptian–Lower Albian was identified in borehole 2-JSN-01-PE in the Jatobá Basin by the presence de *S. variverrucata*, *E. tumulus*, *C. turbatus*, *A. australis*, *C. classoides*, *G. barahoornii*, *V. pallidus*, *C. nuni*, and *S. simplex*. However, the palynological association is largely characterized by Lower Cretaceous species that are very similar to those described in chronologically related deposits by Regali et al. (1974), Lima (1978), Antonioli and Dino (2007), and Portela et al. (2014). The continued presence of *S. variverrucata* in the Romualdo and Crato formations of the Jatobá Basin indicates a late Aptian age, as defined by Regali and Santos (1999). The last occurrence of *S. variverrucata* further supports that the age is not older than late Aptian.

5.2 Paleoenvironment and Paleoclimate inferences

During the late Aptian period in northeast Brazil, the post-rift I sequence was situated within the Lower Cretaceous *Dicheiropollis etruscus/Afropollis* Province (Herngreen et al., 1996), characterized by the prevalence of gymnospermous pollen, including taxa such as *Classopollis*, *Equisetosporites*, *Araucariacites*, *Inaperturopollenites*, *Gnetaceaepollenites*, *Steevesipollenites*, and *Uesuguipollenites*. The more abundant and dispersed groups provide regional evidence of paleoclimate and paleoenvironmental conditions (Jackson, 1994; Souza-Lima and Silva, 2018).

The genus *Classopollis*, linked to the extinct family Cheirolepidiaceae, dominated certain coastal environments in the Mesozoic and was widespread in warm habitats at low paleolatitudes, especially during the Early Cretaceous (Taylor et al., 2009). The dominance of *Classopollis*, indicative of a dry and arid climate (Doyle, 1999; Carvalho et al., 2019), is documented in the deposition of the post-rift I sequence. This implies that the basins experienced a hot and dry paleoclimate characterized by xerophytic flora. Furthermore, the palynomorphy of the basins undergoes changes, with dinoflagellate cysts and foraminiferal test linings appearing suddenly and abundantly in the Jatobá Basin. It is suggested that the basins may reflect various factors related to marine conditions, ecological dynamics, and sedimentary processes during the time of deposition. Accordingly, we combined the palynological and sedimentological datasets to reconstruct paleoclimate changes.

During the deposition of the Barbalha and Marizal formations, the palynoflora consists of plants from the Cheirolepidiaceae and Araucariaceae families, in addition to fern spores, which indicate a hot and wet climate (Santos et al., 2022). According to Cardoso et al. (2023), climatic oscillations were identified during this age, as evidenced by bioclimatic groups associated with humid conditions: hydrophytes, hygrophytes, tropical lowland flora, and upland flora. A relationship between these groups has been suggested (e.g., Carvalho et al., 2017, 2019, 2022).

According to Hashimoto et al. (1987), Assine (2007), and Lima (2018), the Barbalha and Marizal formations are correlated. The Barbalha Formation recovered in the core (Fig. 4) represents depositional sequence 2, as described by Fauth et al. (2023). It represents partially enclosed coastal bodies of water where freshwater from rivers and streams mixes with saltwater from the ocean, corresponding to a confined estuarine deposit within a flooded valley (Guzmán et al., 2023). Varejão et al. (2021a) state that the upper sequence of the Barbalha Formation delineates a transition from a fluvial to a bayhead delta setting, spanning from the lowstand system tract to the transgressive surface. Bayhead deltas typically form in the innermost regions of bays and estuaries along transgressive coastlines (Aschoff et al., 2018).

During the deposition of the Crato Formation, the palynoflora was dominated by an abundance of *Classopollis*. Additionally, taxa such as *Araucariacites*, *Inaperturopollenites*, *Equisetosporites*, and fern spores were present. There was an increase in palynological richness, which is associated with carbonate-rich sediments (e.g., claystone, siltstone, sandstone, limestone) deposited along coastlines spanning a broad latitudinal range. The presence of foraminiferal test linings at 126.5 m (Fig. 4) and 87.41 m (Fig. 6) in the lower part was also noted, associated with the intercalation of siliciclastic and carbonate sedimentation. An intermediate humid paleoenvironment was identified between the two semi-arid paleoenvironmental phases.

The presence of foraminiferal test linings exclusively represents marine benthic paleoenvironments and indicates marine ingression (Decommer, 1982; Tyson, 1995; Goldberg et al., 2019). Their low abundance could be related to proximal marine environments closer to continental sources (Rosner et al., 2011). According to Guzmán et al. (2023), the deposition of the Crato Formation in the Araripe Basin recorded hedbergellid foraminifera, corroborating a marine influence during its formation.

Its high abundance of *Classopollis*, along with intercalated siliciclastic deposits, indicates the development of xerophytic vegetation under arid to semi-arid conditions (Doyle et al., 1982; Carvalho et al., 2017; Souza-Lima and Silva, 2018). It is widely agreed that hot and semi-arid to arid climates predominated in the low-latitude regions during the late Aptian, typically inferred from the prevalent occurrence of *Classopollis* (Doyle et al., 1982; Carvalho et al., 2017; 2019; Arai and Assine, 2020; Santos et al., 2022).

The consistent presence of these microfossils is interpreted as indicative of marine sedimentary environments, with the highest occurrences reported in coastal to shallow shelf settings (Lister and Batten, 1988; Stancliffe, 1989).

The gradual increase in humidity observed in the Crato Formation, according to Kujau et al. (2013) may represent an increase in the intensity of precipitation and/or an extension of the annual humid period (Kujau et al., 2013). These sedimentary characteristics and paleoenvironmental conditions have been reported by Neumann et al. (2003) and Heimhofer et al. (2010). Their interpretation suggests deposition in an estuarine-lacustrine system.

The remarkable similarity observed between the microbialite (Facies 22) spread among siliciclastic rocks and the laminated limestone in the wells exhibits similar characteristics of deposition in both shallow marine settings and hypersaline lakes. This kind of sedimentation occurs in anoxic conditions of the benthonic zone of the sub-marginal area of a closed to semi-closed paleolake (Silveira et al., 2023). Gratzer et al. (2013) also documented the presence of microbialite in the Crato Formation on the Jatobá Basin. Furthermore, Aptian microbialite occurrences on the northeastern basins, such as those of the Codó Formation in the Parnaíba Basin, are reported (Bahniuk et al., 2015).

The presence of marine fossils within the uppermost organic shales of the Crato Formation, just below the evaporites of the Ipubi Formation, further supports evidence of a marine connection (Goldberg et al., 2019).

The Facies F1, F3, F8, F13, F17, F19, F20, F21 (Fig. 2), on the Ipubi Formation, especially the F19 with the massive evaporites, associated to the gypsum precipitation, indicates precipitation in shallow waters under conditions of extreme aridity (Collinson and Thompson, 1982), along with the distribution and abundance of *Classopollis,* in this formation, express a deposition near the coastline under dry climatic conditions (Carvalho et al., 2017, 2019, 2022).

The presence in strata of the Ipubi Formation also confirms, in addition to climatic conditions of aridity, the presence of a body of saline water, since they are often found in saline environments (Alvin, 1982; Carvalho et al., 2017, 2019, 2022).

According to Guzmán et al. (2023), the marine conditions became better established, with the more abundant and diverse presence of foraminifera, suggesting that the Araripe Basin reached a more open circulation with the ocean.

Sedimentological characteristics such as limestone, with siliciclastic intercalations immediately adjacent to the Ipubi Formation evaporites, corroborate the already established marine connection in the close coastal plain (sabkha). This observation aligns with the likely depositional setting, where the evaporitic layer indicates a period when the paleolake water became more saline due to heightened evaporation (Silva, 1988).

During the deposition of the Romualdo Formation, the palynomorphs is diversified is represented by an increase in marine content, her high content in the Jatobá Basin. The abundance and distribution of *Classopollis* along the Romualdo Formation, associated with the presence of *Subtilisphaera*, suggest a semi-closed, marine-influenced body of water, followed by a marine transgression in the Romualdo Formation, the presence of *Classopollis* in marine deposits is indicative of proximity to coastal environments, commonly associated with shallow marine to lagoonal depositional settings, and often with evaporites (Vakhrameev, 1970; Doyle et al., 1982; Michels, et al., 2018; Arai and Assine, 2020).

According to Arai and Assine (2020) the presence of marine palynomorphs (dinoflagellate cysts and foraminiferal linings) together with *Classopollis* indicates marine conditions for the Romualdo Formation.

In our material, these association occurs in the interval between 11 and 28 meters (Fig. 4), suggesting shallow marine conditions.

The Facies F1, F2, F3, F4, F5, F6, F10, F13, F14, F17, F20 presented in this paper, suggest the transition from a fluvial to an estuarine system (Miall, 1977; 1990; 1996), reinforced by *Subtilisphaera* occurrence. This genus occurred in the epicontinental seas of the Cretaceous period and is an opportunistic organism with a high tolerance for variations in salinity (Jain and

Millepied, 1975; Arai, 2000, 2014; Carvalho et al., 2016). Characterized by a deposition of mixed siliciclastic and limestone for the Araripe Basin records a high diversity and abundance of foraminifera species, both benthic and planktonic (Guzmán et al., 2023). The accumulation of these foraminiferal suggest poorly oxygenated conditions in a middle neritic-upper bathyal environment (Kaminski and Kuhnt, 1995; Kaminski et al., 1995; Gradstein et al., 2019).

6. Conclusions

The palynological and sedimentological analyses of the Araripe and Jatobá basins led to the following conclusions:

The late Aptian, of the biozone (P-270), is observed with the last occurrence of *Sergipea variverrucata* a key palynomorph to identify the upper Aptian in the Brazilian basins. Its presence in the Crato, and Romualdo formations clearly a late Aptian stage (local Alagoas stage). The presence of *Sergipea variverrucata* biozone (P-270) in the post-rift I sequence of the Santana Group, integrated with planktic foraminifera, suggests that it was deposited during the Early Aptian to late Aptian in the Jatoba and Araripe basins.

According to our facies and palynological data, the Santana Group was deposited in fluvio-deltaic, lagoonal, and shallow marine (estuarine) environments within the Araripe and Jatobá Basins. The Barbalha Formation, formed during a humid climate, represents a fluvio-deltaic system, whereas the Marizal Formation predominantly exhibits fluvial characteristics indicative of arid conditions. During a wet-dry climate cycle, the Crato and Ipubi Formations are interpreted as parts of a lagoonal system, with the Crato Formation indicating an open lagoon influenced sporadically by marine conditions and the Ipubi Formation representing a semi-closed to closed lagoon under drier conditions. The Romualdo Formation is interpreted as a marine environment; however, differences exist between the two basins. In the Araripe Basin, it is assigned to shallow marine environment, whereas in the Jatobá Basin, it is characterized as a well-developed marine paleoenvironment.

References

Alvin, K.L. 1982. Cheirolepidiaceae: biology, structure and paleoecology. Review of Palaeobotany and Palynology. Vol, 37, pp. 71-98.

Arai, M. 2005. Histórico da palinoestratigrafia marinha no Brasil com ênfase em dinoflagelados Cretáceos: Arquivos do Museu Nacional, Rio de Janeiro, v. 63, pp. 371–384.

Arai, M. 2009. Paleogeografia do Atlântico Sul no Aptiano: um novo modelo a partir de dados micropaleontológicos recentes. Bol. Geociencias da Petrobr. 17, 331–351.

Arai, M. 2014. Aptian/Albian (Early Cretaceous) paleogeography of the South Atlantic: A paleontological perspective. Brazilian Journal of Geology, 44(2), pp. 339-350. https://doi.org/10.5327/Z2317-4889201400020012

Arai, M., Assine, M.L. 2020. Chronostratigraphic constraints and paleoenvironmental interpretation of the Romualdo Member (Santana Formation, Araripe Basin, Northeastern Brazil) based on palynology. Cretaceous Research Vol. 116, 104610. https://doi.org/10.1016/j.cretres.2020.104610

Arai, M., Botelho Neto, J., Lana, C.C., Pedrão, E. 2000. Cretaceous dinoflagellate provincialism in Brazilian marginal basins. Cretaceous Research 21, pp. 351-366. https://doi.org/10.1006/cres.2000.0211

Arai, M., Coimbra, J.C., Silva-Telles, A.C. 2001. Síntese bioestratigráfica da Bacia do Araripe (Nordeste do Brasil). *In:* Simpósio sobre a bacia do araripe e bacias interiores do nordeste, 1-2. Comunicações, Crato, SBP/URCA/DNPM, p. 109–117, pp. 122–124.

Arai, M., Cunha Lana, C., Pedrão, E. 1994. Ecozona *Subtilisphaera* spp.: Registro eocretáceo de um importante episódio ecológico do Oceano Atlântico primitivo: Acta Geológica Leopoldensia, Vol. 17, no. 39/2, pp. 521–538.

Araripe, R.C., Oliveira, D.H., Tomé, M.E., Moura de Mello, R., Barreto, A.M.F. 2021. Foraminifera and ostracoda from the lower cretaceous (Aptian–lower Albian) Romualdo Formation, Araripe basin, northeast Brazil: Paleoenvironmental inferences. Cretaceous Research Vol. 122, 104766. https://doi.org/10.1016/j.cretres.2021.104766.

Araripe, R.C., Pedrosa Lemos, F.A., do Prado, L.A.C., Tomé, M.E., Oliveira, D.H.D., Pereira, P.A., Nascimento, L.R.S., Asakura, Y., Ng, C., Viviers, M.C., Barreto, A.M.F. 2022. Upper Aptian–lower Albian of the southern-central Araripe Basin, Brazil: Microbiostratigraphic and paleoecological inferences. Journal of South American Earth Sciences. Vol. 116, 103814. https://doi.org/10.1016/j.jsames.2022.103814

Aschoff, J.L., Olariu, C., Steel, R.J. 2018. Recognition and significance of bayhead delta deposits in the rock record: A comparison of modern and ancient systems. Sedimentology 65, pp. 62–95. https://doi.org/10.1111/sed.12351

Assine, M.L. 2007. Bacia do Araripe. Bol. Geociencias Petrobras 15, pp. 371-389.

Assine, M.L., Perinotto, J.A.J., Custodio, M.A., Neumann, V.H., Varejão, F.G., Mescolotti, P.C. 2014. Sequências Deposicionais do Andar Alagoas da Bacia do Araripe, Nordeste do Brasil. Boletim de Geociências da Petrobras 22, pp. 3-28.

Azevedo, I.H.R., Lacerda, L.D., Saraiva, A.Á.F., Sial, N.A., Benigno, A.P.A., Aguial, J.E., 2024. Aptian-Albian paleoenvironmental geochemistry: Araripe Basin, Northeastern Brazil. Journal of South American Earth Sciences. Vol. 137, 104856 https://doi.org/10.1016/j.jsames.2024.104856

Bahniuk, A.M., Anjos, S., França, A.B., Matsuda, N., Eiler, J., Mckenzie, J.A., Vasconcelos, C. 2015. Development of microbial carbonates in the Lower Cretaceous Codó Formation (north-east Brazil): implications for interpretation of microbialite facies associations and palaeoenvironmental conditions. Sedimentology. Vol. 62, pp. 155–181. https://doi.org/10.1111/sed.12144

Barreto, A.M.F., Bertotti, A.L., Sylvester, P.J., Prado, L.A.C., Araripe, R.C., Oliveira, D.H., Tom´e, M.E.T.R., Lemos, F.A.P., Nascimento, L.R.L., Pereira, P.A., Albayrak, A.I. 2022. U/Pb geochronology of fossil fish dentine from Romualdo Formation, Araripe Basin, northeast of Brazil. Journal of South American Earth Sciences. Vol. 116, 103774. https://doi.org/10.1016/j.jsames.2022.103774

Beurlen, G., Regali, M.S.P. 1987. O Cretáceo da Plataforma continental do Maranhão e Pará, Brasil: bioestratigrafia e evolução paleoambiental. Bol. Geociencias Petrobras. Vol. 1, pp. 135-155.

Bom M.H.H., Kochhann K.G.D., Heimhofer U., Mota M.A.L., Guerra R.M.G., Simões M.G., Krahl G., Meirelles V., Ceolin D., Fürsich F.T., Lima F.H.O., Fauth G., Assine M.L. 2023. Fossil-bearing concretions of the Araripe Basin accumulated during Oceanic Anoxic Event 1b. Paleoceanography and paleoclimatology, Vol. 38, 11 e2023PA004736. https://doi.org/10.1029/2023PA004736

Bruhn, C. H. 1999. Reservoir architecture of deep-lacustrine sandstones from the Early Cretaceous Recôncavo rift basin, Brazil. AAPG bulletin, 83(9), pp. 1502- 1525. http://dx.doi.org/10.1306/E4FD41F7-1732-11D7-8645000102C1865D

Cardoso da Silva Giannerini, M., de Araujo Carvalho, M., Cunha Lana, C., Santiago, G., de Paula Sá, N., and da Cunha Correia, G. 2023. Late Aptian paleoclimate reconstruction of the Brazilian equatorial margin: inferences from palynology, Clim. Past, 19, 1715–1742, https://doi.org/10.5194/cp-19-1715-2023.

Carvalho, M.A., 2004. Palynological assemblage from Aptian/Albian of the Sergipe Basin: Paleoenvironmental reconstruction. Revista Brasileira de Paleontologia. Vol. 7, 159–168. http://dx.doi.org/10.4072/rbp.2004.2.08

Carvalho, M.A., Mendonça Filho, J.G., Menezes, T.R. 2006. Palynofacies and sequence stratigraphy of the Aptian–Albian of the Sergipe Basin, Brazil. Sedimentary Geology 192, pp. 57-74. https://doi.org/10.1016/j.sedgeo.2006.03.017

Carvalho, R.R., Neumann, V.H., Fambrini, G.L., Vieira, M.M., Rocha, D.A. 2010. Origem e proveniência das sequências siliciclásticas inferior da Bacia de Jatobá. Estudos Geológicos, Vol. 20(2), pp. 113-127.

Carvalho, M.A., Lana, CC., Bengtson, P., Sá, N.D. 2017. Late Aptian (Cretaceous) climate changes in northeastern Brazil: a reconstruction based on indicator species analysis (IndVal). Palaeogeography, Palaeoclimatology, Palaeoecology, Vol. 485, pp. 543-560. https://doi.org/10.1016/j.palaeo.2017.07.011

Carvalho, M.A., Bengtson, P., Lana, C.C., Sá, N.D.., Santiago, G., Giannerini, M.C. 2019. Late Aptian (Early Cretaceous) dry-wet cycles and their effects on vegetation in the South Atlantic: Palynological evidence. Cretaceous Research 100, pp. 172-183. https://doi.org/10.1016/j.cretres.2019.03.021

Coimbra, J.C., Arai, M., Carreño, A.L. 2002. Biostratigraphy of Lower Cretaceous microfossils from the Araripe Basin, northeastern Brazil. Geobios Vol. 35(6), 687-698. https://doi.org/10.1016/S0016-6995(02)00082-7.

Coimbra, J.C., Freire, T.M. 2021. Age of the post-rift Sequence I from the Araripe Basin, Lower Cretaceous, NE Brazil: implications for spatio-temporal correlation. Revista Brasileira de Paleontologia. Vol. 24 (1), pp. 37–46. https://doi.org/10.4072/rbp.2021.1.03

Collinson, J.D, Thompson, D.B. 1982. Sedimentary Structures. Allen and Unwin, London, 194 pp.

Costa, I.P., Milhomem, P.S., Carvalho, M.S.S. 2003. Bacias sedimentares brasileiras: Bacia de Jatobá. Aracaju: Fundação Paleontológica Phoenix (Série Bacias Sedimentares, n. 53).

Costa, I.P., Bueno, G.V., Milhomem, P.S., Silva, H.S.R.L., Kosin, M.D. 2007. Sub-bacias de Tucano Norte e Bacia de Jatobá. Boletim de Geociências da Petrobras 15, pp. 445-453.

Custódio, M.A., Quaglio, F., Warren, L.V., Simões, M.G., Fürsich, F.T., Perinotto, J.A.J., Assine, M.L. 2017. The transgressive-regressive cycle of the Romualdo Formation (Araripe Basin): Sedimentary archive of the Early Cretaceous marine ingression in the interior of Northeast Brazil. Sediment. Geol. 359, pp. 1–15. https://doi.org/10.1016/j.sedgeo.2017.07.010.

Decommer, H. 1982. Etude palynoplanctologique et cadre sédimentologique du Jurassique et du Crétacé du nord de la France Ann. Soc. Geol. Nord, 101 (1982), pp. 161-176

Dino, R. 1992. Palinologia, bioestratigrafia e paleoecologia da formação Alagamar, Cretáceo da Bacia Potiguar, Nordeste do Brasil. Instituto de Geociências, Universidade de São Paulo, São Paulo, Tese, pp.300

Dino, R. 1994. Some new pollen grain species from Lower Cretaceous in northeastern Brazil. Boletim de Geociências da Petrobras. Vol. 8(2), 257-273. https://www.researchgate.net/publication/293103813.

Doyle, J.A. 1999. The rise of angiosperms as seen in the African Cretaceous pollen record. In: Heine, K. (Ed.), Palaeoecology of Africa and the Surrounding Islands. Proceedings of the Third Conference on African Palynology; Johannesburg, pp. 14–19 September 1997. https://www.researchgate.net/publication/291799474

Doyle, J.A., Jardiné, S., Doerenkamp, A. 1982. *Afropollis*, a new genus of early angiosperm pollen, with notes on the Cretaceous palynostratigraphy and paleoenvironments of Northern Gondwana. Bull. Centre Res. Expl. Prod. Elf-Aquitaine 6, pp. 39–117.

Fambrini, G.L., Silvestre, D.C., Barret, A.M., Silva-Filho, W.F. 2020. Estratigrafia da Bacia do Araripe: estado da arte, revisão crítica e resultados novos. Geologia USP. Série Científica, 20(4), pp. 169-212. https://doi.org/10.11606/issn.2316-9095.v20-163467

Fauth, G., Kern, H.P., Villegas - Martín, J., De Lira Mota, M.A., Dos Santos Filho, M.A.B., Santa Catharina, A., Leandro, L.M., Luft-Souza, F., Strohschoen, O., Nauter-Alves, A., Tungo, E.J.F., Bruno, M.D.R., Ceolin, D., Baecker-Fauth, S., Bom, M.H.H., Lima, F.H.O., Santos, A., Assine. M.L. 2023. Early Aptian marine incursions in the interior of northeastern Brazil following the Gondwana breakup. Scientific reports 13:6728 https://doi.org/10.1038/s41598-023-32967-w

Ferreira, N.N., Ferreira, E.P., Ramos, R.R.C., Carvalho, I.S. 2016. Palynological and sedimentary analysis of the Igarapé Ipiranga and Querru 1 outcrops of the Itapecuru formation (lower cretaceous, Parnaíba Basin), Brazil. Journal of South American Earth Sciences, Vol. 66, pp. 15–31. https://doi.org/10.1016/j.jsames.2015.12.005.

Ferreira, N.N., Ferreira, E.P., Ramos, R.R., Carvalho, I.S. 2020. Terrestrial and marine palynomorphs from deposits of the pull-apart rift of West Gondwana (Parnaíba Basin, northern Brazil): Biostratigraphy and relation to tectonic events. Journal of South American Earth Sciences, Vol. 101, 102612. https://doi.org/10.1016/j.jsames.2020.102612

Goldberg, K., Preamor, E., Bardola, T., Souza, P.A. 2019. Aptian marine ingression in the Araripe Basin: implications for paleogeographic reconstruction and evaporite accumulation. Marine and Petroleum Geology, Vol. 107, pp. 214-221. https://doi.org/10.1016/j.marpetgeo.2019.05.011

Gomes, J.M., Rios-Netto, A.M., Borghi, L., Carvalho, I., Mendoça Filho, J.G., Sabaraense, L.D., Araújo, B. 2021. Cyclostratigraphic analysis of the early Cretaceous laminated limestones of the Araripe Basin, NE Brazil: Estimating sedimentary depositional rates. Journal of South American Earth Sciences, Vol. 112, 103563. https://doi.org/10.1016/j.jsames.2021.103563

Gradstein, F.M., Waskowska, A., Kopaevich, L., Watkins, D.K., Friis, H., Pérez Panera, J. 2019. Berriasian planktonic foraminifera and calcareous nannofossils from Crimea Mountains, with reference to microfossil evolution. Swiss Journal of Palaeontology. 138, 213–236. https://doi.org/10.1007/s13358-018-0175-8

Gratzer, R., Neumann, V.H., Vortisch, W., Rocha, D.E.A., Betchel, A. 2013 Stable isotopes of organics and inorganics, clay mineralogy and chemical environment of an Aptian lacustrine succession in northeastern Brazil, In Bojar, A.-V., Melinte-Dobrinescu, M.C., and Smit, J., eds., Isotopic Studies in Cretaceous Research: Geological Society of London, Special Publication 382, pp. 157–182. https://doi.org/10.1144/SP382.4

Guerra-Sommer, M., Degani-Schmidt, I., Mendonça, J.O., Mendonça Filho, J.G., Lopes., F.D.S., Salgado-Campos, V.M.J., Araújo, B., Carvalho, I.S. 2021. Multidisciplinary approach as a key for paleoenvironmental interpretation in a Weichselia-dominant interval from the late Aptian Codó Formation (Parnaíba Basin, Brazil). Journal of South American Earth Sciences 111 103490. https://doi.org/10.1016/j.jsames.2021.103490.

Guerrini, V.B., Matos, S.A., Fürsich, F.T., Rodrigues, M.G., Varejão, F.G., Warren, L.V., Assine, M.A., Simões, M.G. 2024. Early Cretaceous Bivalves of The Romualdo Formation, Araripe

Basin, Northeastern Brazil. Cretaceous Research, 105910. https://doi.org/10.1016/j.cretres.2024.105910

Guzmán, J., Piovesan, E.K., Melo, R.M., Almeida-Lima, D., De Jesus e Sousa, A., Neumann, V.H. 2023. Ostracoda and Foraminifera biostratigraphy and palaeoenvironmental evolution of the Aptian Santana Group, post-rift of the Araripe Basin, Brazil. Gondwana Research. Vol. 124, 18-38. https://doi.org/10.1016/j.gr.2023.06.014

Hashimoto, AT., Appi, C.J., Soldan, A.L., Cerqueira, J.R. 1987. O Neo-alagoas nas bacias do Ceará, Araripe e Potiguar (Brasil): caracterização estratigráfica e paleoambiental. Revista Brasileira de Geociências. Vol. 17, 118-122.

Hay, W.W., Floegel, S., 2012. New thoughts about the Cretaceous climate and oceans. Earth-Science Reviews. Vol. 115, 262–272. https://doi.org/10.1016/j.earscirev.2012.09.008

Heimhofer, U., Hochuli, P. 2010. Early Cretaceous angiosperm pollen from a low-latitude succession (Araripe Basin, NE Brazil). Review of Palaeobotany and Palynology. Vol. 161, 105–126. https://doi.org/10.1016/j.revpalbo.2010.03.010.

Herngreen, G.F, Kedves, M., Kedves, Rovnina, L.V., Smirnova, S.B. 1996. Cretaceous microfloral provinces: a review. In: Jansonius, J., McGregor, D.C. (Eds.), Palynology: Principles and Applications. American Association of Stratigraphic Palynologic, Texas, USA, pp. 1157-1188.

Jackson, S.T. 1994. Pollen and spores in quaternary lake sediments as sensors of vegetation composition: theoretical models and empirical evidence. In: Traverse, A. (Ed.) Sedimentation of Organic Particles. Cambridge University Press, Cambridge, pp. 253–286.

Jain, K.P., Millepied, P. 1975. Cretaceous microplankton from Senegal basin, West Africa. Part II. Systematics and biostratigraphy. Geophytology 5, pp.126–171.

Kaminski, M.A, Kuhnt, W. 1995. Tubular agglutinated foraminifera as indicators of organic carbon flux, in: Kaminski, M.A, Geroch, S., Gasif ski, M. (Eds.), Proceedings of the Fourth International Workshop on Agglutinated Foraminifera 1993. Grzybowski Foundation Special Publication no. 3, Kraków Poland, pp. 141–144.

Kaminski, M.A., Boersma, A., Tyszka, J., Holbourn, A.E.L. 1995. Response of deepwater agglutinated foraminifera to dysoxic conditions in the California Borderland basins, in: Kaminski, M.A., Geroch, S., Gasif ski, M.A. (Eds.), Proceedings 4th International Workshop on Agglutinated Foraminifera, Krakow, 1993. pp. 131–140

Kujau, A., Heimhofer, U., Hochuli, P.A., Pauly, S., Morales, C., Adatte, T., Föllmi, K., Ploch, I., Mutterlose, J. 2013. Reconstructing Valanginian (Early Cretaceous) mid-latitude vegetation and climate dynamics based on spore–pollen assemblages. Review of Palaeobotany and Palynology. 197, pp. 50–69. https://doi.org/10.1016/j.revpalbo.2013.05.003

Lemos, F.A.P., Asakura, Y., Antunes, R.L., Araripe, R.V.C., Prado, L.A.C., Tomé, M.E., Oliveira, D.H., Nascimento, L.R.S., Ng, C., Barreto, A.M.F. 2023. Calcareous nannofossils, biostratigraphy, and paleobiogeography of the Aptian/Albian Romualdo Formation in the Araripe Basin, North-Eastern Brazil. Brazilian Journal of Geology. Vol. 53 (2). https://doi.org/10.1590/2317-4889202320220054

Lima, M.R. 1978. Palinologia da Formação Santana (Cretáceo do Nordeste do Brasil). Instituto de Geociências, Universidade de São Paulo, São Paulo, Tese, pp. 335-392

Lima, Rafael Pereira. 2018. Sequências lacustres pós-rifte na Serra Negra (Bacia de Jatobá) e Serra do Tonã (Sub-bacia de Tucano Norte): correlações estratigráficas regionais e estruturais. Tese, Universidade Federal de Pernambuco Centro de Tecnologia e Geociências Programa de Pós-Graduação em Geociências, Recife, PE. Brasil.

Lister, J.k., D.J. Batten. 1988. Stratigraphic and palaeoenvironmental distribution of Early Cretaceous dinoflagellate cysts in the Hurlands Farm Borehole, West Sussex, England. Palaeontographica B, 210 (1988), pp. 9-89

Lúcio, T., Souza Neto, J. A., Selby, D. 2020. Late Barremian / Early Aptian Re–Os age of the Ipubi Formation black shales: Stratigraphic and paleoenvironmental implications for Araripe Basin, northeastern Brazil. Journal of South American Earth Sciences. Vol 102, 102699. https://doi.org/10.1016/j.jsames.2020.102699

Magnavita, L.P., Szatmari, P., Cupertino, J.A., Destro, N., Roberts, D.G. 2012. The Recôncavo Basin. In: David, G., Roberts, D. G., Bally, A. W. (eds.), Regional Geology and Tectonics: Phanerozoic Rift Systems and Sedimentary Basins. Amsterdam: Elsevier Science. pp. 383-420.

Melo, R.M., Guzmán, J., Almeida-Lima, D., Piovesan, E.K., Neumann, V.H. de M.L., Sousa, A.J. 2020. New marine data and age accuracy of the Romualdo Formation, Araripe Basin, Brazil. Scientific Reports 10, pp. 1–15. https://doi.org/10.1038/s41598-020-72789-8.

Miall, A.D. 1977. A review of the braided-rivers depositional environment. Earth Science Review, 13(1), pp. 1-63. https://doi.org/10.1016/0012-8252(77)90055-1

Miall, A.D. 1990. Principles of Sedimentary Basin Analysis, 2nd ed. xv + 668 pp. Berlin, Heidelberg, New York, London, Paris, Tokyo, Hong Kong, Barcelona: Springer-Verlag. Price DM 128.00 (hard covers). ISBN 3 540 97119 X.

Miall, A.D., 1996. The Geology of Fluvial Deposits: Sedimentary Facies, Basin Analysis and Petroleum Geology. Springer-Verlag, New York, 582 pp.

Michels, F.H., Souza, P.A., Premaor, E. 2018. Aptian-Albian palynologic assemblages interbedded within salt deposits in the Espírito Santo Basin, eastern Brazil: Biostratigraphical and paleoenvironmental analysis. Marine and Petroleum Geology, Vol. 91, pp. 785-799. https://doi.org/10.1016/j.marpetgeo.2018.01.023

Nascimento, L.R.S., Tomé, M.E., Barreto, A.M.F., Oliveira, D.H., Neumann, V.H. 2017. Diagnóstico palinoflorístico do poço 2-JNS-01PE, Cretáceo Inferior, Bacia do Jatobá, nordeste do Brasil. Estudos Geológicos. Vol 27, pp. 118–134. https://doi.org/10.18190/1980-8208/estudosgeologicos.v27n1p118-134

Nascimento, L.R.S.L., Arai, M., Lacerda, J.N.L., Tomé, M.E., Araripe, R., Barreto, A.M.F, de Oliveira, D.H., Lemos., F.P., Prado, L.A.C., Ng, C. 2023. Integrated study of the microfossils of the upper Aptian (Lower Cretaceous) of the Sobradinho and Serra do Mãozinha sections (Araripe Basin, northeastern Brazil): Biostratigraphic and paleoenvironmental inferences. Journal of South American Earth Sciences. Vol. 132, 104644.https://doi.org/10.1016/j.jsames.2023.104644

Neumann, V.H., Cabrera, L. 1999. Una nueva propuesta estratigráfica para la tectonosecuencia post-rifte de la Cuenca de Araripe, Noreste de Brasil. In: Boletim do 5º Simpósio sobre o Cretáceo do Brasil, pp. 279-285.

Neumann, V.H., Borrego, A.G., Cabrera, L., Dino, R. 2003. Organic matter composition and distribution through the Aptian-Albian lacustrine sequences of the Araripe Basin, northeastern Brazil. International Journal of Coal Geology. Vol. 54, pp. 21-40. https://doi.org/10.1016/S0166-5162(03)00018-1

Neumann, V.H., Rocha, D.E.G.A., Moraes, A.S., Sial, A.N., Taboada Castro, M.T., Barbosa, J.A., Fambrini, G.L., Carvalho, R.R. 2010. Microfacies carbonaticas e comportamento isotópico de C e O nos calcários laminados aptianos lacustres da Serra Negra, bacia do Jatobá, nordeste do Brasil. Estudos Geológicos. Vol. 20, n. 1, p. 89-100.

Neumann, V.H., Rocha, D.E.G.A. 2014. Stratigraphy of the Post-Rift Sequences of the Jatobá Basin, Northeastern Brazil. In: STRATI 2013 (Eds R. Rocha, J. Pais, J.C. Kullberg, and S. Finney), Springer International Publishing, pp. 553–557.

Neumann, V.H., Assine, M.L. 2015. Stratigraphic proposal to the post-rift I tectonicsedimentary sequence of Araripe Basin, Northeastern Brazil, Strati 2015. In: 2nd International Congress on Stratigraphy. Berichte des Institutes für Erdwissenschaften der Universitat Graz, 274 pp.

Ponte, F.C., Asmus, H.E. 1978. Geological framework of the Brazilian continental margin. Geol. Rundsch. 67, pp. 201–235.

Ponte, F.C., Ponte Filho, F.C. 1996. Evolução Tectônica e Classificação da Bacia do Araripe. Report of the Departamento Nacional de Produção Mineral: Recife, Brasil, 68 pp.

Portela, H.A., Antonioli L., Dino, R., Garcia, M.J. 2014. Caracterização palinoflorística e paleoambiental da Formação Santana (Cretáceo Inferior), poço 4-BO-1-PE, Bacia do Araripe, Nordeste do Brasil. Revista Brasileira de Paleontologia, 17,363-372. http://dx.doi.org/10.4072/rbp.2014.3.07

Regali, M.S.P., Uesugui, N., Santos, A.S. 1974a. Palinologia dos sedimentos Meso-cenozoicos do Brasil (I). Bol. Tec. Petrobras 17, pp. 177–191.

Regali, M.S.P., Uesugui, N., Santos, A.S., 1974b. Palinologia dos sedimentos Meso-cenozoicos do Brasil (II). Bol. Tec. Petrobras 17, 263–301.

Regali, M.S.P., Uesugui, N., Lima, E.C. 1985. Palinoestratigrafia e paleoambiente da Bacia de Barreirinhas - Maranhão - Brasil. Departamento Nacional de Produção Nacional, Série Geológica n.27. Seção Paleontologia e Estratigrafia 2, pp. 461–470.

Regali, M.S.P. 1987a. Palinomorfos do Barremiano/Albiano brasileiros. Parte II. In: 10th Congresso Brasileiro de Paleontologia, Rio de Janeiro, Anais, Vol. 2. pp. 647–655.

Regali, M.P.S. 1989. *Complicatisaccus cearensis*: uma palinozona do Eocretáceo do Brasil. In: 11st Congresso Brasileiro de Paleontologia, Curitiba, Anais, vol. 1. pp. 235–274.

Regali, M.S.P., Santos, P.R.S. 1999. Palinoestratigrafia e geocronologia dos sedimentos albo-aptianos das bacias de Sergipe e Alagoas – Brasil. In: 5th Simpósio sobre o Cretáceo do Brasil, Serra Negra, Boletim de resumos, pp. 411–419.

Rios-Neto, A.M., Regali, M.S.P., Carvalho, I.S., Freitas, F.I. 2012. Palinoestratigrafia do intervalo Alagoas da Bacia do Araripe, Nordeste do Brasil. Revista Brasileira de Geociências, v.42, n.2, pp. 331-342.

Rocha, D.E.G.A., Leite, J. F. 1999. Estudo hidrogeológico da Bacia do Jatobá – PE. Geologia. Série Hidrogeologia – Estudos e Projetos. Vol. 2: 20pp.

Rocha, D.E.G.A. 2011. Caracterização do intervalo carbonático do sistema lacustre Aptiano da Bacia do Jatobá, NE do Brasil. Recife, Universidade Federal de Pernambuco, Centro de Tecnologia e Geociências. Tese de Doutorado, 145 pp.

Rosner, E. H., Lana, C.C., Le Hérissé & José, A., Melo, H.G. 2011. Bacia do Rio do Peixe (Pb): Novos resultados biocronoestratigráficos e paleoambientais. Paleontologia: Cenários de Vida.

Santos, C.A., Neumann, V.H., Menezes, M.R., Rocha, D.A., Agostinho, S.M. 2011. Caracterização Sedimentológica e micropaleontológica dos calcários bioclásticos da Serra do Periquito, Bacia de Jatobá. Estudos Geológicos, Vol. 21, pp. 21-39.

Santos, A., De Lira Mota, M.A., Kern, H.P., Fauth, G., Paim, P.S.G., Netto, R.G., Sedorko, D., Lavina, E.L.C., Krahl, G., Fallgatter, C., da Silveira, D.M., Aquino, C.D. dos Santos, M.O., Baecker-Fauth, S., Vieira, C.E.L. 2022. Earlier onset of the Early Cretaceous Equatorial humidity belt. Global and Planetary Change. Vol, 208, 103724. https://doi.org/10.1016/j.gloplacha.2021.103724

Schrank, E. 2010. Pollen and spores from the Tendaguru Beds, Upper Jurassic and Lower Cretaceous of southeast Tanzania: Palynostratigraphical and paleoecological implications, Palynology, 34:1, pp. 3-42. https://doi.org/10.1080/01916121003620106

Silva, M.A.M. 1988. Evaporitos do Cretáceo da Bacia do Araripe: ambientes de deposição e história diagenética. Bol. Geociências Petrobras, 21, pp. 53-63.

Silveira, L.F., Borghi, L., Bobco, F.E.R., Araújo, B.C., Kroth, M., Duarte, G., Ferreira, L.O., Mendonça, J.O. 2023. Multiscale characterization of an extensive stromatolite field: a new correlation horizon for the Crato Member, Araripe Basin, Brazil. Journal of Sedimentary Research. Vol. 93 (10), pp. 776–795 https://doi.org/10.2110/jsr.2022.090

Song, Z.C., Shang, Y.K. 2000. Fossils spores and pollen of China. In *The mesozoic spores and pollen* (Vol. 2). Science Press.

Souza-Lima, W., Silva, R.O. 2018. Aptian–Albian paleophytogeography and paleoclimatology from Northeastern Brazil sedimentary basins. Review of Palaeobotany and Palynology. Vol 258, pp. 163-189. https://doi.org/10.1016/j.revpalbo.2018.08.003

Stancliffe. R.P.W. 1989. Microforaminiferal linings: their classification, biostratigraphy and palaeoecology, with special reference to specimens from British Oxfordian sediments. Micropaleontology. Vol. 35, pp. 337-352

Taylor N.T., Taylor L.E., Krings, M. 2009. Paleobotany: The Biology and Evolution of Fossil Plants. Second Edition. Elsevier

Teixeira, M.C., Mendonça Filho, J.G., de Oliveira, A.D., Assine, M.L. 2017. Faciologia orgânica da Formação Romualdo (Grupo Santana, Cretáceo Inferior da Bacia do Araripe): caracterização da matéria orgânica sedimentar e interpretação paleoambiental. Geologia USP. Série Científica, 17(4), pp. 19-44. https://doi.org/10.11606/issn.2316-9095

Tomé, M.E., Lima Filho, M.F., Neumann, V.H. 2014. Taxonomic studies of nonmarine ostracods in the Lower Cretaceous (Aptian-lower Albian) of post-rift sequence from Jatobá and Araripe basins (Northeast Brazil): Stratigraphic implications. Cretac. Res. 48, pp. 153–176. https://doi.org/10.1016/j.cretres.2013.12.007.

Tomé, M.E., Araripe, R., Oliveira, D., Barreto, A.M.F, Prado, L.A.C., Pedrosa, F., Pereira, P., Nascimento, L.R.S. 2022. Early cretaceous ostracoda (Crustacea) from south-central Araripe Basin, Brazil, with descriptions of seven new species. Vol. 5159,4.1 Zootaxa. https://doi.org/10.11646/zootaxa.5159.4.4

Tyson, R.V. 1995. Sedimentary Organic Matter: Organic Facies and Palynofacies. Chapman & Hall, Londres, 615 pp.

Uesugui, N. 1979. Palinologia: técnica de tratamento de amostras. Bol. Tec. Petrobras 22, pp. 229–240.

Vakhrameev, V.A. 1970. Range and paleoecology of Mesozoic conifers: the Cheirolepidiaceae. Paleontological Journal 4, pp. 11-24.

Vallejo, J.D., Piovesan, E.K., Carvalho, M.A., Guzmán, J. 2023. Palynofacies analyses of Santana Group, upper Aptian of the Araripe Basin, northeast Brazil: Paleoenvironmental reconstruction. Journal of South American Earth Sciences. Vol. 121, 104154. https://doi.org/10.1016/j.jsames.2022.104154.

Varejão, F.G., Fürsich, F.T., Warren, L.V., Matos, S.A., Rodrigues, M.G., Assine, M.L., Sales, A.M.F., Simões, M.G. 2019. Microbialite fields developed in a protected rocky coastline: The shallow carbonate ramp of the Aptian Romualdo Formation (Araripe Basin, NE Brazil). Sedimentary Geology. Vol. 389, pp. 103–120. https://doi.org/10.1016/j.sedgeo.2019.06.003.

Varejão, F.G., Warren, L.V., Simões, M.G., Buatois, L.A., Mángano, M.G., Bahniuk Rumbelsperger, A.M., Assine, M.L. 2021a. Mixed siliciclastic–carbonate sedimentation in an evolving epicontinental sea: Aptian record of marginal marine settings in the interior basins of north-eastern Brazil. Sedimentology 68, pp. 2125–2164. https://doi.org/10.1111/sed.12846.

Varejão, F.G., Silva, V.R., Assine, M.L., Warren, L.V., Matos, S.A., Rodrigues, M.G., Fürsich, F.T., Simões, M.G. 2021b. Marine or freshwater? Accessing the paleoenvironmental parameters of the Caldas Bed, a key marker bed in the Crato Formation (Araripe Basin, NE Brazil). Brazilian J. Geol. 51, e2020009. https://doi.org/10.1590/2317-4889202120200009.

Wood, G.D., Gabriel, A.M., Lawson, J.C. 1996. Palynological techniques – processing and microscopy. In: Jansonius, J., McGregor, D.C. (Eds.), Palynology: Principles and Applications. American Association of Stratigraphic Palynologic, Texas, USA, pp. 29–50.

Figure captions

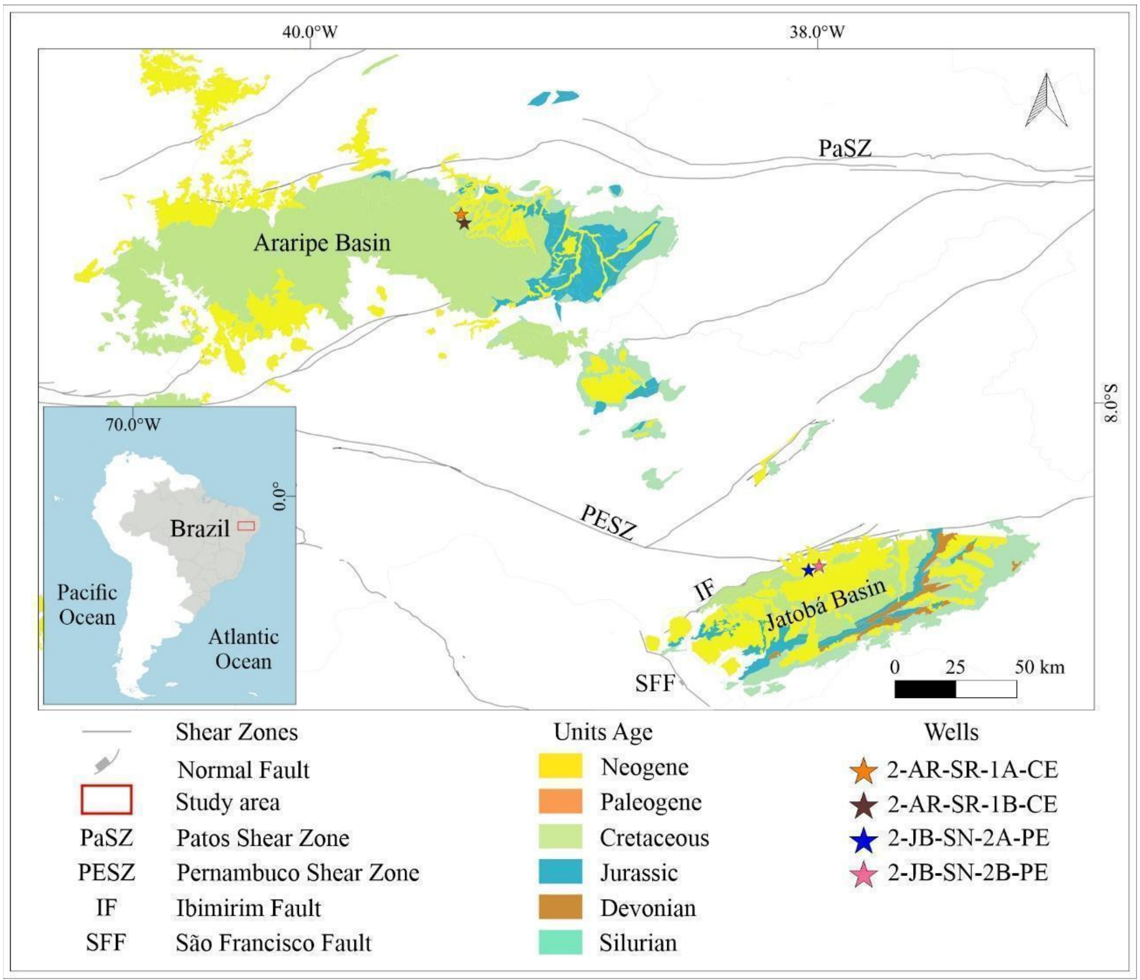

Fig. 1. Location of the Araripe and Jatobá Basin in Northeast Brazil and the position of the well logs used in this work.

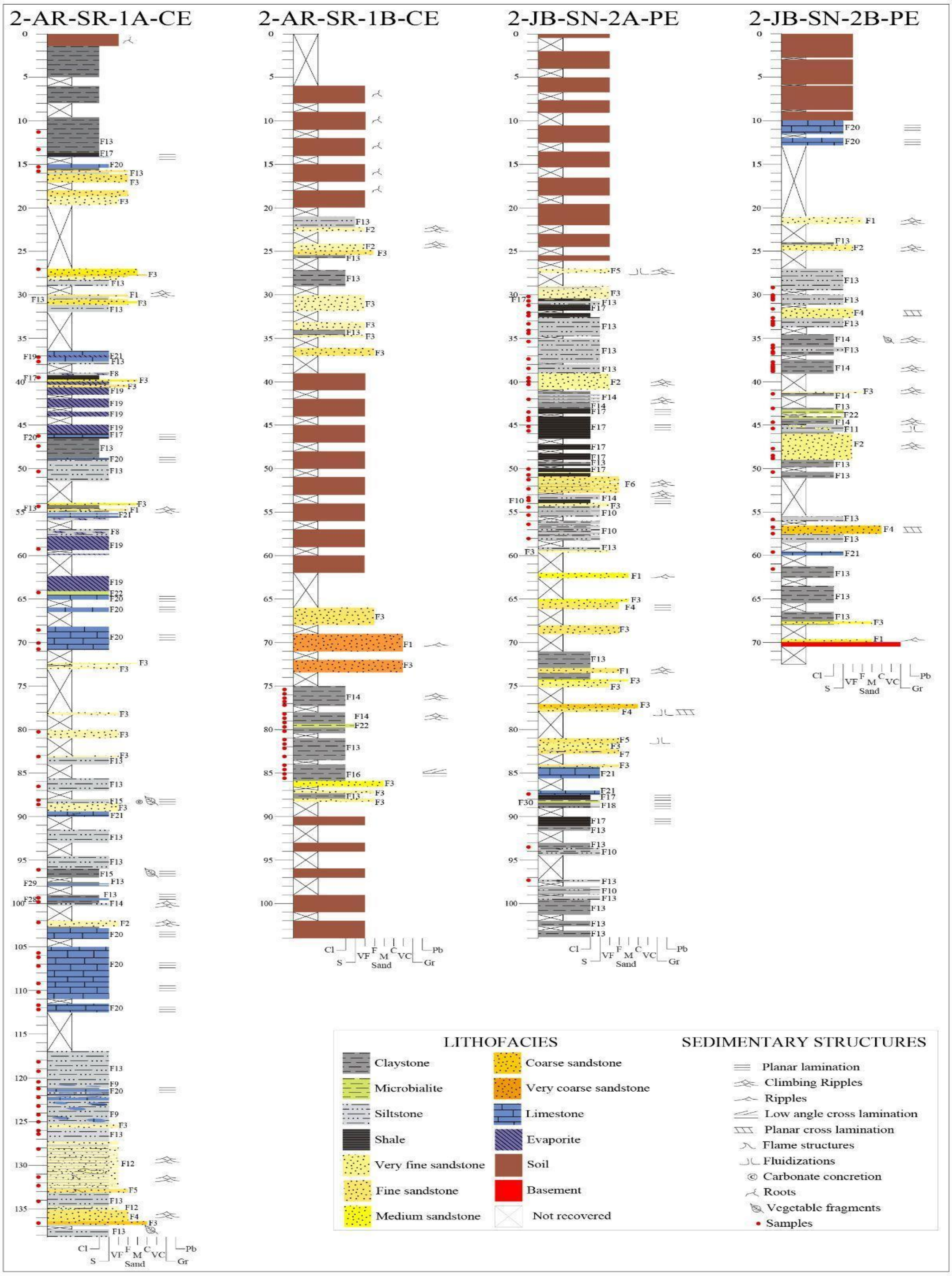

Fig. 2. Sedimentary logs of the wells used in this work, showing palynological sampling positions and sedimentary facies of the Araripe and Jatobá Basin, at a 1:100 scale.

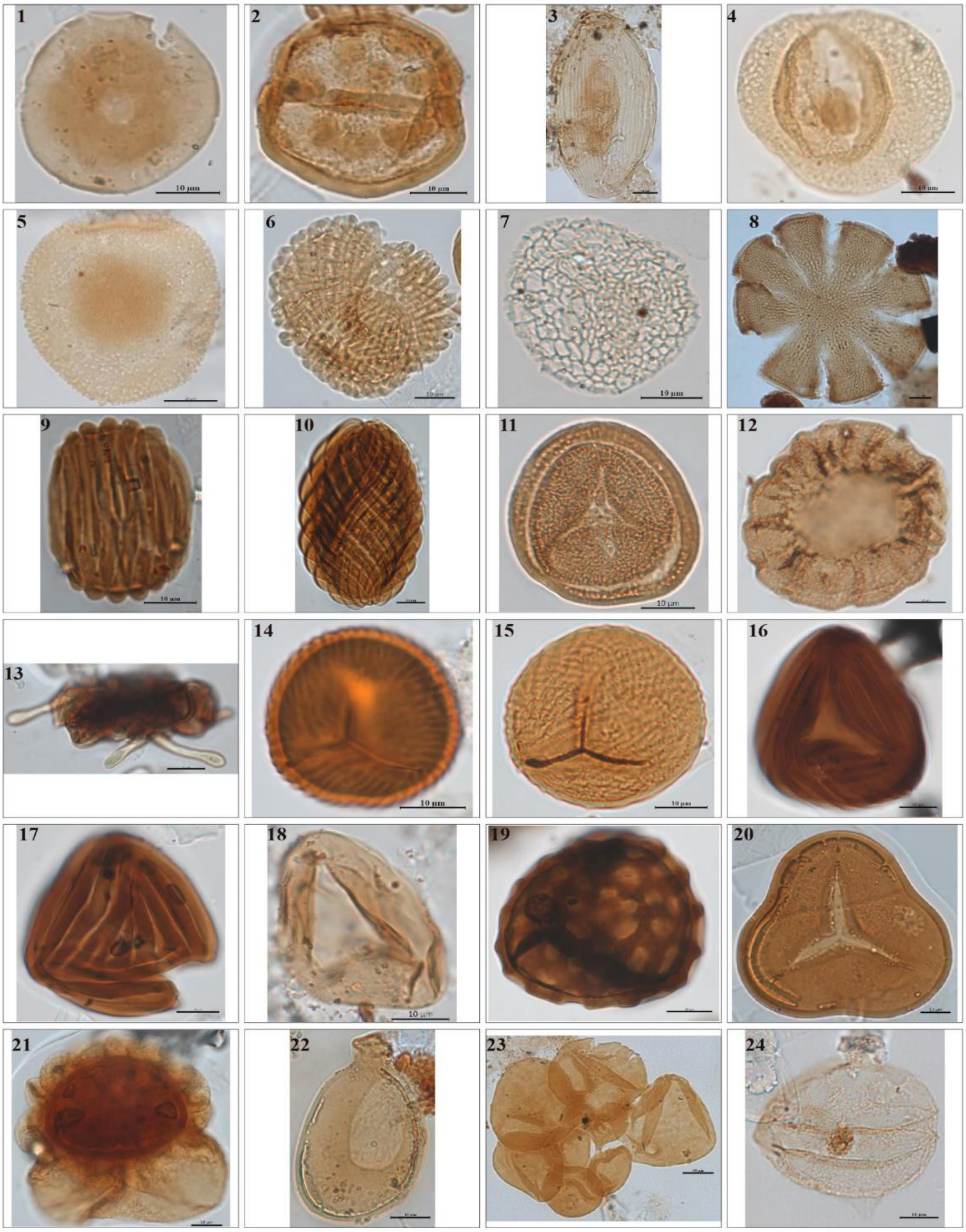

Fig. 3. Palynomorphs from the wells. Scale bar is 10 µm long. 1. *Exesipollenites tumulus* 2. *Sergipe variverrucata.* 3. *Equisetosporites maculosus.* 4. *Complicatisaccus cearensis*. 5. *Uesuguipollenites callosus*. 6. *Trisectoris reticulatus*. 7. *Afropollis jardinus*. 8.*Retistephanocolpites* sp. 9. *Gnetaceaepollenites retangularis*. 10. *Gnetaceaepollenites jansonii*. 11. *Classopollis classoides.* 12. *Callialasporites segmentatus.* 13. *Elaterosporites klaszii.* 14. *Cicatricosisporites avnimelechi* 15. *Cicatricosisporites nuni.* 16. *Cicatricosisporites brevilaesuratus.* 17. *Cicatricosisporites pseudotripartitus.* 18. *Deltoidospora tenuis.* 19. *Ischyosporites foveolatus.* 20. *Deltoidospora australis*. 21. *Paludites mamelonatus*. 22. Foraminiferal lining (*Pyrgo* sp.). 23. Foraminiferal lining. 24. *Subtilisphaera* sp.

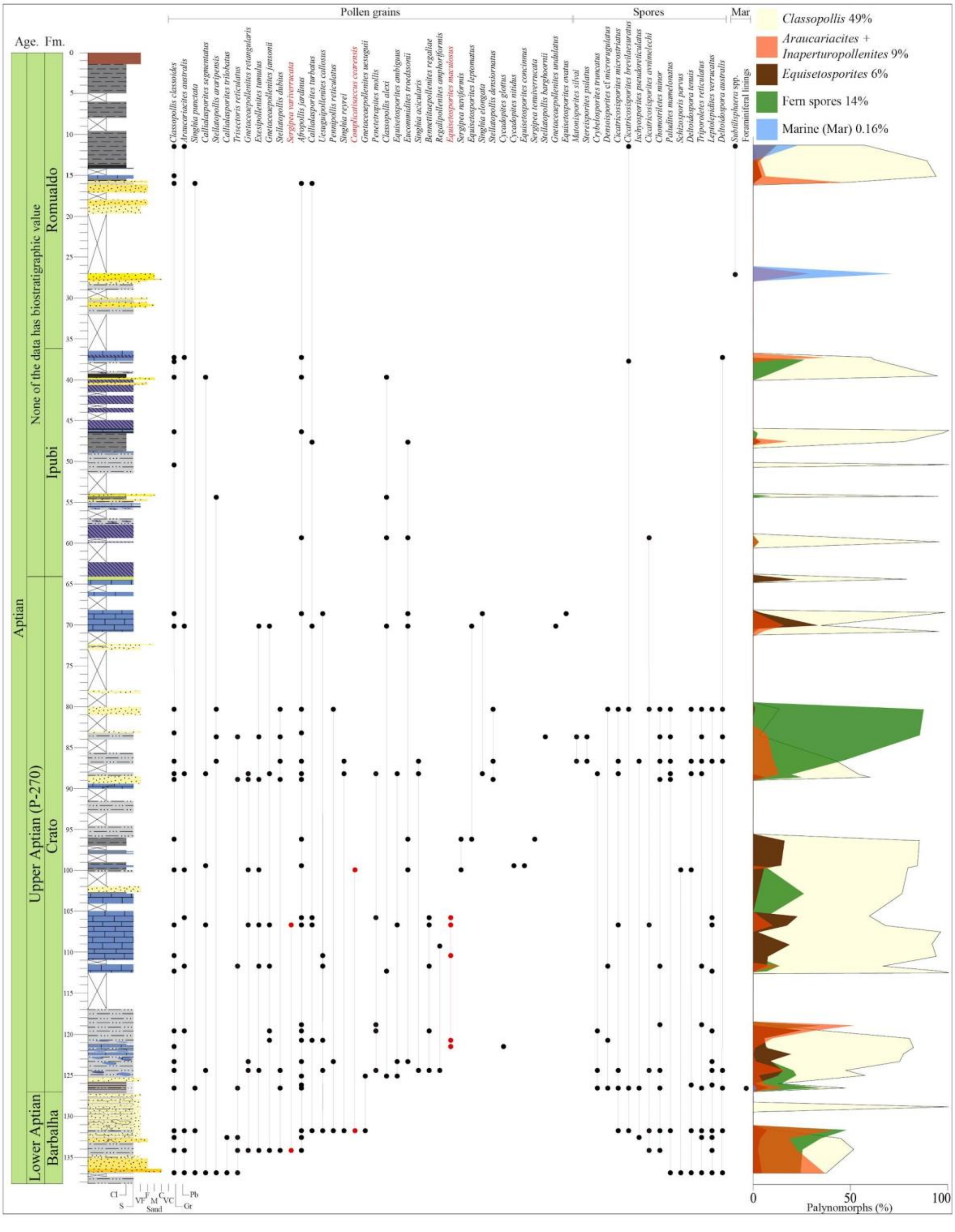

Fig. 4. Stratigraphic distribution of palynofloral genera, highlighting red species with biostratigraphic value. Average spore/pollen grain genera as climate indicators in well 2-AR-SR-1A-CE, Araripe Basin, Fm: Formation.

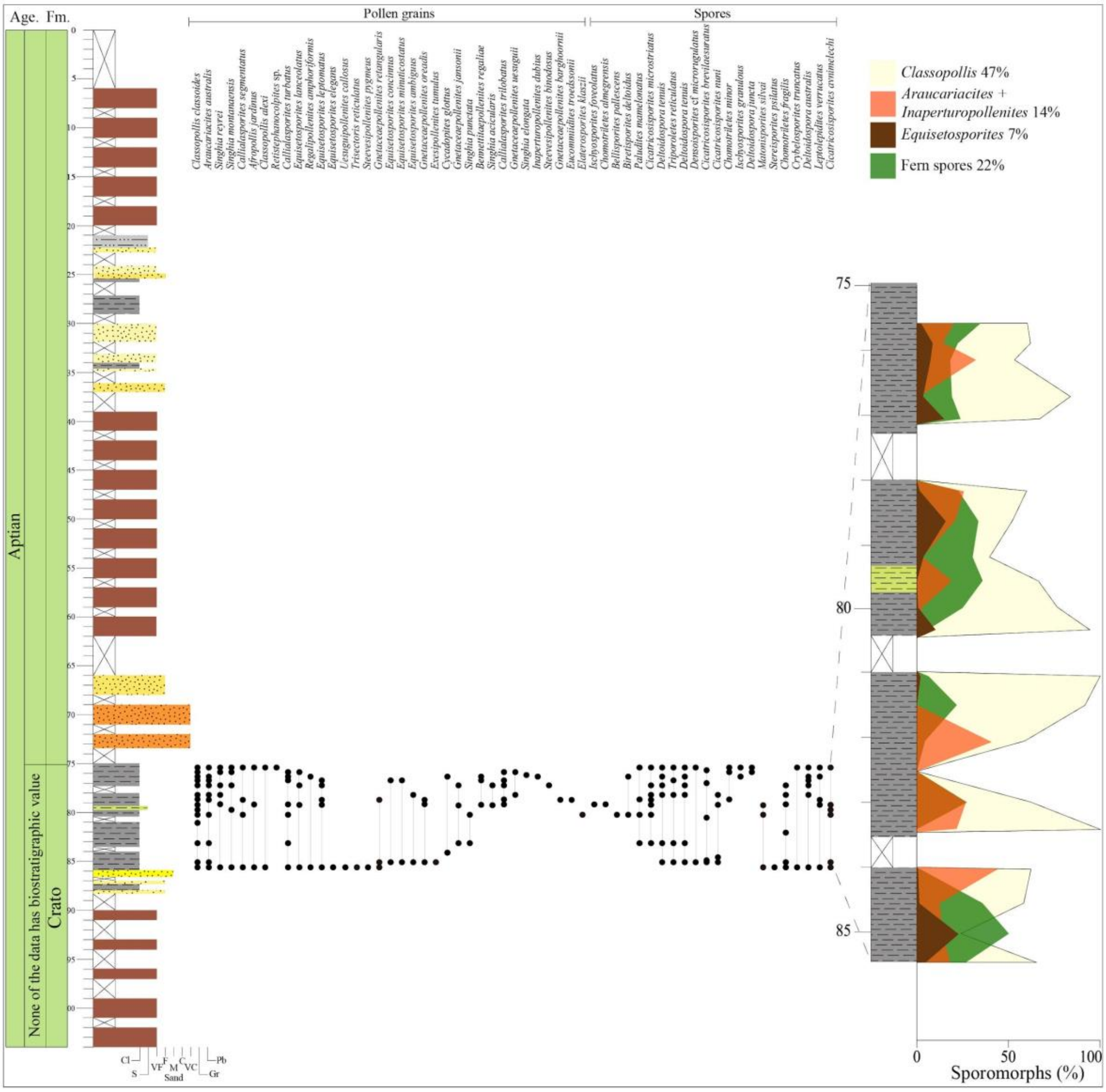

Fig. 5. Stratigraphic distribution of palynofloral genera, highlighting red species with biostratigraphic value. Average spore/pollen grain genera as climate indicators in well 2-AR-SR-1B-CE, Araripe Basin, Fm: Formation.

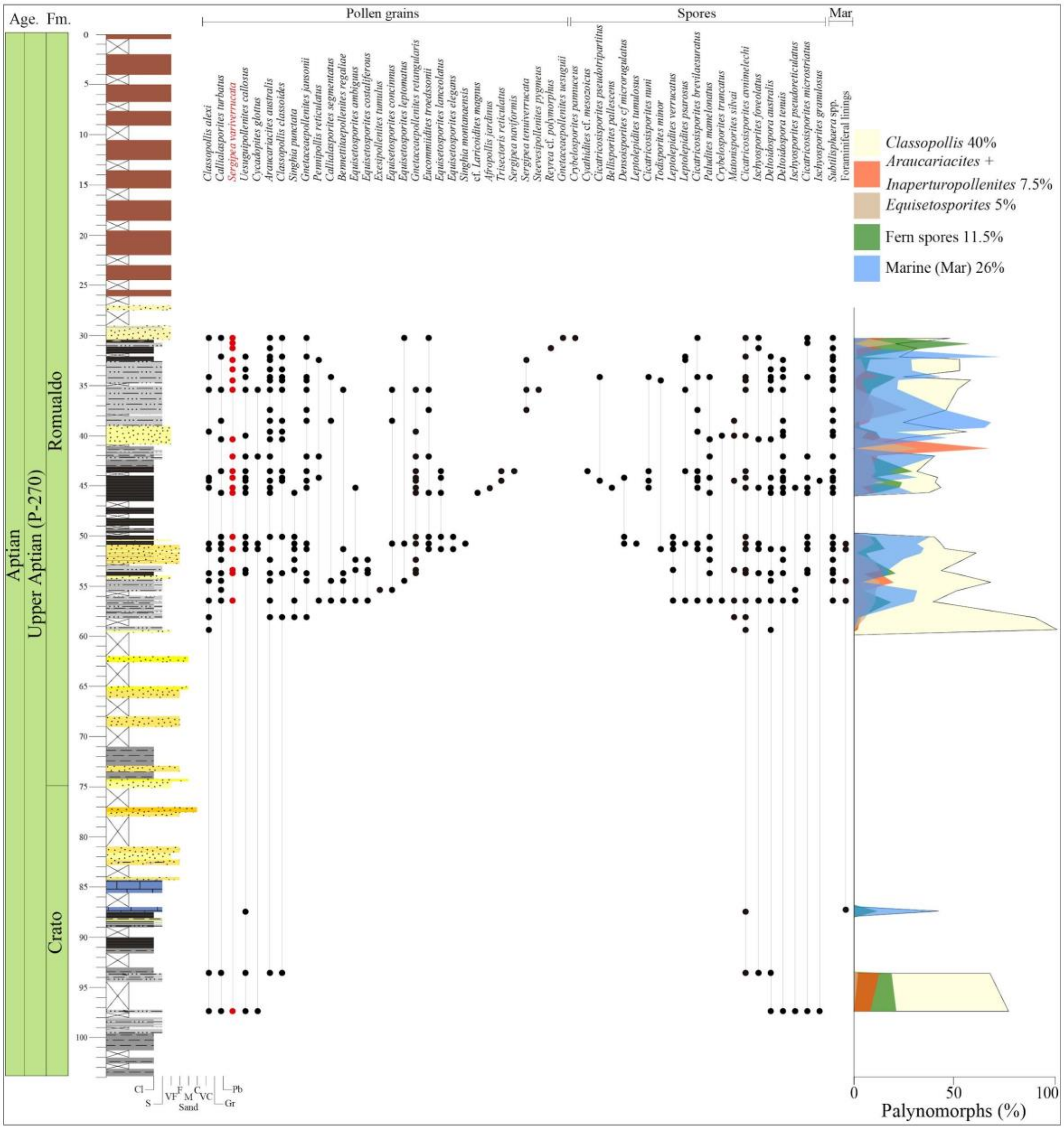

Fig. 6. Stratigraphic distribution of palynofloral genera, highlighting red species with biostratigraphic value. Average spore/pollen grain genera as climate indicators in well 2-JB-SN-2A-PE, Jatobá Basin, Fm: Formation.

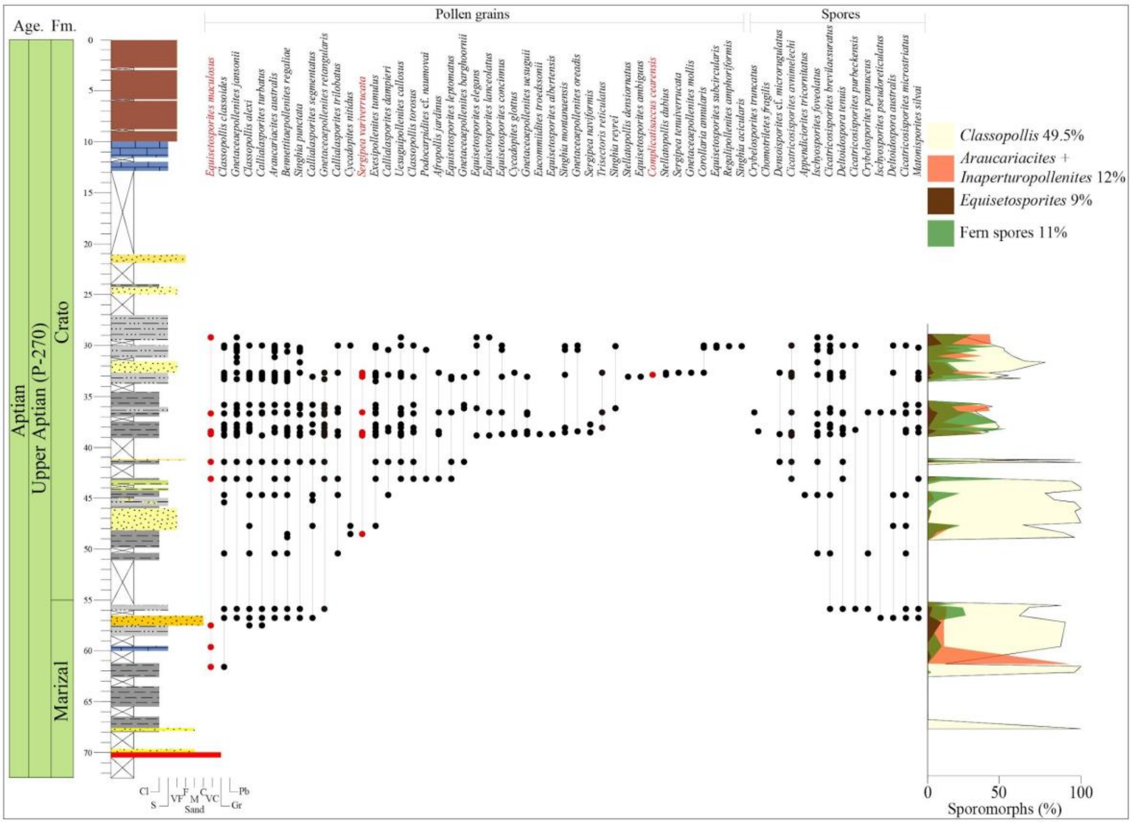

Fig. 7. Stratigraphic distribution of palynofloral genera, highlighting red species with biostratigraphic value. Average spore/pollen grain genera as climate indicators in well 2-JB-SN-2B-PE, Jatobá Basin. Fm: Formation.

6. CONSIDERAÇÕES FINAIS

A presente tese contém os resultados e interpretações da pesquisa em caracterização paleoambiental da fase pós-rifte I das bacias do Araripe e Jatobá, Nordeste do Brasil: inferências palinológicas e palinofaciológicas.

A palinoflora estudada enquadra-se na província Pré-Albiana do Cretáceo Inferior *Dicheiropollis etruscus*/*Afropollis*, preconizada por Herngreen et al. (1996), distinguida pela prevalência de pólen gimnospérmico.

O estudo integrado dos palinomorfos, palinofácies e sedimentologia da fase pós-rifte I das bacias Araripe e Jatobá permitiu a constatação e determinação dos limites nos testemunhos das formações Romualdo, Ipubi, Crato, Barbalha e Marizal, representativas do Aptiano.

Levando em consideração a correlação entre as bacias, a identificação da palinoflora e sua distribuição estratigráfica no Grupo Santana corroboram que seu paleoambiente deposicional ocorreu do Aptiano inferior ao Aptiano superior. Assim, a Formação Barbalha, que foi depositada em um clima úmido, representa um sistema flúvio-deltaico, enquanto a Formação Marizal apresenta predominantemente características fluvial indicativas de condições áridas. Durante um ciclo climático úmido-seco, as Formações Crato e Ipubi são interpretadas como partes de um sistema lagunar, com a Formação Crato indicando uma lagoa aberta, influenciada esporadicamente por condições marinhas, e a Formação Ipubi representando uma lagoa semifechada a fechada sob condições mais secas. A Formação Romualdo é interpretada como ambiente marinho; no entanto, existem diferenças entre as duas bacias. A Bacia do Araripe é interpretada como um ambiente marinho raso do tipo epicontinental, enquanto a Bacia do Jatobá, é caracterizada como um paleoambiente marinho bem estabelecido.

A abundância de palinomorfos de origem continental, aliada à presença de cistos de dinoflagelados e palinoforaminíferos, permite concluir uma deposição sob condições marinhas costeiras. Além disso, a presença de palinoforaminíferos na Formação Crato sustenta que a influência marinha foi mais antiga e que o ambiente deposicional teve uma progressão constante de caráter transicional a completamente marinho.

7. REFERÊNCIAS

ALMEIDA, F.F.M.; HASUI, Y.; BRITO NEVES, B.B.; FUCK, R.A. Brazilian structural provinces: an introduction. **Earth Science Reviews**, v. 17(1-2), p. 1-29, 1981.

ARAI, M.; COELHO, P.S. Statitical analysis of palynological assemblages from the Aptian-Albian of the Araripe Basin, northeast Brazil: a case study of paleoenvironmental significance of Early Cretaceous terrestrial palynomorphs. Asociación Paleontológica Argentina. **VII International Symposium on Mesozooic Terrestrial Ecosystems,** v. 25–28, p. 30–36. Buenos Aires, 2001.

ARAI, M., ASSINE, M.L. Chronostratigraphic constraints and paleoenvironmental interpretation of the Romualdo Formation (Santana group, Araripe Basin, northeastern Brazil) based on palynology. **Cretaceous Research**, v. 116, 104610, 2020.

ASHLEY, G.M. Classification of large-scale subaqueous bedforms: A new look at an old. **Journal of Sedimentary Petrology**, v. 60, p. 160-172, 1990.

ASSINE, M.L. Bacia do Araripe. **Boletim de Geociências da Petrobras**, v. 15, n. 2, p. 371-389, 2007

ASSINE, M.L.; PERINOTTO, J.A.J.; CUSTÓDIO, M.A.; NEUMANN, V.H.M.L.; VAREJÃO F.G.; MESCOLOTTI, P.B. Sequências deposicionais do Andar Alagoas da Bacia do Araripe, Nordeste do Brasil. **Boletim de Geociências da Petrobras**. v. 22, n. 1, p. 3-28, 2014.

BEURLEN, G.; REGALI, M.S.P. O Cretáceo da Plataforma continental do Maranhão e Pará, Brasil: bioestratigrafia e evolução paleoambiental. **Boletim de Geociências da Petrobras,** v. 1, p. 135-155, 1987.

BRITO NEVES, B.B.; SANTOS, E.J.; VAN SCHMUS, W.R**.** Tectonic history of the Borborema Province. *In*: Cordani U.G., Milani E.J., Thomaz Filho A., Campos D.A. (eds.), **Tectonic Evolution of South America**. Rio de Janeiro, 31st International Geological Congress, p. 151-182, 2000.

CARVALHO, M.A. **Paleoenvironmental reconstruction based on palynological and palynofacies analyses of the Aptian-Albian succession in the Sergipe Basin, northeastern Brazil**, Universität Heidelberg, Heidelberg, PhD thesis, p. 192, Germany, 2001.

CARVALHO, M.A.; MENDONÇA FILHO, J.G.; MENEZES, T.R. Paleoenvironmental reconstruction based on palynofacies analysis of the Aptian–Albian succession of the Sergipe Basin, Northeastern Brazil. **Marine Micropaleontology**, v. 59, p. 56-81, 2006a.

CARVALHO, M.A.; MENDONÇA FILHO, J.G.; MENEZES, T.R. Palynofacies and sequence stratigraphy of the Aptian–Albian of the Sergipe Basin, Brazil. **Sedimentary Geology**, v. 192, p. 57-74, 2006b.

CARVALHO, R.R.; NEUMANN, V.H.; FAMBRINI, G.L.; VIEIRA, M.M.; ROCHA, D.A. Origem e proveniência das sequências siliciclásticas inferior da Bacia de Jatobá. **Estudos Geológicos**, v. 20, n. 2, p. 113-127, 2010.

CARVALHO, M.A.; BENGTSON, P.; LANA, C.C.; SÁ, N.D.; SANTIAGO, G.; GIANNERINI, M.C. Late Aptian (Early Cretaceous) dry-wet cycles and their effects on vegetation in the South Atlantic: Palynological evidence. **Cretaceous Research**, v. 100, p. 172-183, 2019.

CESERO, P. DE; PONTE, F.C. Análise comparativa da paleogeologia dos litorais atlânticos brasileiro e africano. **Boletim de Geociências da Petrobras**, v. 11, n. 1/2, p. 1-18, 1997.

CHANG, H.K.; KOWSMANN, R.O.; FIGUEIREDO, A.M.F. New concepts on the development of East Brazilian Marginal Basins. **Episode**s, v. 11, n. 3, 1988.

CHANG, H.K.; KOWSMANN, R.O.; FIGUEIREDO, A.M.F.; BENDER, A.A. Tectonics and stratigraphy of the East Brazil Rift system: an overview. **Tectonophysics**, v. 213, p. 97-138, 1992.

COIMBRA, J.C.; ARAI, M.; CARREÑO, A.L. Biostratigraphy of Lower Cretaceous microfossils from the Araripe Basin, northeastern Brazil. **Geobios**, v. 35, n. 6, p. 687-698, 2002.

COIMBRA, J.C.; FREIRE, T.M. Age of the post-rift sequence I from the Araripe Basin, Lower Cretaceous, NE Brazil: Implications for spatio-temporal correlation. **Revista Brasileira de Paleontologia**, v. 24, n. 1, p. 37-46, 2021.

COSTA, I.P.; MILHOMEM, P.S.; CARVALHO, M.S. Bacias sedimentares brasileiras: Bacia de Jatobá Aracaju: **Fundação Paleontológica Phoenix** (Série Bacias Sedimentares, n. 53, 2003.

COSTA, I.P.; BUENO, G.V; MILHOMEM, P.S.; SILVA, H.S.R; KOSIN, M.D. Sub-bacia de Tucano Norte e Bacia de Jatobá. **Boletim de Geociências da Petrobras**, v. 15, n. 2, p. 445–453, 2007.

COLLINSON, J.D. Alluvial sediments. *In:* Reading, H.G. (Ed.), Sedimentary environments: **Processes, Facies and Stratigraphy**. Third Edition Blackwell Science, London, pp. 37-82, 1996.

CUSTÓDIO, M.A.; QUAGLIO, F.; WARREN, L.V.; SIMÕES, M.G.; FÜRSICH, F.T.; PERINOTTO, J.A.J.; ASSINE, M.L. The transgressive-regressive cycle of the Romualdo Formation (Araripe Basin): Sedimentary archive of the Early Cretaceous marine ingression in the interior of Northeast Brazil. **Sedimentary Geology**, v. 359, p.1-15, 2017.

DINO, R. **Palinologia, bioestratigrafia e paleoecologia da formação Alagamar, Cretáceo da Bacia Potiguar, Nordeste do Brasil**. Instituto de Geociências, Universidade de São Paulo, São Paulo, Brasil, Tese, p. 300, 1992.

DINO, R. Some new pollen grain species from Lower Cretaceous in northeastern Brasil. **Boletim de Geociências da Petrobras**, v. 8, n. 2, p. 257-273, 1994.

FAMBRINI, G.L.; SILVESTRE, D.D.C.; JUNIOR, A.M.B.; DA SILVA-FILHO, W.F. Estratigrafia da Bacia do Araripe: Estado da arte, revisão crítica e resultados novos. **Geol. USP Série Cient**, v. 20, p. 169-212, 2020.

FERREIRA, N.N.; FERREIRA, E.P., RAMOS; R.R.C., CARVALHO, I.S. Palynological and sedimentary analysis of the Igarapé Ipiranga and Querru 1 outcrops of the Itapecuru formation (lower cretaceous, Parnaíba Basin), Brazil. **Journal of South American Earth Sciences,** v. 66, p. 15–31, 2016.

FERREIRA, N.N.; FERREIRA, E.P.; RAMOS, R.R.; CARVALHO, I.S. Terrestrial and marine palynomorphs from deposits of the pull-apart rift of West Gondwana (Parnaíba Basin, northern Brazil): Biostratigraphy and relation to tectonic events. **Journal of South American Earth Sciences**, v. 101, 102612, 2020.

GARCIA, A.J.V. Evolução Sedimentar da Sequência Pré-Rifte das Bacias Costeiras e Interiores do Nordeste Brasileiro. **Pesquisas, Instituto de Geociências, UFRGS**, v. 18, p. 3- 12, 1991.

GOMES, J.M.; RIOS-NETTO, A.M.; BORGHI, L.; CARVALHO, I.; MENDOÇA FILHO, J.G.; SABARAENSE, L.D.; ARAÚJO, B. Cyclostratigraphic analysis of the early Cretaceous laminated limestones of the Araripe Basin, NE Brazil: Estimating sedimentary depositional rates. **Journal of South American Earth Sciences**, v. 112, 103563, 2021.

GONZALEZ, L.D., MASTALERZ, M., MENDONÇA FILHO, J.G. Application of organic facies and biomarkers in characterization of paleoenvironmental conditions and maturity of sediments from the Codó Formation in the west-central part of the São Luís Basin, Brazil. **International Journal of Coal Geology**, v. 225, 103482, 2020.

GOLDBERG, K.; PREAMOR, E.; BARDOLA, T.; SOUZA, P.A. Aptian marine ingression in the Araripe Basin: implications for paleogeographic reconstruction and evaporite accumulation. **Marine and Petroleum Geology**, v. 107, p. 214–221, 2019.

GUZMÁN, J.; FAMBRINI, G.L.; OLIVEIRA, E.V., USMA, C.D. Estratigrafia da Bacia de Jatobá: Estado da Arte. **Estudos Geológicos**, v. 25, n. 1, p. 53-76, 2015.

GUZMÁN, J. **Correlações Bioestratigráficas E Faciológicas Da Fase Pós-Rifte Das Bacias De Araripe, Tucano Norte E Jatobá, Nordeste Do Brasil.** Programa de Pós-Graduação em Geociências da Universidade Federal de Pernambuco, Recife, Brasil, Tese, p.133, 2023.

HERNGREEN, G.F, KEDVES, M., KEDVES, ROVNINA, L.V., SMIRNOVA, S.B. Cretaceous microfloral provinces: a review. *In:* Jansonius, J., McGregor, D.C. (Eds.), Palynology: **Principles and Applications.** American Association of Stratigraphic Palynologic, Texas, USA, p. 1157-1188, 1996.

HEIMHOFER, U., HOCHULI, P.A. Early Cretaceous angiosperm pollen from a lowlatitude succession (Araripe Basin, NE Brazil). **Review of Palaeobotany and Palynology**, v. 161, n. 3–4, p. 105–126, 2010.

JANSONIUS, J.; HILLS, L. **Genera File of Fossil Spores and Pollen.** 3287 cards. Department of Geology, University of Calgary, Calgary, Canada, Special Publication, 1976.

JARAMILLO, C.; RUEDA, M. A Morphological Electronic Database of Cretaceous-Cenozoic and Extant pollen, spores and dinoflagellates from Northern South America. *In*: Morphological DB. **Smithsonian Tropical Research Institute**. Panamá, 2023. Disponível em: http://biogeodb.stri.si.edu/jaramillosdb/web/morphological/. Acesso em: 13 julho 2023.

KUCHLE, J. **Análise tectono-estratigráfica de bacias rifte**. Porto Alegre. Tese de doutorado apresentado ao Programa de Pós-graduação em Geociências do Instituto de Geociências, UFRGS, 2010.

KUCHLE, J.; SCHERER, C. M.D.S. Sismoestratigrafia de bacias rifte: Técnicas, métodos e sua aplicação na Bacia do Recôncavo. **Boletim de Geociências da Petrobras**, v. 18, n. 2, p. 179-206, 2010.

KUCHLE, J.; SCHERER, C.M. DOS S.; BORN, C.C.; ALVARENGA, R. DOS S.; ADEGAS, F. A contribution to regional stratigraphic correlations of the Afro-Brazilian depression - The Dom João Stage (Brotas Group and equivalent units - Late Jurassic) in Northeastern Brazilian sedimentary basins. **Journal of South American Earth Sciences**, v. 31, n. 4, p. 358-371, 2011.

LACERDA, J.N.L.; NASCIMENTO, L.R.; BARRETO, A.M.F. Paleoecology and paleoenvironmental inferences based on palynomorphs from the Romualdo Formation (Lower Cretaceous) of the Araripe Basin, Serrolândia Mine, Pernambuco, northeastern Brazil. **Journal of South American Earth Sciences**, v. 129, 104526, 2023.

LIMA, M.R. **Palinologia da Formação Santana (Cretáceo do Nordeste do Brasil)**. Instituto de Geociências, Universidade de São Paulo, São Paulo, Tese, p. 335-392, 1978.

LIMA, M.R. Palinologia do limito de Jatobá (Cretáceo do nordeste do Brasil). I. Introdução, contexto estratigráfico, identificação de espécies Cretáceas. **Anais do XXXIII Congresso Brasileiro de Geologia**, Rio de Janeiro, p. 536–547, 1984.

LIMA, R.P. **Sequências lacustres pós-rifte na Serra Negra (Bacia de Jatobá) e Serra do Tonã (Sub-bacia de Tucano Norte): correlações estratigráficas regionais e estruturais**. Tese, Universidade Federal de Pernambuco Centro de Tecnologia e Geociências Programa de Pós-Graduação em Geociências, Recife, PE. Brasil, 2018

MAGNAVITA, L.; DESTRO, N.; CARVALHO, M.S.; MILHOMEN, P.S.; SOUZA-LIMA, W. Bacia de Tucano. **Fundação paleontológica Phoenix**, v. 5, p. 22, 2003.

MARTILL, D.M. The preservation of fossil fishes in concretions from the Cretaceous of Brazil. **Palaeontology**, v. 30, p. 1-18, 1988.

MENDES, D.M.; GUZMÁN, J.; NEUMANN, V.H.; PIOVESAN, E.K. Geological and stratigraphic characterization of the region North of Inajá (PE), Jatobá Basin, Northeast Brazil. **Northeast Geosciences Journal**, v. 6, n. 2, p. 32-44, 2020.

MENDONÇA FILHO, J.G.; MENEZES. T.R.; MENDONÇA, J.O. Organic composition (palynofacies analysis). *In*: **7th ICCP training course on dispersed organic matter**. GFZ (Deutsches GeoForschungs Zentrum, Potsdam, Germany. Chapter 5, p. 36-89, 2014.

MIALL, A.D. **The Geology of Fluvial Deposits: Sedimentary Facies, Basin Analysis and Petroleum Geology,** Springer-Verlag, New York, 582 pp, 1996.

MIALL, A.D. **Principles of Sedimentary Basin Analysis**, Springer-Verlag, Berlin, Germany, 616 pp, 2000.

MICHELS, F.H.; SOUZA, P.A.; PREMAOR, E. Aptian-Albian palynologic assemblages interbedded within salt deposits in the Espírito Santo Basin, eastern Brazil: Biostratigraphical and paleoenvironmental analysis. **Marine and Petroleum Geology**, v. 91, p. 785-799, 2018.

NASCIMENTO, D.R., JR.; DA SILVA FILHO, W.F.; FREIRE, J.G., JR.; Dos SANTOS, F.H. Syngenetic and diagenetic features of evaporite-lutite successions of the Ipubi Formation, Araripe Basin, Santana do Cariri, NE Brazil. **Journal of South American Earth Sciences**, v. 72, p. 315-327, 2016.

NASCIMENTO, L.R.D.S.L., TOMÉ, M.E.T.R., BARRETO, A.M.F., HOLANDA DE OLIVEIRA, D., NEUMANN, V.H. Biostratigraphic analysis based on palynomorphs and ostracods from core 2-JNS-01PE, Lower Cretaceous, Jatobá Basin, northeastern Brazil. **Journal of South American Earth Sciences**, v. 76, p. 115-136, 2017.

NASCIMENTO, L.R.S.L.; ARAI, M.; LACERDA, J.N.L.; TOMÉ, M.E.; ARARIPE, R.; BARRETO, A.M.F; OLIVEIRA, D.H.; LEMOS., F.P.; PRADO, L.A.C.; NG, C. Integrated study of the microfossils of the upper Aptian (Lower Cretaceous) of the Sobradinho and Serra do Mãozinha sections (Araripe Basin, northeastern Brazil): Biostratigraphic and paleoenvironmental inferences. **Journal of South American Earth Sciences**, v. 132, 104644, 2023.

NEUMANN, V.H. **Estratigrafía, Sedimentología, Geoquímica y Diagénesis de los Sistemas Lacustres Aptienses-Albienses de la Cuenca de Araripe (Noreste de Brasil)**. Tese, Universidad de Barcelona, Barcelona, España, 1999.

NEUMANN, V.H.; CABRERA, L. Una nueva propuesta estratigráfica para la tectono sequência Pós-rifte de la Cuenca de Araripe, Noreste de Brasil, *In*: **5° Simpósio Sobre o Cretáceo Do Brasil**. UNESP, Rio Claro, p. 279–285, 1999.

NEUMANN, V.H.; BORREGO, A.G.; CABRERA, L.; DINO, R. Organic matter composition and distribution through the Aptian-Albian lacustrine sequences of the Araripe Basin, northeastern Brazil. **International Journal of Coal Geology**, v. 54, p. 21–40, 2003.

NEUMANN, V.H.; ROCHA, D.E.G.A. Stratigraphy of the Post-Rift Sequences of the Jatobá Basin, Northeastern Brazil. (R. Rocha et al., Eds.) *In*: Strati 2013 First International Congress on Stratigraphy at the Cutting Edge of Stratigraphy. **Anais Springer International Publishing Switzerland**, 2014.

NEUMANN, V.H.; ASSINE, M. Stratigraphic proposal to the Post-Rift I Tectonic-Sedimentary Sequence of Araripe Basin, Northeastern Brazil. *In*: **Strati 2015 – 2nd International Congress on Stratigraphy.** Berichete des Institutes für Erdwissenschaften der Universtät Graz, p. 274, 2015.

NEVES, S.P. Comparative geological evolution of the Borborema Province and São Francisco Craton (eastern Brazil): Decratonization and crustal reworking during West Gondwana assembly and implications for paleogeographic reconstructions. **Precambrian Research**, v. 355, 2021.

NICHOLS, G. **Sedimentology and Stratigraphy**. Second Edition. Wiley Blackwell, West Sussex, UK. 419 pp, 2009.

OLIVEIRA, R.G. **Arcabouço geofísico, isostasia e causas do magmatismo Cenozoico da Província Borborema e sua margem continental (Nordeste do Brasil).** Tese, Universidade Federal do Rio Grande do Norte, Natal, Brasil, p. 411, 2008.

PONTE, F.C.; ASMUS, H.E. Geological framework of the Brazilian continental margin. **Geologische Rundschau**, v. 67, p. 201-235, 1978.

PORTELA, H.A. **Estudo Palinológico e Palinofaciológico da Formação Santana, Bacia do Araripe, Nordeste do Brasil**. Faculdade de Geologia, Universidade do Estado do Rio de Janeiro, Rio de Janeiro, dissertação de mestrado, p. 133, 2008.

PORTELA, H.A.; ANTONIOLI L.; DINO R.; GARCIA M.J. Caracterização palinoflorística e paleoambiental da Formação Santana (Cretáceo Inferior), poço 4-BO-1-PE, Bacia do Araripe, Nordeste do Brasil. **Revista Brasileira de Paleontologia**, v. 17, p. 363-372, 2014.

POSAMENTIER, H.W.; WALKER, R. Facies models revisited. **SEPM**, Oklahoma, United States of America, 520 pp, 2006.

PROSSER, S. Rift-related linked depositional systems and their seismic expression. In: WILLIAMS, G.D.; DOBB, A. (Eds.). **Geological Society of London Special Publication**, Lyell Collection, v. 71, p. 35-66, 1993.

READING, H.G. **Sedimentary environments: Processes, Facies and Stratigraphy.** Blackwell Science, London, Third Edition, 704 pp, 1996.

REGALI, M.S.P.; UESUGUI, N.; SANTOS, A.S. Palinologia dos Sedimentos Meso-Cenozóicos do Brasil (1). **Boletim de Tecnologia da Petrobras**, v. 17, ed. 3, 177190, 1974a.

REGALI, M.S.P.; UESUGUI, N.; SANTOS, A.S. Palinologia dos Sedimentos Meso-Cenozóicos do Brasil (11). **Boletim de Tecnologia da Petrobras**, v. 17, ed. 4, 263301, 1974b.

REGALI, M.S.P., UESUGUI, N., LIMA, E.C. Palinoestratigrafia e paleoambiente da Bacia de Barreirinhas - Maranhão - Brasil. Departamento Nacional de Produção Nacional, **Série Geológica** n.27. Seção Paleontologia e Estratigrafia, v. 2, p. 461-470, 1985.

REGALI, M.S.P. Palinomorfos do Barremiano/Albiano brasileiros. Parte II. *In:* 10th Congresso Brasileiro de Paleontologia, Rio de Janeiro, **Anais**, v. 2, p. 647–655, 1987.

REGALI, M.S.P.; VIANA, C.F. Sedimentos do NeojurássicoEocretáceo do Brasil: Idade e correlação com a escala internacional**.** **Petrobras**, Rio de Janeiro, p. 95, 1989.

REGALI, M.S.P. *Complicatisaccus cearensís*: uma palinozona do Eocretáceo do Brasil. *In*: 11st Congresso Brasileiro de Paleontologia, Curitiba, **Anais,** v. 1. p. 235-274, 1989a.

REGALI, M.S.P. Biocronoestratigrafia e paleoambiente do eocretáceo das bacias do Araripe (CE) e Rio do Peixe (PB) NE-PE. *In*: **Simpósio sobre a Bacia do Araripe e Bacias Interiores do Nordeste**, v. 1, Atas, p.163-171, 1990.

REGALI, M.S.P.; SANTOS, P.R.S. Palinoestratigrafia e geocronologia dos sedimentos albo-aptianos das bacias de Sergipe e Alagoas – Brasil. *In*: 5th Simpósio sobre o Cretáceo do Brasil, Serra Negra, **Boletim de resumo,** p. 411-419, 1999.

REGALI, M.S.P. Palinoestratigrafia dos sedimentos cretácicos da Bacia do Araripe e das Bacias Interiores do Nordeste – Brasil. *In*: **Simpósios Sobre a Bacia do Araripe e Bacias Interiores do Nordeste**, p. 101-106, 2001

RIOS-NETO, A.M.; REGALI, M.S.P.; CARVALHO, I.S.; FREITAS, F.I. Palinoestratigrafia do intervalo Alagoas da Bacia do Araripe, Nordeste do Brasil. **Revista Brasileira de Geociências**, v. 42, n. 2, p. 331-342, 2012.

ROCHA, D.E.G.A. **Caracterização do intervalo carbonático do sistema lacustre Aptiano da Bacia do Jatobá, NE do Brasil**. Recife, Universidade Federal de Pernambuco, Centro de Tecnologia e Geociências. Tese de Doutorado, p. 128, 2011.

ROCHA, D.E.G.A. & LEITE, J. F. Estudo hidrogeológico da Bacia do Jatobá – PE. Geologia. Série Hidrogeologia. **Estudos e Projetos,** v. 2, p. 20, 1999.

SANTOS, E.J. **O complexo granítico Lagoa das Pedras: acresção e colisão na região de Floresta (Pernambuco), Província Borborema.** Tese, Instituto de Geociências da Universidade de São Paulo, São Paulo, Brasil, p. 228, 1995.

SANTOS, C.A.; NEUMANN, V.H.; MENEZES, M.R.; ROCHA, D.A.; AGOSTINHO, S.M. Caracterização Sedimentológica e micropaleontológica dos calcários bioclásticos da Serra do Periquito, Bacia de Jatobá. **Estudos Geológicos**, v. 21, p. 21-39, 2011.

SCHALLER, H. Revisão estratigráfica da Bacia de Sergipe/Alagoas. **Boletim de Tecnologia da Petrobras**, v. 12, p. 21-86, 1969.

SCHERER, C., M. DOS S.; DE SÁ, E. F. J.; CÓRDOBA, V. C.; SOUSA, D. DO S.; AQUINO, M. M.; CARDOSO, F. M. C. Tectono-stratigraphic evolution of the Upper Jurassic–Neocomian rift succession, Araripe Basin, Northeast Brazil. **Journal of South American Earth Sciences**, v. 49, p. 106-122, 2014.

SCHERER, C.M.S.; GOLDBERG, K.; BARDOLA, T. Facies architecture and sequence stratigraphy of an early post-rift fluvial succession, Aptian Barbalha Formation, Araripe Basin, northeastern Brazil. **Sedimentary Geology.** v, 322, n. 1, p. 43-62, 2015.

SOUZA-LIMA, W.; SILVA, R.O. Aptian–Albian paleophytogeography and paleoclimatology from Northeastern Brazil sedimentary basins. **Review of Palaeobotany and Palynology**, v. 258, p. 163-189, 2018.

TEIXEIRA, M.C.; MENDONÇA FILHO, J.G.; DE OLIVEIRA, A.D.; ASSINE, M.L. Faciologia orgânica da Formação Romualdo (Grupo Santana, Cretáceo Inferior da Bacia do Araripe): caracterização da matéria orgânica sedimentar e interpretação paleoambiental. **Geologia Série Científica**, v. 17, n. 4, p. 19–44, 2017.

TOMÉ, M.E., LIMA FILHO, M.F., NEUMANN, V.H. Taxonomic studies of nonmarine ostracods in the Lower Cretaceous (Aptian-lower Albian) of post-rift sequence from Jatobá and Araripe basins (Northeast Brazil): Stratigraphic implications. **Cretaceous Research**, v. 48, p. 153–176. 2014.

TUCKER, M.E. **Rochas sedimentares: Guia geológico de campo**. Bookman editora LTDA, Porto Alegre, Brazil, 336 pp, 2014.

TYSON, R.V. **Sedimentary Organic Matter: Organic Facies and Palynofacies**. Chapman & Hall, Londres, p. 615, 1995.

TRAVERSE, A. **Paleopalynology.** Secon edition. Springer, Pennsylvania, USA, p. 813, 2007.

VALLEJO, J.D.; PIOVESAN, E.K.; CARVALHO, M.A.; GUZMÁN, J. Palynofacies analyses of Santana Group, upper Aptian of the Araripe Basin, northeast Brazil:

Paleoenvironmental reconstruction. **Journal of South American Earth Sciences**, v. 121, 104154, 2023.

VAN SCHMUS W.R.; KOZUCH M.; BRITO NEVES B.B. Precambrian history of the Zona Transversal of the Borborema Province, NE Brazil: Insights from Sm-Nd and U-Pb geochronology. **Journal of South American Earth Sciences**, v. 31, n. 2-3, p. 227-252, 2011.

VAREJÃO, F.G.; WARREN, L.V.; PERINOTTO, J.A.; NEUMANN, V.H.; FREITAS, B.T.; ALMEIDA, R.P.; ASSINE, M.L. Upper Aptian mixed carbonate-siliciclastic sequences from Tucano Basin, Northeastern Brazil: Implications for paleogeographic reconstructions following Gondwana break-up. **Cretaceous Research**, v. 67, p. 44–58, 2016.

VAREJÃO, F.G.; WARREN, L.V.; SIMÕES, M.G.; BUATOIS, L.A.; MÁNGANO, M.G.; RUMBELSPERGER, A. M.; ASSINE, M.L. Mixed siliciclastic–carbonate sedimentation in an evolving epicontinental sea: Aptian record of marginal marine settings in the interior basins of north-eastern Brazil. **Sedimentology**, v. 68, p. 2125-2164, 2021a.

VAREJÃO, F.G.; SILA, V.R.; ASSINE, M.L.; WARREN L.V.; MATOS S.A.; RODRIGUES M.G.; FÜRSICH. F.T.; SIMÕES M.G. Marine or freshwater? Accessing the paleoenvironmental parameters of the Caldas Bed, a key marker bed in the Crato Formation (Araripe Basin, NE Brazil). **Brazilian Journal of Geology**, v.51, n. 1, 2020009, 2021b.

WALKER, R.G.; JAMES, N.P. **Facies Models: Response to Sea Level Change**. Geological Association of Canada, 409 pp, 1992.

APÊNDICE A- TESTEMUNHO 2-AR-SR-1A-CE. BACIA ARARIPE, REPRESENTATIVA DO GRUPO SANTANA, FORMAÇÕES ROMUALDO, IPUBI, CRATO E BARBALHA

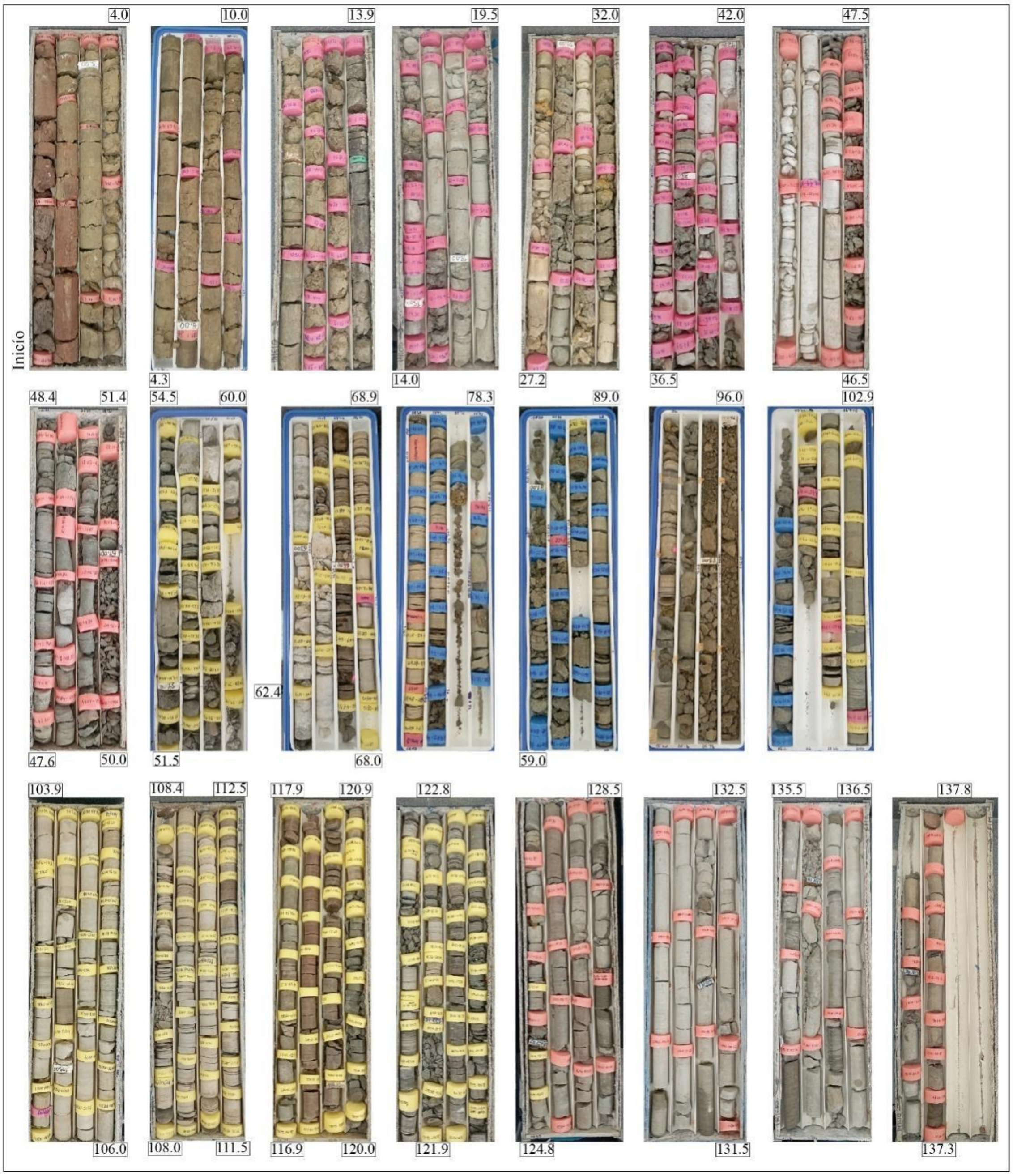

APÊNDICE B- TESTEMUNHO 2-AR-SR-1B-CE. BACIA ARARIPE, REPRESENTATIVO DA FORMAÇÃO CRATO

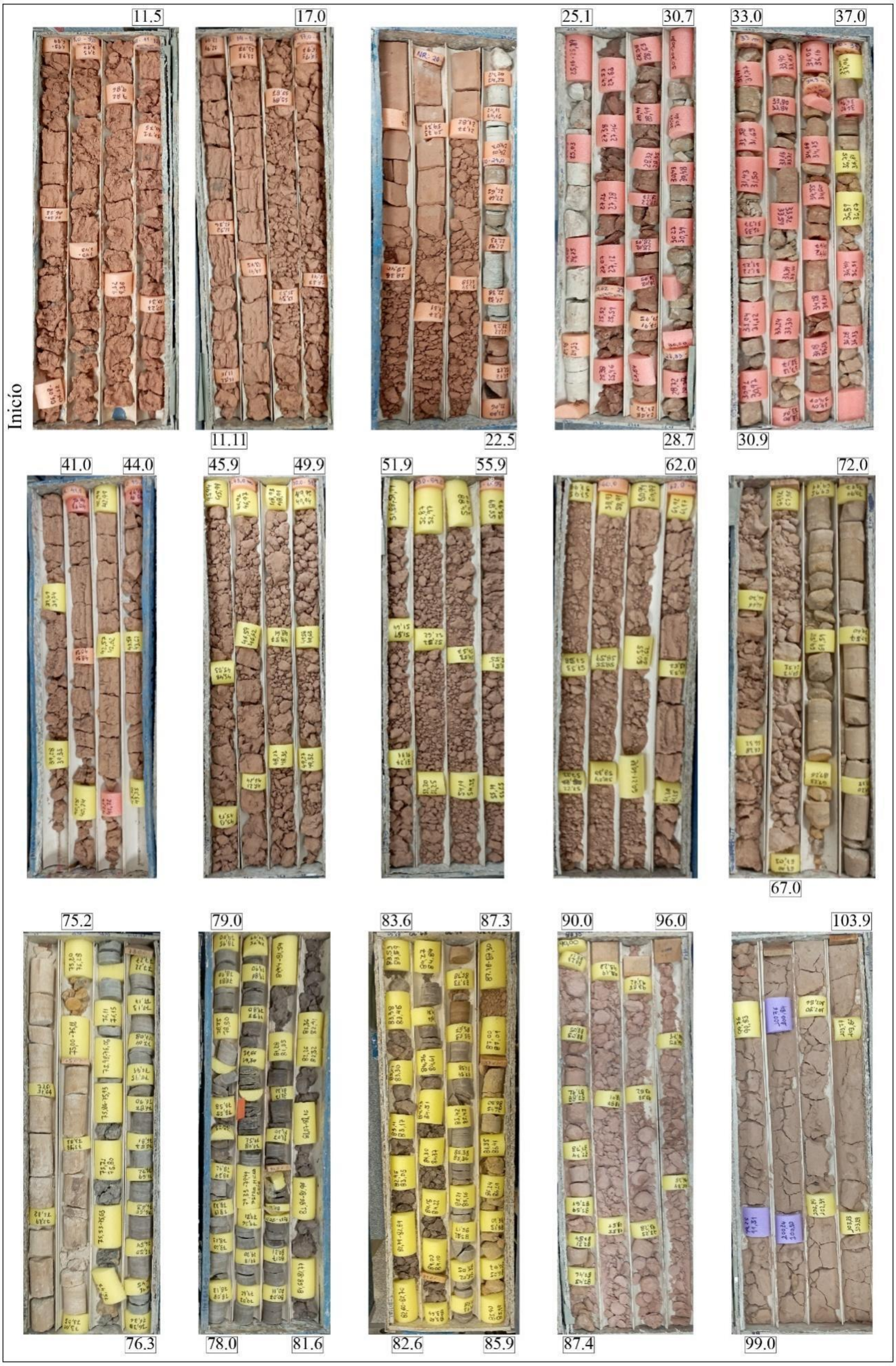

APÊNDICE C- TESTEMUNHO 2-JB-SN-2A-PE DA BACIA DO JATOBÁ, REPRESENTATIVO DAS FORMAÇÕES ROMUALDO E CRATO

APÊNDICE D- TESTEMUNHO 2-JB-SN-2B-PE DA BACIA JATOBÁ, REPRESENTATIVO DAS FORMAÇÕES CRATO E MARIZAL

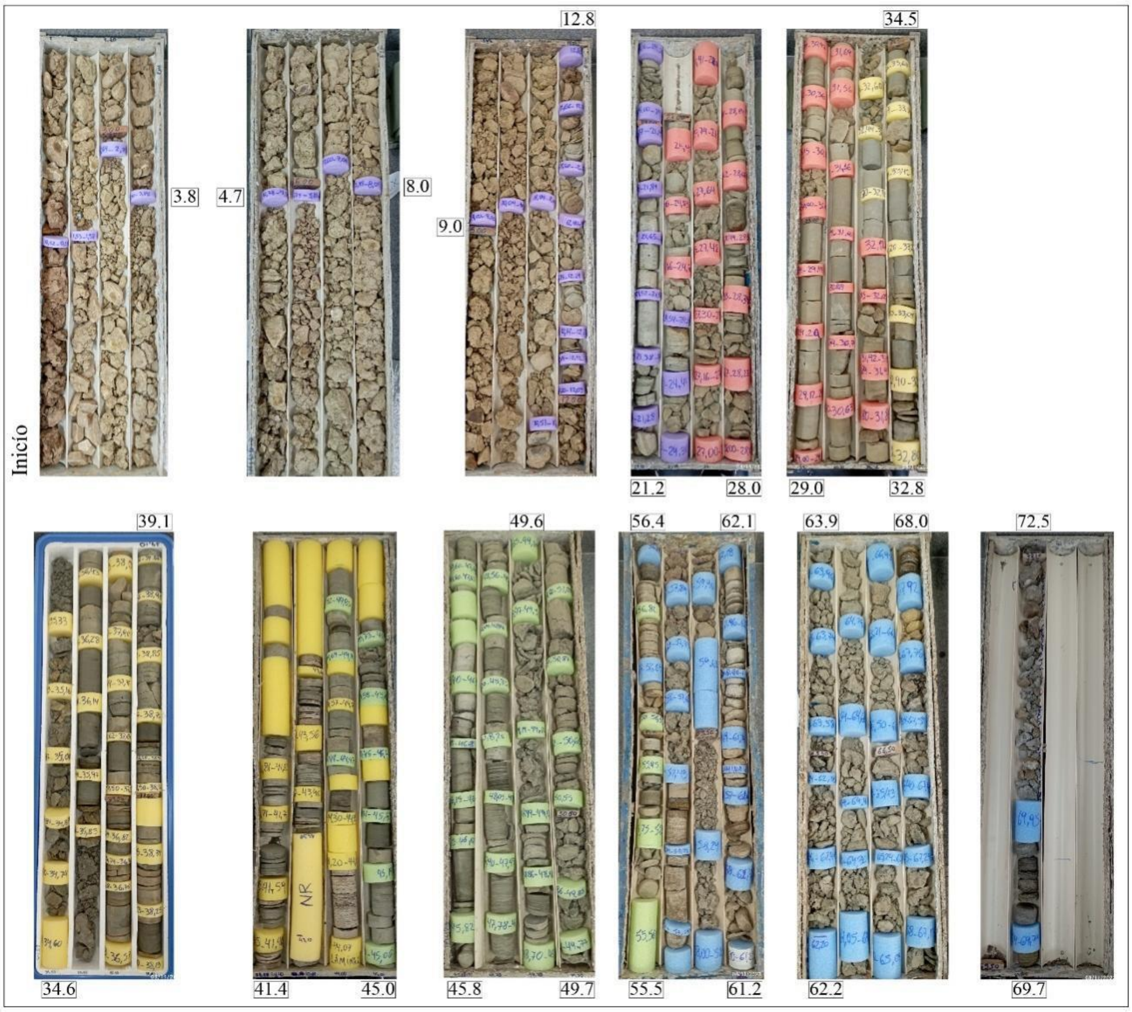

APÊNDICE E- ARTIGO PUBLICADO EM *JORNAL OF SOUTH AMERICAN EARTH SCIENCES*

Journal of South American Earth Sciences 121 (2023) 104154

Contents lists available at ScienceDirect

Journal of South American Earth Sciences

journal homepage: www.elsevier.com/locate/jsames

Palynofacies analyses of Santana Group, upper Aptian of the Araripe Basin, northeast Brazil: Paleoenvironmental reconstruction

Juan David Vallejo [a,b,*], Enelise Katia Piovesan [a,b], Marcelo de Araujo Carvalho [c], Juliana Guzmán [a,b]

[a] *Programa de Pós-graduação em Geociências (PPGEOC), Centro de Tecnologia e Geociências (CTG), Universidade Federal de Pernambuco (UFPE), Av. da Arquitetura, S/n - Cidade Universitária, 50740-550, Recife, PE, Brazil*

[b] *Laboratório de Micropaleontologia Aplicada (LAGESE/LITPEG), Departamento de Geologia (DGEO), Universidade Federal de Pernambuco (UFPE), Av. da Arquitetura, S/n - Cidade Universitária, 50740-550, Recife, PE, Brazil*

[c] *Laboratório de Paleoecologia Vegetal, Departamento de Geologia e Paleontologia, Museu Nacional, Universidade Federal do Rio de Janeiro, Brazil*

ARTICLE INFO

Keywords:
Sedimentary organic matter
Palynology
Post-rift sequence

ABSTRACT

We present the paleoenvironmental analysis based on sedimentary organic matter (SOM) of alluvial-lacustrine-transitional deposits that crop out in the east portion of the Araripe Basin, Ceará State, Brazil. Samples were collected from the Barbalha, Crato, Ipubi and Romualdo formations, Santana Group. For the palynofacies analyses, the kerogen categories were counted and grouped. The described SOM were subdivided into six groups: Structureless, which consists of resin and amorphous organic matter (AOM); Terrigenous, which consists of non-opaque biostructured-phytoclast; Opaque, which consists of equidimensional, lath and corroded of black color; Sporomorphs, which consist of spores and pollen grains; Freshwater, constituted by *Botryococcus* and *Pediastrum* microplankton and Marine elements, represented by dinoflagellate cysts and foraminiferal lining. The stratigraphic distribution of the seven palynofacies reflects a change from fluvial system to a lacustrine environment, as well as the first marine incursion on Serra da Mãozinha section (Crato Formation). In the top of the Santana Group recorded a transition from a lacustrine environment close to a fluvio-deltaic source to an estuarine system, marked by the presence of *Subtilisphaera*, during the late Aptian. The palynological data presented indicates that the entire Santana Group is of Aptian age considering the conspicuous presence of *Sergipea variverrucata* in the sections.

1. Introduction

The paleoenvironmental evolution of the Araripe Basin has been subject of several studies related to some controversies about the time of the marine ingression in this basin. Varejão (2019) suggested that the depositional history of this basin is much more complex than previously thought. The Aptian Stage recorded episodes of oceanic crust creation worldwide, warming punctuated by rapid cooling events, ocean anoxia events (OAE) (Benigno et al., 2021), with major changes in sea level, climate, and in the marine plankton communities (Huber et al., 2011; Huber and Leckie, 2011). Due to changes and the break-up of the Gondwana Supercontinent, the rocks of the Araripe Basin provide an excellent opportunity to investigate the environmental depositional conditions in which the organic matter was accumulated and preserved (Neumann et al., 2003).

The analysis of palynofacies preserved in the sedimentary record is important due to their potential for paleoenvironmental interpretation; it also provides an insight on transgressive-regressive systems tracts in the depositional history (Tyson, 1995; Candel et al., 2013). There are several important contributions to palynology for the basin, but few focus on palynofacies (e.g., Lima, 1978; Arai and Coelho, 2001; Coimbra et al., 2002; Neumann et al., 2003; Heimhofer and Hochuli, 2010; Teixeira et al., 2017; Goldberg et al., 2019; Arai and Assine, 2020). Nevertheless, no study has focused on the complete Santana Group, Post-rift Sequence I of the Lower Cretaceous.

Palynofacies analysis is an interdisciplinary approach that integrates

* Corresponding author. Programa de Pós-graduação em Geociências (PPGEOC), Centro de Tecnologia e Geociências (CTG), Universidade Federal de Pernambuco (UFPE), Av. da Arquitetura, S/n - Cidade Universitária, 50740-550, Recife, PE, Brazil.

E-mail addresses: juandavidv85@gmail.com (J.D. Vallejo), enelise.katia@ufpe.br (E.K. Piovesan), mcarvalhomn@gmail.com (M. de Araujo Carvalho), julitaguzmang@gmail.com (J. Guzmán).

https://doi.org/10.1016/j.jsames.2022.104154
Received 11 October 2022; Received in revised form 6 December 2022; Accepted 6 December 2022
Available online 8 December 2022
0895-9811/© 2022 Elsevier Ltd. All rights reserved.

the study of palynomorphs as well as the entire organic content of sediments, which reflects the original conditions in the source area and the depositional environment (Tyson, 1995; Atta-Peters et al., 2013). This paper presents palynological results developed after palynofacies analysis of the Santana Group, Araripe Basin, aiming to contribute to a better understanding of the geological evolution of Araripe Basin during the Aptian.

2. Geological settings

The Araripe Basin (Fig. 1) is located in the Precambrian São José do Caiano Terrain of the Transversal Zone Domain of the Borborema Province, between the Pernambuco Shear Zone at north and the Patos Shear Zone at south (Brito Neves et al., 2000). This basin is an extensive and complex interior basin of northeast Brazil, covering part of the territory of Pernambuco, Piauí and mainly Ceará states (Assine et al., 2014). The origin and evolution of the Araripe Basin occurred through different tectonic phases (Brito Neves, 1990), related to the fragmentation of the Gondwana supercontinent and the opening of the South Atlantic Ocean (Asmus and Ponte, 1973; Ponte and Asmus, 1978; Garcia et al., 2005; Scherer et al., 2015). Stratigraphic framework consists of megasequences generated in different tectonic regimes point out to the polygenetic evolution of this basin (Assine, 1992, 2007; Ponte and Appi, 1990; Ponte and Ponte Filho, 1996; Neumann and Cabrera, 1999). Different sequences, limited by unconformities of regional extent, were deposited in different paleogeographic scenarios showing a complex tectono-sedimentary evolution (Assine, 2007; Assine et al., 2014; Neumann and Assine, 2015).

The Araripe Basin is divided into two geographic physiognomies, the Vale do Cariri and Chapada do Araripe. The Vale Cariri extends to the east where the Cariri Formation (Paleozoic) of the syneclysis sequence occurs, the Brejo Santo and Missão Velha formations (Upper Jurassic) from the beginning of the rift sequence and the Abaiara Formation (Berriasian–Hauterivian) from the rift climax sequence. The Chapada do Araripe is found on the west, it mainly encompasses units of the Post-rift I sequence, correspondent to the Santana Group and Post-rift II sequence, represented by Araripina and Exu formations (Cretaceous) (Assine, 2007; Assine et al., 2014; Neumann and Assine, 2015).

In this work, we studied all formations of the Santana Group. The Santana Group was deposited during the Aptian (Alagoas local stage) and comprises, from bottom to top, the Barbalha, Crato, Ipubi and Romualdo formations (Assine et al., 2014; Neumann and Assine, 2015), their strata are only observable in outcrops restricted to the slopes of the Araripe Plateau (Fig. 2). The Santana Group recorded a complete transgressive-regressive cycle, limited at the base by a pre-Aptian unconformity (Ponte and Ponte Filho, 1996; Assine, 2007) and contains some of the most important fossil-bearing strata of Brazil and is correlated with the Aptian sequences of Brazilian and African marginal basins (Neumann and Assine, 2015). These lithological units comprehend mixed carbonate-evaporite-siliciclastic depositional system tracts (Assine et al., 2014) related to short-lived marine ingressions (Arai, 2014; Assine et al., 2016; Custódio et al., 2017; Fürsich et al., 2019; Varejão et al., 2019, 2020).

The Barbalha Formation characterizes the initial sedimentary record of the Post-rift I (Assine, 1992). Proposed by Ponte and Appi (1990) as Rio da Batateira Formation, this unit exhibits an intercalation of sandstones and shales, including the black shales named as Batateira Beds (Hashimoto et al., 1987). The Barbalha Formation can be subdivided into two large fining-upward cycles, starting up with sandy conglomerates to coarse-grained sandstones, which pass upwards to fine-grained

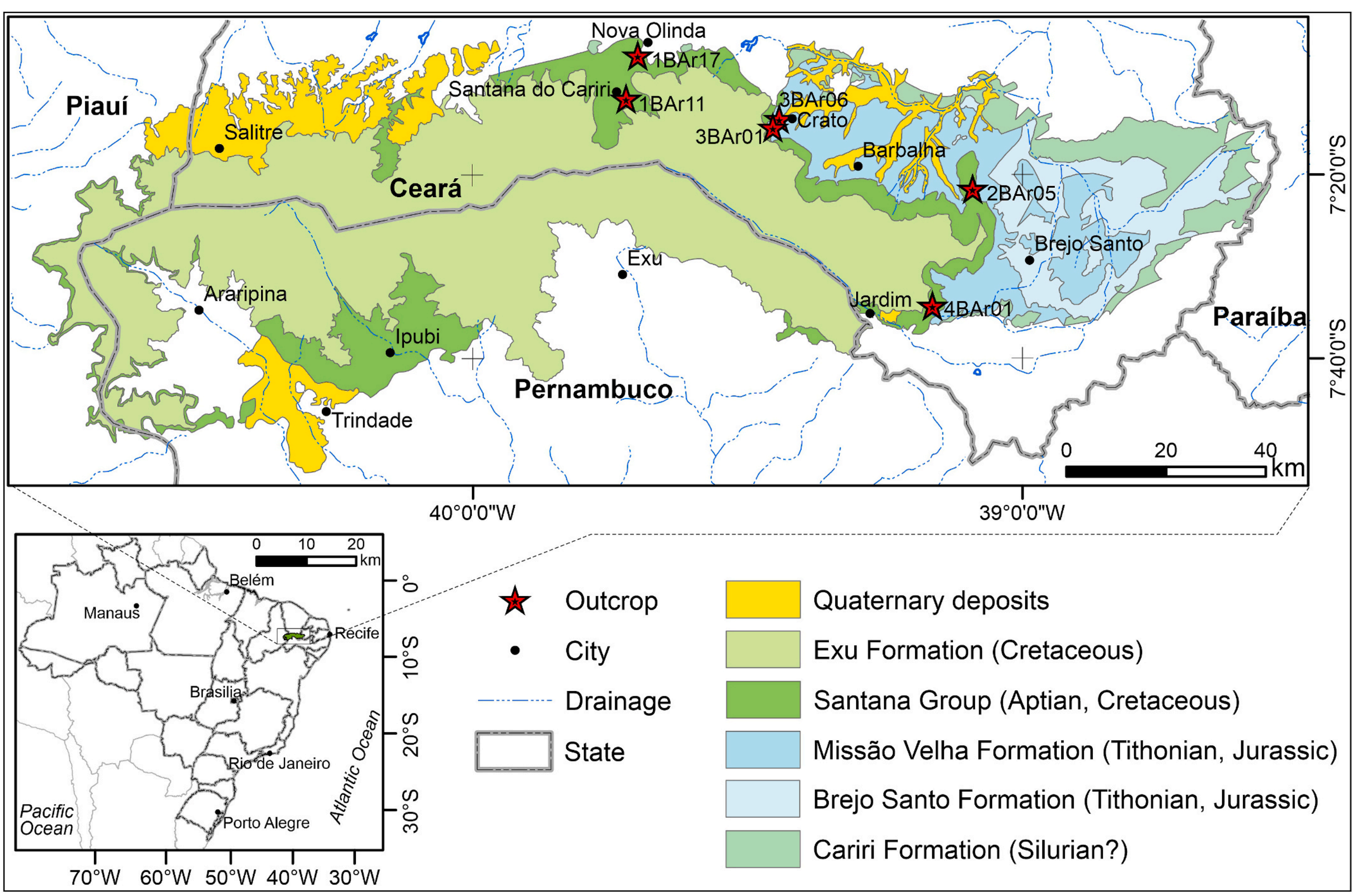

Fig. 1. Location map of the Araripe Basin in Northeastern Brazil showing the lithostratigraphic units and studied outcrops. The Santana Group strata display restricted spatial distribution, only being observables in outcrops on the slopes of the Araripe Plateau.

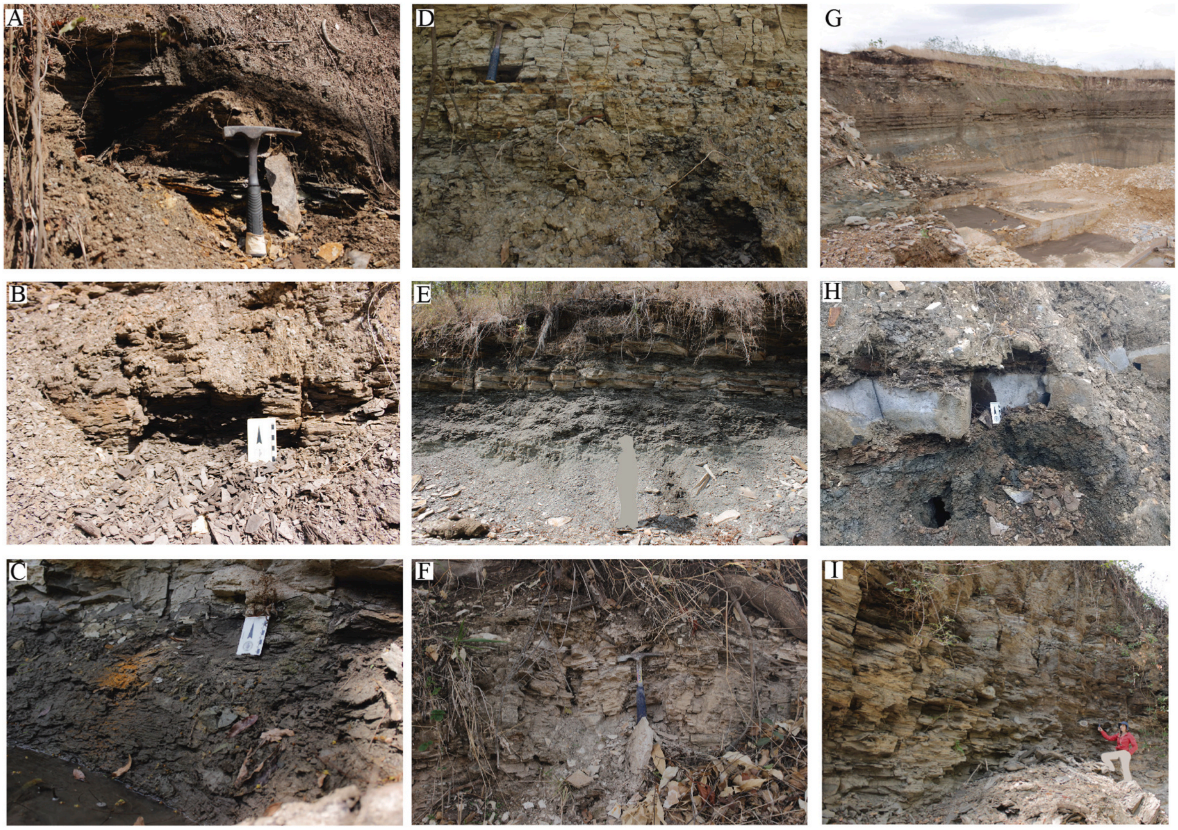

Fig. 2. Outcrops of the Santana Group: (A–D) Batateira River, Barbalha Formation (E) Batateira River, Crato Formation; (F) Serra da Mãozinha, Crato Formation; (G) Três Irmãos Quarry, Crato Formation; (H) Conceição Preta Quarry, Ipubi Formation; (I) Sítio Sobradinho, Romualdo Formation.

sandstones and mudstones and with a vertical association facies typical of a high accommodation system tract (transgressive) materialized by river channel facies (Assine et al., 2014; Scherer et al., 2015) and composed by fluvial and lacustrine deposits (Assine, 1992, 2007; Fambrini et al., 2019). According to recent studies developed by Varejão et al. (2021), the Barbalha Formation may be subdivided into two facies associations, fluvial channel or overbank deposits and bayhead delta. These facies are characterized by intervals comprising conglomerate, pebbly sandstone, mudstone, successions of shale and heterolithic facies deposited under a dry warm semiarid climate (Chagas et al., 2007). The Barbalha Formation represents the record of the onset of the first lake system, characterized by anoxic conditions, which led to the preservation of significant amount of the organic matter (Assine, 2007; Assine et al., 2014).

Deposits of the Crato Formation are composed predominantly of limestones with planar and parallel laminations, interspersed with shale intercalations (Neumann, 1999; Neumann and Cabrera, 1999). The diversity, abundance and well-preserved fossil content made this formation a famous *Konservat-Lagerstätte* (Martill et al., 2007). The mixed carbonate-siliciclastic succession was initially interpreted as exclusively deposited in a lacustrine system (Neumann, 1999; Neumann and Cabrera, 1999; Martill et al., 2007), but recent detailed stratigraphic studies show a transgressive surface followed by tide-dominated bay deposits with distinct subtidal, intertidal and supratidal portions, demonstrating intermittent marine incursions in a broad non-marine environment that represents the Crato Formation (Varejão et al., 2021).

The Ipubi Formation is characterized by the presence of evaporites, consisting of discontinuous gypsum layers associated with green and black shales (Neumann, 1999; Assine, 2007; Neumann and Assine, 2015; Fabin et al., 2018). According to Coimbra et al. (2002), the depositional system occurs in restricted portions of an extensive carbonate lagoon, which was interpreted as a coastal sabkha submitted to marine influence by Bobco et al. (2017). This coastal depositional environment setting has been interpreted as susceptible to the relative sea level changes, under arid to semi-arid climatic conditions (Assine, 2007; Assine et al., 2014; Bobco et al., 2017; Fabin et al., 2018; Goldberg et al., 2019; Moura et al., 2020; Coimbra and Freire, 2021).

The Romualdo Formation comprises a wide range of lithologies, including stratified conglomerates, fine to medium grained sandstones, limestones, marls and shales, which characterize a coastal to marine environment (Assine et al., 2014). This sedimentary succession records the establishment of an epicontinental sea in the Araripe Basin during the late Aptian, it shows an abundance of ostracodes, pollen grains, spores, dinoflagellate cysts, foraminifera and mollusks (e.g., Assine, 2007; Coimbra et al., 2002; Heimhofer and Hochuli, 2010; Custódio et al., 2017; Fürsich et al., 2019; Melo et al., 2020; Arai and Assine, 2020; Araripe et al., 2022).

3. Material and methods

3.1. Studied sections

Thirty-nine samples obtained from the alluvial-lacustrine-transitional deposits of Santana Group were analyzed (Table 1), including five samples from the Barbalha Formation, 19 from the Crato Formation, six from the Ipubi Formation and nine samples from the Romualdo Formation, collected of outcrops in the northeast, east and southeast edges of the basin (Fig. 1).

The Barbalha Formation outcrops along the Batateira River, correspond to the "Batateiras Geossítio" at the area of the Sítio Fundão State Park, municipality of Crato, Ceará State, the samples were obtained along the riverbed above the surface taking different sections (Fig. 2).

The samples 3BAr01a and 3BAr01b (N9200385/E451227) corresponds to the "Batateira beds" (correlated with the "Amargosa beds" of

Table 1
Selected samples for palynofacies analysis of Santana Group.

Formation	Outcrops	Sample	No. Samples
Romualdo	Sítio Sobradinho	4BAr01a-m	9
Ipubi	Conceição Preta Quarry	1BAr11a-f	6
Crato	Três Irmãos Quarry	1BAr17a-g	7
	Serra do Mãozinha	2BAr05a-g	7
	Batateira River	3BAr06a-e	5
Barbalha	Batateira River	3BAr05a	5
		3BAr03	
		3BAr02	
		3BAr01a	
		3BAr01b	
	Total		39

the Marizal Formation in the Recôncavo, Tucano and Jatobá basins, also located in Brazilian Northeast) and has a height of 1.70 m of black bioclastic shales, where a sample was collected at the level that presented the least alteration. Crossing the river in a southwesterly direction, three more samples from the outcrops 3BAr02 (N9200279/E450993), 3BAr03 (N9200254/E450933), and 3BAr05a (N9198829/E450069) of mudstones and gray shales interspersed with sandstones of the Barbalha Formation were collected. Near the "Cascata do Lameiro" and Avenida José Ribeiro de Andrade, municipality of Crato, Ceará, the Barbalha Formation is overlaid by the Crato Formation. The 3BAr06 outcrop (N9198774/E449987) constitutes of black shales and laminated limestone from the base of the Crato Formation (Fig. 3).

Located in the municipality of Abaiara, Ceará state, the outcrop 2BAr05 (N9213217 E422963) at the top of the "Serra do Mãozinha", samples from the Crato Formation were obtained along the road, consisting of massive and laminated calcarenite ranging in color from light brown to gray, interspersed with calcilutite from light brown to whitish-orange, with gray to greenish-gray shale are interspersed. In the cities of Nova Olinda and Santana do Cariri, Ceará State, mines of limestone exploration from the Crato Formation for cement or slabs, and gypsum from the Ipubi Formation are founded. The Três Irmãos Quarry, outcrop 1BAr17 (N9213217/E 422963), presents laminated limestones interspersed with siltstones, shales and fine levels of gypsum of the Crato Formation.

The Sítio Sobradinho, outcrop 4BAr01 (N9163029/E481969), located to the southeast of the Araripe Plateau, corresponds to an outcrop of approximately 100 m height that records the thickest and most complete stratigraphic section of the Romualdo Formation. In this section, transitional coastal deposits such as: fine-grained quartz arenites, mudstones, siltstones, shales, limestones are found in interstratified levels and as concretions, lie discordantly on the carbonate-siliciclastic facies of the Crato Formation. The stratigraphic section depicts a transgressive regressive cycle, composed by transgressive and highstand systems tracts (Custódio et al., 2017). At the Sítio Sobradinho outcrop, 8 m thick interval was analyzed.

3.2. Samples preparation

The samples were prepared according to the method described in Tyson (1995) and Mendonça Filho et al. (2011) using conventional acid treatment involving the dissolution of all mineral constituents with hydrochloric acid (HCl) and hydrofluoric acid (HF) to remove carbonates and silicates. Enough HCl (37%) was added, to completely cover the sample leaving it to rest for 24 h. The samples were rinsed with distilled water and HF (40%) was subsequently added, covering the sample and left to react for 24 h. The samples were washed again with distilled water and sieved through a 10 μm opening net. HCl (10%) was added to the residue, to cover the sample for 24 h and finally washed with distilled water. Denser particles were separated from the organic residue using sodium polytungstate with a specific density of 2.0 g/cm3. The residual matter was mounted on the slides using polyvinyl Alcohol (PVA) and *Norland Optical Adhesive* cured under ultraviolet light and analyzed under transmitted light microscopy and fluorescence.

For paleoenvironmental study based on palynofacies, we counted at least 300 organic particles in each sample. The Sedimentary Organic Matter (SOM) was classified according to Tyson (1995) and Mendonça Filho et al. (2011, 2014). For each sample was determined the relative abundance in percentage of SOM and the representative constituents were photographed using a digital Axiocam 503 camera mounted on a Zeiss microscope (Axio Imager A.2). All slides and residues are stored and cataloged in the Applied Micropaleontology Laboratory (LMA) of the Federal University of Pernambuco (UFPE).

Three main constituents of kerogen were recognized, based on the classification scheme proposed by Tyson (1995); Carvalho et al. (2006) and Mendonça Filho et al. (2011, 2014) and include Amorphous Organic Matter (AOM), Phytoclasts (Opaque and Non-Opaque) and Palynomorphs. The amorphous organic matter (AOM) includes the structureless dispersed particulate organic matter (kerogen) whether of marine or non-marine origin. The non-opaque phytoclasts refers to microscopic particles of plant derived kerogen including all structured terrestrial plant fragments such as cuticles, wood remains and tracheids. The opaque phytoclasts (black debris) include all oxidized brownish black to black woody tissues, or carbonized particles of plant derived kerogen. The palynomorphs refers to all acid-resistant, organic walled microfossils (e.g. spores, pollen grains and dinoflagellates cysts).

Based on quantitative and qualitative variations in the kerogen constituents, different palynofacies constituents can be observed (e.g., Carvalho et al., 2006; Carvalho et al., 2013; Atta-Peters et al., 2013; Atta-Peters and Achaegakwo, 2015) which revealed their link, to different depositional paleoenvironments.

4. Results

The three main kerogen groups and their subgroups of sedimentary organic matter (SOM) were identified: Amorphous organic matter group (AOM and resin), Phytoclast group (Opaque and non-opaque) and Palynomorph group (sporomorphs, freshwater microplankton, marine microplankton and zoomorphs) (Fig. 4), reflecting seven different palynofacies (Fig. 5).

To assess the distribution pattern of the kerogens, their percentages were plotted revealing distinct intervals and depositional environment changes, variations in the stratigraphic distribution of the sections of the six associations are grouped and shown (Figs. 3 and 5). The associations were recognized, namely based on origin and state of preservation, being designated by the most dominant particle: Structureless (AOM), Terrigenous (non-opaque phytoclast-biostructured: striate, striped, banded, pitted, cuticle and degraded), Opaque (equidimensional, lath, and corroded), Sporomorph (spores and pollen grain), Freshwater (*Botryococcus* and *Pediastrum*) and Marine microplankton (dinoflagellate cysts and foraminiferal test linings).

The associations differ in their proportions of kerogen groups and subgroups, show a high average of terrigenous particles inputs, nevertheless highlighting, structureless with a general average abundance of 21.3%, followed by the opaques with 20.7%. The marine component was the least abundant component recovered one (Fig. 5) (Table 2).

4.1. Marine microplankton

Marine elements had the least abundant association (average 0.1% of the total kerogen) (Table 2). It is composed of dinoflagellate cysts and foraminiferal test linings. Despite the low abundance of marine elements in the upper section Sítio Sobradinho, a prominent feature is the presence of dinoflagellate cysts of the genus *Subtilisphaera* normally is associated with restricted low-salinity marine environments (Jain and Millepied, 1975).

Foraminiferal lining observed in the Serra do Mãozinha had the lower abundance in the marine component, these are dominated by

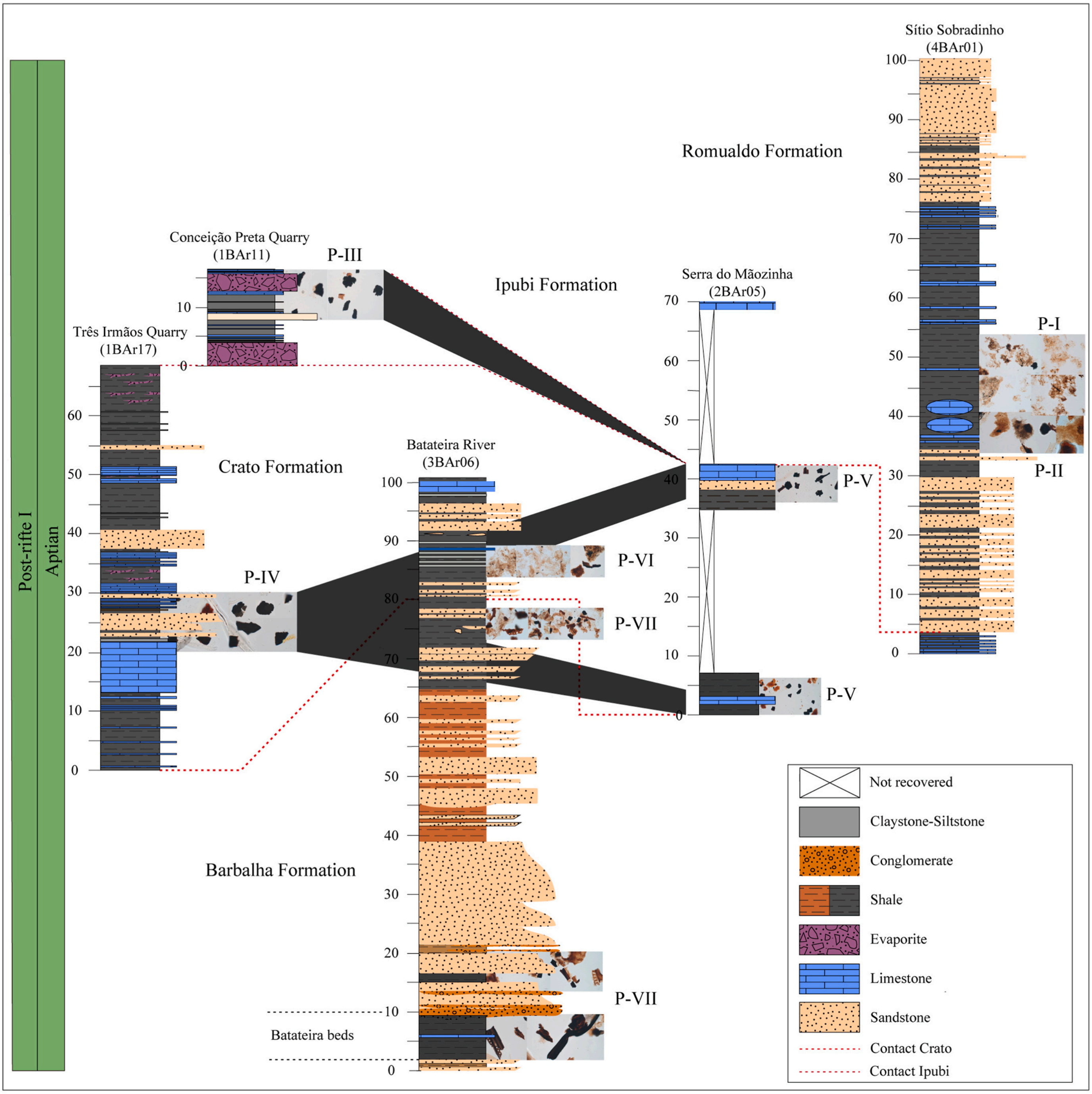

Fig. 3. Lithology, sample points and palynofacies data for along the Santana Group. All figures at a magnification of 40×. Palynofacies P-VII: non-opaque phytoclasts dominant with AOM. Palynofacies P-VI: AOM dominant with opaques and sporomorphs. Palynofacies P–V: opaques dominant with AOM. Palynofacies P-IV: opaques dominant with non-opaque phytoclasts. Palynofacies P-III: opaques dominant. Palynofacies P-II: sporomorphs with opaques and presence of freshwater microplankton and marine elements. Palynofacies P–I: AOM dominant with low presence of marine microplankton.

dinoflagellate cysts, although, marine elements occurrence in the Crato and Romualdo formations, indicating a marine water influence in the Araripe Basin during the deposition of these units.

4.2. *Freshwater microplankton*

This association is composed of *Botryococcus* and *Pediastrum* and presented very low abundance (average 0.5% of the total kerogen) (Table 2). Freshwater palynofacies occurs in almost all investigated sections, its absence was only observed in the Conceição Preta Quarry section. Batateira River section presents dominance of *Botryococcus*, with a coloration ranging from light brown to golden yellow in transmitted white light and has an intense yellow color under fluorescence. This type of microplankton, according to Mendonça Filho et al. (2011), can be found in lagoon, lake, fluvial and delta facies, or in a freshwater input redeposition area (Tyson, 1993, 1995). In the lower part of the Sítio Sobradinho section, *Pediastrum* was dominant, being translucent under fluorescence it has a color range from yellow to yellow-green. According to Mendonça Filho et al. (2010), the predominance of algae of the genus *Pediastrum* over the algae of the genus *Botryococcus*

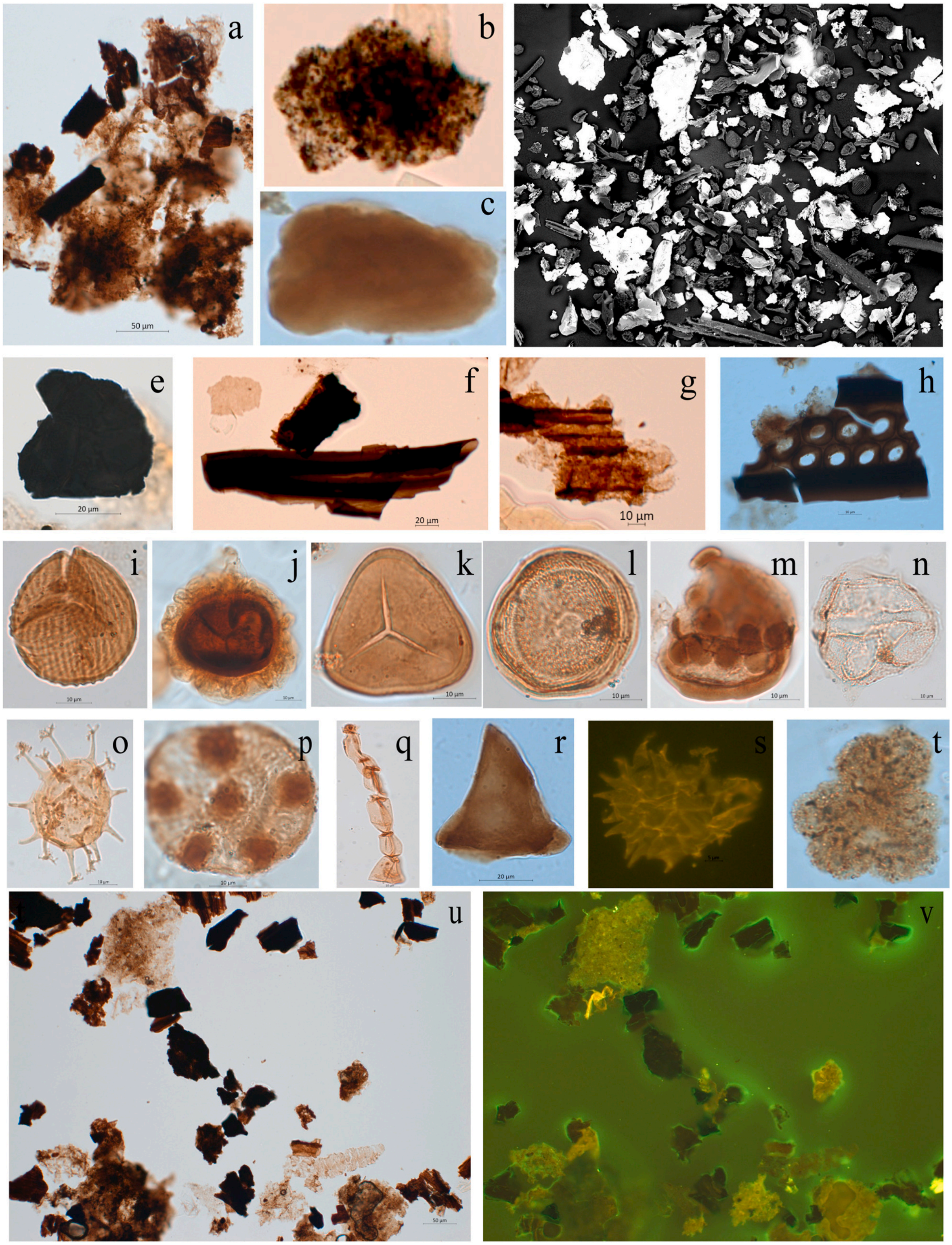

Fig. 4. Typical constituents of SOM recognized in the Santana Group. a, b. Amorphous Organic Matter; c. Resin; d. Image of Sedimentary Organic Matter taken on a SEM; e. Equidimensional Opaque phytoclast; f. Non-Opaque Banded; g. Non-Opaque Striped phytoclast; h. Non-Opaque Pitted phytoclast; i. *Cicatricosisporites avnimelechi;* j. *Paludites mamelonatus;* k. *Deltoidospora hallii;* l. *Classopollis classoides;* m. *Sergipea variverrucata*; n. *Subtilisphaera* sp.; o. Acritarch; p. *Maranhites* sp.; q. Foraminiferal lining; r. Scolecodont; s. *Pediastrum;* t. *Botryococcus;* u, v. Particulate organic matter distribution 20X. v. Fluorescence mode.

demonstrates the lake's high level, these were found in a range of fresh to brackish water habitats, but particularly in oligotrophic to mesotrophic ponds, lakes and slow-moving bodies of water of widely varying pH (Batten, 1996).

4.3. Sporomorphs

This association is composed by pollen grains and spores of continental origin. The assemblage is well preserved, consisting mainly of gymnosperm pollen grains associated to fern spores and rare Aptian

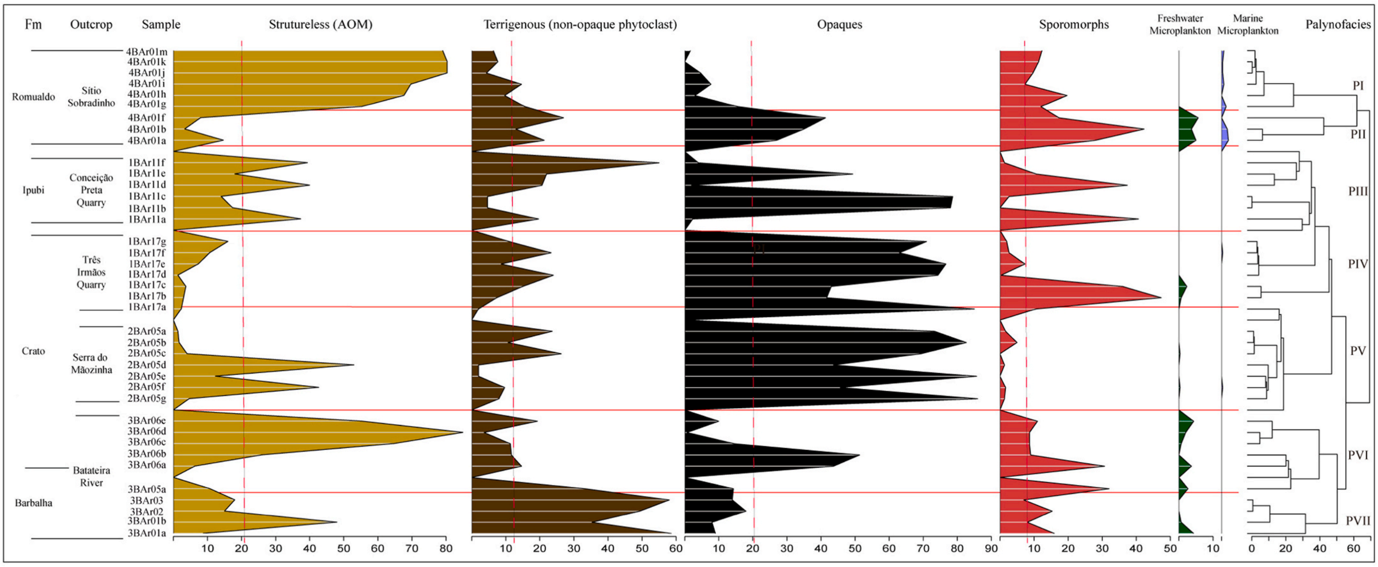

Fig. 5. Distribution of organic components in each sample along the Santana Group, based on outcrops, Dashed line: General average, Fm: Formation.

Table 2
Average abundance of organic components for the studied sections. In bold the most significant organic components.

Formation	Outcrop	Struteless	Terrigenous	Opaques	Sporomorphs	Freshwater	Marine
Romualdo	Sítio Sobradinho	**67.7**	13.0	7.7	12.3	0.0	**0.7**
Ipubi	Conceição Preta Quarry	27.7	20.2	26.7	6.7	0.0	0.0
Crato	Três Irmãos Quarry	3.7	11.0	**71.0**	7.3	0.0	0.0
	Serra do Mãozinha	4.7	9.7	**73.3**	1.3	0.0	0.0
	BatateiraRiver	**55.3**	11.7	14.7	9.0	2.0	0.0
Barbalha	Batateira River	15.0	**49.3**	14.0	15.3	0.7	0.0
General Average		21.3	12.3	20.7	8.2	0.5	0.1

angiosperm pollen grains (typical of the Alagoas local Stage flora). Sporomorphs presents a general average of 8.2% of the total kerogen and occurs predominantly in Batateira River section, it reaches an average of 15.3% (Table 2).

The palynological data of the sections indicated a typicall Aptian association (e.g., Regali and Viana, 1989; Regali and Santos, 1999), more specifically to the upper Aptian (P-270 Palynozone) based in the records of *Sergipea variverrucata* (Regali et al., 1974; Regali and Viana, 1989; Regali and Santos, 1999). Several taxa had been determined (e.g., *Cicatricosisporites avnimelechi*, *Paludites mamelonatus*, *Deltoidospora australis*, *Densoisporites australis*, *Leptolepidites verrucatus* and *Klukisporites foveolatus*, in addition to *Afropollis jardinus*, *Afropollis zonatus*, *Bennettitaepollenites regaliae*, *Callialasporites dampieri*, *Callialasporites segmentatus*, *Callialasporites trilobatus*, *Araucariacites australis*, *Equisetosporites concinnus*, *Equisetosporites elegans*, *Gnetaceaepollenites retangulares*, *Gnetaceaepollenites jansonii*, *Sergipea variverrucata*, *Singhia montanaensis*, *Stellatopollis araripensis*, *Stellatopollis densiornatus*, *Stellatopollis dubius*, *Trisectoris reticulatus* and *Uesuguipollenites callosus*) correlated to those reported from the upper Aptian Brazilian marginal basins (e.g., Regali et al., 1974; Lima, 1978; Dino, 1992; Regali and Santos, 1999; Heimhofer and Hochuli, 2010; Carvalho et al., 2019).

4.4. *Terrigenous (non-opaque phytoclast)*

In our material, the terrigenous elements are essentially composed of continental organic particles: non-opaque biostructured phytoclasts. The terrigenous particles show a general average of 12.3% of the total kerogen and occurs predominantly at the Batateira River section (Table 2). It is mainly found in the base of the studied section, which corresponds to the Batateira Beds.

Terrigenous particles are well preserved, structured (mainly striate, banded and cuticles), and its predominance suggests the proximity to a fluvial-deltaic source and moderately dysoxic condition (Tyson, 1995; Kholeif and Ibrahim, 2010). Generally, large amounts of phytoclast particles are deposited by rivers in estuaries and deltas, both close to shorelines (Carvalho et al., 2006).

4.5. *Structureless (AOM)*

Structureless is the most abundant components in the association (average of 21.3% of the total kerogen). It is composed of AOM usually occurring heterogeneously, thick and thin shapes (sometimes small in size) in dark brown color, containing inclusions (e.g., small fragments of phytoclast) and of lower fluorescence. Structureless particles occur in all investigated sections. In the Sítio Sobradinho section, AOM it is the most abundant particularly the AOM thick type, Batateira River has nearly the same abundance, but thinner AOM. A large amount of AOM results from the combination of the high preservation rate and low-energy environment attributed to dysoxic-anoxic conditions (Carvalho et al., 2006).

4.6. *Opaques*

Opaque particles are composed exclusively by phytoclasts of black color even at the grain boundary (corroded and equidimensional). The association averages 20.7% (Table 2) of total kerogen and occurs predominantly in Serra do Mãozinha and Três Irmãos Quarry sections, being dominated by corroded shape.

The opaque phytoclasts are derived from the oxidation of woody materials either during prolonged transport or post-depositional alteration; the high values of the black debris indicate oxidizing conditions and either proximity to terrestrial sources or redeposition of organic matter from fluvio-deltaic environment of deposition (Tyson, 1989;

Atta-Peters et al., 2013).

Based on the association and distribution of the kerogen group, seven palynofacies were identified (PI-PVII) (Fig. 5). The Palynofacies I (P–I) occurs between (4BAr01m-4BAr01g), Sítio Sobradinho (Romualdo Formation) and is characterized by the high abundance of AOM (50.81%) and absence of freshwater microplankton. The low average of marine microplankton in the P1 is represented by the dinocyst *Subtilisphaera*. The Palynofacies II (P-II) (4BAr01f-4BAr01a) also recorded in samples from Sítio Sobradinho (Romualdo Formation) is characterized by the highest abundance of sporomorphs (18%), opaque phytoclasts (15.33%) followed with lower presence of freshwater microplankton (1.61%) and marine elements. The Palynofacies III (P-III) is recorded in the site Conceição Preta Quarry (Ipubi Formation) and is characterized by the highest proportion of opaque phytoclasts (35%) with presence of AOM (30%) and lower presence of non-opaque phytoclasts (20.5%) and sporomorphs (15%). The Palynofacies IV (P-IV) is recorded in the site Três Irmãos Quarry (Crato Formation) and is characterized by the highest proportion of opaque phytoclasts (66%), and low presence of sporomorphs (14%) followed by non-opaque phytoclasts (13%) and AOM (6.43%). The Palynofacies V (P–V) identified in samples from the outcrop Serra do Mãozinha is dominated by opaque phytoclast (70%) with lower presence of AOM (17.5%) and rare sporomorphs (1.57%). The low presence of marine microplankton is represented by the presence of foraminiferal lining. The Palynofacies VI (P-VI) Batateira River (Crato Formation) is composed mainly by AOM (48%) and a lower presence of opaque phytoclast (24%) and sporomorphs (13.6%) with freshwater microplankton (2.13%). The Palynofacies VII (P-VII), which occurs in Batateira River (Barbalha Formation), is dominated by non-opaque phytoclasts (41.42%) with presence of AOM (26.32%) and lower presence of sporomorphs (15%) and rare freshwater microplankton (1.54%).

5. Discussion

The Aptian Stage in the Araripe Basin is characterized by transgressive-regressive cycles, related to the fragmentation of Gondwana and the opening of the South Atlantic Ocean (Assine, 2007; Coimbra et al., 2002). The transition from a fluvial-lacustrine to an open marine environment in the Santana Group is recognizable from the palynofacies data. Therefore, the averages of palynofacies associations are considered for the analyzed sections as the proportional abundance groups not only reflecting the biological origin as well as the paleoenvironmental evolution and reinforce the evidence of intermittent marine incursions in a broad non-marine setting, as pointed by Varejão et al. (2021). The proposed changes in environmental conditions over time are supported by the stratigraphic correlation framework of the Lower Cretaceous deposits of the interior basins of NE Brazil and the sedimentary events recorded in the Brazilian marginal basins (e.g., Arai and Assine, 2020; Melo et al., 2020; Coimbra and Freire, 2021).

The lower part of the Batateira River studied section corresponds to the Batateira Bed, which represent the first lacustrine cycle of Santana Group, under anoxic conditions (Assine, 2007), with a trend of slightly increased salinity (Pontes et al., 2021), represented by the P-VII and is dominated by non-opaque phytoclasts. According to Pontes et al. (2021) it encompasses fluvial braided systems gradually replaced by a lacustrine establishment, where AOM show a decreasing trend following the Batateira Beds, this decrease is accompanied by an increasing trend of opaque particles (Fig. 5). The Barbalha Formation (lower Batateira river section) exhibits characteristics of a proximal environment, close to the parent flora. The genera *Cicatricosisporites*, *Psilatriletes*, *Classopollis* and *Equisetosporites* are dominants, characterizing an inner shelf settings as most terrestrial organic matter close to the fluvial-deltaic source (Mendonça Filho et al., 2011). The fact that terrestrial particles are dominant, followed by the abundance of the sporomorphs assemblage indicates proximity to source (e.g., rivers) in a lacustrine system.

In the Crato Formation (upper Batateira river section), AOM shows a conspicuous increasing upward trend in this section. This is accompanied by the presence of *Botryococcus* and an increased number of opaque particles, followed by an abrupt decrease of non-opaque phytoclasts reflected in the P-VI (Fig. 5). These different peaks of change in SOM occurred in freshwater to saline lacustrine zones (Neumann et al., 2003). The presence of *Botryococcus* clearly suggests deposition under brackish conditions (Tyson, 1995; Batten, 1996). According to Tyson (1995) if there is a reduction in the water depth, as a function of the increased evaporation taxa, an increase in salinity also occurs. The paleoenvironmental interpretation for this section is supported using ternary diagram (Mendonça Filho et al., 2014). Fig. 6 shows that, except for three samples (3BAr01a, 3BAr05a and 3BAr06a), all other samples indicate high salinity conditions in the deposition of Batateira river section, there is evidence of brackish conditions with freshwater influence in the deposition sites. As demonstrated by Varejão et al. (2021) this is intrinsically related to unconfined bayhead and hypersaline lacustrine environments.

The relative abundance of AOM increases from proximal to distal direction under dysoxic to anoxic shelf environments (Tyson, 1996). The renewed input of freshwater, during episodes of lacustrine water level rise and spread, could reflect a fluvial system, considering that in basins with preservation of AOM and with reducing conditions the allochthonous terrestrial material is only dominant near the fluvial-deltaic sources or with turbidites (Tyson, 1993). The lower average of freshwater and the absence of dinoflagellate cysts allows to infer a brackish lagoonal to lagoonal coastal plain paleoenvironment in transitional phase with oxygen-deficient (dysoxic-anoxic) conditions, deposited under black shales.

The Crato Formation at the Serra do Mãozinha is composed of laminated limestone interspersed with very fine sand and shale, where opaque particles clearly show a conspicuous increase in all section (Fig. 5). On the other hand, the increasing trend of AOM observed in the Batateira River was the opposite. Even so, small amounts of terrigenous particles are recorded. A low presence of marine elements shows the existence of short-lived marine incursions in the Crato Formation (Goldberg et al., 2019; Varejão et al., 2020; Varejão et al., 2021). This association is reflected in the P–V and is characterized by high contents of opaque phytoclasts (e.g., corroded). These particles are derived from the oxidation of woody materials either during prolonged transport or during post-depositional alteration, the high values indicate oxidizing conditions and either proximity to terrestrial sources or redeposition of organic matter from fluvio-deltaic environment (Tyson, 1989; Kholeif and Ibrahim, 2010; Atta-Peters et al., 2013). Evidence of subaerial exposure or, at least, extremely shallow conditions with rare foraminiferal lining, reinforce the intermittent marine incursions (Goldberg et al., 2019; Varejão et al., 2021) and the occurrence of marine to lagoonal coastal plain in a transitional environment.

Along the Três Irmãos Quarry, the Crato Formation deposits recorded a conspicuous predominance of opaque phytoclasts (e.g., corroded) with a presence of terrigenous particles, reflected in the P-IV this section is similar to the Serra do Mãozinha section. The opaque phytoclasts dominate the sedimentary organic matter recorded in the samples from these two sections, which contain minor amounts of AOM and sporomorphs particles. This association reflects oxidizing depositional paleoenvironmental that tends to destroy the majority of less resistant organic particles (Mendonça Filho et al., 2011, 2014).

Represented by an evaporite pack (Assine, 1992; Ponte and Appi, 1990), the Ipubi Formation is interpreted as originating in coastal environments (supratidal), susceptible to relative variations in sea level (Assine, 2007). AOM and opaque particles are the most abundant in Conceição Preta Quarry, represented in the P-III reflecting a depositional trend that was strongly controlled by the evaporitic sequence generated in a coastal sabkha environment, deposited in restricted portions of a carbonate lagoon (Bobco et al., 2017). The high average of AOM, greater than sporomorphs, indicates enhanced preservation in reducing conditions and increased stability of the water column, resulting in dysoxic or

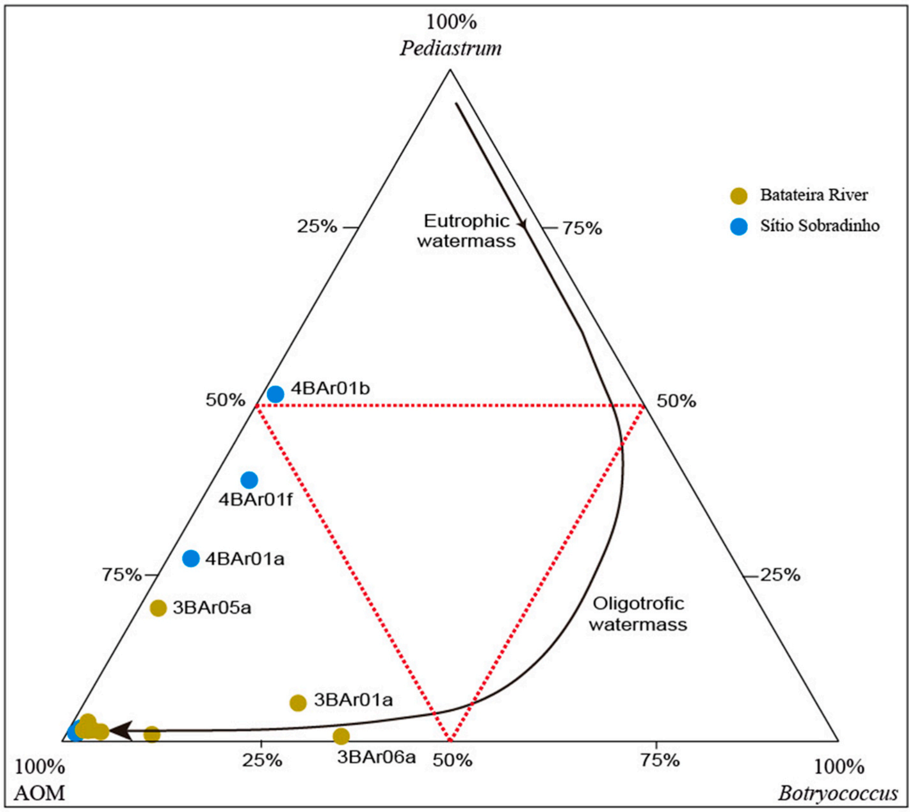

Fig. 6. Ternary diagram. Palynomorphs and AOM assemblages are represented by the content of AOM, *Pediastrum* and *Botryococcus* indicates the salinity conditions in the deposition sites and to distinguish the trophic state in lacustrine environments.

anoxic bottom conditions (Tyson, 1993, 1995). Our data on the Conceição Preta Quarry reinforces the idea of Bobco et al. (2017) that suggested a deposition of this formation subaqueous and intra sedimentary settings in a coastal sabkha under anoxic conditions, hypersaline in an environment transitional under the influence of marine transgression (Moura et al., 2020).

The age of the Romualdo Formation, upper unit of Santana Group, is assigned to the late Aptian (Melo et al., 2020; Arai and Assine, 2020). The Sítio Sobradinho section is strongly dominated by AOM, low average of terrigenous and palynomorphs, indicative of mixed siliciclastic-carbonate marine ramp paleoenvironment (Melo et al., 2020). According to Tyson (1995), high percentages of AOM indicate deposition in reducing environments, temporarily suboxic/anoxic with high preservation of autochthonous planktonic organic material or microbial benthic material. The base of the sedimentary succession (4BAr01a-4BAr01f) represented by the P-II, suggests a transitional environment with a reduction in salinity concentration (Fig. 6) this reduction could be explained by the presence of *Pediastrum* which is less tolerant to elevated salinities (Tyson, 1993). After the marine conditions established and shown in the P–I, the occurrence of *Subtilisphaera* Ecozone, a typical Tethyan dinocyst assemblage (Arai, 2014; Arai et al., 2000), demonstrates the circulation of marine waters in the Araripe Basin during its deposition reinforcing the interpretation of Custódio et al. (2017), Teixeira et al. (2017), Melo et al. (2020), Arai and Assine (2020). The existence of marine components, associated with higher amounts of AOM which results from a combination of the high preservation rate and lower energy environments, in dysoxic conditions Tyson (1993); Teixeira et al. (2017).

6. Conclusions

This research provides a new contribution to the palaeoenvironmental conditions during the Aptian and, more precisely, late Aptian in the Araripe Basin. Our data from outcrops in the Santana Group suggested a depositional trend that is strongly controlled by a fluvial input to a shallow marine environment. The knowledge on the biology of certain plankton groups reveals significant evidence regarding salinity and water depth. Therefore, palynofacies analysis provides essential information on sedimentary processes and palaeoenvironment within a depositional system. On the other hand, the occurrence of foraminiferal lining reinforces a marine influence.

CRediT authorship contribution statement

Juan David Vallejo Ramírez: Writing – review & editing, Writing – original draft, Methodology, Investigation, Conceptualization. **Enelise Katia Piovesan:** Writing – review & editing, Writing – original draft, Conceptualization. **Marcelo de Araujo Carvalho:** Writing – review & editing, Writing – original draft, Conceptualization. **Juliana Guzmán:** Writing – review & editing, Writing – original draft.

Declaration of competing interest

The authors declare that they have no known competing financial interests or personal relationships that could have appeared to influence the work reported in this paper.

Data availability

The data that has been used is confidential.

Acknowledgments

The authors would like to acknowledge the Brazilian National

Petroleum Agency (ANP) and PETROBRAS for financial support through the following projects: “ARTUNJA: Correlações bioestratigráficas dos sistemas flúvio-lacustres das fases rifte e pós-rifte das bacias do Araripe, Jatobá e Tucano Norte, NE do Brasil/n. 2017/00263-2”; “Implantação da infraestrutura do Laboratório de Micropaleontologia Aplicada da Universidade Federal de Pernambuco/n. 2018/00320-9” and “Bioestratigrafia de alta resolução e paleoambientes das bacias do Araripe, Tucano Norte e Jatobá (seções rifte e pós-rifte)/n. 2019/00280-0”. EKP thanks the Conselho Nacional de Desenvolvimento Científico e Tecnológico –CNPq (grant n. 309766/2021-4). We also thank the reviewers and the editor for their useful suggestions and comments.

References

Arai, M., Botelho, N., Lana, C., Pedrão, E., 2000. Cretaceous dinoflagellate provincialism in Brazilian marginal basins. Cretac. Res. 21 (2–3), 351–366. https://doi.org/10.1006/cres.2000.0211.

Arai, M., Coelho, P.S., 2001. Statitical analysis of palynological assemblages from the Aptian-Albian of the Araripe Basin, northeast Brazil: a case study of paleoenvironmental significance of Early Cretaceous terrestrial palynomorphs. Asociación Paleontológica Argentina. VII International Symposium on Mesozooic Terrestrial Ecosystems 25–28, 30–36. Buenos Aires.

Arai, M., 2014. Aptian/albian (early cretaceous) paleogeography of the South Atlantic: a paleontological perspective. Braz. J. Genet. 44 (2), 339–350. https://doi.org/10.5327/Z2317-4889201400020012.

Arai, M., Assine, M.L., 2020. Chronostratigraphic constraints and paleoenvironmental interpretation of the Romualdo Formation (Santana group, Araripe Basin, northeastern Brazil) based on palynology. Cretac. Res. 116, 104610 https://doi.org/10.1016/j.cretres.2020.104610.

Asmus, H.E., Ponte, F.C., 1973. The Brazilian marginal basins. In: NAIRN, A.E.M., STEHILI, F.G. (Eds.), The Ocean Basins and Margins, Volume 1 – the South Atlantic. Plenum Press, New York, pp. 87–133.

Assine, M.L., 1992. Análise estratigráfica da Bacia do Araripe, nordeste do Brasil. Rev. Bras. Geociencias 22 (3), 289–300.

Assine, M.L., 2007. Bacia do Araripe. Bol. Geociencias Petrobras 15, 371–389.

Assine, M.L., Perinotto, J.A. de J., Custódio, M.A., Neumann, V.H., Varejão, F.G., Mescolotti, P.C., 2014. Sequências deposicionais do Andar Alagoas da Bacia do Araripe, Nordeste do Brasil. Bol. Geociencias Petrobras 22, 3–28.

Assine, M.L., Quaglio, F., Warren, L.V., Simões, M.G., 2016. Comments on paper by M. Arai “aptian/albian (early cretaceous) paleogeography of the South Atlantic: a paleontological perspective”. Braz. J. Genet. 46 (1), 3–7. https://doi.org/10.1590/2317-4889201620150046A.

Atta-Peters, Achaegakwo, C.A., 2015. Palynofacies and palaeoenvironmental significance of the Albian – cenomanian succession of the Epunsa - 1 well, onshore Tano basin, western Ghana. J. Afr. Earth Sci. 114, 1–12. https://doi.org/10.1016/j.jafrearsci.2015.10.020.

Atta-Peters, D., Agama, C.I., Asiedu, D.K., Apesegah, E., 2013. Palynology, palynofacies and palaeoenvironments of sedimentary organic matter from Bonyere-1 Well, Tano basin, western Ghana. Int. Lett. Nat. Sci. 5, 27–45. https://doi.org/10.56431/p-i2vlvk.

Araripe, R.A., Pedrosa Lemos, F.A., do Prado, L.A., Tomé, M.E., Oliveira, D.H., Pereira, P. A., Nascimento, L.R., Asakura, Y., Ng, C., Viviers, M.C., Barreto, A.F., 2022. Upper aptian-lower albian of the southern-central Araripe Basin, Brazil: microbiostratigraphic and paleoecological inferences. J. S. Am. Earth Sci. 116–103814. https://doi.org/10.1016/j.jsames.2022.103814.

Batten, D., 1996. Palynofacies and palaeoenvironmental interpretation. In: Jansonius, J., McGregor, D.C. (Eds.), Palynology: Principles and Applications, vol. 3. Americam Association of Stratigraphic Palynologist Foundation, pp. 1011–1064.

Benigno, A.P., Saraiva, A.Á., Sial, A.N., Lacerda, 2021. Mercury chemostratigraphy as a proxy of volcanic-driven environmental changes in the Aptian-Albian transition, Araripe Basin, northeastern Brazil. J. S. Am. Earth Sci. 107, 103020. https://doi.org/10.1016/j.jsames.2020.103020.

Bobco, F.E.R., Goldberg, K., Bardola, T.P., 2017. Modelo deposicional do Membro Ipubi (Bacia do Araripe, nordeste do Brasil) a partir da caracterização faciológica petrográfica e isotópica dos evaporitos. Pesqui. em Geociencias 44 (3), 431–451. https://doi.org/10.22456/1807-9806.83267.

Brito Neves, B.B., 1990. A Bacia do Araripe no contexto geotectônico regional. In: simpósio sobre a Bacia do Araripe e bacias interiores do Nordeste. Crato. Atas. Grato. DNPM 1, 21–33.

Brito Neves, B.B., Santos, E.J., Van Schmus, W.R., 2000. Tectonic history of the Borborema province, northeastern Brazil. In: Cordani, U.G., Milani, E.J., Thomaz Filho, A., Campos, D.) (Eds.), Tectonic Evolution of South America, Eds. 31st International Geological Congress, Rio de Janeiro, p. 21.

Candel, S.M., Borromei, A.M., Martínez, M.A., Bujalesky, G., 2013. Palynofacies analysis of surface sediments from the Beagle Channel and its application as modern analogues for Holocene records of Tierra del Fuego, Argentina. BioOne Res. 37 (1), 62–76. https://doi.org/10.1080/01916122.2012.718994.

Carvalho, M.A., Mendonça Filho, J.G., Menezes, T.R., 2006. Palynofacies and sequence stratigraphy of the aptian–albian of the sergipe basin, Brazil. Sediment. Geol. 192, 57–74. https://doi.org/10.1016/j.sedgeo.2006.03.017.

Carvalho, M.A., Ramos, R.C., Crud, M.B., Witovisk, L., Kellner, A.W., Silva, H.P., Grillo, O.N., Riff, D., Romano, P.S., 2013. Palynofacies as indicators of paleoenvironmental changes in a cretaceous succession from the larsen basin, james ross island, Antarctica. Sediment. Geol. 295, 53–66. https://doi.org/10.1016/j.sedgeo.2013.08.002.

Carvalho, M.A., Bengtson, P., Lana, C.C., de Sá, N.P., Santiago, G., da Giannerini, M.C.S., 2019. Late Aptian (Early Cretaceous) dry–wet cycles and their effects on vegetation in the South Atlantic: palynological evidence. Cretac. Res. 100, 172–183. https://doi.org/10.1016/j.cretres.2019.03.021.

Chagas, D.B., Assine, M.L., Freitas, F.I., 2007. Sedimentary facies and depositional environments of the Barbalha Formation, Araripe basin, northeastern Brazil. Geociencias 26, 313–322. https://www.researchgate.net/publication/286738532.

Coimbra, J.C., Arai, M., Carreño, A.L., 2002. Biostratigraphy of lower cretaceous microfossils from the Araripe Basin, northeastern Brazil. Geobios 35 (6), 687–698. https://doi.org/10.1016/S0016-6995(02)00082-7.

Coimbra, J.C., Freire, T.M., 2021. Age of the post-rift Sequence I from the Araripe Basin, lower cretaceous, NE Brazil: implications for spatio-temporal correlation. A J. Braz. Soc. Paleontol. 24 (1), 37–46. https://doi.org/10.4072/rbp.2021.1.03.

Custódio, M.A., Quaglio, F., Warren, L.V., Simões, M.G., Fürsich, F.T., Perinotto, J.A.J., Assine, M.L., 2017. The transgressive-regressive cycle of the Romualdo Formation (Araripe Basin): sedimentary archive of the early cretaceous marine ingression in the interior of northeast Brazil. Sediment. Geol. 359, 1–15. https://doi.org/10.1016/j.sedgeo.2017.07.010.

Dino, R., 1992. Palinologia, Bioestratigrafia e Paleoecologia da Formação Alagamar-Cretáceo da Bacia Potiguar, Nordeste do Brasil. Tese de Doutorado, Instituto de Geociências da USP, p. 299p.

Fabin, C.E., Correia Filho, O.J., Alencar, M.L., Barbosa, J.A., Miranda, T.S., Neumann, V. H., Gomes, I.F., Santana, F.R., 2018. Stratigraphic relations of the Ipubi Formation: siliciclastic-evaporitic succession of the Araripe Basin. Annal. Braz. Acad. Sci. 90 (2), 2049–2071. https://doi.org/10.1590/0001-3765201820170526.

Fambrini, G.L., Silvestre, D., Menezes-Filho, A.B., Da Costa, A.C., Neumann, V.H., 2019. Architectural and facies characterization of the aptian fluvial Barbalha Formation, Araripe Basin, NE Brazil. In: Geoscience to Engineering. Geological Society of London, Special Publications, pp. 119–150. https://doi.org/10.1144/SP488-2017-275, 488.

Fürsich, F.T., Custódio, M.A., Matos, S.A., Hethze, M., Quaglio, F., Warren, L.V., Assine, M., Simões, M.G., 2019. Analysis of a cretaceous (late aptian) high-stress ecosystem: the Romualdo Formation of the Araripe Basin, northeastern Brazil. Cretac. Res. 95, 268–296. https://doi.org/10.1016/j.cretres.2018.11.021.

Garcia, A.J.V., Da Rosa, A.A.S., Goldberg, K., 2005. Paleoenvironmental and paleoclimatic control on early diagenetic processes and fossil record in Cretaceous continental sandstones of Brazil. J. S. Am. Earth Sci. 19 (3), 243–258. https://doi.org/10.1016/j.jsames.2005.01.008.

Goldberg, K., Preamor, E., Bardola, T., Souza, P.A., 2019. Aptian marine ingression in the Araripe Basin: implications for paleogeographic reconstruction and evaporite accumulation. Mar. Petrol. Geol. 107, 214–221. https://doi.org/10.1016/j.marpetgeo.2019.05.011.

Hashimoto, A.T., Appi, C.J., Soldan, A.L., Cerqueira, J.R., 1987. O Neo-Alagoas nas bacias do Ceará. Araripe e Potiguar (Brasil): caracterização estratigráfica e paleoambiental. Rev. Bras. Geociencias 17 (2), 118–122.

Heimhofer, U., Hochuli, P.A., 2010. Early Cretaceous angiosperm pollen from a low-latitude succession (Araripe Basin, NE Brazil). Rev. Palaeobot. Palynol. 161 (3–4), 105–126. https://doi.org/10.1016/j.revpalbo.2010.03.010.

Huber, B.T., Leckie, M., 2011. Planktic foraminiferal species turnover across deep-sea Aptian/Albian boundary sections. J. Foraminifer. Res. 41 (1), 53–95. https://doi.org/10.2113/gsjfr.41.1.53.

Huber, B.T., Macleod, K.G., Gröcke, D.R., Michal Kucera, M., 2011. Paleotemperature and paleosalinity inferences and chemostratigraphy across the Aptian/Albian boundary in the subtropical North Atlantic. Paleoceanogr. Paleoclimatol. 26 (4), PA4221. https://doi.org/10.1029/2011PA002178.

Jain, K.P., Millepied, P., 1975. Cretaceous microplankton from Senegal basin, west africa. II. Systematics and biostratigraphy. Geophytology 5, 126–171.

Kholeif, S., Ibrahim, M., 2010. Palynofacies analysis of inner continental shelf and middle slope sediments offshore Egypt, south-eastern mediterranean. Geobios 43 (3), 333–347. https://doi.org/10.1016/j.geobios.2009.10.006.

Lima, M.R., 1978. Palinologia da Formação Santana (Cretáceo do Nordeste do Brasil). Instituto de Geociências, Universidade de São Paulo, São Paulo, Tese de Doutoramento, pp. 335–392p.

Martill, D.M., Bechly, G., Loveridge, R.F., 2007. Window into an Ancient World. In: The Crato Fossil Beds of Brazil. Cambridge University Press, p. 625.

Melo, R.M., Guzmán, J., Almeida-Lima, D., Piovesan, E.K., Neumann, V., Sousa, A.J., 2020. New marine data and age accuracy of the Romualdo Formation, Araripe basin, Brazil. Sci. Rep. 10, 15779 https://doi.org/10.1038/s41598-020-72789-8.

Mendonça Filho, J.G., Chagas, R.B.A., Menezes, T.R., Mendonça, J.O., Da Silva, F.S., Sabadinisantos, E., 2010. Organic facies of the oligocene lacustrine system in the cenozoic taubaté basin, southern Brazil. Int. J. Coal Geol. 84, 166–178. https://doi.org/10.1016/j.coal.2010.07.004.

Mendonça Filho, J.G., Menezes, T.R., Mendonça, J.O., 2011. Organic composition (palynofacies analysis). In: 4th ICCP Training Course on Dispersed Organic Matter, pp. 33–81 (Chapter 5).

Mendonça Filho, J.G., Menezes, T.R., Mendonça, J.O., 2014. Organic composition (palynofacies analysis). In: 7th ICCP Training Course on Dispersed Organic Matter. GFZ (Deutsches GeoForschungs Zentrum, Potsdam, Germany, pp. 36–89 (Chapter 5).

Moura, W.A.L., Araújo, J.C.M., Lúcio, T., Souza Neto, J.A., 2020. Paleoambiente deposicional e origem da matéria orgânica dos folhelhos betuminosos da Formação Ipubi, porções leste e sudeste da Bacia do Araripe, NE do Brasil: evidência de N-Alcanos e Isoprenoides. Estudos Geológicos. 30 (1), 31–44. https://periodicos.ufpe.br/revistas/estudosgeologicos/index.

Neumann, V.H., 1999. Estratigrafía, Sedimentología, Geoquímica y Diagénesis de lós Sistemas Lacustres Aptienses-Albienses de la Cuenca de Araripe (Noreste de Brasil). Universidad de Barcelona, Ph.D. thesis, p. 244.

Neumann, V.H., Cabrera, L., 1999. Una nueva propuesta estratigráfica para la tectonosecuencia post-rifte de la Cuenca de Araripe, Noreste de Brasil. In: Simpósio sobre o Cretáceo do Brasil, 5, Boletim de Resumos, Serra Negra, UNESP/IGCE, pp. 279–285.

Neumann, V., Assine, M., 2015. Strati 2015 – 2nd International Congress on Stratigraphy. In: Stratigraphic Proposal to the Post-Rift I Tectonic-Sedimentary Sequence of Araripe Basin, Northeastern Brazil. Berichete des Institutes für Erdwissenschaften der Universtät Graz, p. 274.

Neumann, V.H., Borrego, A.G., Cabrera, L., Dino, R., 2003. Organic matter composition and distribution through the Aptian-Albian lacustrine sequences of the Araripe Basin, northeastern Brazil. Int. J. Coal Geol. 54, 21–40. https://doi.org/10.1016/S0166-5162(03)00018-1.

Ponte, F.C., Appi, C.J., 1990. Proposta de revisão da coluna estratigráfica da Bacia do Araripe. In: Congresso Brasileiro de Geologia, 36. Sociedade Brasileira de Geologia, Natal, pp. 211–226.

Ponte, F.C., Asmus, H.E., 1978. Geological framework of the Brazilian continental margin. Geol. Rundsch. 67, 201–235.

Ponte, F.C., Ponte Filho, F.C., 1996. Evolução Tectônica e Classificação da Bacia do Araripe. Report of the Departamento Nacional de Produção Mineral: Recife, Brazil, p. 68.

Pontes, N.V., das Chagas, D.B., de Souza, A.C.B., do Nascimento Junior, D.R., da Silva Filho, W.F., Capilla, R., Garcia, A.J.V., de Araújo Nogueira Neto, J., 2021. Organic and isotopic geochemistry of evaporites and shales of the Santana group (Araripe Basin, Brazil): clues on the evolution of depositional systems and global correlation during the lower cretaceous. Minerals 1 (8), 795. https://doi.org/10.3390/min11080795.

Regali, M.S.P., Uesugui, N., Santos, A.S., 1974. Palinologia dos sedimentos Meso-Cenozóicos do Brasil (II). Bol. Tec. Petrobras 17 (4), 263–301.

Regali, M.S.P., Santos, P.R.S., 1999. Palinoestratigrafia e geocronologia dos sedimentos albo-aptianos das bacias de Sergipe e Alagoas – Brasil. In: 5th Simpósio sobre o Cretáceo do Brasil, Serra Negra, Boletim de resumo, pp. 411–419.

Regali, M.S.P., Viana, C.F., 1989. Sedimentos do Neojurássico-Eocretáceo do Brasil: Idade e correlação com a escala internacional. Petrobras, p. 95.

Scherer, C.M.S., Goldberg, K., Bardola, T., 2015. Facies architecture and sequence stratigraphy of an early post-rift fluvial succession, Aptian Barbalha Formation, Araripe Basin, northeastern Brazil. Sediment. Geol. 322 (1), 43–62. https://doi.org/10.1016/j.sedgeo.2015.03.010.

Teixeira, M.C., Mendonça Filho, J.G., de Oliveira, A.D., Assine, M.L., 2017. Faciologia orgânica da Formação Romualdo (Grupo Santana, Cretáceo Inferior da Bacia do Araripe): caracterização da matéria orgânica sedimentar e interpretação paleoambiental. Geol. Usp. Série Científica 17 (4), 19–44. https://doi.org/10.11606/issn.2316-9095.v17-347.

Tyson, R.V., 1989. Late jurassic palynofacies trends, piper and kimmeridge clay formation, UK onshore and offshore. In: Batten, D.J., Keen, M.C. (Eds.), Northwest European Micropalaeontology and Palynology. British Micropalaeontological Society Series, pp. 135–172.

Tyson, R.V., 1993. Palynofacies analysis. In: Jenkins, D.J. (Ed.), Applied Micropalaeontology. Kluwer Academic Publishers, Dordrecht, pp. 153–191.

Tyson, R.V., 1995. Sedimentary Organic Matter: Organic Facies and Palynofacies. Chapman & Hall, Londres, p. 615.

Tyson, R.V., 1996. Sequence-stratigraphical Interpretation of Organic Facies Variations in Marine Siliciclastic Systems; General Principles and Application to the Onshore Kimmeridge Clay Formation, vol. 103. Geological Society, London, Special Publications, UK, pp. 75–96. https://doi.org/10.1144/GSL.SP.1996.103.01.0.

Varejão, F.G., 2019. Abordagem multi-indicadores do sistema misto carbonáticosiliciclástico da Formação Crato: evolução sedimentar, paleogeografia e tectônica. PhD thesis. Universidade Estadual Paulista "Júlio de Mesquita Filho", p. 163.

Varejão, F.G., Fürsich, F.T., Warren, L.V., Matos, S.A., Rodrigues, M.G., Assine, M.L., Sales, A.M.F., Simões, M.G., 2019. Microbialite fields developed in a protected rocky coastline: the shallow carbonate ramp of the Aptian Romualdo Formation (Araripe Basin, NE Brazil). Sediment. Geol. 389, 103–120. https://doi.org/10.1016/j.sedgeo.2019.06.003.

Varejão, F.G., Sila, V.R., Assine, M.L., Warren, L.V., Matos, S.A., Rodrigues, M.G., Fürsich, F.T., Simões, M.G., 2020. Marine or freshwater? Accessing the paleoenvironmental parameters of the caldas bed, a key marker bed in the Crato Formation (Araripe Basin, NE Brazil). Braz. J. Genet. 51 (1), e2020009 https://doi.org/10.1590/2317-4889202120200009.

Varejão, F.G., Warren, L.V., Simões, M.G., Buatois, L.A., Mángano, M.G., Rumbelsperger, A.M., Assine, M.L., 2021. Mixed siliciclastic–carbonate sedimentation in an evolving epicontinental sea: Aptian record of marginal marine settings in the interior basins of north-eastern Brazil. Sedimentology 68, 2125–2164. https://doi.org/10.1111/sed.12846.

APÊNDICE F- ARTIGO PUBLICADO EM *CRETACEOUS RESEARCH*

Cretaceous Research xxx (xxxx) xxx

Contents lists available at ScienceDirect

Cretaceous Research

journal homepage: www.elsevier.com/locate/CretRes

Sedimentary organic matter and paleoenvironmental reconstruction of the Santana Group (Lower Cretaceous), Araripe Basin, Northeast Brazil

Juan David Vallejo [a, b, *], Regina Buarque de Gusmão [a, b], Marcelo de Araujo Carvalho [c], Claus Fallgatter [a, b], Enelise Katia Piovesan [a, b]

[a] Applied Micropaleontology Laboratory (LAGESE/LITPEG), Department of Geology, Federal University of Pernambuco, Recife-PE, Av. Da Arquitetura, s/n, CEP 50740-540, Brazil
[b] Graduate Program in Geosciences, Technology and Geosciences Centre, Federal University of Pernambuco, Recife-PE, Av. da Arquitetura, s/n, CEP 50740-550, Brazil
[c] Plant Paleoecology Laboratory (LAPAV), Department of Geology and Paleontology, National Museum, Federal University of Rio de Janeiro, Rio de Janeiro-RJ, Brazil

ARTICLE INFO

Article history:
Received 23 May 2024
Received in revised form
19 September 2024
Accepted in revised form 27 September 2024
Available online xxx

Keywords:
Palynofacies
Late Aptian
Post-rift I sequence
Biozone

ABSTRACT

Depositional controls of the Santana Group in the Araripe Basin are still being debated. The main controversial subject is their marine influence and paleoenvironmental evolution. In this study, palynofacies analysis was performed on 59 samples from one core drilled at Sítio Romualdo in the Araripe Basin to investigate sedimentary organic matter. Three palynofacies associations (structureless, continental particles, and aquatic + opaque) were identified. The Santana Group consist of Barbalha, Crato, Ipubi and Romualdo formations. Based on palynofacies associations we conclude that the depositional setting of the Barbalha Formation reflects a fluvially-fed lacustrine system under oxic conditions. The Crato Formation, associated with tidal flats, coastal lakes, and lagoons within an open bay environment, represents a bayhead delta system. The Ipubi Formation corresponds to a coastal plain typical of sabkha paleoenvironments, characterized by low energy under reducing conditions, during drier climate conditions. The Romualdo Formation records mainly an estuarine paleoenvironment characterized by dysoxic to anoxic conditions. The presence of palynomorph groups typifies a late Aptian age for the Santana Group, which is based on the range of guide species marked mainly by the presence of *Sergipea variverrucata* biozone (P-270), as well as the occurrence of *Complicatisaccus cearensis* and *Equisetosporites maculosus*. The identification of marine palynomorphs (dinoflagellate cysts *Subtilisphaera* and foraminiferal test linings) are indicative of several, local marine incursions.

© 2024 Elsevier Ltd. All rights are reserved, including those for text and data mining, AI training, and similar technologies.

1. Introduction

The Araripe Basin contains a succession that includes rocks deposited during the extensional process of the Gondwana break-up and the opening of the South Atlantic Ocean during the Early Cretaceous. This period was marked by significant global changes in climate and physiography, including changes in sea level, ocean circulation, and anoxic events (Cooper, 1977; Carvalho et al., 2019), leading to the establishment of much diversified sedimentary environments through an alluvial–fluvial–deltaic–lacustrine to an evaporitic to open marine context from late Aptian to Late Albian (Souza-Lima and Silva, 2018). Recent research has shed light on the paleoenvironmental evolution in the Araripe Basin, particularly focusing on depositional events during the Santana Group sedimentation (Goldberg et al., 2019; Arai and Assine, 2020; Melo et al., 2020; Pontes et al., 2021; Varejão et al., 2021a; Fauth et al., 2023; Guzmán et al., 2023; Vallejo et al., 2023).

The Santana Group, which is part of the Post-rift I sequence (Neumann, 1999; Neumann and Cabrera, 1999; Assine et al., 2014; Neumann and Assine, 2015), consists of the following lithostratigraphic units from base to top: Barbalha (Batateira Beds), Crato,

* Corresponding author.
E-mail address: juandavidv85@gmail.com (J.D. Vallejo).

https://doi.org/10.1016/j.cretres.2024.106016
0195-6671/© 2024 Elsevier Ltd. All rights are reserved, including those for text and data mining, AI training, and similar technologies.

Please cite this article as: J.D. Vallejo, R.B. de Gusmão, M. de Araujo Carvalho *et al.*, Sedimentary organic matter and paleoenvironmental reconstruction of the Santana Group (Lower Cretaceous), Araripe Basin, Northeast Brazil, Cretaceous Research, https://doi.org/10.1016/j.cretres.2024.106016

UNCORRECTED PROOF

Ipubi, and Romualdo formations. These formations are characterized by transgressive-regressive cycles (Coimbra et al., 2002; Assine, 2007; Goldberg et al., 2019; Varejão et al., 2021a, 2021b; Vallejo et al., 2023). The Santana Group is well known for its extensive deposits of laminated limestones, gypsum evaporites, sandstones, carbonate concretions, mudstones, siltstones, and black shales, as well as its complex depositional history (Assine et al., 2014; Varejão, 2019; Fambrini et al., 2020). Although the transgressive-regressive cycle is clear, its impact on the evolution of the paleoenvironment remains controversial.

The Post-rift sequence I consists of rocks of late Aptian–Early Albian age (Ponte and Appi, 1990; Assine, 1992; Arai et al., 2001; Coimbra et al., 2002; Araripe et al., 2022; Bom et al., 2023; Lemos et al., 2023), whereas the variety and abundance of well-preserved ostracods, foraminifera, and palynomorphs indicate a late Aptian age (Arai and Assine, 2020; Melo et al., 2020; Coimbra and Freire, 2021; Guzmán et al., 2023). However, certain discrepancies still exist, particularly concerning the position of the Aptian–Albian boundary (Heimhofer and Hochuli, 2010) and the depositional paleoenvironmental assigned to the Alagoas local Stage (Regali et al., 1974; Beurlen and Regali, 1987) and the subdivision into subzones added by Regali and Santos (1999).

Palynofacies analysis offers an interdisciplinary approach to paleoenvironmental reconstruction, extending beyond the examination of palynomorphs alone and encompassing the entire organic content. Particulate organic matter plays a crucial role as a sedimentary component, offering valuable insights into the source area and depositional setting. The composition and distribution of sedimentary organic matter in marine paleoenvironments has been closely linked to variations in sea level, as demonstrated by several authors (e.g., Tyson, 1995; Carvalho et al., 2006; Teixeira et al., 2017; Goldberg et al., 2019; Vallejo et al., 2023).

This study aims to contribute palynological data and to establish paleoenvironmental conditions during deposition of the Santana Group in the Early Cretaceous from the Araripe Basin, based on palynofacies characteristics.

2. Geological setting

The Araripe Basin (Fig. 1) is located in the northeast of Brazil, within the Borborema Province. It is one of the most extensive and complex of the interior basins, with 9000 km^2 of surface area, mostly developed during the Late Jurassic and Early Cretaceous periods, during the Gondwana break-up and the opening of the South Atlantic Ocean (Asmus and Ponte, 1973; Ponte and Asmus, 1978; Garcia et al., 2005; Assine, 2007; Assine et al., 2014; Scherer et al., 2015). NE-SW and E-W-oriented faults are considered the main structural control of the basin (Fambrini et al., 2011; Scherer et al., 2014).

In this basin, a series of depositional events produces one of the most complex polycyclic systems all in the interior basins, comparable to those of the intracratonic and marginal basins of Brazil (Arai, 2006). The tectonic-sedimentary sequences present a complex setting, which continues to generate various proposals and subdivisions concerning its temporal and geographic emplacement (Ponte and Appi, 1990; Ponte and Ponte Filho, 1996; Assine, 2007; Assine et al., 2014; Neumann and Assine, 2015). The most accepted division for Araripe Basin, is based on regional unconformities: (a) Paleozoic sequence (Upper Ordovician–Lower Silurian), composed of the Cariri Formation; (b) The early rift sequence (Upper Jurassic), Brejo Santo and Missão Velha formations; (c) The rift climax sequence (Lower Cretaceous), Abaiara Formation and (d) post-rift sequences. The post-rift is divided into the post-rift I sequence, corresponding to the Alagoas-Stage (Santana Group), and the post-rift II sequence, which includes the Araripina and Exu formations of the Araripe Group (summarized by Fambrini et al., 2020).

The focus of this study, the post-rift sequence I, is represented by the deposits of the Santana Group, which include, from bottom to top, the Barbalha, Crato, Ipubi and Romualdo formations (Neumann and Cabrera, 1999; Assine et al., 2014; Neumann and Assine, 2015; Custódio et al., 2017; Varejão et al., 2021a, 2021b; Guzmán et al., 2023).

The Barbalha Formation comprises the initial deposition of the post-rift I sequence, where marine transgressive events are clearly identifiable (Fauth et al., 2023). It shows deposition within fluvial and lacustrine environments (Assine, 2007; Neumann and Assine, 2015; Scherer et al., 2015), This unit consists of two sequences: depositional sequence 1, controlled by allogenic processes and corresponding to fluvial channels with laterally well-developed overbanks, and depositional sequence 2, which represents overbank deposits in an underdeveloped floodplain within the river system (sensu Assine et al., 2014; Scherer et al., 2015; Fambrini et al., 2019; Varejão et al., 2021a; Fauth et al., 2023).

The black shales of the Batateira Beds (depositional sequence 1) were deposited under dysoxic/anoxic conditions (Ponte and Appi, 1990) and are considered a lacustrine system (Assine, 2007; Chagas et al., 2007), ranging from brackish to freshwater conditions (Fauth et al., 2023).

The Crato Formation is a fully developed paleolake with a carbonate depocenter that has been continuously expanding over time. It is composed of six rhythmite limestone-claystone shoals intercalated with shales, forming a succession up to 50–70 m thick (Neumann, 1999; Neumann and Cabrera, 1999). The limestone layers of the Crato Formation represent a transgressive event that is followed by tide-dominated bay deposits, which are recorded with specific subtidal, intertidal, and supratidal portions (Varejão et al., 2021b). Overlaying the Crato Formation, the Ipubi Formation is composed of evaporite beds combined with green and black shales, up to 30 m thick, related to extreme arid conditions (Assine et al., 2014). It consists of shales and overlying evaporite deposits, indicating a transition of lacustrine to marine settings (Fabin et al., 2018; Goldberg et al., 2019). These deposits were formed in a supralittoral zone of a coastal sabkha type (Coimbra et al., 2002; Bobco et al., 2017; Varejão et al., 2021b). The depositional setting has been interpreted as a coastal environment associated with relative sea level changes under arid to semi-arid conditions (Assine, 2007; Assine et al., 2014; Bobco et al., 2017; Fabin et al., 2018; Goldberg et al., 2019; Coimbra and Freire, 2021; Carvalho et al., 2022).

The Romualdo Formation record the final deposition of the Santana Group. Its lower portion consist of sandstones beds intercalated with shales, followed by a transgressive event represented by ostracod-bearing green shales. The presence of stratified conglomerates, sandstones, limestones, marls and shales, along with records of marine palynomorphs (e.g., dinocysts and foraminiferal linings) and carbonate microfossils (e.g., foraminifera and ostracods), suggests well-established marine conditions during deposition (Assine et al., 2014; Custódio et al., 2017; Arai and Assine, 2020; Melo et al., 2020; Coimbra and Freire, 2021; Araripe et al., 2021, 2022; Vallejo et al., 2023). The distribution and abundance of carbonate microfossils suggest its chronostratigraphic positioning in the upper Aptian (Melo et al., 2020). According to Custódio et al. (2017), the Romualdo Formation sequence comprises a transgressive-regressive cycle with a depositional dip towards the southeast, decreasing in thickness towards the northwest, and source areas located at the northern portion of the basin. In the eastern part of the basin, facies associations are indicative of a deepening-upward sequence on a mixed siliciclastic carbonate marine ramp with the full establishment of the seaway (Melo et al., 2020; Guzmán et al., 2023).

UNCORRECTED PROOF

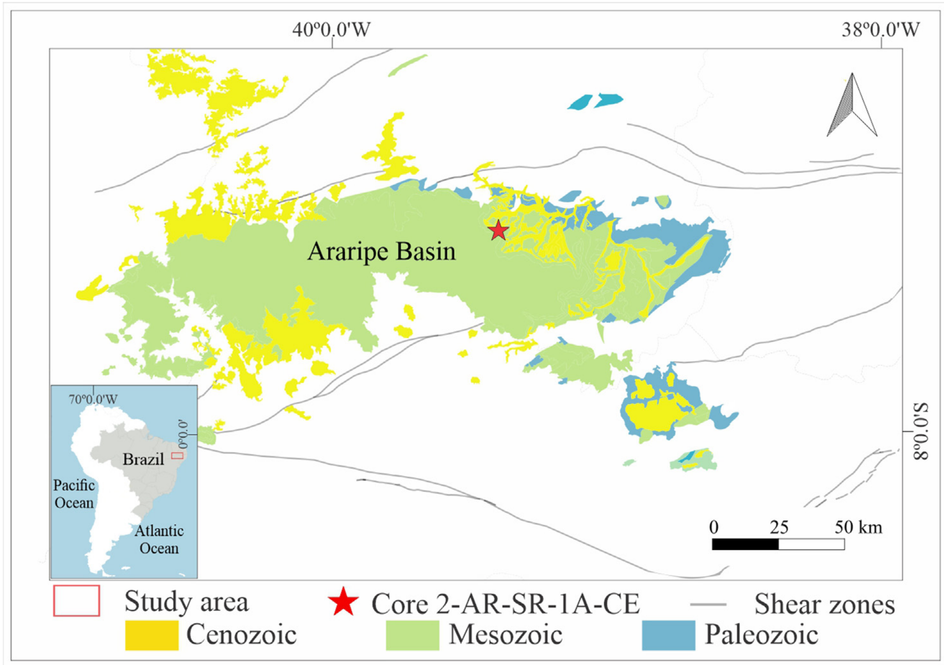

Fig. 1. Location of the Araripe basin in Brazil. Q4

3. Material and methods

The study was carried out using samples collected from the well core 2-AR-SR-1A-CE, which is located at coordinates 7°17′32″N, 39°23′35″E. The well reached a depth of 141 m and encompassed the Romualdo, Ipubi, Crato, and Barbalha formations of the Santana Group, Araripe Basin. For the palynofacies analysis, a total of 59 samples were collected from the interval 11.29–137.87 m. These samples were prepared according to the method described in Tyson (1995) and Mendonça Filho et al. (2010), using conventional acid treatment involving the dissolution of all mineral constituents using hydrochloric acid (HCl) and hydrofluoric acid (HF) to remove carbonates and silicates, respectively. HCl acid (37 % concentration) was added until it completely covered the sample and was left resting for 24 h. The samples were rinsed with distilled water and HF acid (40 % concentration) was then added, covering the sample, and left to react for 24 h. The samples were washed again with distilled water and sieved through a 10 μm opening net. HCl acid (10 % concentration) was added to the residue, to cover the sample for 24 h and finally washed with distilled water. The residual organic matter was divided into two parts: one for the analysis of non-oxidized sedimentary organic matter (SOM), classified using the terminology from Mendonça Filho and Menezes (2011); the other part was oxidized using nitric acid (HNO_3) (65 % concentration) to clean and concentrate the palynomorphs. The residual matter was mounted on slides using polyvinyl Alcohol (PVA) and Norland Optical Adhesive cured under ultraviolet light. In each slide, the counting of 300 particles of SOM was performed following the methods described by Mendonça Filho et al. (2011). At least 300 palynomorphs were counted in each sample using a transmitted-light microscope. When necessary, incident blue light (ultra-violet fluorescence mode) was applied. The representative constituents were photographed using a digital Axiocam 503 camera mounted on a Zeiss microscope (Axio Imager A.2) with 20X air objective, and 63X, 100X oil immersion. All slides and residues were stored and cataloged in the Applied Micropaleontology Laboratory (LMA) of the Federal University of Pernambuco (UFPE) under the collection number LMA-P00223 - LMA-P00281.

3.1. Palynofacies analysis

Based on the classification scheme proposed by Mendonça Filho et al. (2011): the Amorphous group consists of amorphous organic matter (AOM) strictly derived from phytoplankton and bacteria, as well as the pseudoamorphous subgroup originating from macrophyte tissue, in addition to resin produced by terrestrial plants in tropical climates; the Phytoclast group includes both opaque and non-opaque subgroups containing mostly woody tissue that is brown in color, as well as cuticles and membranes; finally, the Palynomorphs group refers to all acid-resistant, organic walled microfossils (e.g., spores, pollen grains, algae, foraminiferal test linings and dinoflagellates cysts). Detailed descriptions of SOM are available in the literature (e.g., Tyson, 1995; Batten, 1996; Carvalho et al., 2006, 2013; Mendonça Filho et al., 2010).

3.2. Data analysis

The data obtained from the quantitative analyses of SOM components were recalculated to percentage values. The cluster analysis (R-mode) was conducted to establish associations between the SOM categories, allowed us to organize the samples studied into three palynofacies associations, based on the abundance of groups and sub-groups of SOM (Fig. 4). In addition, the average for each Q5 formation was calculated based on these associations (Table 1) and

Table 1
Average abundance of the sedimentary organic matter association (SOMA) from well 2-AR-SR-1A-CE. The most significant of the associations are highlighted in bold.

Formation	Structureless	Continental particles	Aquatic + Opaque
Romualdo	38.1	**29.0**	32.9
Ipubi	**48.8**	6.3	44.9
Crato	**44.7**	**33.5**	21.8
Barbalha	6.1	**30.9**	**63.0**
General average	**41.2**	**25.4**	**33.4**

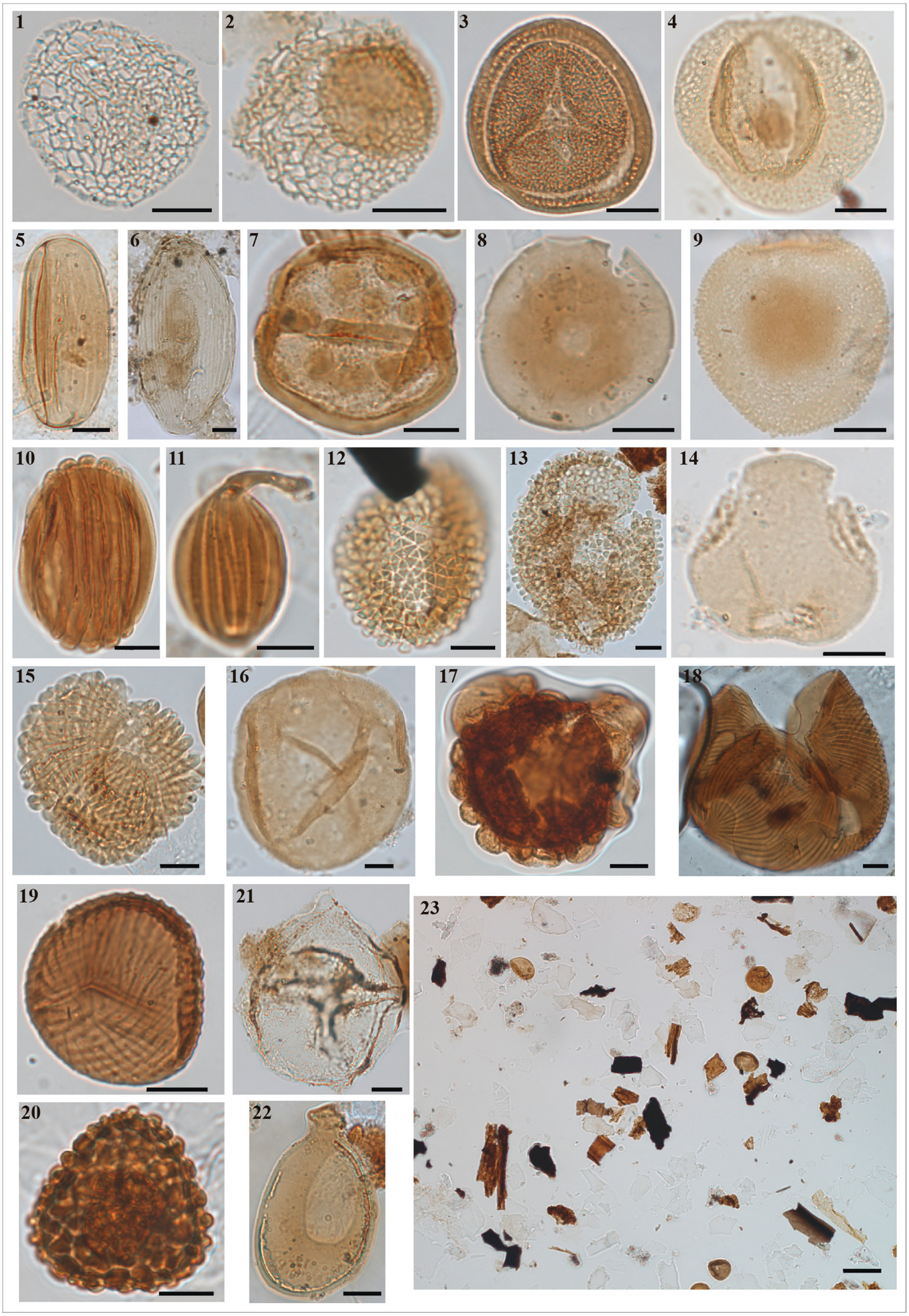

Fig. 2. The main palynomorphs from the 2-AR-SR-1A-CE well. Scale bar is 10 μm long. 1. *Afropollis jardinus* (sample LMA-P00256, coords. 16–65); 2. *Afropollis operculatus* (sample LMA-P00247, coords. 9–105); 3. *Classopollis classoides* (sample LMA-P00254, coords. 12.8–70.8); 4. *Complicatisaccus cearensis* (sample LMA-P00249, coords. 5–101); 5. *Equisetosporites leptomatus* (sample LMA-P00251, coords. 3–94); 6. *Equisetosporites maculosus* (sample LMA-P00246, coords. 3–96.7); 7. *Sergipea variverrucata* (sample LMA-P00225, coords. 11.8–77.9); 8. *Exesipollenites tumulus* (sample LMA-P00225, coords. 5.5–71.3); 9. *Uesuguipollenites callosus* (sample LMA-P00236, coords. 20–72); 10. *Gnetaceaepollenites retangularis* (sample LMA-P00233, coords. 4–80.8); 11. *Regalipollenites amphoriformis* (sample LMA-P00232, coords. 4–103); 12. *Stellatopollis araripensis* (sample LMA-P00227,

were plotted using the RiojaPlot website to describe the paleoenvironmental interpretations. This plotting revealed distinct changes in the depositional paleoenvironment, alongside data from sedimentological descriptions.

4. Results and discussion

4.1. Age constrains

The palynologic record reveals a common assemblage dominated by terrestrial components, containing the following species of biostratigraphic value: *Exesipollenites tumulus, Sergipea variverrucata, Equisetosporites maculosus* and *Complicatisaccus cearensis*. These palynomorphs define the "*Tricolpites*" – *Exesipollenites tumulus* Zone proposed by Muller et al. (1987), this is found in Zone 5 and is correlated to selected contemporary palynozonations identified in Brazil (Regali et al., 1974; Beurlen and Regali, 1987; Regali, 1987; Regali and Viana, 1989; Regali and Santos, 1999).

The last occurrence of *Sergipea variverrucata* at depth of 106.7 m, indicates the biozone (P-270) proposed by Regali and Santos (1999). Additionally, the last presence of *Complicatisaccus cearensis* at depths of 99 m indicates the biozone (P-280) proposed by Regali and Santos (1999). Furthermore, the presence of *Equisetosporites maculosus* at a depth 105.7 m–121.7 m delineates the upper boundary of the biozone (P-270) (Dino, 1992, 1994).

Based on the palynological assemblage from the recovered deposits of the Santana Group (Fig. 2), the biostratigraphic result indicates a late Aptian age, as defined according to the Brazilian palynological zoning (Regali and Santos, 1999). This places the local biozone (P-270) in the studied section, where a moderate abundance of *Equisetosporites maculosus* and the presence of *Complicatisaccus cearensis* occur (Fig. 3).

The age of the Cretaceous deposits of the Araripe Basin is in constant debate. Previous biostratigraphic studies suggest a late Aptian age for the Romualdo Formation (Melo et al., 2020; Guzmán et al., 2023). However, the high diversity and abundance of foraminifera species, both benthic and planktonic (e.g., *Hedbergella* and *Gubkinella*), suggest that the accumulation of these planktonic foraminifera genera may be related to the Oceanic Anoxic Event (OAE1b), which occurred between the latest Aptian and the Early Albian (Ferraro et al., 2020). Based on the high-resolution multiproxy analysis, which integrates stable isotopes, elemental data, and microfossils, suggests that deposition likely occurred from the late Aptian–Early Albian (Bom et al., 2023). According to Lemos et al. (2023), calcareous nannofossils are recorded in the Romualdo Formation, indicating an Aptian–Albian age.

The stratigraphic positions of our recorded species with biostratigraphic value are illustrated in Fig. 3. The presence of dinoflagellates cysts (dinocysts) from the genus *Subtilisphaera* has been documented in several northeastern basins of Brazil, including São Luís, Potiguar, Parnaíba, Tucano, Sergipe, Araripe, and Ceará basins (Arai et al., 2000; Arai, 2009, 2014; Gonzalez et al., 2020) and reinforces the marine transgressive event in the late Aptian (Arai and Assine, 2020). However, the absence of species with biostratigraphic value in samples from the Ipubi and Romualdo formations hinders the establishment of local biozones. According to Melo et al. (2020) and Guzmán et al. (2023), a late Aptian age is suggested for the intermediate part of the Romualdo Formation based on samples from the same core (2-AR-SR-1A-CE). This aligns with the reference records of Teixeira et al. (2017), Arai and Assine (2020), and Vallejo et al. (2023), which suggest that the last occurrence of *S. variverrucata* in this formation corresponds to biozone P-270 (Regali and Santos, 1999), indicating a late Aptian age. Controversially, Lúcio et al. (2020) presented Re–Os elemental and isotopic data suggesting that the black shales from the Ipubi Formation were deposited during the latest Barremian–earliest Aptian. However, the authors ignored the previous robust biostratigraphic results from Araripe Basin (Coimbra and Freire, 2021). As reported by Guzmán et al. (2023), the presence of *Favusella hoterivica* at the top of the Barbalha Formation suggests a chronostratigraphic position in the lower Aptian, corresponding to the occurrence of the *Leupoldina cabri* Zone. This was confirmed by Fauth et al. (2023), who dated the deposits of the Barbalha Formation for the first time based on the recovery of the planktonic foraminifera genera *Leupoldina* sp. and *Globigerinelloides* spp.

4.2. Sedimentary organic matter composition (SOM)

The identification of the main groups of SOM shows that Amorphous Group predominate, reaching an average of 42 % of total kerogen. It is composed of amorphous organic matter (AOM), pseudoamorphous matter, and a low presence of resin. The Phytoclast Group is characterized by an abundance of particles, with a predominance of opaques (33 % of total kerogen). These opaques are primarily corroded type. Additionally, non-opaque phytoclasts (15 % of total kerogen) are mainly composed of non-biostructured and biostructured particles, primarily of striate and banded types, in addition to cuticles. The Palynomorphs Group is the least abundant, consisting mainly of pollen grains predominantly from gymnosperms and pteridophyte spores, comprising only 11 % of total kerogen. Additionally, some freshwater algae, as well as rare occurrence of foraminiferal test linings and dinocysts (e.g., *Subtilisphaera* sp.), were identified (Supplementary data). There were also occurrences of acritarchs (e.g., *Maranhites* spp.), probably reworked from Devonian rocks (Brito and Quadros, 1995).

4.3. Sedimentary organic matter association (SOMA)

Three sedimentary organic matter associations (SOMA) were revealed by cluster analysis dendrogram (Fig. 4) designated by their composition, affinity, and dominant particles of SOM: Association I: Structureless, Association II: Continental particles, and Association III: Aquatic + opaque particles. The SOMA ranges inproportion across the well, considering the kerogen groups and subgroups. For the analysis, the most significant association is the one with an average percentage higher than the overall average of SOMA (Table 1 and Fig. 5).

The structureless SOMA show slightly higher percentages of structureless particles, averaging 41.2 % (Table 1). These particles are composed of AOM and pseudomorphs particles. AOM particles typically exhibit heterogeneous distribution, with an average of 36.5 %. It varies in color from yellow to dark and light brown, containing inclusions such as fragments of phytoclasts and palynomorphs, and showing weak or no fluorescence. Significant quantities of AOM arise from environments with high preservation rates and low energy in aquatic settings (Carvalho et al., 2006). Its preservation is closely related to dysoxic-anoxic conditions and is thus associated with high primary productivity (Tyson, 1993).

coords. 5–83); 13. *Stellatopollis densiornatus* (sample LMA-P00242, coords. 19.6–69); 14. *Penetetrapites mollis* (sample LMA-P00232, coords. 4–94); 15. *Trisectoris reticulatus* (sample LMA-P00226, coords. 10–95.8); 16. *Araucariacites australis* (sample LMA-P00225, coords. 52–63); 17. *Paludites mamelonatus* (sample LMA-P00256, coords. 17–98); 18. *Cicatricosisporites microstriatus* (sample LMA-P00253, coords. 4.3–66.9); 19. *Cicatricosisporites avnimelechi* (sample LMA-P00256, coords. 19–70); 20. *Leptolepidites verrucatus* (sample LMA-P00254, coords. 17–70.3); 21. *Subtilisphaera* sp. (sample LMA-P00277, coords. 9–100); 22. Foraminiferal test linings (*Pyrgo* sp.) (sample LMA-P00230, coords. 10–71.8); 23. Sedimentary organic matter distribution 20X. Scale bar is 50 μm long.

UNCORRECTED PROOF

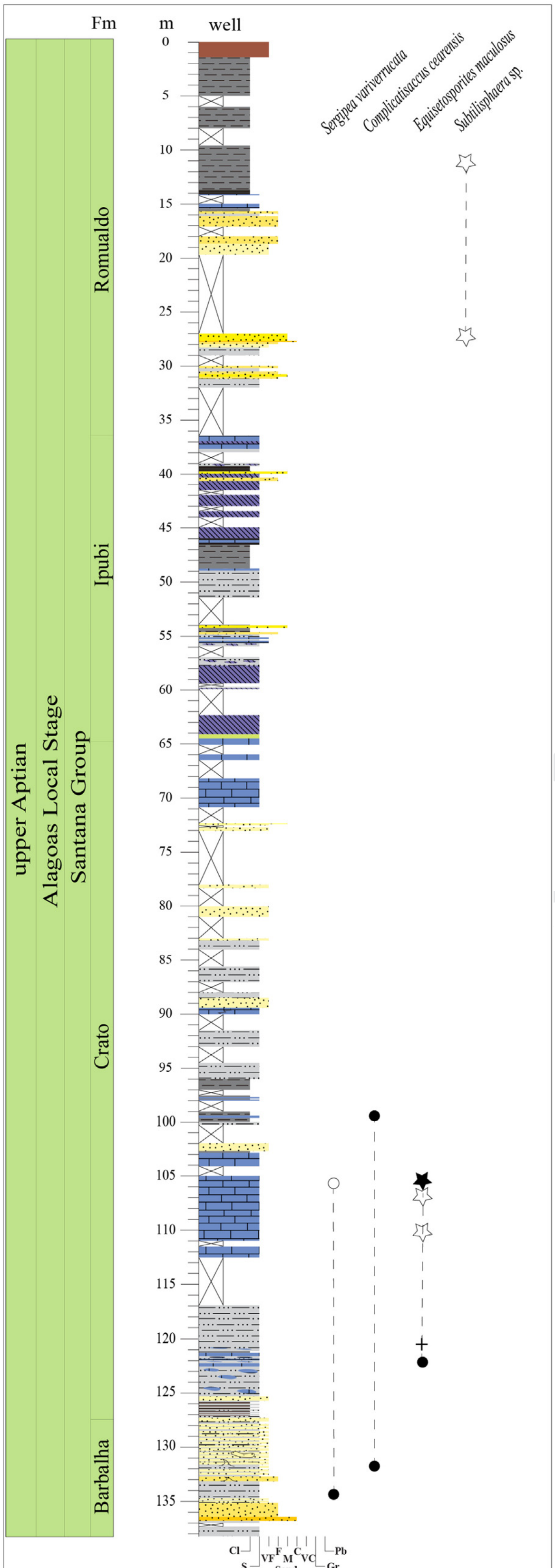

Fig. 3. Distribution and stratigraphic abundance of species with biostratigraphic value in the Santa Group of the Araripe Basin. Fm: Formations; m: meters.: ● present: 1 specimen; ○ present: 2 specimens; + present: 3 specimens; ☆ present: 4–6 specimens; ★ Abundant: ≥15 specimens.

Particles categorized as pseudoamorphous show a diffuse boundary, brown color, absence of inclusions, and lack of fluorescence. These particles are most likely derived from the oxidation of poorly preserved or degraded phytoclasts (Tyson, 1995). This association occurs predominantly in the Ipubi Formation.

The SOMA aquatic + opaque elements consist of opaque phytoclasts and marine elements such as dinocysts and foraminiferal linings, as well as freshwater algae with an average of 33.4 % (Table 1). The average predominance of opaque phytoclasts in this association is 32.7 %, primarily composed of corroded opaques. According to Tyson (1993), opaque phytoclast particles are derived primarily from the oxidation of translucent material that was transported over a prolonged period. In addition, freshwater microplankton are present with very low content, with average of 0.7 % (e.g., *Botryococcus*). Some marine microplankton, specifically dinocysts of the genus *Subtilisphaera*, were also identified in the Romualdo Formation. In addition, foraminiferal test linings were retrieved from a sample located at the base of the Crato Formation. The few well-preserved specimens identified have a single-chamber shape. The presence of these marine elements has been interpreted as a consistent indicator of marine sedimentary environments, with the highest frequencies reported in coastal to shallow shelf settings (Lister and Batten, 1988; Stancliffe, 1989).

The SOMA continental is primarily composed of terrestrial particles, such as non-opaque (translucent phytoclast), cuticle, membrane, biostructured (e.g., striate, banded, pitted), sporomorphs (pollen grains and spores) and resin. This association show average of 25.4 % (Table 1) of the total kerogen. It is mainly found in biostructured particles, with an average of 13 %, primarily striate and banded forms, followed by sporomorphs at an average of 9.9 %, and very low values for cuticles, resin, and membrane. The SOMA consists entirely of terrestrial particles and is associated with a fluvial-deltaic source (Tyson, 1995).

5. Paleoenvironmental significance from palynofacies analysis

Based on the palynofacies associations revealed in core 2-AR-SR-1A-CE, various depositional conditions are interpreted (Fig. 5).

The structureless organic matter association is dominant, indicating deposition under anoxic conditions. According to Carvalho et al. (2013) this association is terrestrially influenced, as indicated by a moderate presence of pseudoamorphous particles that are mostly derived from the oxidation of translucent material. The high AOM content may also be related to significant aquatic productivity and/or significantly less input of sediments (Neumann et al., 2003). The level of fluorescence exhibited by the AOM particles reflects the general redox background of the depositional environment. The weak or absent fluorescence suggests that at least part of the AOM derives from phytoclast degradation; however, two possibilities are raised: a terrestrial origin (phytoclast-derived) and/or plankton-derived poorly preserved (Tyson, 1995). The highest average of structureless is found in the Ipubi Formation (see Table 1), followed by the Crato Formation, where high AOM preservation is attributed to reducing conditions. Therefore, this result does not completely exclude the possibility that some of the AOM was derived from phytoclasts; their content may be moderate to high due to turbiditic input and/or proximity to the source (Tyson, 1995).

The association of aquatic + opaque is composed primarily of opaque particles. High values indicate oxidizing conditions and either proximity to terrestrial sources or redeposition of terrestrial organic matter from fluvio-deltaic sources (Tyson, 1989). The presence of aquatic palynomorphs is lower; however, they were deposited in either marine or brackish environments. Foraminiferal

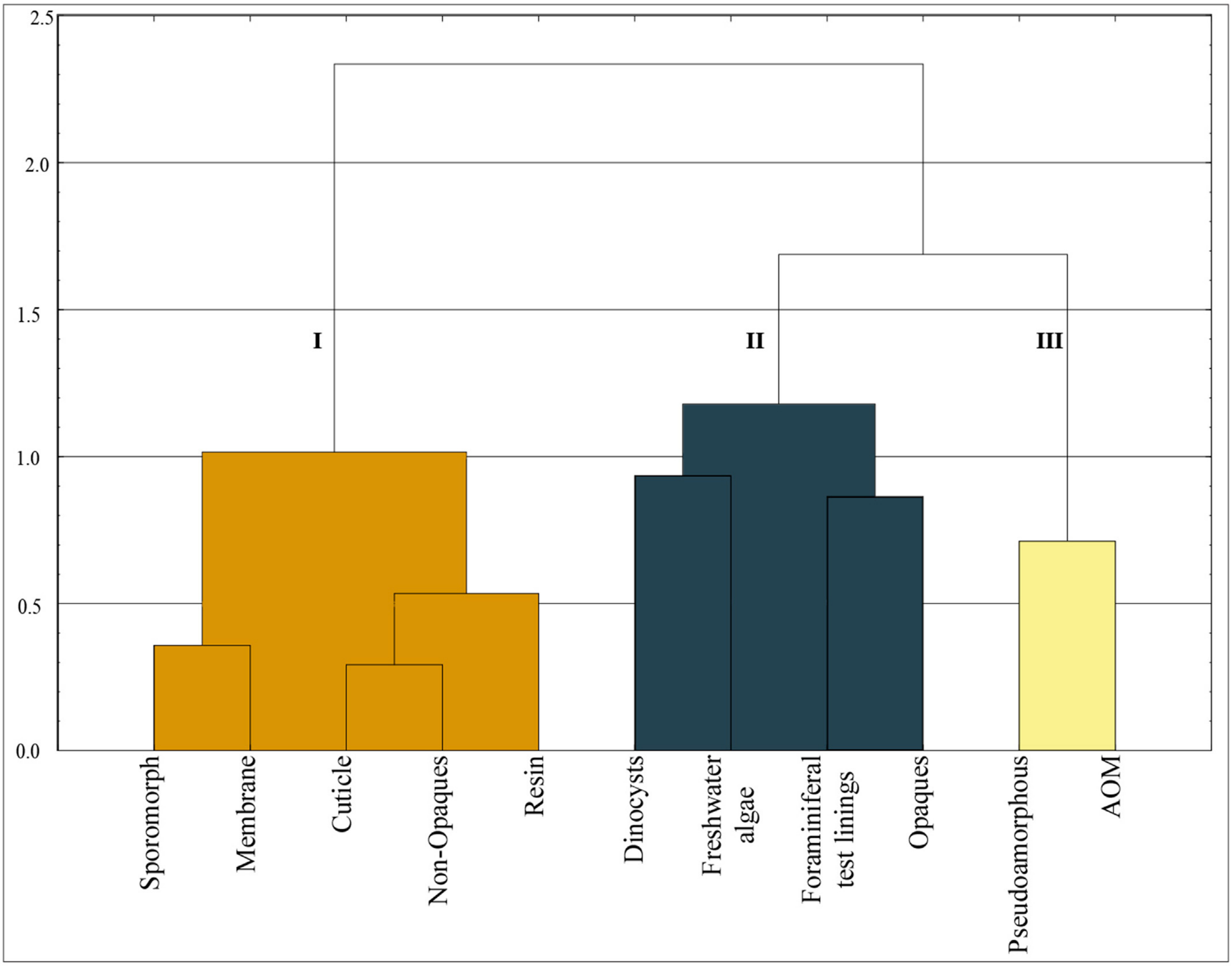

Fig. 4. Categories of SOM from the well core samples in this paper include three sedimentary organic matter associations (SOMA): Assoc. I - continental particles; Assoc. II - marine microplankton, freshwater microplankton, and opaque particles; Assoc. III - structureless particles.

linings are of benthic origin and indicate marine depositional environments or estuarine marshes of variable salinity. Dinoflagellate cysts are mostly of marine origin, suggesting near-shore environments (Batten, 1996). The highest average of aquatic + opaque is observed in the Barbalha Formation (see Table 1). The continental association represents environments close to the source. It is composed exclusively of fragments of tissues derived from higher plants, comprising translucent woody material in addition to terrestrial palynomorphs, which include the most abundant taxa: *Classopollis*, *Afropollis*, *Araucariacites*, *Equisetosporites*, *Gnetaceaepollenites*, *Inaperturopollenites*, *Stellatopollis*, *Crybelosporites*, *Cyathidites*, *Cicatricosisporites*, and *Paludites* (Fig. 6). The continental association is the least abundant and is found along the entire log, mainly in the Crato, Barbalha, and Romualdo formations (see Table 1).

5.1. Implications from palynofacies

Lithology changes reflect a variety of depositional paleoenvironments, enabling inference about the transition from a fluvial-lacustrine environment to a marine setting, as identified through SOM analysis.

5.2. Barbalha Formation

The Barbalha Formation (127–138 m) consist of amalgamated sandstone beds with climbing ripples, followed by siltstones. These deposits show an average of 63.0 % of aquatic and opaque associations. The occurrence of freshwater microplankton (e.g., *Botryococcus* and *Pediastrum*) is relatively low, although these algae and their variations are indicative of a body of water with changes in both salinity and primary productivity (Gonzalez et al., 2020). This suggests differing ecological preferences: *Pediastrum* are stenohaline and less tolerant to increases in salinity, in contrast to the euryhaline *Botryococcus* (Batten, 1996). The presence of *Botryococcus* suggests deposition under oligotrophic and euryhaline conditions (Tyson, 1995).

The palynofacies composition exhibits a clearly proximal fluvio-deltaic signature with opaque phytoclasts derived from the oxidation of translucent particles that have undergone prolonged transport (Tyson, 1995; Kholeif and Ibrahim, 2010; Carvalho et al., 2013). The distribution of the depositional sequence proposed by Assine et al. (2014), Scherer et al. (2015), and Fauth et al. (2023) suggests that this interval is part of sequence 2. It was deposited during the transition from a fluvial to a bayhead delta environment

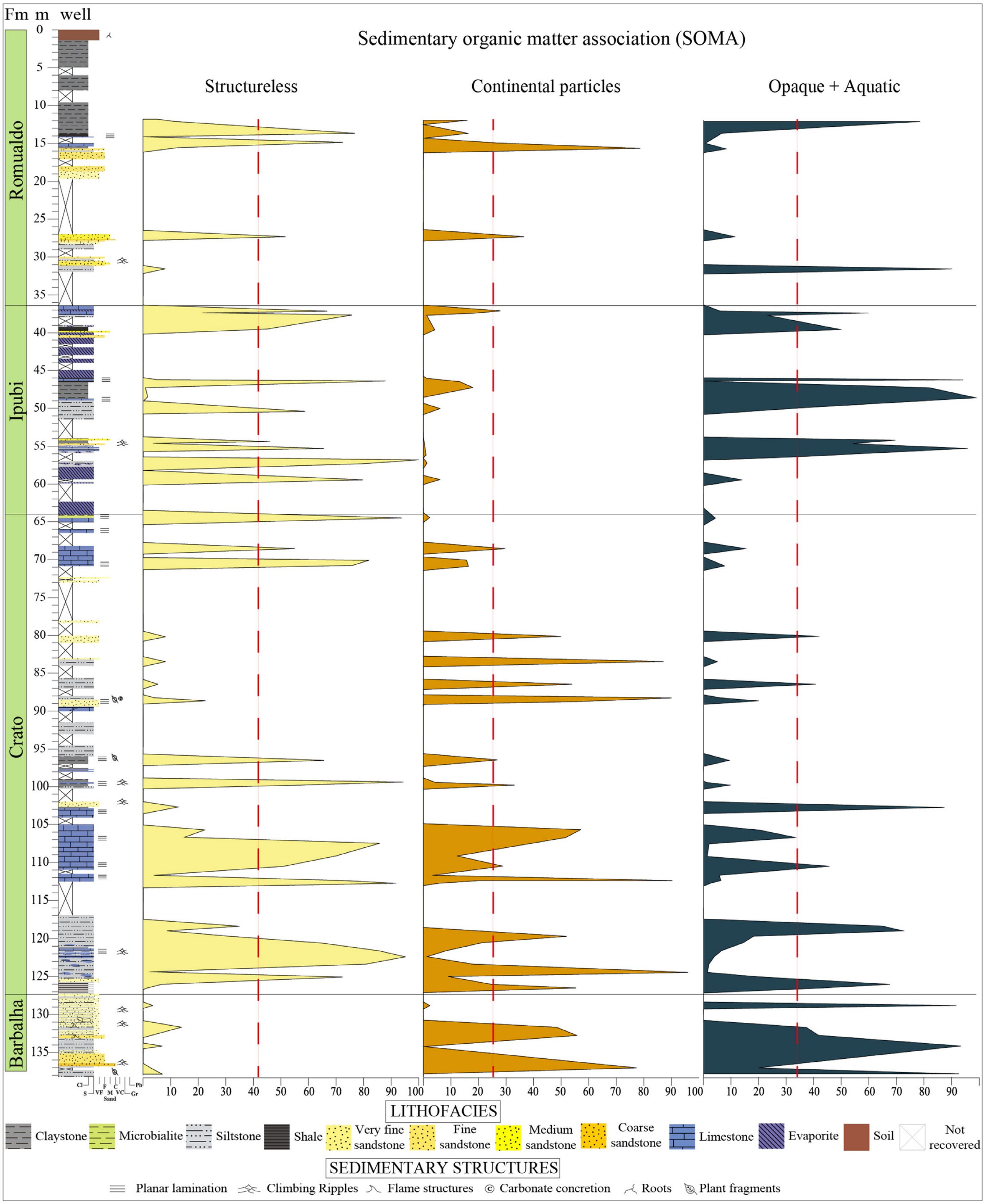

Fig. 5. Stratigraphic distribution of sedimentary organic matter association (SOMA) from well 2-AR-SR-1A-CE. Fm: Formations; m: meters. The dashed line represents the general average value. Barbalha Formation (characterized by the dominance of opaque + aquatic and continental particles); Crato Formation (dominated by structureless particles and continental particles); Ipubi Formation (dominated by structureless particles and aquatic + opaque) Romualdo Formation dominated by structureless particles and aquatic + opaque).

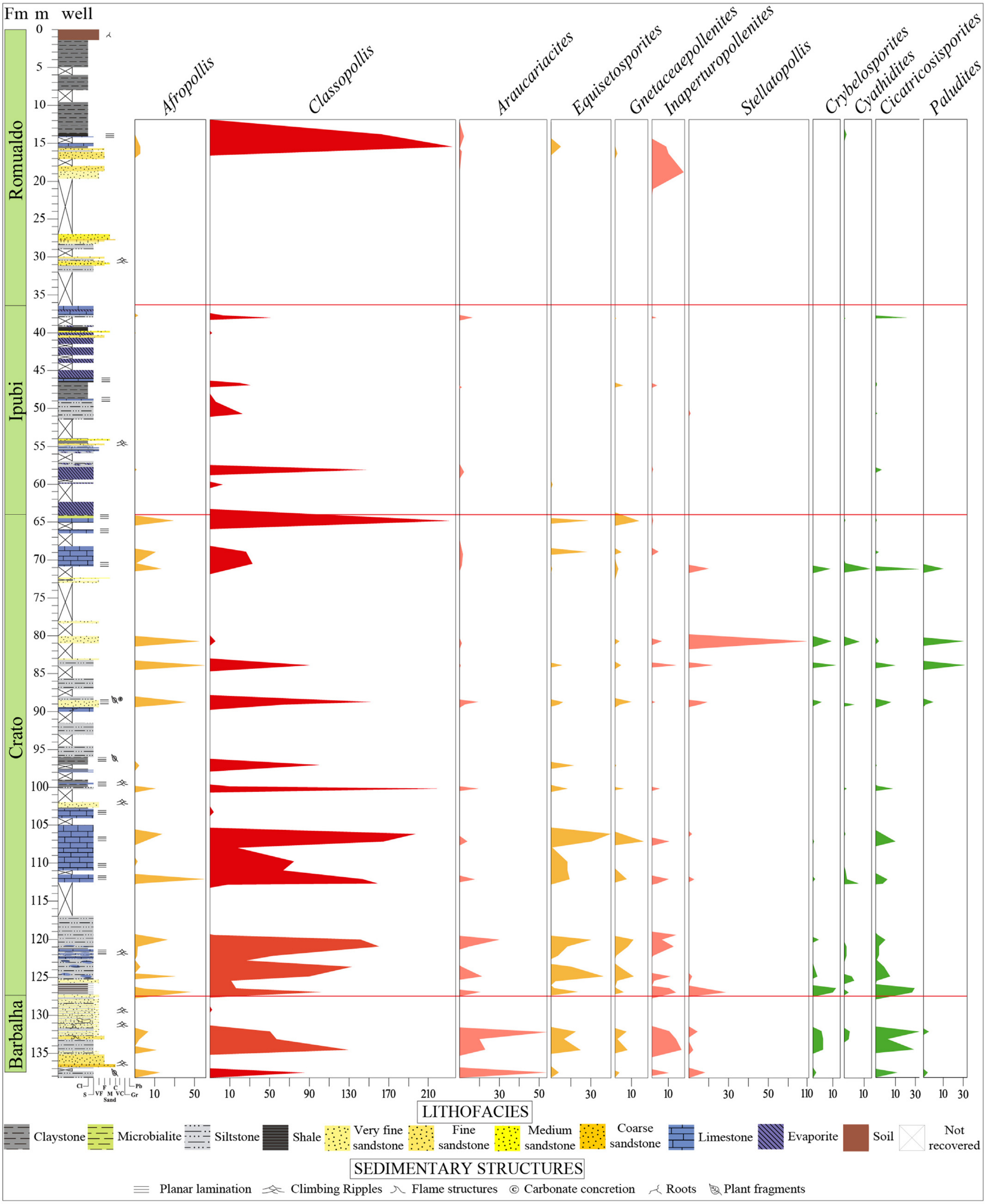

Fig. 6. The distribution of the main pollen grains and spores is observed along well 2-AR-SR-1A-CE. Fm: Formations; m: meters.

(Varejão et al., 2021a). The lower abundance of AOM, associated with a high presence of opaque phytoclast, suggests an establishment of the fluvial system during the Barbalha Formation deposition. The presence of exclusively terrestrially derived organic particles and their high percentages is primarily associated with proximal depositional conditions. The predominance of pollen grains from xerophytic plants, mainly of the *Classopollis* (Cheirolepidiaceae), suggest a hot and arid climate, as previously observed by Carvalho et al. (2017; 2019). The increase of *Araucariacites*, *Inaperturopollenites*, and fern spores (e.g., *Crybelosporites*, *Cicatricosisporites*) (Fig. 6) reflects more humid conditions (Carvalho et al., 2017, 2019; Santos et al., 2022).

5.3. Crato Formation

According to SOMA, the Crato Formation (64–127 m) exhibits a clear proximal signature, as demonstrated by the average of continental particles (33.5 %). Based on lithological characteristics, a connection with a lagoonal coastal plain, that seems to have been opened (Silveira et al., 2023), due to a relatively high sea level (Tucker, 2014). On the other hand, the SOM and carbonate contents show a wide variation of facies, with different peaks of change in SOM occurring in freshwater to saline lacustrine zones (Neumann et al., 2003; Vallejo et al., 2023). Based on faunal considerations by Guzmán et al. (2023) and palynomorph records by Vallejo et al. (2023), in addition to the main taxa recorded (e.g., *Classopollis*, *Equisetosporites*, *Inaperturopollenites*, *Araucariacites*, *Cicatricosisporites*, *Afropollis*, *Gnetaceaepollenites*, *Stellatopollis*), it is proposed that the deposition of the Crato Formation occurred under freshwater conditions, encompassing mudflats, coastal lakes, and lagoons within a bay system. Marine palynomorphs were recorded at a depth of 126 m, and record the presence of foraminiferal test linings, which supports the deposition in a coastal hypersaline lake. This finding agrees with Vallejo et al. (2023) in the Serra do Mãozinha, indicating the first ingressions of seawater (Goldberg et al., 2019; Varejão et al., 2021a, 2021b; Fauth et al., 2023; Vallejo et al., 2023). This occurrence shows that marine to brackish conditions followed coastal lakes within a bayhead, as proposed by Guzmán et al. (2023), the presence of agglutinated foraminifera (e.g., *Bathysiphonids, Rhabdamminids, Rhizammids*, *Gaudryinella alexandria*, *Recurvoides* sp.) indicates a deposition in a confined transitional environment under anoxic conditions. In agreement with the SOM analysis, a lower energy environment, attributed to dysoxic and anoxic conditions, is proposed.

The continuous presence of *Classopollis* sp. associated with pollen grains such as *Gnetaceaepollenites* and *Equisetosporites*, reflects a hot and arid climate (Carvalho et al., 2019, 2022). According to Doyle et al. (1982), the decline of araucariaceous pollen (*Araucariacites*) perhaps reflects an effect of aridization. Carvalho et al. (2017; 2019; 2022) stated that arid conditions are characterized by sea-level lowstands, while warm and humid conditions are correlated with rising sea levels. These humid conditions are recorded by several peaks in the abundance of the genera such as *Crybelosporites*, *Cyathidites, Cicatricosisporites*, and *Paludites*; their occurrence represents a humid phase.

5.4. Ipubi Formation

The Ipubi Formation consist of an evaporite package (Ponte and Appi, 1990; Assine, 1992) and is interpreted as a coastal environment (supratidal) that are susceptible to relative variations in sea level (Coimbra et al., 2002; Assine, 2007). It shows a high average of structureless particles (48.8 %), in addition to presenting a high average association of opaque + aquatic elements, mainly opaque phytoclasts. The high proportion of AOM in sediments suggests enhanced preservation under reducing conditions and increased water column stability, with more reducing features and good to excellent AOM preservation (Tyson, 1993, 1995; Ibrahim et al., 2002). Carvalho et al. (2006) suggested that the substantial accumulation of AOM results from both high preservation rates and a low-energy environment associated with dysoxic-anoxic conditions. Based on the observed palynofacies assemblage, they proposed a brackish/lagoonal environment for deposition. In our study, a conspicuous increase in AOM accompanied by the presence of *Botryococcus* and an increase in opaque phytoclasts suggests a brackish lagoonal to coastal plain paleoenvironment in a transitional phase with oxygen-deficient (dysoxic-anoxic) conditions.

5.5. Romualdo Formation

The Romualdo Formation consist of an intercalation of fine-grained sandstones, siltstones, limestones and mudstones and record the establishment of marine conditions (Melo et al., 2020; Guzmán et al., 2023), deposited during the Oceanic Anoxic Event (OAE) 1b (Bom et al., 2023). The highest average of structureless particles (38 %) is observed, followed by the association of opaque + aquatic (32.9 %). The most abundant opaques are corroded, exhibiting a dark to black color and a range sizes. The presence of structureless particles shows high abundance. The high percentage of AOM is the result of well preservation rates and low-energy settings, indicating preservation under reducing conditions and increased stability of the water column (Tyson, 1993, 1995; Batten, 1996; Carvalho et al., 2006; Kholeif and Ibrahim, 2010). According to Bom et al. (2023), changes in water-column structure and oxygen levels allowed for better preservation of the organic matter. Various aspects, such as intensified hydrological cycles, potential submarine volcanism, increased continental runoff, organic matter input, and nutrient delivery to the epicontinental sea, contributed to the further enhancement of organic matter preservation. The predominance of structureless association, as well as the presence of aquatic + opaques association and continental particles showing an average of 29 %, suggests an estuarine setting. This proposal is also supported by the low content of the marine palynomorph. The high occurrence of opaque phytoclasts indicates a high energy oxidizing condition (Tyson, 1993). The good preservation of AOM, with a low abundance of palynomorphs, indicate a transitional proximal-distal paleoenvironment, suggesting deposition in nearshore to coastal settings (Teixeira et al., 2017). A relative abundance of *Classopollis* sp, is observed, indicating adaptation to arid climates and hypersaline soils of coastal habitats (Michels et al., 2018).

Some marine microplankton (genus *Subtilisphaera*) were identified, associated with restricted low-salinity conditions (Jain and Millepied, 1975; Arai, 2014). The deposition of sedimentary organic matter occurred in a marine-influenced, possibly coastal, environment under arid and warm conditions.

6. Conclusion

The main contribution of this work is the analysis of sedimentary organic matter covering the entire Santana Group, detailing the paleoenvironmental conditions during the late Aptian. Palynofacies analysis was used to reconstruct the depositional setting of part of the Araripe Basin. Our results clearly indicate that the conditions during the deposition of the post-rift sequence I show punctual marine influence.

The Santana Group of the Araripe Basin was initially deposited in a fluvial system. Later, sediments were deposited in a lagoon system connected to tidal flats, coastal lakes, and lagoons within an open bay, coinciding with a relative sea-level rise. This transition from a lacustrine bay reflects a shallow marine environment typical of an epicontinental sea, with a saline/lacustrine character. Therefore, the Santana Group is interpreted as being deposited in a fluvial system, transitioning through a lagoonal and an open bay environment into a marine setting during the late Aptian.

CRediT authorship contribution statement

Juan David Vallejo: Writing – review & editing, Writing – original draft, Methodology, Investigation, Formal analysis, Conceptualization. **Regina Buarque de Gusmão:** Writing – review & editing, Writing – original draft. **Marcelo de Araujo Carvalho:** Writing – review & editing, Software, Conceptualization. **Claus Fallgatter:** Writing – review & editing, Conceptualization. **Enelise Katia Piovesan:** Writing – review & editing, Conceptualization.

Declaration of competing interest

The authors declare that they have no known competing financial interests or personal relationships that could have appeared to influence the work reported in this paper.

Data availability

I have shared my data in the appendix file.

References

Arai, M., 2006. Revisão estratigráfica do Cretáceo Inferior das bacias interiores do Nordeste do Brasil. Geociencias 25 (1), 7–15.

Arai, M., 2009. Paleogeografia do Atlântico Sul no Aptiano: um novo modelo a partir de dados micropaleontológicos recentes. Boletim de Geociencias da Petrobras 17, 331–351.

Arai, M., 2014. Aptian/Albian (Early Cretaceous) paleogeography of the South Atlantic: a paleontological perspective. Brazilian Journal of Genetics 44 (2), 339–350. https://doi.org/10.5327/Z2317-4889201400020012.

Arai, M., Assine, M.L., 2020. Chronostratigraphic constraints and paleoenvironmental interpretation of the Romualdo Member (Santana Formation, Araripe Basin, Northeastern Brazil) based on palynology. Cretaceous Research 116, 104610. https://doi.org/10.1016/j.cretres.2020.104610.

Arai, M., Botelho Neto, J., Lana, C.C., Pedrão, E., 2000. Cretaceous dinoflagellate provincialism in Brazilian marginal basins. Cretaceous Research 21, 351–366. https://doi.org/10.1006/cres.2000.0211.

Arai, M., Coimbra, J.C., Silva-Telles, A.C., 2001. Síntese bioestratigráfica da Bacia do Araripe (Nordeste do Brasil). In: Simpósio sobre a Bacia do Araripe e bacias interiores do Nordeste. SBP/URCA/DNPM, Comunicações, Crato, pp. 1–2, 109–117, 122–124.

Araripe, R.C., Lemos, F.A.P., Prado, L.A.C., Tomé, M.E.T.R., Oliveira, D.H., Pereira, P.A., Nascimento, L.R., Asakura, Y., Ng, C., Viviers, M.C., Barreto, A.F., 2022. Upper Aptian–lower Albian of the southern-central Araripe Basin, Brazil: Microbiostratigraphic and paleoecological inferences. Journal of South American Earth Sciences 116, 103814. https://doi.org/10.1016/j.jsames.2022.103814.

Araripe, R.C., Oliveira, D.H., Tomé, M.E., Mello, R.M., Barreto, A.F., 2021. Foraminifera and Ostracoda from the Lower Cretaceous (Aptian–lower Albian) Romualdo Formation, Araripe Basin, northeast Brazil: Paleoenvironmental inferences. Cretaceous Research 122, 104766. https://doi.org/10.1016/j.cretres.2021.104766.

Assine, M.L., 1992. Análise estratigráfica da Bacia do Araripe, nordeste do Brasil. Revista Brasileira de Geociencias 22 (3), 289–300.

Assine, M.L., 2007. Bacia do Araripe. Boletim de Geociencias da Petrobras 15 (2), 371–389.

Assine, M.L., Perinotto, J.A.J., Custodio, M.A., Neumann, V.H., Varejão, F.G., Mescolotti, P.C., 2014. Sequências Deposicionais do Andar Alagoas da Bacia do Araripe, Nordeste do Brasil. Boletim de Geociencias da Petrobras 22, 3–28.

Asmus, H.E., Ponte, F.C., 1973. The Brazilian marginal basins. In: Nairn, A.E.M., Stehli, F.G. (Eds.), The Ocean Basins and Margins 1 – the South Atlantic. Plenum Press, New York, pp. 87–133.

Batten, D., 1996. Palynofacies and palaeoenvironmental interpretation. In: Jansonius, J., McGregor, D.C. (Eds.), Palynology: Principles and Applications, American Association of Stratigraphic Palynologists Foundation, pp. 1011–1064. College Station.

Beurlen, G., Regali, M.S.P., 1987. O Cretáceo da Plataforma continental do Maranhão e Pará, Brasil: bioestratigrafia e evolução paleoambiental. Boletim de Geociencias da Petrobras 1, 135–155.

Bobco, F.E.R., Goldberg, K., Bardola, T.P., 2017. Modelo deposicional do Membro Ipubi (Bacia do Araripe, nordeste do Brasil) a partir da caracterização faciológica petrográfica e isotópica dos evaporitos. Pesquisas em Geociencias 44 (3), 431–451. https://doi.org/10.22456/1807-9806.83267.

Bom, M.H.H., Kochhann, K.G.D., Heimhofer, U., Mota, M.A.L., Guerra, R.M., Simões, M.G., Krahl, G., Meirelles, V., Ceolin, D., Fürsich, F., Lima, F.H.O., Fauth, G., Assine, M.L., 2023. Fossil-bearing concretions of the Araripe Basin accumulated during oceanic anoxic event 1b. Paleoceanography and Paleoclimatology 38, e2023PA004736. https://doi.org/10.1029/2023PA004736.

Brito, I.M., Quadros, L.P., 1995. Retrabalhamento do Devoniano no Cretáceo Inferior da Bacia do Araripe. Anais da Academia Brasileira de Ciências 67 (4), 493–496. Rio de Janeiro.

Carvalho, M.A., Bengtson, P., Lana, C.C., Sá, N.D., Santiago, G., Giannerini, M.C., 2019. Late Aptian (Early Cretaceous) dry-wet cycles and their effects on vegetation in the South Atlantic: Palynological evidence. Cretaceous Research 100, 172–183. https://doi.org/10.1016/j.cretres.2019.03.021.

Carvalho, M.A., Lana, C.C., Bengtson, P., Sá, N.D., 2017. Late Aptian (Cretaceous) climate changes in northeastern Brazil: a reconstruction based on indicator species analysis (IndVal). Palaeogeography, Palaeoclimatology, Palaeoecology 485, 543–560. https://doi.org/10.1016/j.palaeo.2017.07.011.

Carvalho, M.A., Lana, C.C., Sá, N.D., Santiago, G., Giannerini, M.C., Bengtson, P., 2022. Influence of the intertropical convergence zone on early Cretaceous plant distribution in the South Atlantic. Scientific Reports 12, 12600. https://doi.org/10.1038/s41598-022-16580-x.

Carvalho, M.A., Mendonça Filho, J.G., Menezes, T.R., 2006. Palynofacies and sequence stratigraphy of the Aptian–Albian of the Sergipe Basin, Brazil. Sedimentary Geology 192, 57–74. https://doi.org/10.1016/j.sedgeo.2006.03.017.

Carvalho, M.A., Ramos, R.C., Crud, M.B., Witovisk, L., Kellner, A.W., Silva, H.P., Grillo, O.N., Riff, D., Romano, P.S., 2013. Palynofacies as indicators of paleoenvironmental changes in a Cretaceous succession from the Larsen Basin, James Ross Island, Antarctica. Sedimentary Geology 295, 53–66. https://doi.org/10.1016/j.sedgeo.2013.08.002.

Chagas, D.B., Assine, M.L., Freitas, F.I., 2007. Fácies sedimentares e ambientes deposicionais da Formação Barbalha no Vale do Cariri, Bacia do Araripe, Nordeste do Brasil. Geociências UNESP 26, 313–322.

Coimbra, J.C., Arai, M., Carreño, A.L., 2002. Biostratigraphy of Lower Cretaceous microfossils from the Araripe Basin, northeastern Brazil. Geobios 35 (6), 687–698. https://doi.org/10.1016/S0016-6995(02)00082-7.

Coimbra, J.C., Freire, T.M., 2021. Age of the post-rift Sequence I from the Araripe Basin, Lower Cretaceous, NE Brazil: implications for spatio-temporal correlation. Revista Brasileira de Paleontologia 24 (1), 37–46. https://doi.org/10.4072/rbp.2021.1.03.

Cooper, M.R., 1977. Eustacy during the Cretaceous: Its implications and importance. Palaeogeography, Palaeoclimatology, Palaeoecology 22, 1–60. https://doi.org/10.1016/0031-0182(77)90032-3.

Custódio, M.A., Quaglio, F., Warren, L.V., Simões, M.G., Fürsich, F.T., Perinotto, J.A.J., Assine, M.L., 2017. The transgressive-regressive cycle of the Romualdo Formation (Araripe Basin): sedimentary archive of the Early Cretaceous marine ingression in the interior of northeast Brazil. Sedimentary Geology 359, 1–15. https://doi.org/10.1016/j.sedgeo.2017.07.010.

Dino, R., 1992. Palinologia, bioestratigrafia e paleoecologia da formação Alagamar, Cretáceo da Bacia Potiguar, Nordeste do Brasil. Instituto de Geociências. Universidade de São Paulo, São Paulo, p. 300. Tese de Doutorado.

Dino, R., 1994. Some new pollen grain species from Lower Cretaceous in northeastern Brasil. Boletim de Geociencias da Petrobras 8 (2), 257–273. https://www.researchgate.net/publication/293103813.

Doyle, J.A., Jardiné, S., Doerenkamp, A., 1982. *Afropollis*, a new genus of early angiosperm pollen, with notes on the Cretaceous palynostratigraphy and paleoenvironments of Northern Gondwana. Bull. Centre Res. Expl. Prod. Elf-Aquitaine 6, 39–117.

Fabin, C.E., Correia Filho, O.J., Alencar, M.L., Barbosa, J.A., Miranda, T.S., Neumann, V.H.M.L., Gomes, I.F., Santana, F.R., 2018. Stratigraphic Relations of the Ipubi Formation, Siliciclastic- Evaporitic Succession of the Araripe Basin. Anais da Academia Brasileira de Ciências 90 (2 Suppl. 1), 2049–2071. https://doi.org/10.1590/0001-3765201820170526.

Fambrini, G.L., de Lemos, D.R., Tesser, Jr., S., De Araújo, J.T., Da Silva-Filho, W.F., de Souza, B.Y.C., Neumann, V.H., 2011. Estratigrafia, arquitetura deposicional e faciologia da Formação Missão Velha (Neojurássico-Eocretáceo) na área-tipo, Bacia do Araripe, Nordeste do Brasil: Exemplo de sedimentação de estágio de início de rifte a clímax de rifte. Geologia USP: Série Científica 11, 55–87. http://www.repositorio.ufc.br/handle/riufc/65263.

Fambrini, G.L., Silvestre, D., Menezes-Filho, A.B., Da Costa, A.C., Neumann, V.H., 2019. Architectural and facies characterization of the Aptian fluvial Barbalha Formation, Araripe Basin, NE Brazil. In: Geoscience to Engineering. Geological Society of London, Special Publications, pp. 119–150. https://doi.org/10.1144/SP488-2017-275, 488(1.

Fambrini, G.L., Silvestre, D.D.C., Junior, A.M.B., Da Silva-Filho, W.F., 2020. Estratigrafia da Bacia do Araripe: Estado da arte, revisão crítica e resultados novos. Geologia USP: Série Científica 20, 169–212. https://doi.org/10.11606/issn.2316-9095.v20-163467.

Fauth, G., Kern, H.P., Villegas, J., De Lira, M.A., Marcos Antonio Batista, M.A., Amanda Santa, A., Maia, L., Luft-Souza, F., Strohschoen, O., Andressa Nauter-Alves, A., Tungo, E.J.F., Rodrigues, M.D., Ceolin, D., Baecker-Fauth, S., Hünnig, M.H., De Oliveira, F.H., Santos, A., Assine, M., 2023. Early Aptian marine incursions in the interior of northeastern Brazil following the Gondwana breakup. Scientific Reports 13, 6728. https://doi.org/10.1038/s41598-023-32967-w.

UNCORRECTED PROOF

Ferraro, S., Coccioni, R., Sabatino, N., Del Core, M., Sprovieri, M., 2020. Morphometric response of late Aptian planktonic foraminiferal communities to environmental changes: A case study of *Paraticinella rohri* at Poggio le Guaine (central Italy). Palaeogeography, Palaeoclimatology, Palaeoecology 538, 109384. https://doi.org/10.1016/j.palaeo.2019.109384.

Garcia, A.J.V., Da Rosa, A.A.S., Goldberg, K., 2005. Paleoenvironmental and paleoclimatic control on early diagenetic processes and fossil record in Cretaceous continental sandstones of Brazil. Journal of South American Earth Sciences 19 (3), 243–258. https://doi.org/10.1016/j.jsames.2005.01.008.

Goldberg, K., Preamor, E., Bardola, T., Souza, P.A., 2019. Aptian marine ingression in the Araripe Basin: implications for paleogeographic reconstruction and evaporite accumulation. Marine and Petroleum Geology 107, 214–221. https://doi.org/10.1016/j.marpetgeo.2019.05.011.

Gonzalez, L.C., Mastalerz, M., Mendonça Filho, J.G., 2020. Application of organic facies and biomarkers in characterization of paleoenvironmental conditions and maturity of sediments from the Codó Formation in the west-central part of the São Luís Basin, Brazil. International Journal of Coal Geology 225, 103482. https://doi.org/10.1016/j.coal.2020.103482.

Guzmán, J., Piovesan, E.K., Melo, R.M., Almeida-Lima, D., De Jesus e Sousa, A., Neumann, V.H., 2023. Ostracoda and Foraminifera biostratigraphy and palaeoenvironmental evolution of the Aptian Santana Group, post-rift of the Araripe Basin, Brazil. Gondwana Research 124, 18–38. https://doi.org/10.1016/j.gr.2023.06.014.

Heimhofer, U., Hochuli, P., 2010. Early Cretaceous angiosperm pollen from a low-latitude succession (Araripe Basin, NE Brazil). Review of Palaeobotany and Palynology 161, 105–126. https://doi.org/10.1016/j.revpalbo.2010.03.010.

Ibrahim, M., Al-Saad, H., Kholeif, S., 2002. Chronostratigraphy, palynofacies, source rock potential, and organic thermal maturity of Jurassic rocks of Qatar. GeoArabia 7, 675–696. https://doi.org/10.2113/geoarabia0704675.

Jain, K.P., Millepied, P., 1975. Cretaceous microplankton from Senegal Basin, West Africa. II. systematics and biostratigraphy. Geophytology 5, 126–171.

Kholeif, S., Ibrahim, M., 2010. Palynofacies Analysis of Inner Continental Shelf and Middle Slope Sediments offshore Egypt, South-eastern Mediterranean. Geobios 43 (3), 333–347. https://doi.org/10.1016/j.geobios.2009.10.006.

Lemos, F.A.P., Asakura, Y., Antunes, R.L., Araripe, R.V.C., Prado, L.A.C., Tomé, M.E.T., Oliveira, D.H., Nascimento, L.R.S., Ng, C., Barreto, A.M.F., 2023. Calcareous nannofossils, biostratigraphy, and paleobiogeography of the Aptian/Albian Romualdo Formation in the Araripe Basin, North-Eastern Brazil. Brazilian Journal of Genetics 53 (2). https://doi.org/10.1590/2317-4889202320220054.

Lister, J.K., Batten, D.J., 1988. Stratigraphic and palaeoenvironmental distribution of Early Cretaceous dinoflagellate cysts in the Hurlands Farm Borehole, West Sussex, England. Palaeontographica Abteilung B Band 210, 9–89.

Lúcio, T., Souza Neto, J.A., Selby, D., 2020. Late Barremian/Early Aptian Re-Os age of the Ipubi Formation black shales: Stratigraphic and paleoenvironmental implications for Araripe Basin, northeastern Brazil. Journal of South American Earth Sciences 102, 102699. https://doi.org/10.1016/j.jsames.2020.102699.

Melo, R.M., Guzmán, J., Almeida-Lima, D., Piovesan, E.K., Neumann, V.H., Sousa, A.J., 2020. New marine data and age accuracy of the Romualdo Formation, Araripe Basin, Brazil. Scientific Reports 10, 15779. https://doi.org/10.1038/s41598-020-72789-8.

Mendonça Filho, J.G., Menezes, T.R., 2011. Organic matter: concepts and definitions. In: Flores, D., Marques, M. (Eds.), ICCP Training Course on Dispersed Organic Matter. ICCP, Porto, pp. 1–12.

Mendonça Filho, J.G., Menezes, T.R., Mendonça, J.O., Oliveira, A.D., Carvalho, M.A., Sant'Anna, A.J., Souza, J.T., 2010. Palinofácies. In: Carvalho, I.S. (Ed.), Paleontologia. Interciência, Rio de Janeiro, pp. 379–413.

Mendonça Filho, J.G., Menezes, T.R., Mendonça, J.O., 2011. Organic composition (Palynofacies Analysis). In: 4th ICCP Training Course on Dispersed Organic Matter. ICCP, Porto, pp. 33–81.

Michels, F.H., Souza, P.A., Premaor, E., 2018. Aptian-Albian palynologic assemblages interbedded within salt deposits in the Espírito Santo Basin, eastern Brazil: Biostratigraphical and paleoenvironmental analysis. Marine and Petroleum Geology 91, 785–799. https://doi.org/10.1016/j.marpetgeo.2018.01.023.

Muller, J., Di Giacomo, E., Van Erve, A.W., 1987. A palynological zonation for the cretaceous, tertiary, and quaternary of northern South America. American Association of Stratigraphic Palynologists Contributions Series 19, 7–76.

Neumann, V.H., 1999. Estratigrafía, Sedimentología, Geoquímica y Diagenesis de los Sistemas Lacustres Aptienses-Albienses de la Cuenca de Araripe (Noreste do Brasil). Universidade de Barcelona, Barcelona, p. 233. PhD thesis.

Neumann, V.H., Assine, M.L., 2015. Stratigraphic proposal to the post-rift I tectonicsedimentary sequence of Araripe Basin, Northeastern Brazil, Strati 2015. In: 2nd International Congress on Stratigraphy. Berichte des Institutes für Erdwissenschaften der Universitat Graz, p. 274.

Neumann, V.H., Borrego, A.G., Cabrera, L., Dino, R., 2003. Organic matter composition and distribution through the Aptian-Albian lacustrine sequences of the Araripe Basin, northeastern Brazil. International Journal of Coal Geology 54, 21–40. https://doi.org/10.1016/S0166-5162(03)00018-1.

Neumann, V.H., Cabrera, L., 1999. Uma nueva proposta estratigráfica para la tectonosecuencia post-rifte de la Cuenca de Araripe, Noreste de Brasil. In: Boletim do 5º Simpósio sobre o Cretáceo do Brasil, pp. 279–285.

Ponte, F.C., Appi, C.J., 1990. Proposta de revisão da coluna estratigráfica da Bacia do Araripe. In: Congresso Brasileiro de Geologia, vol. 36. Sociedade Brasileira de Geologia, Anais, SBG, Natal, pp. 211–226.

Ponte, F.C., Asmus, H.E., 1978. Geological framework of the Brazilian continental margin. Geologische Rundschau 67, 201–235.

Pontes, N.V., das Chagas, D.B., de Souza, A.C.B., do Nascimento Junior, D.R., da Silva Filho, W.F., Capilla, R., Garcia, A.J.V., de Araújo Nogueira Neto, J., 2021. Organic and isotopic geochemistry of evaporites and shales of the Santana group (Araripe Basin, Brazil): clues on the evolution of depositional systems and global correlation during the lower cretaceous. Minerals 1 (8), 795. https://doi.org/10.3390/min11080795.

Ponte, F.C., Ponte Filho, F.C., 1996. Evolução Tectônica e Classificação da Bacia do Araripe. Report of the Departamento Nacional de Produção Mineral, p. 68. Recife, Brasil.

Regali, M.S.P., 1987. Palinomorfos do Barremiano/Albiano brasileiros. Parte II. 10th Congresso Brasileiro de Paleontologia 2, 647–655. Rio de Janeiro, Anais.

Regali, M.S.P., Santos, P.R.S., 1999. Palinoestratigrafia e geocronologia dos sedimentos Albo-Aptianos das bacias de Sergipe e Alagoas – Brasil. In: Boletim do 5th Simpósio sobre o Cretáceo do Brasil, pp. 411–419. Serra Negra-SP.

Regali, M.S.P., Uesugui, N., Santos, A.S., 1974. Palinologia dos Sedimentos Meso-Cenozóicos do Brasil (1). Boletim Tec. da Petrobras 17 (3), 177190.

Regali, M.S.P., Viana, C.F., 1989. Sedimentos do neo-jurássico Eocretáceo do Brasil: Idade e correlacão com a escala internacional. Petrobras, Rio de Janeiro, p. 95.

Santos, A., De Lira Mota, M.A., Kern, H.P., Fauth, G., Paim, P.S.G., Netto, R.G., Sedorko, D., Lavina, E.L.C., Krahl, G., Fallgatter, C., da Silveira, D.M., Aquino, C.D., dos Santos, M.O., Baecker-Fauth, S., Vieira, C.E.L., 2022. Earlier onset of the Early Cretaceous Equatorial humidity belt. Global and Planetary Change 208, 103724. https://doi.org/10.1016/j.gloplacha.2021.103724.

Scherer, C.M.S., Goldberg, K., Bardola, T., 2015. Facies architecture and sequence stratigraphy of an early post-rift fluvial succession, Aptian Barbalha Formation, Araripe Basin, northeastern Brazil. Sedimentary Geology 322 (1), 43–62. https://doi.org/10.1016/j.sedgeo.2015.03.010.

Scherer, C.M.S., Jardim de Sá, E.F., Córdoba, V.C., Sousa, D.C., Aquino, M.M., Cardoso, F.M.C., 2014. Tectono-stratigraphic evolution of the Upper Jurassic - Neocomian rift succession, Araripe Basin, Northeast Brazil. Journal of South American Earth Sciences 49, 106–122. https://doi.org/10.1016/j.jsames.2013.10.007.

Silveira, L.F., Borghi, L., Bobco, F.E.R., Araújo, B.C., Kroth, M., Duarte, G., Ferreira, L.O., Mendonça, J.O., 2023. Multiscale characterization of an extensive stromatolite field: A new correlation horizon for the Crato member, Araripe Basin, Brazil. Journal of Sedimentary Research 93, 776–795. https://doi.org/10.2110/jsr.2022.090.

Souza-Lima, W., Silva, R.O., 2018. Aptian–Albian paleophytogeography and paleoclimatology from Northeastern Brazil sedimentary basins. Review of Palaeobotany and Palynology 258, 163–189. https://doi.org/10.1016/j.revpalbo.2018.08.003.

Stancliffe, R.P.W., 1989. Microforaminifera linings: Their Classification, Biostratigraphy and Palaeoecology, with special reference to specimens from British Oxfordian sediments. Micropaleontology 35, 337–352. https://doi.org/10.2307/1485676.

Teixeira, M.C., Mendonça Filho, J.G., de Oliveira, A.D., Assine, M.L., 2017. Faciologia orgânica da Formação Romualdo (Grupo Santana, Cretáceo Inferior da Bacia do Araripe): caracterização da matéria orgânica sedimentar e interpretação paleoambiental. Geologia USP: Série Científica 17 (4), 19–44. https://doi.org/10.11606/issn.2316-9095.v17-347.

Tucker, M.E., 2014. Rochas sedimentares: Guia geológico de campo Maurice E. Tucker: tradução Rualdo Menegat. 4. Bookman, Porto Alegre, p. 344.

Tyson, R.V., 1989. Late Jurassic palynofacies trends, Piper and Kimmeridge Clay Formation, UK onshore and offshore. In: Batten, D.J., Keen, M.C. (Eds.), Northwest European Micropalaeontology and palynology. British Micropalaeontological Society Series, pp. 135–172.

Tyson, R.V., 1993. Palynofacies analysis. In: Jenkins, D.J. (Ed.), Applied Micropalaeontology. Kluwer Academic Publishers, Dordrecht, pp. 153–191.

Tyson, R.V., 1995. Sedimentary Organic Matter: Organic Facies and Palynofacies. Chapman & Hall, Londres, p. 615.

Vallejo, J.D., Piovesan, E.K., Carvalho, M.A., Guzmán, J., 2023. Palynofacies analyses of Santana Group, upper Aptian of the Araripe Basin, northeast Brazil: Paleoenvironmental reconstruction. Journal of South American Earth Sciences 121, 104154. https://doi.org/10.1016/j.jsames.2022.104154.

Varejão, F.G., 2019. Abordagem multi-indicadores do sistema misto carbonáticosiliciclástico da Formação Crato: evolução sedimentar, paleogeografia e tectônica. PhD thesis. Universidade Estadual Paulista "Júlio de Mesquita Filho, p. 163.

Varejão, F.G., Silva, V.R., Assine, M.L., Warren, L.V., Matos, S.A., Rodrigues, M.G., Fürsich, F.T., Simões, M.G., 2021b. Marine or freshwater? Accessing the paleoenvironmental param of the Caldas Bed, a key marker bed in the Crato Formation (Araripe Basin, NE Brazil). Brazilian Journal of Genetics 51 (1), 2020009. https://doi.org/10.1590/2317-4889202120200009.

Varejão, F.G., Warren, L.V., Simões, M.G., Buatois, L.A., Mángano, M.G., Bahniuk Rumbelsperger, A.M., Assine, M.L., 2021a. Mixed siliciclastic–carbonate sedimentation in an evolving epicontinental sea: Aptian record of marginal marine settings in the interior basins of north-eastern Brazil. Sedimentology 68, 2125–2164. https://doi.org/10.1111/sed.12846.

Appendix A. Supplementary data

Supplementary data to this article can be found online at https://doi.org/10.1016/j.cretres.2024.106016.

APÊNDICE G- ABUNDÂNCIA ABSOLUTA DAS ESPÉCIES DETERMINADAS

Taxon	Autor	Araripe		Jatobá		Total geral
		2-AR-SR-1A-CE	2-AR-SR-1B-CE	2-JB-SN-2A-PE	2-JB-SN-2B-PE	
Afropollis jardinus	Doyle, Jardiné and Doerenkamp, 1982	133	4		12	149
Appendicisporites tricornitatus	Weyland and Greifeld 1953				1	1
Araucariacites australis	Cookson, 1947	91	124	260	365	840
Bellisporites pallescens	Pocock, 1970		1	3		4
Bennettitaepollenites regaliae	Dino, 1994	16	3	7	132	158
Biretisporites deltoidus	Dettmann, 1963		2			2
Callialasporites dampieri	Dev, 1961				11	11
Callialasporites segmentatus	(Balme, 1957) Srivastava, 1963	12	8	5	34	59
Callialasporites trilobatus	(Balme) Dev 1961	2	11		16	29
Callialasporites turbatus	(Balme, 1957) Schultz, 1967	15	15	36	27	93
cf. *Laricoidites magnus*	(Potonié) Potonié Thomson and Thiegart 1950			7		7
Chomotriletes almegrensis	Pocock, 1962		3			3
Chomotriletes fragilis	Pocock, 1962		24		3	27
Chomotriletes minor	(Kedves, 1961) Pocock, 1970	26	5			31
Cicatricosisporites microstriatus	Jardiné and Magloire, 1963	15	13	31	42	101
Cicatricosisporites purbeckensis	Norris, 1969				3	3
Cicatricosisporites avnimelechi	Horowitz, 1970	24	22	79	47	172
Cicatricosisporites brevilaesuratus	Couper, 1958	10	8	23	55	96
Cicatricosisporites nuni	Horowitz, 1970		6	10		16
Cicatricosisporites pseudotripartitus	(Bolchovitina) Dettmann, 1963			2		2
Classopollis alexi	Burger, 1965	10	12	239	528	789
Classopollis classoides	(Pflug, 1953) Pocock and Jansonius, 1961	548	212	148	759	1667
Classopollis torosus	(Reissinger) Couper, 1958				139	139
Complicatisaccus cearensis	Regali, 1987	2			1	3
Corollaria annularis	Malyawkina, 1953				7	7
Crybelosporites pannuceus	(Brenner) Srivastava, 1975			2	5	7
Crybelosporites truncatus	Lima, 1979	7	3	2	2	14
Cyathidites cf. *mesozoicus*	(Thiegart) Potonié, 1956			1		1
Cycadopites glottus	(Brenner) Wingate, 1980	2	6	7	7	22
Cycadopites nitidus	(Balme) de Jersey, 1964	6			4	10
Deltoidospora australis	(Couper, 1953) Pocock, 1970	19	14	29	10	72
Deltoidospora cf. *hallii*	Miner, 1935			5		5
Obtusisporis juncta	(Kara-Murza) Pocock,1970		2			2
Deltoidospora tenuis	Lima, 1978	12	12	38	29	91
Densoisporites cf. *microrugulatus*	Brenner, 1963	6	3	4	8	21
Elaterosporites klaszii	(Jardine and Magloire, 1965)		1			1
Equisetosporites albertensis	Singh, 1964				8	8
Equisetosporites ambiguus	(Hedlund 1966) Singh, 1983	25	2	12	2	41
Equisetosporites concinnus	Singh, 1964	1	2	10	27	40
Equisetosporites costaliferous	(Brenner 1968) Lima, 1980			5		5
Equisetosporites elegans	Lima, 1980		4	3	24	31
Equisetosporites lanceolatus	Lima, 1980		10	17	9	36
Equisetosporites leptomatus	Lima, 1980	3	18	6	8	35
Equisetosporites maculosus	Dino, 1994	28		2	29	59
Equisetosporites minuticostatus	Lima, 1980		2			2
Equisetosporites ovatus	(Pierce, 1961) Singh, 1964	1		1		2
Equisetosporites subcircularis	Lima, 1980				8	8
Eucommiidites troedssonii	(Erdtman, 1948) Potonie, 1958	16	1	15	1	33
Exesipollenites tumulus	Balme, 1957	14	1	2	118	135
Gnetaceaepollenites barghoornii	(Pocock) Lima, 1980		3		13	16
Gnetaceaepollenites jansonii	(Pocock) Lima, 1980	23	7	49	113	192
Gnetaceaepollenites mollis	(Srivastava) Lima, 1979				1	1
Gnetaceaepollenites oreadis	Srivastava, 1968		3		13	16
Gnetaceaepollenites retangularis	Lima, 1980	20	7	70	87	184
Gnetaceaepollenites uesuguii	Lima, 1979	3	2	1	25	31
Gnetaceaepollenites undulatus	(Regali et al. 1974) Lima, 1979	1				1
Inaperturopollenites dubius	(Potonie and Venitz) Pflug and Thomson, 1953		1			1
Ischyosporites foveolatus	(Pocock) Fensome, 1987	15	1	18	27	61
Ischyosporites granulosus	Tralau, 1968		4	4		8
Ischyosporites pseudoreticulatus	(Couper) Döring, 1965	3		5	2	10
Leptolepidites psarosus	Norris, 1969			14		14
Leptolepidites tumulosus	(Döring 1964) Srivastava, 1975			1		1
Leptolepidites verrucatus	Couper, 1953	60	12	13		85
Matonisporites silvai	Lima, 1979	5	4	7	47	63
Paludites mamelonatus	Lima, 1979	100	6	34		140
Penetetrapites mollis	Hedlund and Norris, 1968	18				18
Pennipollis reticulatus	(Brenner 1963) Friis Pedersen and Crane, 2000	8		15		23
Regalipollenites amphoriformis	(Regali et al. 1974) Lima, 1979	5	2		1	8
Reyrea polymorphus	Herngreen, 1973			1		1
Schizosporis parvus	Cookson and Dettmann, 1959	3				3
Sergipea naviformis	Regali, Uesugui and Santos, 1974	3		1	4	8
Sergipea tenuiverrucata	Regali, Uesugui and Santos, 1974	1		7	1	9
Sergipea variverrucata	Regali, Uesugui and Santos, 1974	3		86	16	105
Singhia acicularis	Lima, 1980	8	3		1	12
Singhia elongata	(Horowitz) Lima, 1980	3	2			5
Singhia montanaensis	(Brenner 1968) Lima, 1980		10	3	21	34
Singhia punctata	Lima, 1980	10	2	19	79	110
Singhia reyrei	Lima, 1980	5	7		2	14
Steevesipollenites binodosus	Stover, 1964		1			1
Steevesipollenites pygmeus	Azema and Boltenhagen, 1974		1	4		5
Stellatopollis araripensis	Lima, 1989	16				16
Stellatopollis barghoornii	Doyle, 1976	1				1
Stellatopollis densiornatus	Lima, 1989	11			2	13
Stellatopollis dubius	Lima, 1989	43			2	45
Stereisporites psilatus	(Ross) Manum, 1954	4	1			5
Todisporites minor	Couper, 1958			3		3
Triporoletes reticulatus	(Pocock 1962) Playford, 1971	23	8			31
Trisectoris reticulatus	Heimhofer and Hochuli, 2010	12	2	4	7	25
Uesuguipollenites callosus	Dino, 1994	15	1	151	45	212

APÊNDICE H- TABELA DE DISTRIBUIÇÃO ESTRATIGRÁFICA DAS ABUNDÂNCIAS ABSOLUTAS DOS PALINOMORFOS DO TESTEMUNHO 2-AR-SR-1A-CE

Hole ID	From	To	Sample #	*Afropollis*	*Afropollis jardinus*	*Afropollis operculatus*	*Afropollis zonatus*	*Araucariacites*	*Araucariacites australis*	*Bennettitaepollenites*	*Bennettitaepollenites regaliae*	*Callialasporites*	*Callialasporites segmentatus*	*Callialasporites trilobatus*	*Callialasporites turbatus*	*Classopollis*	*Classopollis* (Tétrade)	*Classopollis alexi*	*Classopollis classoides*	*Complicatisaccus cearensis*	*Conferticulcites*	*Cycadopites*	*Cycadopites nitidus*	*Dichatopollenites*	*Equisetosporites*	*Equisetosporites ambiguus*	*Equisetosporites concinnus*	*Equisetosporites leptomatus*	*Equisetosporites maculosus*	*Equisetosporites ovatus*	*Equisetosporites reyrei*
AR-SR-1A-CE	11,29	11,31	25b					2								8			3												
AR-SR-1A-CE	13,29	13,32	32					1	3							116	12		29			1			4						
AR-SR-1A-CE	15,08	15,12	38	5												171	17		34			1			9						
AR-SR-1A-CE	15,95	15,97	46	5	2			2		1					4	28			5						2						
AR-SR-1A-CE	27,02	27,05	58																			1									
AR-SR-1A-CE	31,23	31,27	68																													
AR-SR-1A-CE	37,17	37,2	78	3	1			4											12												
AR-SR-1A-CE	37,4	37,43	81					3	2							46			9												
AR-SR-1A-CE	39,49	39,51	92	1	1								1			23		3	6												
AR-SR-1A-CE	46,18	46,22	109		1											2			1												
AR-SR-1A-CE	46,38	46.40	111													28															
AR-SR-1A-CE	47,57	47,6	121					2				1			1	37						5			2						
AR-SR-1A-CE	48,75	48,78	127B																													
AR-SR-1A-CE	50,31	50,33	136													2			1			1									
AR-SR-1A-CE	54,36	54,39	147													14		1													
AR-SR-1A-CE	54,4	54,43	148																													
AR-SR-1A-CE	54,74	54,76	150																													
AR-SR-1A-CE	55,34	55,37	155																													
AR-SR-1A-CE	57,72	57,54	164																													
AR-SR-1A-CE	59,61	59,65	168	1	1			4								125	18	1				2									
AR-SR-1A-CE	64,37	64,4	178													7									2						
AR-SR-1A-CE	68,43	68,46	187	26	3					3						195	4		5						11					1	
AR-SR-1A-CE	70	70,04	202	11					3	4					2		23	2	1			13			23			1			
AR-SR-1A-CE	70,83	70,85	209	1				2								39															
AR-SR-1A-CE	80,18	80,21	216	17	2							1				12			5						1						
AR-SR-1A-CE	83,51	83,55	222	54	4			2											5		1										
AR-SR-1A-CE	86,62	86,65	230	37	26			1				1				38	9		24		2				1						
AR-SR-1A-CE	88,16	88,19	234	45	3	8		8	9	1		2	1			112	1		2						11	1					
AR-SR-1A-CE	88,83	88,86	238	21	5			5				2				46			22						7						
AR-SR-1A-CE	96,25	96,69	245	4	2	1										79	5		16						19			2			
AR-SR-1A-CE	99,39	99,41	250													18									3						
AR-SR-1A-CE	99,78	99,8	253	4	9			2	15			3	4			173	11		19	1		6	6		14		1				
AR-SR-1A-CE	102,9	102,9	264													3															
AR-SR-1A-CE	105,7	105,8	277	25	3	1				1	3				1	162	1					1			38				15		
AR-SR-1A-CE	106,7	106,8	285	6	2	5		5	3	5	9	7	3		1	135	1		21			1		1	28	5			4		
AR-SR-1A-CE	107,5	107,5	292													25									1						
AR-SR-1A-CE	109	109,1	303	2												65	12								15				1		
AR-SR-1A-CE	110,4	110,5	316													53	14								1				5		
AR-SR-1A-CE	111,7	111,7	324	64		7		11	3		1	1				112	1		26						17						
AR-SR-1A-CE	112,4	112,4	333	2						1		2				148	5		1						3						
AR-SR-1A-CE	112,5	112,6	335													16		1													
AR-SR-1A-CE	118,3	118,4	347																													
AR-SR-1A-CE	119	119	352	1	2											4															
AR-SR-1A-CE	119,5	119,6	357	18	19	6		25	5	3	1	2				17	7		24		1				31						
AR-SR-1A-CE	120,5	120,5	365	3	9	2		5				4			2	133	9		13						12				3		
AR-SR-1A-CE	121,7	121,7	377	2												42	8		8						5				1		
AR-SR-1A-CE	122,3	122,4	384													31	2								9						
AR-SR-1A-CE	123,2	123,2	391	5	1			2		2						19	4		23			3			7						
AR-SR-1A-CE	124,4	124,4	404	37		4		12		1	2	2	1			71			2		3				3	18					
AR-SR-1A-CE	125	125	410	2	2											17	1	1				1			3	1					
AR-SR-1A-CE	126	126	417		5											22	2								2						
AR-SR-1A-CE	126,5	126,5	420	13	16		3	11				3				66	7		26		1				16						
AR-SR-1A-CE	128,9	128,9	431													2															
AR-SR-1A-CE	131,7	131,8	440	7		5		69	11			8			3	3			25	1					14						1
AR-SR-1A-CE	132,7	132,8	443		3			1		4		3		1		1			51						8						
AR-SR-1A-CE	134	134,1	448	3	11		1	8	14	2		4				58			69						5						
AR-SR-1A-CE	136,9	137	459	23		3		52	23	1		11	2	1		72			15						9						
AR-SR-1A-CE	137,9	137,9	466													1					1										

Sample #	*Eucommiidites troedssonii*	*Exesipollenites*	*Exesipollenites tumulus*	*Gnetaceaepollenites*	*Gnetaceaepollenites jansonii*	*Gnetaceaepollenites retangularis*	*Gnetaceaepollenites uesugii*	*Gnetaceaepollenites undulatus*	*Inaperturopollenites*	*Monosulcites*	*Monosulcites glottus*	*Penetetrapites mollis*	*Pennipollis reticulatus*	*Proxapertites*	*Psilatricolpites*	*Regalipollenites amphoriformis*	*Retitricolpites*	*Sergipea tenuiverrucata*	*Sergipea variverrucata*	*Singhia*	*Singhia acicularis*	*Singhia elongata*	*Singhia punctata*	*Singhia reyrei*	*Steevesipollenites*	*Stellatopollis*	*Stellatopollis araripensis*	*Stellatopollis barghoornii*	*Stellatopollis densiornatus*	*Stellatopollis dubius*	*Trisectoris reticulatus*	*Uesuguipollenites callosus*
25b																																
32									4																							
38	1								13																							
46				2					29														1									
58									2																							
68																																
78									3																							
81									4																							
92				1																												
109																																
111																																
121	1			5					5											3					2							
127B																																
136																																
147																											1					
148																																
150																																
155																																
164																																
168	2								2																							
178																																
187	3			22					1	7										11		1			2							3
202	2		1	2	3			1	6						1					2												
209				1																												
216				3									4												2	8	4		2	2		
222			1	4					9											5					2	73	7	1	7	14	3	
230		1		4					16					1						7	5			2		17	2			5		
234			1	6	2	2			3			5									1	2		1		12				5	1	
238				1	1	1																			5	8			2			
245	2			1						7							2	1														
250																																
253	3		1	3		2			7																							
264																																
277				6					6	2		2					2								4	3						
285		1	1	13	5	8			11										2						2							
292																																
303		1														1																
316		5		1																												7
324			4	4	3				11						1											5					2	1
333									3						9																	
335																	1															
347																																
352									18			1																				
357				6	6				7			2		5											4							
365				6	2				15																3							2
377				1					1		2																					
384																																
391	3			4		1							1	1																		
404			2	12		4			13			8				4	2			1	2				4					3		1
410				1			1		2																1	1						
417				1					11																	13						
420				6					16					3									2		4	19				6	2	
431																																
440				6			2		1				3							1			5		1	8						1
443				2					22					1																	1	
448			3	5	1	2			27					2					1							2				2	2	
459		1		3					9	2													2		1	11	2				1	
466																																

Sample #	*Aequitriradites*	*Appendicisporites*	*Arcellites*	*Biretisporites*	*Camarozonosporites*	*Cardioangulina*	*Chomotriletes minor*	*Cicatricosisporites*	*Cicatricosisporites avnimelechi*	*Cicatricosisporites brevilaesuratus*	*Cicatricosisporites microstriatus*	*Concavissimisporites*	*Crybelosporites*	*Crybelosporites truncatus*	*Cyathidites*	*Cymatiosphaera*	*Deltoidospora*	*Deltoidospora australis*	*Deltoidospora tenuis*	*Densoisporites*	*Densoisporites* cf. *microrugulatus*	*Echinatisporis*	*Foveotriletes*	*Ischyosporites foveolatus*	*Ischyosporites pseudoreticulatus*	*Klukisporites*	*Leptolepidites verrucatus*	*Matonisporites*	*Matonisporites silvai*	*Paludites mamelonatus*	*Perotriletes*	*Psilatriletes* 25-50um
25b								1		1																						
32								1									2	1															2
38																	1	1														
46																																
58																																
68																																
78																																
81		1			1			15									1	1				1										
92																	1															1
109																																
111								1																							
121								1																							
127B																																
136																																
147								1																							
148																																
150																																
155																																
164																																
168								4									1														
178																																
187								1																								1
202								3																							
209																																1
216	2					2	1	31	6	2	2	2	16				8	3	4	1	1		1				1			11		24
222		1		1			1	3					17		2		4	2											3	37	3	14
230					1		1	1			2	1	21					2	2					2	1	1	2		1	35		
234							1	8			2		7	1					2											6		
238								6					3									1				1				2		5
245								1																							
250								1																							
253								9									1		1	1								1				2
264																																
277								6					1				1										4					
285								1	2		1		1				3										7					
292																																
303																																
316																																1
324							4	6					2			1	1				2						4					2
333					1			4																								8
335																																
347																																
352							5	2								2	1																
357								6					1	2			1										1					
365								3									2				1											2
377								3									1															2
384								1																							
391								3					1				2										1					
404	3	1					3	6	2		1		2	1	1		1	3						1			3					3
410								1												1												5
417		3						3					14						1								2					
420		4			4		2	23		3	2		6	3	5		5	2		3	2				1		8					4
431																																
440	6	2			1		5	25	9	1	5		5		2		3	2	1			7	2	9			4		1	5		5
443			1		3			7					6				3							1	1	1	5					4
448					3		3	31	1				6													1	14					
459	6				1			16					3		9			2	1				2	2			3	1		4		
466																																

Sample #	*Reticulatisporites*	*Reticulatus arcuatus*	*Rouseisporites*	*Scabratriletes*	*Schizosporites parvus*	*Schizosporites*	*Stereisporites*	*Stereisporites psilatus*	*Todisporites*	*Triporoletes reticulatus*	*Verrucosisporites*	**Total**	*Subtilisphaera* sp.	Acritarco	Diatomacea	*Maranhites* sp.	Pyrgo	Escolecodonte	Prasinofita	Indeterminados
25b												15	6							7
32												176								69
38												253								32
46												81								42
58												3	3							9
68												0								
78												23								13
81									2			86								24
92												38								12
109												4								
111												29								7
121												65						8		14
127B												0								
136												4								
147												17								7
148												0								
150												0								
155												0								
164												0								
168									1			162								43
178												9								6
187												300								110
202											1	105								56
209												44								1
216									2	2		185		5						156
222				8		2			3	2	2	297		3		3				115
230								1	1	5	3	282								74
234			1									273								50
238											1	145								53
245												142			4					55
250												22								13
253					1							300						3		39
264											1	4								2
277									1		2	291								
285												300								82
292												26								20
303												97								47
316											1	88				2				54
324						4						300	1							46
333											1	188								123
335												18								6
347												0								
352						2						38		23		8				42
357												200						3		112
365												231								37
377									1			77								45
384												43								51
391												83								62
404												243		3		2				72
410												41								19
417						3			2			84		5			2			44
420			3									300		12						133
431												2								1
440	2		2				2		1		8	290		15		3			1	
443			1	3							5	139								53
448											1	282								178
459		3	1		2							300		8		4				133
466																				

APÊNDICE I - TABELA DE DISTRIBUIÇÃO ESTRATIGRÁFICA DAS ABUNDÂNCIAS ABSOLUTAS DOS PALINOMORFOS DO TESTEMUNHO 2-AR-SR-1B-CE

Hole ID	From	To	Sample #	*Afropollis*	*Afropollis jardinus*	*Afropollis zonatus*	*Araucariacites*	*Araucariacites australis*	*Bennettitaepollenites*	*Bennettitaepollenites regaliae*	*Callialasporites segmentatus*	*Callialasporites trilobatus*	*Callialasporites turbatus*	*Classopollis*	*Classopollis* (Tétrade)	*Classopollis alexi*	*Classopollis classoides*	*Confertisulcites*	*Cycadopites*	*Echimonocolpites*	*Elaterosporites klaszii*	*Equisetosporites*	*Equisetosporites ambiguus*
AR-SR-1B-CE	75,6	75,6	155		1			39	2		1		2	74	8	8	56					9	
AR-SR-1B-CE	75,9	75,9	157									1		26	3		3		1			5	
AR-SR-1B-CE	76,1	76,2	159	1				12	1	1			1	33	3		5					8	
AR-SR-1B-CE	76,7	76,7	165	1				2		1		1	2	47			9		2			1	
AR-SR-1B-CE	77,1	77,1	169					9	1			3		93	2		12			1		17	
AR-SR-1B-CE	78,2	78,2	173				16	4	2					65			18		5			4	1
AR-SR-1B-CE	78,7	78,7	178					24			2	5		69	4		22		6			24	
AR-SR-1B-CE	79,2	79,2	183	1	1		5		1	1		1	2	66	2		5					9	
AR-SR-1B-CE	79,5	79,5	188				4							14			1		1				
AR-SR-1B-CE	80,1	80,1	194				8	3	1		2		3	64	8		32				1	1	
AR-SR-1B-CE	80,4	80,4	197	1									1	21			7					4	
AR-SR-1B-CE	81,1	81,1	198				1							24			3					1	
AR-SR-1B-CE	81,5	81,5	201											4									
AR-SR-1B-CE	82,1	82,1	204											4									
AR-SR-1B-CE	82,7	82,7	206																				
AR-SR-1B-CE	83	83,1	208				8	8					1	58	5		5		1				
AR-SR-1B-CE	83,4	83,5	211											4									
AR-SR-1B-CE	84,1	84,1	213	1			4							7	3							1	
AR-SR-1B-CE	84,6	84,6	217				2							27	1							2	
AR-SR-1B-CE	85	85,1	221	1				12	1					11	6		8	2				21	
AR-SR-1B-CE	85,6	85,6	225	2	2	3	4	11	4		3		3	99	6	4	26	2		3		14	1

Sample #	*Equisetosporites concinnus*	*Equisetosporites elegans*	*Equisetosporites lanceolatus*	*Equisetosporites leptomatus*	*Equisetosporites minuticostatus*	*Eucommiidites troedssonii*	*Exesipollenites*	*Exesipollenites tumulus*	*Gnetaceaepollenites*	*Gnetaceaepollenites barghoornii*	*Gnetaceaepollenites jansonii*	*Gnetaceaepollenites oreadis*	*Gnetaceaepollenites retangularis*	*Gnetaceaepollenites uesuguii*	*Inaperturopollenites*	*Inaperturopollenites dubius*	*Monosulcites glottus*	*Penetetrapites*	*Podocarpidites*	*Regalipollenites amphoriformis*	*Retistephanocolporites*	*Retitricolpites*	*Singhia*	*Singhia acicularis*	*Singhia elongata*	*Singhia montanaensis*	*Singhia punctata*	*Singhia reyrei*	*Steevesipollenites*	*Steevesipollenites binodosus*	*Steevesipollenites pygmeus*	*Stellatopollis*	*Trisectoris reticulatus*
155							1		8						4						1					3		1	6				
157			2						1						8										2	3		1	3				
159									1						12	1																	
165	1			2	1				1						1							1							2				
169			3	4					8		3			1	12		5			1		2		1		2		1	3	1			
173									1					1	18							9						1	1			1	
178				5		1			2	3		1	2		14							1							1				
183			4	4					3		2	1			13							1		2		1		2	3				
188																																	
194									1						1				1								1						
197																																	
198																																	
201																																	
204															3																		
206																																	
208											2				14												1						
211															1																		
213															4																		
217															6																		
221	1				1			1				1	2		5		1						1										
225		4	1	3					3				3		26			3		1		3	5			1		1			1		2

Sample #	*Tucanopollis*	*Uesuguipollenites callosus*	*Aequitriradites*	*Appendicisporites*	*Arcellites*	*Auritulinasporites*	*Bellisporites pallescens*	*Biretisporites deltoidus*	*Camarozonosporites*	*Chomotriletes almegrensis*	*Chomotriletes fragilis*	*Chomotriletes minor*	*Cicatricosisporites*	*Cicatricosisporites avnimelechi*	*Cicatricosisporites brevilaesuratus*	*Cicatricosisporites microstriatus*	*Cicatricosisporites nuni*	*Concavissimisporites*	*Crybelosporites*	*Crybelosporites truncatus*	*Cyathidites*	*Cyclogranisporites*	*Cymatiosphaera*
155			4									2	17	8	2	2				2	3		
157												2	2										
159	1												6					1				1	
165													4										
169	1							1			4		16			1					4		
173	5										4		11			1	3						
178												1	32			4			4		4		
183	2				1	1				3	5		18	2	1	1	1				2		
188													4	2							1		
194							1		2				11	6	1	2					1		
197								1					2										
198													1										
201																							
204																							
206																							
208	1										1		13			2			1				
211																							
213																							
217													11		2		1				2		
221				2					1		3		25	1	2		1						
225		1		2							7		13	3					1	1	5		1

Sample #	*Deltoidospora*	*Deltoidospora australis*	*Deltoidospora juncta*	*Deltoidospora tenuis*	*Densoisporites*	*Densoisporites cf. microrugulatus*	*Echinatisporis*	*Foveotriletes*	*Granulatisporites*	*Ischyosporites*	*Ischyosporites foveolatus*	*Ischyosporites granulosus*	*Klukisporites*	*Leptolepidites*	*Leptolepidites verrucatus*	*Matonisporites silvai*	*Paludites mamelonatus*	*Perotrilites*	*Pilosisporites*	*Psilatriletes 25-50um*	*Rouseisporites*	*Schizosporis*	*Stereisporites*	*Stereisporites psilatus*	*Todisporites*	*Undulatisporites*	*Verrucosisporites*	**Total**
155	3	2	1	1		2		1	1	7		3	1	1	2		2		1	2	2						4	300
157			1						2					2													3	71
159		2		2								1																93
165		4					1						1		1						1							87
169	1	2		1						1				1				1									3	222
173	5	2		1	1									4							2							186
178					3					4					4		1			6					1		5	255
183	4									2	1			6	2	2						2					5	191
188																												27
194	3									4						1	2								1			162
197																												37
198					1																						1	32
201					1																							5
204																											1	8
206																												0
208	5			1						1				2			1				2					1		134
211																												5
213					1																							21
217	1																				1						1	57
221				6	3	1							1										1				3	125
225	5	2					3						1	3	3	1								1			3	300

APÊNDICE J - TABELA DE DISTRIBUIÇÃO ESTRATIGRÁFICA DAS ABUNDÂNCIAS ABSOLUTAS DOS PALINOMORFOS DO TESTEMUNHO 2-JB-SN-2A-PE

Hole ID	From	To	Sample #	Afropollis	Afropollis operculatus	Alisporites	Araucariacites	Araucariacites australis	Bennettitaepollenites	Bennettitaepollenites regaliae	Callialasporites	Callialasporites segmentatus	Callialasporites turbatus	cf Laricoidites magnus	Classopollis	Classopollis (Tétrade)	Classopollis alexi	Classopollis classoides	Confertisulcites	Cycadopites	Equisetosporites	Equisetosporites ambiguus	Equisetosporites concinnus	Equisetosporites costaliferous	Equisetosporites elegans	Equisetosporites lanceolatus	Equisetosporites leptomatus	Equisetosporites maculosus	Equisetosporites ovatus	Eucommiidites troedssonii	Exesipollenites	Exesipollenites tumulus	Gnetaceaepollenites	Gnetaceaepollenites jansonii	Gnetaceaepollenites retangularis	Gnetaceaepollenites uesugii
JB-SN-2A-PE	29.25	29.31	2																																	
JB-SN-2A-PE	30.35	30.39	3					11					1		38		4	7			8												4	6		
JB-SN-2A-PE	30.9	30.97	4												1						1															
JB-SN-2A-PE	31.36	31.41	5				5	3							24						2												6			
JB-SN-2A-PE	32.08	32.11	6					2							66						3												9			
JB-SN-2A-PE	32.22	32.26	7												17	2																		1		1
JB-SN-2A-PE	32.37	32.42	8					3					1		76			14		1	7												4			
JB-SN-2A-PE	33.57	33.64	9				1	3							81	3		17			9									1			4			
JB-SN-2A-PE	34.08	34.19	10					14	2		1	1			52	2	5	4			3												4	1		
JB-SN-2A-PE	34.47	34.54	11					2							43	2		10			1													1		
JB-SN-2A-PE	35.31	35.35	12					9		1			1		102	3	6	10			11		5				3			1			4	2	2	
JB-SN-2A-PE	37.39	37.43	13				7	2			1				43															1			3	3		
JB-SN-2A-PE	38.84	38.89	14					13				1	2		83	4		6			4		1										1	1		
JB-SN-2A-PE	39.2	39.23	15								2				22																		1			
JB-SN-2A-PE	39.85	39.87	16				3	5			1				79		11	23			12												4		6	
JB-SN-2A-PE	40.25	40.28	17					15	1		1		1		48			8			7												2			
JB-SN-2A-PE	41.32	41.36	18																									2								
JB-SN-2A-PE	42.00	42.03	19					9							100	4				2	8									2			8	1	5	
JB-SN-2A-PE	43.62	43.66	20					29	4		2		1		50	15		15		3	33					9							16	5	9	
JB-SN-2A-PE	44.14	44.17	21				76		4						100	6	4	4			27					3							11		5	
JB-SN-2A-PE	44.83	44.86	22				8	8							102		5	2		4	45										1		10	15	5	
JB-SN-2A-PE	45.17	45.20	23	2	1			32	4						103	7	15			9	62	5											9	4	11	
JB-SN-2A-PE	45.79	45.84	24	1			60	4	6				3	7	100	10					36					3				6			1		2	
JB-SN-2A-PE	50.06	50.09	25	2				15					2		102	1		4		2	17				1	1				1			4		4	
JB-SN-2A-PE	50.73	50.78	26	1			4	10	4				6		101	17	17		1		20		3				1		1	2			7	1	5	
JB-SN-2A-PE	51.21	51.25	27				3			2			2		103	7	36			2	9				2	1				1			5	1		
JB-SN-2A-PE	51.70	51.75	28												37					1	1															
JB-SN-2A-PE	52.28	52.31	29					6					3		102	9					13	3		2											1	
JB-SN-2A-PE	53.45	53.50	30	1			2	3					2		100					4	26	2		1									12		8	
JB-SN-2A-PE	53.82	53.85	31				7	11		2					86	6	10	9		2	9			1									7	1	7	
JB-SN-2A-PE	54.54	54.47	32				7	17	3	1		2	2		103	18	15			3	27						2						1	5		
JB-SN-2A-PE	55.40	55.43	33				3						1		75						10		1									2	6			
JB-SN-2A-PE	56.51	56.53	34					23	3	1	2	1	2		102	6	1				37	2		1									10			
JB-SN-2A-PE	58.08	58.12	35			1		4	1						101	24	24	3		1	10													1		
JB-SN-2A-PE	59.36	59.40	36				1				1				89	1	21				1															
JB-SN-2A-PE	65.42	65.45																																		
JB-SN-2A-PE	68.36	68.39																																		
JB-SN-2A-PE	74.46	74.49																																		
JB-SN-2A-PE	74.86	74.90																																		
JB-SN-2A-PE	77.36	77.4																																		
JB-SN-2A-PE	82.44	82.47																																		
JB-SN-2A-PE	87.41	87.45	43												7																					
JB-SN-2A-PE	88.48	88.51																																		
JB-SN-2A-PE	90.40	90.43																																		
JB-SN-2A-PE	93.69	93.73	46				5	7			1		2		93	12	19				3															
JB-SN-2A-PE	97.27	97.30					14				2		4		83	9	46	12		1													2			

Hole ID	From	To	Sample #	Inaperturopollenites	Monocolpollenites	Monosulcites glottus	Pennipollis reticulatus	Proxapertites	Retitrescolpites	Reyrea cf. polymorphus	Sergipea cf tenuiverrucata	Sergipea naviformis	Sergipea	Sergipea variverrucata	Singhia	Singhia montanaensis	Singhia punctata	Steevesipollenites	Steevesipollenites cf pygmaeus	Stellatopollis	Trichotomosulcites	Trisectoris reticulatus	Uesuguipollenites callosus	Aequitriradites	Appendicisporites	Bellisporites pallescens	Boseisporites	Camarozonosporites	Chomotriletes
JB-SN-2A-PE	29.25	29.31	2																										
JB-SN-2A-PE	30.35	30.39	3	7									1	1														1	
JB-SN-2A-PE	30.9	30.97	4											1															
JB-SN-2A-PE	31.36	31.41	5	3						1				1											1				
JB-SN-2A-PE	32.08	32.11	6																										
JB-SN-2A-PE	32.22	32.26	7																										
JB-SN-2A-PE	32.37	32.42	8	2			3				4			4				1		2			12						
JB-SN-2A-PE	33.57	33.64	9	6										3				1					4						
JB-SN-2A-PE	34.08	34.19	10	11									4												2			2	
JB-SN-2A-PE	34.47	34.54	11	2										1				1					3		1				
JB-SN-2A-PE	35.31	35.35	12	7		2					2		1	1					4				2		1		3		
JB-SN-2A-PE	37.39	37.43	13								1							1		1									
JB-SN-2A-PE	38.84	38.89	14	10																					1				
JB-SN-2A-PE	39.2	39.23	15																										
JB-SN-2A-PE	39.85	39.87	16	9														1		1			4						
JB-SN-2A-PE	40.25	40.28	17	10	1			1						1				1							1				
JB-SN-2A-PE	41.32	41.36	18	4																									
JB-SN-2A-PE	42.00	42.03	19	50		1	5						1	2									7		2		3		1
JB-SN-2A-PE	43.62	43.66	20	7	2							1	5	9						1		3	12	1	2		4		4
JB-SN-2A-PE	44.14	44.17	21	1			3							8									19						1
JB-SN-2A-PE	44.83	44.86	22	13										14								1	2						4
JB-SN-2A-PE	45.17	45.20	23	18	4				3				1	26				3					21		2	3	4		3
JB-SN-2A-PE	45.79	45.84	24	33										2			3			1			17				3		
JB-SN-2A-PE	50.06	50.09	25	6										1	2		3			1			4				2		
JB-SN-2A-PE	50.73	50.78	26	12		1			1				1	2		3	5						8						1
JB-SN-2A-PE	51.21	51.25	27	6		1			1					1	1		3						5						1
JB-SN-2A-PE	51.70	51.75	28	1																									
JB-SN-2A-PE	52.28	52.31	29	5											1		1												
JB-SN-2A-PE	53.45	53.50	30	29	2			1					1	1			1				1		15					1	
JB-SN-2A-PE	53.82	53.85	31	11	1									1						2			13				3		
JB-SN-2A-PE	54.54	54.47	32	21																									2
JB-SN-2A-PE	55.40	55.43	33	5	1																								
JB-SN-2A-PE	56.51	56.53	34	23			4							1			1										2		
JB-SN-2A-PE	58.08	58.12	35	5													2												
JB-SN-2A-PE	59.36	59.40	36	2																									
JB-SN-2A-PE	65.42	65.45																											
JB-SN-2A-PE	68.36	68.39																											
JB-SN-2A-PE	74.46	74.49																											
JB-SN-2A-PE	74.86	74.90																											
JB-SN-2A-PE	77.36	77.4																											
JB-SN-2A-PE	82.44	82.47																											
JB-SN-2A-PE	87.41	87.45	43																				1		1				
JB-SN-2A-PE	88.48	88.51																											
JB-SN-2A-PE	90.40	90.43																											
JB-SN-2A-PE	93.69	93.73	46	4																2			1					1	
JB-SN-2A-PE	97.27	97.30		6		2								5						5			1						

Hole ID	From	To	Sample #	Cicatricosisporites	Cicatricosisporites avnimelechi	Cicatricosisporites brevilaesuratus	Cicatricosisporites microstriatus	Cicatricosisporites mini	Cicatricosisporites pseudotripartitus	Concavissimisporites	Crybelosporites	Crybelosporites pannuceus	Crybelosporites truncatus	Cyathidites	Cyathidites cf mesozoicus	Cyclogranisporites	Deltoidospora	Deltoidospora australis	Deltoidospora cf halli	Deltoidospora tenuis	Densoisporites cf. microrugulatus	Ischyosporites	Ischyosporites foveolatus	Ischyosporites granulosus	Ischyosporites pseudoreticulatus	Klukisporites	Leptolepidites	Leptolepidites psarosus	Leptolepidites tumulosus	Leptolepidites verrucatus	Matonisporites	Matonisporites silvai	Paludites mamelonatus	Schizosporites	Todisporites	Todisporites minor	Verrucosisporites	Total	Subtilisphaera	Palinoforaminifero
JB-SN-2A-PE	29.25	29.31	2																																			0		
JB-SN-2A-PE	30.35	30.39	3	8	4	2	1				2	2										1	2			2					1							114	9	
JB-SN-2A-PE	30.9	30.97	4	1			1										1																					6		
JB-SN-2A-PE	31.36	31.41	5	17							3							3					1			2									1			73	7	
JB-SN-2A-PE	32.08	32.11	6	8													5	2										2										97	205	
JB-SN-2A-PE	32.22	32.26	7	6							3																											30	15	
JB-SN-2A-PE	32.37	32.42	8	3	3												3	1		2						1		4										151	50	
JB-SN-2A-PE	33.57	33.64	9	6							1						4	1		1						1												147	57	
JB-SN-2A-PE	34.08	34.19	10	15	2	3	11	1	1		1			3			2	2		1													2					152	105	
JB-SN-2A-PE	34.47	34.54	11	6	1						1							4								2										2		83	23	
JB-SN-2A-PE	35.31	35.35	12	4	1													1		2		1				1		2						1			4	200	58	
JB-SN-2A-PE	37.39	37.43	13	1		1																				1												66	42	
JB-SN-2A-PE	38.84	38.89	14	3																3						1	1					1					2	138	235	
JB-SN-2A-PE	39.2	39.23	15	2																																		27	37	
JB-SN-2A-PE	39.85	39.87	16	11		1					5			1						1												1					1	180	45	
JB-SN-2A-PE	40.25	40.28	17	7									1	2				2		1			1			1	2						5					120	92	
JB-SN-2A-PE	41.32	41.36	18																																			6		
JB-SN-2A-PE	42.00	42.03	19	5	2		2													1						1							2				2	226	119	
JB-SN-2A-PE	43.62	43.66	20	18	19	5		2			3			7	1		4			7							11	4		3					1		1	328	130	
JB-SN-2A-PE	44.14	44.17	21	14	3	2	3										3	1		1	1					2							3					305	149	
JB-SN-2A-PE	44.83	44.86	22	42	10	3		1	1					8			4			2				2		3	8					1						324	27	
JB-SN-2A-PE	45.17	45.20	23	32	8	2	1	6						4			5	2		5			1		1	5	10								1			435	173	
JB-SN-2A-PE	45.79	45.84	24	17			3							1			3	1		2						3	7						3					338	127	
JB-SN-2A-PE	50.06	50.09	25	7	5		1							3							1					2	3			2			1					200	182	
JB-SN-2A-PE	50.73	50.78	26	16	3	2	2							5			3				2		3			2	1	1	1	3			1					280	156	1
JB-SN-2A-PE	51.21	51.25	27	22	2	1					3			3			3	2		3							3			2			5			1		243	165	1
JB-SN-2A-PE	51.70	51.75	28				1										1						1			1												44	23	
JB-SN-2A-PE	52.28	52.31	29	10												1				1							1						3					162	52	
JB-SN-2A-PE	53.45	53.50	30	14	2		1				1			3			4		5								1			1		2			1			248	32	
JB-SN-2A-PE	53.82	53.85	31	12	2		2				2			2			2	1		2		1	3				1						3	1	1		3	227	32	
JB-SN-2A-PE	54.54	54.47	32								1			1				1								1	1											234	3	8
JB-SN-2A-PE	55.40	55.43	33	2													3								1	1												111		52
JB-SN-2A-PE	56.51	56.53	34	17	5	1					2		1	1			6	1		1			2		2	3	5	1		2		1	6					279	101	
JB-SN-2A-PE	58.08	58.12	35	4	1																											1						183		5
JB-SN-2A-PE	59.36	59.40	36		1													1																				118		
JB-SN-2A-PE	65.42	65.45																																				0		
JB-SN-2A-PE	68.36	68.39																																				0		
JB-SN-2A-PE	74.46	74.49																																				0		
JB-SN-2A-PE	74.86	74.90																																				0		
JB-SN-2A-PE	77.36	77.4																																				0		
JB-SN-2A-PE	82.44	82.47																																				0		
JB-SN-2A-PE	87.41	87.45	43		1																																	10		7
JB-SN-2A-PE	88.48	88.51																																				0		
JB-SN-2A-PE	90.40	90.43																																				0		
JB-SN-2A-PE	93.69	93.73	46	16	4									4			3	1					4				1								1			184		
JB-SN-2A-PE	97.27	97.30		17			2			1				4			4	2		2				2	1	2	1											230		

APÊNDICE K - TABELA DE DISTRIBUIÇÃO ESTRATIGRÁFICA DAS ABUNDÂNCIAS ABSOLUTAS DOS PALINOMORFOS DO TESTEMUNHO 2-JB-SN-2B-PE

Hole ID	From	To	Sample #	*Afropollis*	*Afropollis jardinus*	*Araucariacites*	*Araucariacites australis*	*Bennettitaepollenites*	*Bennettitaepollenites regaliae*	*Callialaorites dampieri*	*Callialaorites segmentatus*	*Callialaorites trilobatus*	*Callialaorites turbatus*	*Classopollis*	*Classopollis* (Tétrade)	*Classopollis alexi*	*Classopollis classoides*	*Classopollis torosus*	*Complicatisaccus cearensis*	*Conferisulcites*	*Corollaria annularis*	*Cycadopites*	*Cycadopites glottus*	*Cycadopites nitidus*	*Echimonocolpites*	*Equisetoorites*	*Equisetoorites aff lanceolatus*	*Equisetoorites aff reyrei*	*Equisetoorites ambiguus*	*Equisetoorites cf albertensis*	*Equisetoorites concinnus*	*Equisetoorites elegans*	*Equisetoorites leptomatus*	*Equisetoorites maculosus*	*Equisetoorites subcircularis*	*Eucommiidites*	*Eucommiidites aff Troedssonii*
	12.83	12.85																																			
JB-SN-2B-PE	28	28.04	6																																		
JB-SN-2B-PE	28.17	28.22	7																																		
JB-SN-2B-PE	28.33	28.39	8																																		
JB-SN-2B-PE	28.62	28.68	9																																		
JB-SN-2B-PE	28.78	28.84	10																																		
JB-SN-2B-PE	29.26	29.29	11			1								12												12						1					
JB-SN-2B-PE	30	30.06	12	4			24		7			1	5	94	4	6	26				3	1		1		28		1			11	1			1	1	
JB-SN-2B-PE	30.15	30.2	13				2																			2											
JB-SN-2B-PE	30.44	30.46	14	1		6	34		9	2				54	23		28				2					32					5				7	2	
JB-SN-2B-PE	30.6	30.63	15			2	1							1												3											
JB-SN-2B-PE	31.13	31.165	16			17	4	1						28	2											64											
JB-SN-2B-PE	31.65	31.69	17																							0											
JB-SN-2B-PE	31.89	31.92	18																							5											
JB-SN-2B-PE	32.75	32.8	19				45		2				1	79	7	18	26	18			2	3				10						7					
JB-SN-2B-PE	32.9	32.95	20	8	1	15	13	1	5	2		2	1	73	10	11	10		1				4			44	1							3			
JB-SN-2B-PE	33.05	33.08	21			3	12		2					23	3	83	99	7				4				6										4	
JB-SN-2B-PE	33.2	33.23	22			9	11		3		6		1	87	6	42	47					3				8			2		3		2				
JB-SN-2B-PE	33.39	33.42	23				20		2				1	98	3	37	48	32				3				5							1				
JB-SN-2B-PE	35.94	35.97	24			2	12		7		1		1	59	5	33	41	26		2		3				14										1	
JB-SN-2B-PE	36.1	36.14	25	3		27		8	2		1	1		99	24							3				38		1				10				3	
JB-SN-2B-PE	36.53	36.57	26		3		33		8			1	2	42	17							0				66	4				1		2			1	
JB-SN-2B-PE	36.74	36.76	27				13		2		1		3	96	9	15	24	8				2				19								5			
JB-SN-2B-PE	37.74	37.77	28						8		6		1	98	5	21	26	8				1				5											
JB-SN-2B-PE	38.03	38.07	29				17		3	1				98	9	17	28	9								26											
JB-SN-2B-PE	38.35	38.39	30	1			1		9		4	1		96	6	19	29	7		1		3			1	4											
JB-SN-2B-PE	38.58	38.59	31	2			14		5	1	3			96	3	1	19	5								12								2			
JB-SN-2B-PE	38.67	38.7	32	6	3	1	12		5					46	23	19	26					7	2			36				8	7			2		3	
JB-SN-2B-PE	38.82	38.85	33	4	4	7		2	3			2		42	10	24	32					1	1			34	4					5		3		7	1
JB-SN-2B-PE	41.45	41.49	34											16																							
JB-SN-2B-PE	41.55	41.59	35			1	1		7	2	5		3	98	14	21	29	11				2				5							1	3		2	
JB-SN-2B-PE	41.81	41.85	36											11																							
JB-SN-2B-PE	43.37	43.4	37		1		8		3			2		99	7	28	42	8				3				8							2	2		2	
JB-SN-2B-PE	43.5	43.56	38											56	10																						
JB-SN-2B-PE	44.04	44.07	39											7																							
JB-SN-2B-PE	44.2	44.24	40											6																							
JB-SN-2B-PE	44.44	44.47	41											2																							
JB-SN-2B-PE	44.82	44.85	42			13	2			3	1			72	11	24	28									2											
JB-SN-2B-PE	45.19	45.23	43			1								16												2											
JB-SN-2B-PE	45.58	45.62	44					1						11	7		8																				
JB-SN-2B-PE	46.15	46.19	45			1								5																							
JB-SN-2B-PE	46.4	46.45	46											2												1											
JB-SN-2B-PE	47.6	47.65	47											3																							
JB-SN-2B-PE	47.9	47.93	48			3		3			1			48	5	14						1		2		17											
JB-SN-2B-PE	48.56	48.59	49						2			3		68	6									1		4											
JB-SN-2B-PE	48.99	49.03	50			1			1					35								1				2											
JB-SN-2B-PE	50.64	50.68	51				13		1			3		2	5	51	55					3				9											
JB-SN-2B-PE	55.5	55.64	52											4		1										2											
JB-SN-2B-PE	55.91	55.95	53			35	45		25				3	29		23	38									18											
JB-SN-2B-PE	56.64	56.69	54			27	28		11		5		3	39		20	45					25				15											
JB-SN-2B-PE	57.39	57.43	55										2	57	20											3								2			
JB-SN-2B-PE	59.61	59.73	56											13	5											5								4			
JB-SN-2B-PE	61.38	61.43	57											71	9							4				14								3			
JB-SN-2B-PE	61.69	61.74	58												7		5					1															
JB-SN-2B-PE	62.14	62.18	59												1																						
JB-SN-2B-PE	67.84	67.92	60											7																							

Sample #	*Exesipollenites*	*Exesipollenites tumulus*	*Gnetaceaepollenites barghoornii*	*Gnetaceaepollenites jansonii*	*Gnetaceaepollenites mollis*	*Gnetaceaepollenites oreadis*	*Gnetaceaepollenites retangularis*	*Gnetaceaepollenites uesuguii*	*Gnetaceapollenites*	*Inaperturopollenites*	*Monocolpopollenites*	monosulcate (monocolpate)	*Pennipollis*	*Podocarpidites cf naumovai*	*Podocarpites*	*Proxapertites*	*Regalipollenites amphoriformis*	*Reticolpites*	*Sergipea*	*Sergipea naviformis*	*Sergipea tenuiverrucata*	*Sergipea variverrucata*	*Singhia*	*Singhia acicularis*	*Singhia montanaensis*	*Singhia punctata*	*Steevesipollenites*	*Stellatopollis*	*Stellatopollis densiornatus*	*Stellatopollis dubius*	*Trichotomosulcites*	*Trisectoris reticulatus*	*Uesuguipollenites callosus*
6																																	
7																																	
8																																	
9																																	
10																																	
11				4						5													1										1
12		3		1		6			13	14							1						1	1	4		1						10
13				1					0	5													1			3							
14		2		5		3			11	29				1											2	1	2						
15				2					5	6																3							
16				2					8	77																3							
17				1					0	4																							
18										29																							
19		1					5		8				1									2				12	5			1			2
20	8	4		1	1		3		12	21											1	1			2		12			1		3	5
21		5					3		4	8													6				7						
22		12	1				4	3								1			2			2	1				8		2				1
23		1		2						7	3												2				5						
24		5	2	1			8		9	7	4		2										5			6	8						
25		10	9	7			3		4	5	3		2													1	16						1
26		4		10			8	6	6	24	2	2	1		1	1											4				1	3	5
27		11		8			5	6	8	9			1									2	1			4	13						3
28		6		1			4		16	13									2	1			6				21						1
29		8		3			4		8	8			1										6		2	3	11					1	1
30		13		6		4	5	4		9									1				7		11	7	16						
31		11		8			9	3	10	8									3	3		2	10				12						7
32		7		4			1	3	2	12		1			1				6			3				5	7	1					4
33	4	7		5			8		4	13	3		3		1			2				3				5	7	1					1
34																																	
35		4	1	5			8		3	5																14	10						2
36																																	
37		3		5			7		5	4				1					1								4						1
38									1																								
39																																	
40																																	
41																																	
42									2	26																	3						
43																																	
44																																	
45																																	
46																																	
47																																	
48		1								22																	6						
49									1	10												1											
50																																	
51									3			2	1														3						
52									2																								
53				10			2		6		12												8			4	3						
54				21					1			4	2													8	5						
55									1																								
56									1																								
57									1	2																							
58																																	
59																																	
60																																	

Sample #	*Appendiciorites*	*Appendiciorites tricornitatus*	*Aquitriradites*	*Belliorites*	*Boseiorites*	*Camarozonoorites*	*Chomotriletesfragilis*	*Cicatricosiorites*	*Cicatricosiorites avnimelechi*	*Cicatricosiorites brevilaesuratus*	*Cicatricosiorites microstriatus*	*Cicatricosiorites purbeckensis*	*Crybeloorites*	*Crybeloorites pannuceus*	*Crybeloorites truncatus*	*Cyathidites*	Deltoidoora	*Deltoidoora australis*	*Deltoidoora tenuis*	*Densoiorites*	*Densoiorites cf microrugulatus*	*Echinatioris*	*Foveotriletes*	*Ischyoorites*	*Ischyoorites foveolatus*	*Ischyoorites pseudoreticulatus*	*Leptolepidites*	*Matoniorites silvai*	*Schizea*	*Schizea certa*	*Schizoori*	*Todiorites*	*Verrucosiorites*	**Total**	Acritarco	*Maranhites* sp.
																																		0		
6																7																		7		
7																																		0		
8																																		0		
9																																		0		
10																																		0		
11								10		1															1									49		
12								3	10			1				5	3	1	1						1							1		300		
13								5		1							3																	23		
14								16		8	6						2								3		3	1						300	2	
15								3		4							3																	33		
16								9		5						1									2									223		
17								4		1																								10		
18								5																	1									40		
19								4	1	2							2	1	2		3			3				2	1	1				277		
20	1							11	2	1						4									1									300		
21								4		3						1	9			1				1					1				**1**	300		1
22								5	3		1					1			2	3							7	4		1		2	**4**	300		
23								5		2							2											3					**3**	285		
24						7		6			3		3							5		1		1			4	3	2			1		300	1	
25						1		14		2							1														1			300		
26			4			1		12	5		1			2	2	2	1		1					1		1	8				1			300	1	
27	1									6	2						1	2	2	1			1		5		3	3	1			1	3	300		
28								11		4							7								5		1			1			3	282		
29						1				3						1	3		5	1				1			1	1					3	284		
30	2			1		1		8			3	1					5		4					3			5			1			1	300		
31							3	21	6							5	4						2		2		7			1				300		
32			1			1		11	4		6					3	2							2			6							299		
33			2		1	1		9	7	1	1					2	3		1		3		4	1	2		5	1				2		299		
34								2																										18		
35	1							6	5							2			5	3	2			5	1		3		2	1	1		**3**	297		
36																																		11		
37	2							12	4							2	3		4	4				5			3	4		1			**7**	297		
38								3																										70		
39																																		7		
40																																		6		
41																																		2		
42		1						7		2	1						4	2		1					2									207		
43																															3			22		
44																1	1																	29		
45																																		6	1	
46								1																										4		
47																																		3		
48								9			4						2	1									4							143		
49								1																									**1**	98		
50								1																										41		
51										4	3			1			3								1								**2**	165		
52								3																										12		
53								11		5	4	1		2		3	5		2									6						300		
54								11			7							3								1		19						300		
55																																		85		
56								3									1																	32		
57																																		104		
58																																		13		
59																				1														2		
60																																		7		